32086

National Library of Canada | Bibliothèque nationale du Canada | CANADIAN THESES ON MICROFICHE | THÈSES CANADIENNES SUR MICROFICHE

NAME OF AUTHOR/*NOM DE L'AUTEUR* CONRAD MORTIMER BROWNLEE WALKER

TITLE OF THESIS/*TITRE DE LA THÈSE* DIELECTRIC CONSTANTS OF WATER-DMSO SOLUTIONS, AND NUMERICAL MODELLING OF MICROWAVE HEATING

UNIVERSITY/*UNIVERSITÉ* UNIVERSITY OF ALBERTA.

DEGREE FOR WHICH THESIS WAS PRESENTED/ *GRADE POUR LEQUEL CETTE THÈSE FUT PRÉSENTÉE* Phd.

YEAR THIS DEGREE CONFERRED/*ANNÉE D'OBTENTION DE CE GRADE* 1977

NAME OF SUPERVISOR/*NOM DU DIRECTEUR DE THÈSE* DR. W.A.G. Voss, AND DR. W.R. TINGA

Permission is hereby granted to the NATIONAL LIBRARY OF CANADA to microfilm this thesis and to lend or sell copies of the film.

The author reserves other publication rights, and neither the thesis nor extensive extracts from it may be printed or otherwise reproduced without the author's written permission.

L'autorisation est, par la présente, accordée à la BIBLIOTHÈQUE NATIONALE DU CANADA de microfilmer cette thèse et de prêter ou de vendre des exemplaires du film.

L'auteur se réserve les autres droits de publication; ni la thèse ni de longs extraits de celle-ci ne doivent être imprimés ou autrement reproduits sans l'autorisation écrite de l'auteur.

DATED/*DATÉ* March. 18th, 1977 SIGNED/*SIGNÉ* [signature]

PERMANENT ADDRESS/*RÉSIDENCE FIXE* 4111-112A ST., EDMONTON ALBERTA, CANADA.

NL-91 (3-74)

National Library of Canada

Cataloguing Branch
Canadian Theses Division

Ottawa, Canada
K1A 0N4

Bibliothèque nationale du Canada

Direction du catalogage
Division des thèses canadiennes

NOTICE

The quality of this microfiche is heavily dependent upon the quality of the original thesis submitted for microfilming. Every effort has been made to ensure the highest quality of reproduction possible.

If pages are missing, contact the university which granted the degree.

Some pages may have indistinct print especially if the original pages were typed with a poor typewriter ribbon or if the university sent us a poor photocopy.

Previously copyrighted materials (journal articles, published tests, etc.) are not filmed.

Reproduction in full or in part of this film is governed by the Canadian Copyright Act, R.S.C. 1970, c. C-30. Please read the authorization forms which accompany this thesis.

THIS DISSERTATION
HAS BEEN MICROFILMED
EXACTLY AS RECEIVED

AVIS

La qualité de cette microfiche dépend grandement de la qualité de la thèse soumise au microfilmage. Nous avons tout fait pour assurer une qualité supérieure de reproduction.

S'il manque des pages, veuillez communiquer avec l'université qui a conféré le grade.

La qualité d'impression de certaines pages peut laisser à désirer, surtout si les pages originales ont été dactylographiées à l'aide d'un ruban usé ou si l'université nous a fait parvenir une photocopie de mauvaise qualité.

Les documents qui font déjà l'objet d'un droit d'auteur (articles de revue, examens publiés, etc.) ne sont pas microfilmés.

La reproduction, même partielle, de ce microfilm est soumise à la Loi canadienne sur le droit d'auteur, SRC 1970, c. C-30. Veuillez prendre connaissance des formules d'autorisation qui accompagnent cette thèse.

LA THÈSE A ÉTÉ
MICROFILMÉE TELLE QUE
NOUS L'AVONS REÇUE

THE UNIVERSITY OF ALBERTA

THE DIELECTRIC CONSTANT OF WATER-DMSO SOLUTIONS, AND THE NUMERICAL MODELLING OF MICROWAVE HEATING

by

(C) CONRAD M.B. WALKER

A THESIS

SUBMITTED TO THE FACULTY OF GRADUATE STUDIES AND RESEARCH

IN PARTIAL FULFILMENT OF THE REQUIREMENTS FOR THE DEGREE

OF DOCTOR OF PHILOSOPHY

IN

ELECTRICAL ENGINEERING

DEPARTMENT OF ELECTRICAL ENGINEERING

EDMONTON, ALBERTA

SPRING, 1977

THE UNIVERSITY OF ALBERTA

FACULTY OF GRADUATE STUDIES AND RESEARCH

The undersigned certify that they have read, and recommend to the Faculty of Graduate Studies and Research, for acceptance, a thesis entitled "Dielectric Constant of Water-DMSO Solutions, and the Numerical Modelling of Microwave Heating", submitted by Conrad M.B. Walker in partial fulfilment of the requirements for the degree of Doctor of Philosophy in Electrical Engineering.

.....

.....

Supervisors

.....

.....

.....

.....

External Examiner

Date March 15, 1977

ABSTRACT

A cavity perturbation method for wide temperature range dielectric measurements is described. It is used to measure the complex dielectric constant of aqueous-DMSO solutions in the temperature range -60°C to +100°C, for concentrations from 0 to 100%. The results indicate that the relaxation frequency drops from 18 Ghz to 3 Ghz as the concentration is increased from 0 to 70%. A further concentration increase causes the relaxation frequency to increase to 9 Ghz. At temperatures below freezing, the value of ϵ'' is increased by the addition of DMSO, and its rate of change with temperature is reduced. The cryobiological implications of this result are examined.

A numerical model of plane wave microwave heating of canine kidneys is developed. Details of 1.5 mm and larger are represented in the model. The model shows that microwave energy absorbtion is enhanced by DMSO perfusion, and that adjustment of DMSO concentration can provide control of heating uniformity. Uniform perfusion is found to be essential if heating is to be uniform. Steep gradients in the electric field are found to exist at the interfaces to the renal sinus. The compositions of the solutions residing in the renal pelvis and vascular structure of the kidney are found to have considerable effect on the heating uniformity.

ACKNOWLEDGEMENT

The author wishes to express his appreciation to Dr. W.A.G. Voss and Dr. W.R. Tinga for their encouragement and assistance during the course of this project.

The assistance and co-operation of Mr. A. Huizinga, Dr. C. Leibowitz, Mr. D. Malenka and other staff members and graduate students in the Department of Electrical Engineering is also gratefully acknowledged.

The patience and understanding of Rosemary, Tamara and Conrad is deeply appreciated.

The author is indebted to the National Research Council for the financial assistance provided.
(Grants: NRC A7626 and A2272)

CONTENTS

	Title	Page
Chapter 1. Introduction.		
1.1	Microwave Thawing.	1
1.2	Advantages and Disadvantages of Microwave Thawing.	2
1.3	Cryoprotective Agents and their Use.	4
1.4	The Role of Dielectric and Thermal Properties.	6
1.5	The Importance of Numerical Modelling.	9
1.6	Methodology.	11
Chapter 2. Measurement of Dielectric Properties.		
2.1	Review of Dielectric Measurement Technique.	13
2.2	Advantages of the Method Used.	15
2.3	Theoretical Description of the Method.	17
Chapter 3. Measurement Technique.		
3.1	Description of Apparatus.	22
3.2	Temperature Measurement and Control.	25
3.3	Calibration Procedure.	28
3.4	Corrections for Cavity Expansion and Contraction.	32
3.5	Measurement Procedure.	33
3.6	Varying Temperature Measurements (-60 to +20°C).	33
3.7	Varying Temperature Measurements (+20 to +100°C).	35
3.8	Varying Concentration Measurements.	35
3.9	Data Reduction.	36
Chapter 4. Results of Dielectric Measurements.		
4.1	Presentation.	42
4.2	Comparison with Literature for Distilled Water.	44
4.3	Measurements on Various Concentrations.	48
4.4	Comparison of Cole-Cole Plots for Water and DMSO.	62
4.5	Relaxation of a 70% Solution of DMSO in Water.	63
4.6	5% Dextran.	64
4.7	10% DMSO and Various Additives.	67
4.8	Behaviour of ϵ' with Concentration.	70
4.9	Behaviour of ϵ'' with Concentration.	72
4.10	Biological Implications.	72
4.11	Concluding Remarks.	82
Chapter 5. Electromagnetic Field Modelling.		
5.1	A Review of Some Existing Techniques.	83
5.2	Reasons for Choice of the Method Used.	86
5.3	Description of the method.	88
5.4	The Yee Algorithm.	88
5.5	Lattice Truncation Conditions.	93
5.6	The Symmetry Conditions.	96
5.7	The Plane Wave Source Condition.	96
5.8	Stability Criterion.	97
5.9	Computer Program.	98
5.10	Comparison of Exact and Time-domain Solutions.	99

5.11 Calculation of Absorbed Power. 100

Chapter 6. The Kidney Model.
6.1 Modelling of Heating Processes. 103
6.2 Reasons for Choice of the Canine Kidney. 104
6.3 Modelling the Kidney. 105
6.4 The Dielectric Properties of the Model. 105
6.5 Results Obtained with the Model. 112
6.6 Condition 1. The Datum Model 137
6.7 Condition 2. Effect of Frequency 145
6.8 Condition 3. Effect of Reducing DMSO Concentration. 153
6.9 Condition 4. Temperature Effect. 161
6.10 Condition 5. The Effect of No Perfusion. 170
6.11 Condition 6. Total Perfusion of the Pelvis. 170
6.12 Condition 7. 1000 Mhz Heating at 20°C. 184
6.13 Condition 8. Reversed Radiation Direction. 192
6.14 Comparison with Experimental Results. 192
6.15 Concluding Remarks. 195

Chapter 7. Suggested Further Research.
7.1 Dielectric and Thermal Property Measurement. 198
7.2 Numerical Heating Models. 199

Conclusions. 202

References. 204

Appendices.
(A) Computer programs for analysis of dielectric data. 212
(B) Computer program for electromagnetic heating model. 219
(C) Properties of DMSO. 229
(D) Tables of measured dielectric data. 230

LIST OF TABLES

Table	Description	Page
3.1	Data Recording Form.	24
3.2	Calibration Liquids.	28
6.1	Dielectric Data for Beef and Kidney.	132
6.2	Dielectric Data for Fat.	133
6.3	Dielectric Data for Water and DMSO.	134
6.4	Model Parameters.	135

LIST OF FIGURES

Figure	Description	Page
2.1	Cavity Arrangement.	18
2.2	Field Configurations.	18
2.3	$\epsilon' = F_1(\Delta f)$.	20
2.4	$\epsilon'' = F_2(\epsilon').(\Delta T)^{-0.50}$.	20
3.1	Block Diagram of Equipment for Wide Temperature Range Measurements of Dielectric Constant.	23
3.2	Ten-turn Pot Reading vs. Frequency Shift.	24
3.3	ϵ' vs. Frequency Shift.	30
3.4	$\epsilon''(25)$ vs. $(\epsilon'-1)$.	30
3.5	ϵ'' vs. Attenuation.	31
3.6	Dial Correction vs. Temperature.	31
3.7	ϵ' vs. Frequency Shift as Measured and Calculated.	38
3.8	ϵ'' vs. $(\epsilon'-1)$ as Measured and Calculated.	39
4.1	ϵ' vs. Temp. for Distilled Water.	46
4.2	ϵ'' vs. Temp. for Distilled Water.	47
4.3	ϵ' vs. Temp. for 1% DMSO in Water.	49
4.4	ϵ'' vs. Temp. for 1% DMSO in Water.	50
4.5	ϵ' vs. Temp. for 5% DMSO in Water.	51
4.6	ϵ'' vs. Temp. for 5% DMSO in Water.	52
4.7	ϵ' vs. Temp. for 10% DMSO in Water.	53
4.8	ϵ'' vs. Temp. for 10% DMSO in Water.	54
4.9	ϵ' vs. Temp. for 20% DMSO in Water.	55
4.10	ϵ'' vs. Temp. for 20% DMSO in Water.	56
4.11	ϵ' vs. Temp. for 70% DMSO in Water.	57
4.12	ϵ'' vs. Temp. for 70% DMSO in Water.	58
4.13	ϵ' vs. Temp. for 100% DMSO in Water.	59
4.14	ϵ'' vs. Temp. for 100% DMSO in Water.	60
4.15	ϵ' vs. Temp. for Water and 5% Dextran.	65
4.16	ϵ'' vs. Temp. for Water and 5% Dextran.	66
4.17	ϵ' vs. Temp. for Various Compounds in Water.	68
4.18	ϵ'' vs. Temp. for Various Compounds in Water.	69
4.19	ϵ' vs. Concentration for DMSO at Various Temperatures.	71
4.20	ϵ'' vs. Concentration for DMSO at Various Temperatures.	73
4.21	Loss Tangent vs. DMSO Concentration at Various Temperatures.	74
4.22	The Binary H_2O-DMSO Phase System.	75
4.23	Cole-Cole Plot for Ice at -10.9°C.	76
4.24	Cole-Cole Plots for Solutions of Water and DMSO.	77
4.25	Temperature Behaviour of the Relaxation Frequency.	78
4.26	Typical Debye Curve for a Dielectric with	78

	a Single Relaxation Frequency.	
5.1	Position of Field Components About a Unit Cell of the Yee Lattice.	90
5.2	Lattice Used to Test the Program on a Sphere.	90
7.3	Electric Fields Within a Dielectric Sphere.	101
6.1	Dorsal and Transverse Views, with Dimensions, of a Canine Kidney.	106
6.2	Arrangement of the Lattice Around the Kidney.	106
6.3	Dorsal Section of Kidney and Cast of Pelvis.	111
6.4	Transverse Section of Kidney.	111
6.5	(1-5) The 15 Planes of the Dielectric Media Lattice.	112
6.6	(8-11,13,15) Results: Datum Set.	138
6.7	(8-11,13,15) Results: Frequency Effect.	146
6.8	(5,8-10,12,15) Results: Perfusate Effect.	154
6.9	(5,8-11,13,15) Results: Temperature Effect.	162
6.10	(5,8-11,13,15) Results: Perfusion Effect.	171
6.11	(9-11,13,15) Results: Tubule Effect.	178
6.12	(5,8,9,11,13,15) Results: Temperature Effect, 1000 Mhz.	185

LIST OF SYMBOLS

Symbol	Meaning
AT	Attenuation, dB
c	Velocity of light
C_a, C_b	Constants
c_c	Specific heat of container
c_s	Specific heat of sample
$\underline{E}$	Electric field vector
$\underline{\tilde{E}}$	Proportional electric field vector
E_{inc}	Incident electric field
f	Frequency
f_D	Relaxation frequency
F^n	Function at time increment n
H	Magnetic field vector
HI	Heating index
H_ℓ	Latent heat of fusion
i, j, k	Number of space increments in the x, y, z directions respectively
J	Joule's equivalent
k	$1/\delta$
l(m)	Integer constant for tissue type m
loss tangent	ϵ''/ϵ'
m	Tissue type integer
m_c	Mass of container
m_s	Mass of sample
N	Number of lattice points
N_x, N_y, N_z	Number of points in x, y, z directions
P	Absorbed power
P_a	Absorbed power
P_i	Incident power
P_ℓ	Power loss
P_N	Normalised absorbed power
P_{Nmax}	Max. normalised absorbed power
P_r	Reflected power
R, R_a, R_b	Constants
t	Time
T	Cavity transmission
v_{max}	Maximum phase velocity in the media
x, y, z	Co-ordinates
δ	Increment between lattice points
δt	Time increment
ϵ	Permittivity
ϵ_o	Free space permittivity
ϵ^*	Complex dielectric constant
ϵ'	Real part of relative dielectric constant
ϵ_∞	High frequency dielectric constant
ϵ'_r	Maximum value of ϵ' in scatterer
ϵ_s	Static dielectric constant
ϵ''	Imaginary part of relative dielectric constant
$\epsilon''(25)$	Equivalent imaginary part of dielectric

	constant to produce a cavity attenuation of 25 dB
η	Impedance of free space
θ	Temperature
θ_i	Initial temperature
θ_f	Final temperature
λ, λ_m	Wavelength in tissue type m
λ_o	Free space wavelength
λ_m	Maximum wavelength in scatterer
μ	Permeability
μ/μ_o	Permeability of free space
σ	Conductivity

Chapter 1. Introduction

(1.1) Microwave Heating.

The expansion of the biological sciences has led to a need for techniques for the preservation of biological material. Low temperature storage, as developed by the science of cryobiology, has provided one solution to this problem. There are three phases involved in the process of low temperature storage. These are: (a) the cooling of the tissue, (b) its storage at a low temperature and (c) its recovery from the frozen state. The present work is primarily concerned with the use of microwaves in the third phase, though certain aspects of the first two phases are important. Microwave heating is dependent on the dielectric constant and so factors which influence this constant must be considered. In particular, account must be taken of the type of cryoprotective agent, the degree of perfusion with the agent, and the temperature range.

The use of microwaves for the recovery of frozen organs was first reported by Andjus (1) in 1953. Subsequent investigations, including comparisons with conduction heating, have been made by Kenney (2), Holst (3), Hamilton (4), Ketterer (5,6), Burns (7) and others. The major difficulties encountered are achieving and controlling the heating rate, attaining reasonable heating uniformity, and

stopping the process at some desired temperature. Research aimed at resolving these problems has lagged considerably behind the other areas of cryobiological investigation, but the increasing availability of microwave apparatus is aiding in these studies. Systems designed to solve one or more of these problems have been described by Rzepecka (8), Rajotte (9), Walker (10) and others, although most of these systems are primarily useful for small samples.

(1.2) The Advantages and Disadvantages of Microwave Heating.

The two types of heating employed in cryobiology are microwave heating and conventional heating, which employs heat transfer by conductive or convective techniques. In the latter case, it is usually necessary to immerse the tissue in a liquid (often water) to prevent surface evaporation. In microwave heating, however, the surrounding air temperature is not affected, and so liquid immersion is not necessary. If it is required, liquids with suitably low dielectric loss, such as fluorocarbon, can be used (11).

For conventional heating, the delicate nature of biological materials limits the temperature of the surrounding liquid to less than 50°C. This effectively limits the heating rate. As the size of the heated sample increases, this limitation becomes more severe. In addition, heat transfer requires that there be a temperature gradient

from the sample surface to its interior, and so acceptably uniform heating is not possible except for very small samples. These two factors represent a physical limitation of conventional heating.

In the case of microwave heating, energy is dissipated throughout the sample. Heating uniformity is a function of the disposition of the dielectric constants in the sample and the design of the heating apparatus, factors over which there is some degree of control. In addition, heating rate is limited by the available microwave power. Therefore, uniformity and heating rate are governed by technological factors, and so the potential for improvement does exist.

There are three main problems with microwave heating. These are: (a) The amount of dissipated energy is governed by temperature dependent dielectric properties. (b) Temperature measurement during heating is difficult because of electromagnetic field perturbation by the measuring probe. (c) The coupling structure must often be specifically designed for a given sample if optimum uniformity and energy transfer are to be achieved.

An investigation into the temperature dependence of the dielectric constants of tissue and cryoprotective agents will aid in the solution of the first problem, and this is dealt with in Chapter 4. A viable first order solution to

the second problem has been presented elsewhere (10). The numerical model of microwave heating dealt with in Chapters 5 and 6 represents a first step towards the solution of the third problem.

(1.3) Cryoprotective Agents and their Uses.

When biological tissue is cooled through the temperature range from -60°C to +10°C, ice-formation causes changes in intercellular fluid concentrations with resulting changes in osmotic pressure. These effects cause potentially damaging stresses to be established within the cellular structure of the tissue, and for this reason, the present microwave heating study is limited to this crucial temperature range.

The cryoprotective agents used to protect tissue from damage during freezing are basic to the science of cryopreservation. There are two major types of cryoprotective agent commonly employed. These are: (a) some relatively low molecular weight materials (70-400D) such as dimethyl sulfoxide (DMSO) and glycerol, which act by permeating the intercellular spaces of the tissue, and (b) some high molecular weight materials such as polyvinyl-pyrrolidone (PVP) and dextran which are extracellular and are believed to lessen the rise in extracellular ice-concentration as ice forms, thereby protecting the cell

surface rather than the cell interior (12). The two types of agent are sometimes used in conjunction with one another.

DMSO is the liquid which is primarily investigated in this work since it is both an effective cryoprotective agent, and, being a highly polar liquid, is of some interest in the area of dielectric theory. Ashwood-Smith (13) has reviewed many of the important properties of DMSO as related to cryobiology, and Szmant (14) has summarised some of the physical properties of the liquid (see Appendix C).

The compound DMSO was first prepared in 1866, but only came into general use after World War II when its radioprotective and cryoprotective properties were discovered. Its ability to penetrate cell membranes aroused considerable interest in biological and medical circles, but reports of disturbances to the lens of the eye halted clinical tests. These tests have again begun, but the full potential of the compound has yet to be realised, though it has certainly proved important in cryobiology. The uses and properties of the liquid are discussed in considerable detail in the literature (15). Values of some dielectric properties are included there, while other measurements have been reported by Bourgoin (16) and Doucet (17), though these were not at the frequency and concentrations employed in the present work.

(1.4) The Role of Dielectric and Thermal Properties.

A considerable amount of dielectric data for biological materials has appeared in the literature during the past three decades. Among the major contributors are England (18) and Schwann (19), with extensive compilations by Tinga (20) and Presman (21). Knowledge of these data are important for theoretical investigation in several areas. These are: (a) For analysis of electrocardiography and other related electrical measurements of body function. (b) For the detemination of the electrical properties of tissue at high frequencies. In microwave diathermy, this is a pre-requisite to understanding how high frequency electrical currents penetrate the body and produce heat. (c) For the analysis of the deleterious effects of electromagnetic radiation on humans. (d) For analysis of microwave cooking of foods and other industrial processes. (e) For theoretical studies involving the formulation of equations describing material behaviour over a wide range of frequencies and temperatures.

In each case, the conditions under which the data is obtained depend on the intended application. For example, data for frozen foods as well as foods at room temperature are important in studying microwave thawing and tempering, whereas bulk properties of human body tissue at normal body temperature (37°C) are of interest in the study of the biological effects of microwave radiation. The theoretical

study of microwave heating in cryobiology is still in its infancy and so dielectric properties measured under the conditions pertaining to cryopreserved tissue are only just beginning to appear in the literature (22). These conditions include tissue which can be in a wide range of temperatures and is often perfused with a cryoprotective agent. A wide variety of cryoprotective agents can be used and it is difficult to estimate the degree of perfusion for any given case.

There is some evidence to suggest that the dielectric properties of tissue are governed by the properties of the intercellular fluids for frequencies in the microwave region (19). Further, there is an interest in the dielectric properties of aqueous solutions of the cryoprotective agent, DMSO, for a wide range of temperatures. On these grounds, it was decided to make the dielectric property measurements on DMSO for the conditions mentioned, and then, in conjunction with literature data for appropriate frozen foods, to obtain estimates for the dielectric properties of perfused tissues. These properties are required for the numerical microwave heating model. Some data for perfused kidney tissue is available in the literature (22), and this is used to aid in making the estimates.

Although they are not used in this work, thermal properties are also important and a detailed examination of

microwave heating should consider the specific and latent heats and the conductivity of the material. Specific heat and conductivity are also temperature dependent properties, but there is little data regarding their behaviour for the materials of interest in cryobiology. Tressler (23), Awberry (24), Dickerson (25), Ohlsson (26) and Hill (27) have made measurements on the specific and latent heats and conductivities of various meats and other foodstuffs, and some conclusions regarding the behaviour of frozen organs can be drawn from these measurements.

It is recognised that complex materials like biological tissues do not freeze or thaw at a single well-defined temperature, but rather over a range of temperatures. Therefore, to make heat transfer calculations more manageable, Dickerson (25) has suggested the use of the enthalpy of the materials of interest. The existence of tables of enthalpy for various bio-materials under various conditions would be a great asset to microwave heating in cryobiology.

Dielectric and thermal properties are thus a pre-requisite for optimum design of microwave heating apparatus. In addition, reasonably accurate data regarding these properties are especially important when numerical modelling techniques are employed.

(1.5) The Importance of Numerical Modelling.

Numerical modelling techniques have the advantage of being easy to apply when many different variables are involved. In the case of heating studies, the effects of changes in dielectric and thermal properties can quickly be assessed, and possible solutions to problems of heating uniformity can be assessed In many situations, the measurements required to characterise system behaviour are difficult to perform, and the use of numerical modelling is the only remaining recourse.

For instance, there are considerable difficulties involved in making temperature measurements on microwave-heated materials. These difficulties are compounded if temperature distributions are required, as is the case if heating uniformity is of importance. Furthermore, the existence of numerous variables such as the composition of the cryoprotective agent, the heating rate adopted and the possibility of a combination of thermal and microwave heating mean that the direct experimental approach, if at all possible, would require many replications.

The use of a numerical modelling techniques in this situation would allow the interdependence of the different variables to be examined, and could lead to new techniques for controlling uniformity. One possibility would be the

introduction of liquids with carefully chosen dielectric properties to specific areas of the sample being heated. A similar approach using metal balls rather than liquids has been employed in the literature (7). Another possibility is the simultaneous use of microwave and conduction heating, or of multifrequency heating (7). The evaluation of these and other approaches could certainly be simplified by the use of modelling techniques.

In the past, theoretical microwave heating studies have been performed on geometrically simple shapes such as cylindrical 'roasts' (28) and infinite slab 'hamburgers' (29). If inhomogeneous dielectric properties were considered at all, they were usually arranged in a geometrically simple fashion. For these reasons, the bulk properties of the materials of interest were usually sufficient. In the present work, a numerical model which is able to account for relatively small (1.5mm) structural inhomogeneities is employed, and so the properties of the individual tissue types with and without perfusion over a range of temperatures are required. More detailed models investigating other microwave effects have appeared in the literature (30,31,32), but body temperature properties (±10°C) of normal tissue were usually required in these cases.

The model adopted in the present work considers plane

wave illumination of a canine kidney. Though some situations justify the use of a plane wave, the model is not restricted to this type of illumination. It is possible to simulate different types of incident wavefront, and even to model heating within a cavity. The main limitations are memory capacity and processing time.

(1.6) Methodology.

Chapters 2 and 3 deal with the development of a system to measure dielectric properties over a wide range of temperatures. Some of the problems encountered with the measurements are discussed in Chapter 3.

In Chapter 4, the results of the dielectric measurements are presented, and some of the theoretical and biological implications of these results are discussed. In particular, the behaviour of the water-DMSO system in relation to its phase diagram is examined. In addition, changes in the dielectric properties as a function of temperature are discussed in relation to their effect on microwave heating.

Chapter 5 deals with the creation of a numerical model designed to study microwave heating effects. Application of this model to the canine kidney is described in Chapter 6, where the results obtained with the model are also

discussed.

The two sections of Chapter 7 deal respectively with suggested further research on the measurement of dielectric and thermal properties, and the use of the numerical model.

Chapter 2. Measurement of Dielectric Properties

(2.1) Review of Dielectric Measurement Technique

There are a great many different methods of making dielectric measurements, and it is not the present purpose to exhaustively review these techniques. The subject of dielectric measurements in general is adequately treated in the literature, for example, Bussey (33) and Altschuler (34).

Broadly speaking, there are three general classes of dielectric measurement technique for use at microwave frequencies. These are (a) Standing wave methods, (b) Perturbation methods and (c) Time domain techniques. For a given application, individual methods are judged according to the following criteria:

(1) Accuracy and precision of the method.

(2) Sample size and configuration.

(3) Frequency range where the method is applicable.

(4) Available and required apparatus.

(5) Ease of temperature control.

Because the dielectric constant of biological materials even varies for samples from the same piece of tissue, accuracy and precision are not of primary importance. Furthermore, because the main concern in this work is with

microwave heating, and because much of this heating is done in the ISM (Industrial, Scientific and Medical) band at 2450 Mhz, the frequency range from 2 to 3 Ghz is of special importance.

What is important in biological measurements, however, is sample size and configuration, and ease of temperature control. The method was therefore selected with these particular requirements in mind.

In general, standing wave methods require carefully shaped samples of rather large volume and accurately known dimensions, because the samples are required to fit appropriate waveguide structures. At the frequencies of interest, the apparatus would be bulky and difficult to incorporate into a suitable temperature control system. On the other hand, time domain techniques, that of Iskander and Stuchly (35) being a good example, require only small samples and could easily be incorporated into a temperature control system. The disadvantage of this technique is that a sampling oscilloscope and an appropriate facility for Fourier Analysis are required. A time domain reflectometer with good spectral density at frequencies to 3 Ghz is also necessary. Because these facilities were not available, the cavity perturbation technique was chosen. This method adequately fulfils above criteria.

Of the many perturbation techniques available, three in particular were examined. The first of these was developed by Rueggenberg (36); the samples under study need not necessarily be small as usually demanded by perturbation theory. Furthermore, samples of arbitrary shape can be measured, although calibration samples of identical shape and known dielectric properties are required. This method is potentially useful for measurements of whole organs. The second method is due to Rzepecka (37); its chief advantage is that the cavity employed is a section of waveguide, with attendant ease of fabrication. Special arrangements for temperature control in this method are also a desirable feature, but measurements on high-loss materials do require very small samples. The third method examined, and the one finally chosen, was that of Risman and Bengtsson (38), described below.

(2.2) Advantages of the Method Used

The principal advantages of the cavity perturbation method developed by Risman are enumerated below:

(1) The cavity employed is reasonably small and can easily be placed inside a temperature controlled environment, permitting control of sample temperature. Coaxial cable feed to the cavity helps in this respect.

(2) The samples themselves are contained in glass or

teflon tubes which hold about 2ml of liquid. Coring techniques could easily be used for solid samples, as described by Bengtsson (39). The use of teflon tubes is necessary when freezing water, in order to prevent tube breakage.

(3) Careful cavity design minimises the existence of spurious resonances, which reduces the possibility of making incorrect measurements.

(4) The measurements themselves are based on a series of easily obtained calibration liquids, thus ensuring <±5% accuracy throughout the range of ϵ' and ϵ''.

(5) In addition to the cavity, only a variable frequency source, some means of frequency measurement (good to about 1Mhz at 2450 Mhz) and some means of measuring cavity attenuation are required. Absolute frequency measurements are not necessary since it is the frequency shift which is important, and so, few requirements are placed on the frequency measuring equipment. In this particular case, use was made of the sweep-reference output of the source. This output provides a voltage which is proportional to frequency, and it proved possible to use it, rather than a more direct method of frequency measurement.

(6) Actual measurements are very easy to make, consisting of an adjustment for resonance followed by a frequency and attenuation measurement.

(7) Simple graphical techniques could be used to obtain

the values of ϵ' and ϵ'' from the measurements of frequency shift and attenuation, though these would be tedious for the many measurements contemplated. However, computer techniques were used here.

(8) A cavity designed and built in Sweden by Risman and his associates was available. This reduced local manufacture of a cavity to a simple copying process.

(2.3) Theoretical Description of the Method.

The cavity chosen was cylindrical of diameter 96 mm and height 178 mm, and was operated in the TM012 mode. Samples of up to 5mm in diameter were allowed. The diameter to height ratio was chosen to avoid other resonances. For the same reason, vertical slots were made in the cavity walls and the cavity was divided into three sections, each section being electrically insulated from the others. Insulating discs and a teflon cone axially supported the sample within the cavity. The cone automatically centred the sample within the cavity. The inner surfaces of the cavity were gold-plated. A removable top facilitated sample insertion. The physical arrangement of the cavity is shown in figure 2.1. Figure 2.2 shows the field configuration within the cavity. The E-field is parallel to the sample and vanishes at its ends. Because the tangential component of the E-field is continuous at the boundary between the air and the sample,

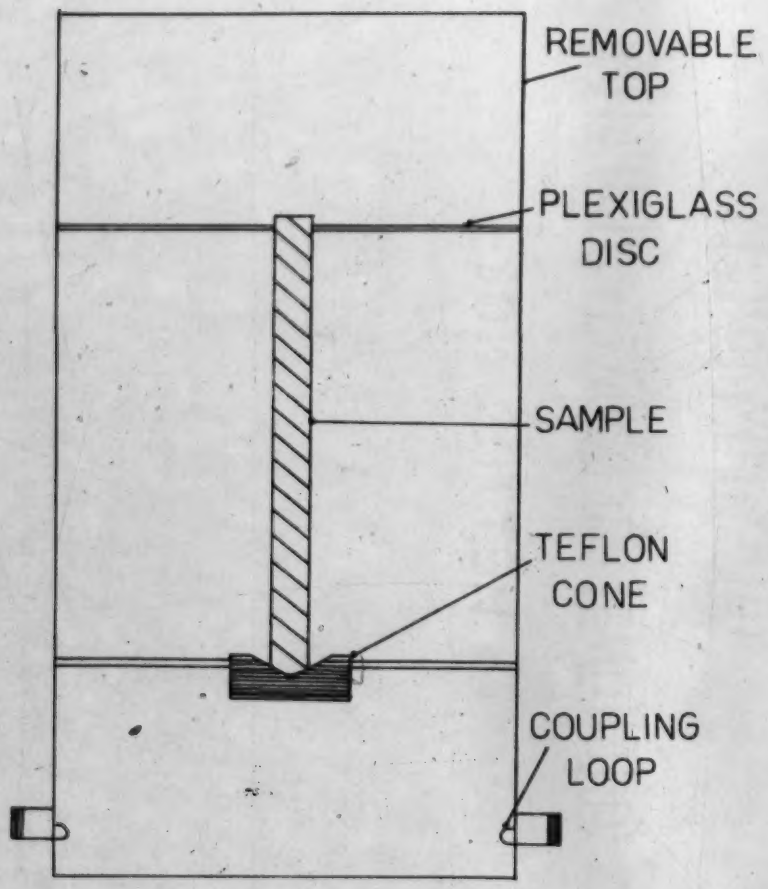

FIGURE 2.1 CAVITY ARRANGEMENT

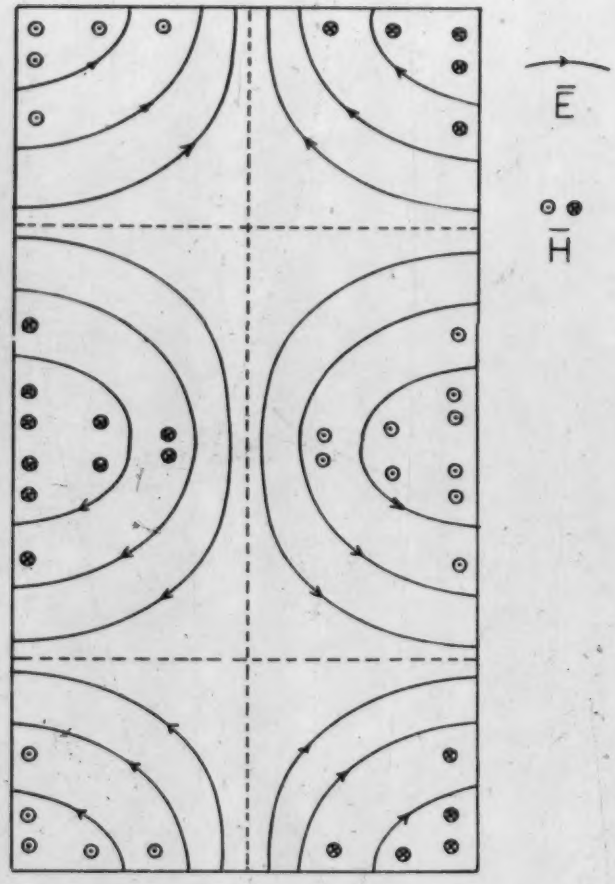

FIGURE 2.2 FIELD CONFIGURATION

there is good field penetration into the sample.

The coupling loops are arranged as shown in figure 2.1. Investigations have indicated that coupling varies with ϵ' in the most favourable way, since cavity transmission increases with ϵ' for fixed ϵ'' of the sample. This gives good resolution for a wide range of ϵ' because ϵ'' is often low when ϵ' is low. Cavity perturbation methods are, in practice, not absolute methods, and so calibration procedures must generally be used. Using a number of well defined reference substances, Risman (38) established the following relationships between ϵ', ϵ'', the frequency shift and the attenuation.

$$\epsilon' - 1 = F_1\{\Delta f\} \quad \ldots\ldots (2.1)$$

$$\epsilon'' = \Delta T^{-0.50} \cdot F_2\{\epsilon' - 1\} \quad \ldots\ldots (2.2)$$

where F_1 and F_2 are functions of the indicated variables.

According to first order perturbation theory, F_1 is a constant and the factor $(\Delta T)^{-0.50}$ can be derived assuming weak coupling and Q(unloaded) >> Q(loaded). Typical curves obtained using these assumptions are shown in figures 2.3 and 2.2. Details regarding the liquids used in the calibration procedure are covered in Chapter 3.

The accuracy of the method is hard to estimate, but

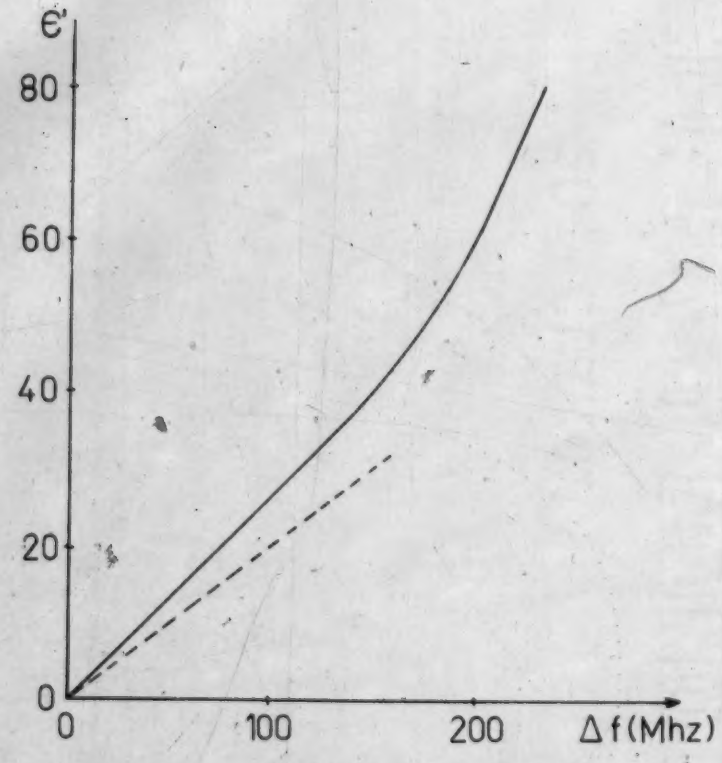

FIGURE 2.3 $\epsilon' = F_1(\Delta f)$ FOR THE TM012 CAVITY WITH 5mm DIA. SAMPLE

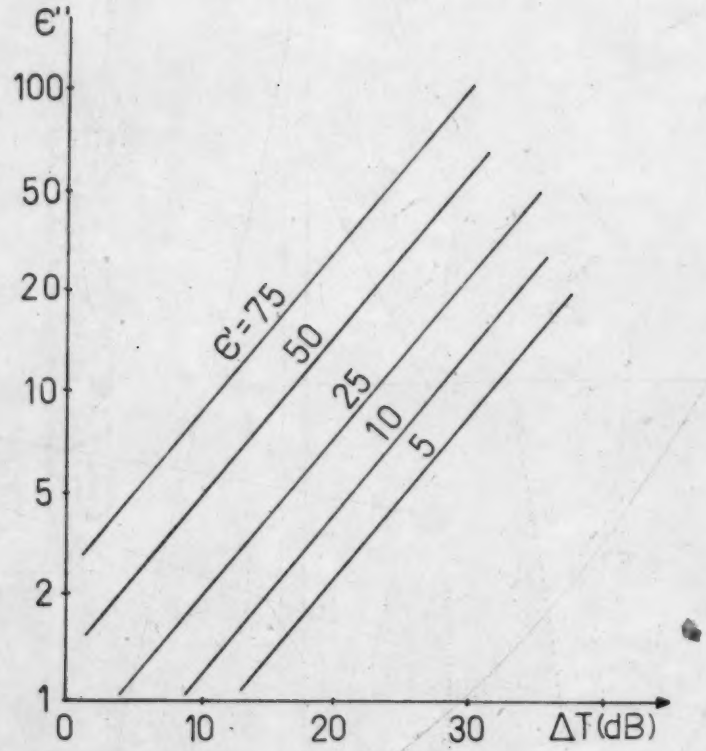

FIGURE 2.4 $\epsilon'' = F_2(\epsilon').(\Delta T)^{-0.50}$ FOR THE TM012 CAVITY WITH 5mm DIA. SAMPLE

measurements on water over a wide temperature range correlates better than ±5% with von Hippel's data (40) when corrected for frequency (see figures 4.1 and 4.2 in Chapter 4). For other liquids, especially those with the higher values of ϵ' and ϵ'', inaccuracy is about ±10%, becoming about ±20% at points far removed from calibration points. The precision or reproducibility of the method is good, the spread being on the order of 1-2% for liquids at the same temperature.

Chapter 3. Dielectric Measurement Technique

(3.1) Description of Apparatus.

Figure 3.1 is a block diagram of the measuring equipment. The cavity is the one discussed in Chapter 2.

A signal at the resonant frequency of the cavity containing the sample (2500-3000 Mhz) is fed through the isolator and cavity and detected on a power meter. The use of a power meter is preferred over the use of a crystal detector because linearity is easier to achieve over the wide dynamic range required. A voltage proportional to frequency is fed from the signal generator to a potentiometer circuit as shown in figure 3.1. When the voltage derived from the reference voltage and the 10-turn pot is equal to that derived from the signal generator, the reading on the meter is reduced to zero. At any other point, the meter reads full scale. Tests using a frequency counter confirmed that this circuit is consistently capable of giving frequency shift readings to an accuracy of better than 1 Mhz, which is more than adequate for the dielectric measurements. Figure 3.2 is a plot of the reading on the 10-turn pot vs. the output frequency of the generator as measured on a frequency counter. Because the source is a voltage-tuned backward wave oscillator, any fluctuations in the sweep reference voltage will also appear as changes in

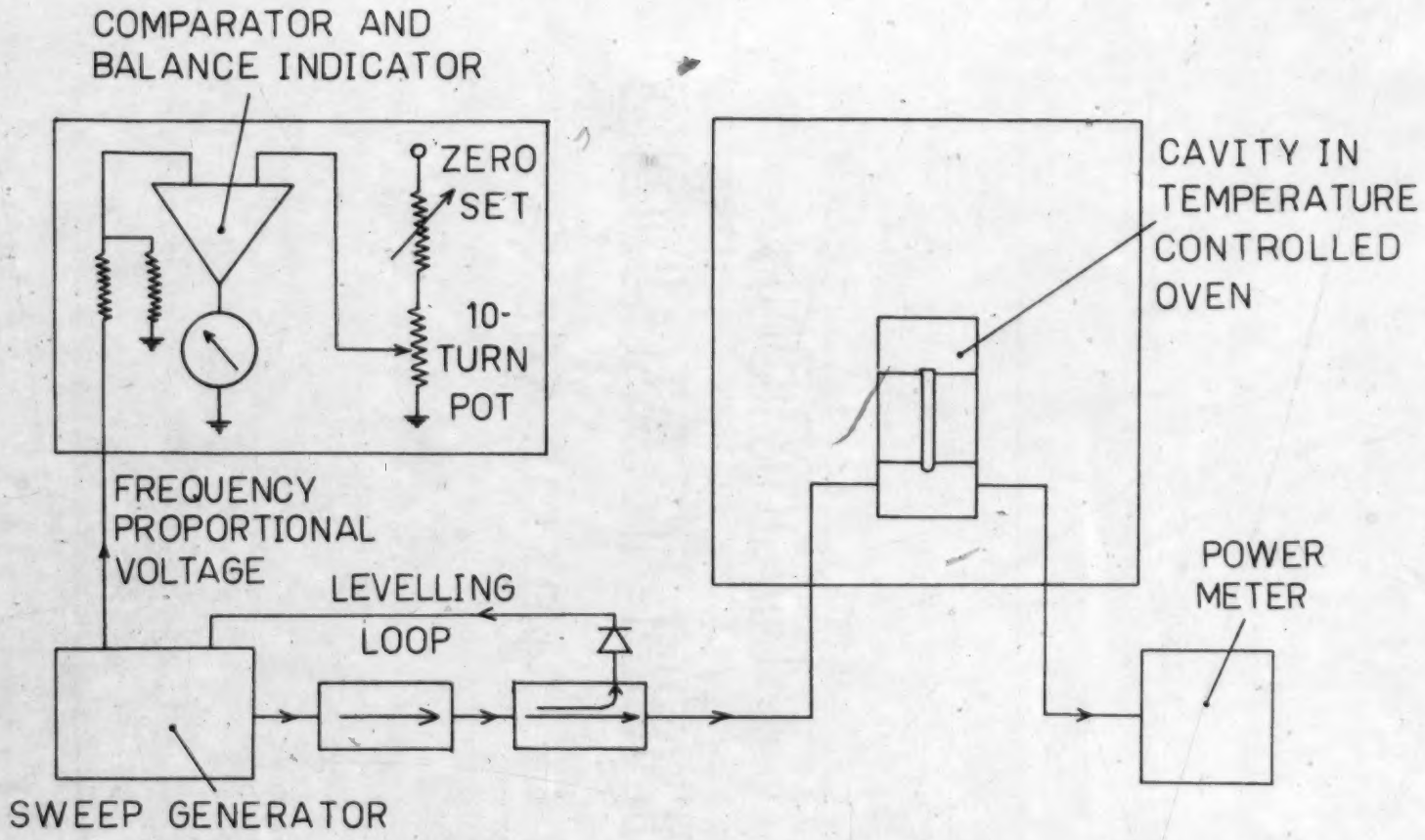

FIGURE 3.1 BLOCK DIAGRAM OF EQUIPMENT FOR WIDE TEMPERATURE RANGE MEASUREMENTS OF DIELCTRIC CONSTANT

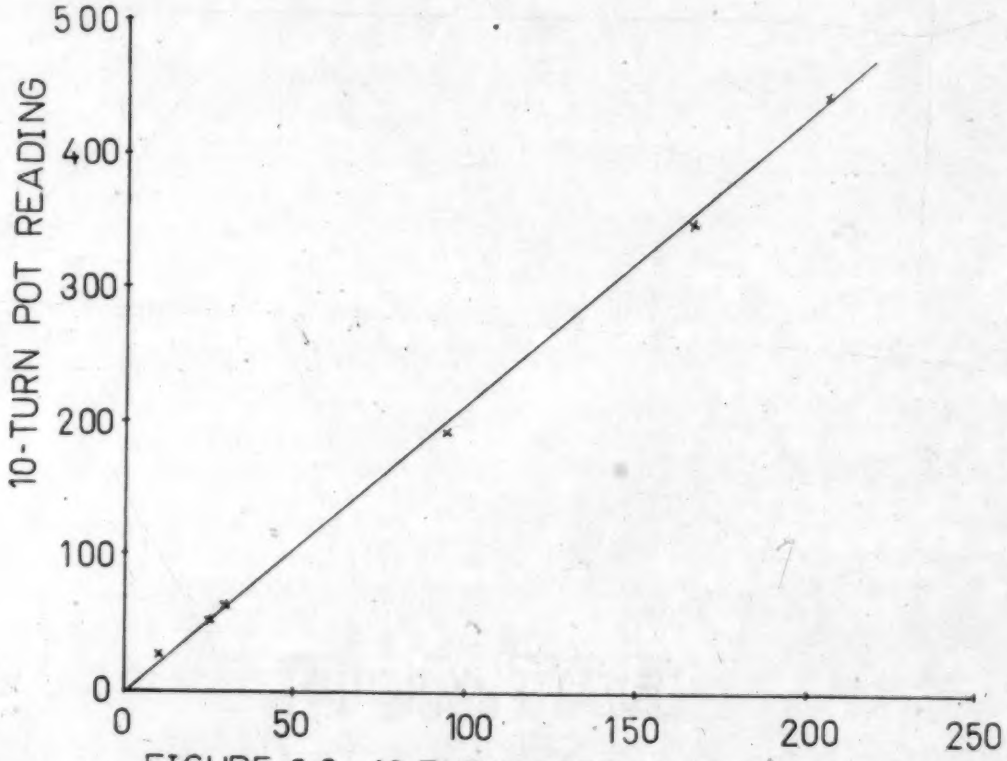

FIGURE 3.2 10-TURN POT READING VS. FREQ. SHIFT IN MHZ.

DATE:	MATERIAL:	APPARATUS:
EXPERIMENTAL NOTES		

TIME MINS.	TEMP. °C	CORRECTION	FREQUENCY SHIFT (REL. UNITS)	ATTENUATION (DB)	ϵ'	ϵ''

TABLE 3.1 DATA RECORDING FORM

frequency. Therefore, long-term fluctuations in measurements of frequency shift by use of the sweep reference voltage are expected to be small, and this is indeed the case.

The cavity and its coaxial air-line feed cables are contained in a Delta-Design temperature controlled oven. Air line is used here because of its ability to withstand wide variations in temperature. All R.F. interconnections are kept as short as possible to reduce losses to a minimum. The operating temperature of the oven can be controlled to within ±1°C over the temperature range -80° to +500°C. Liquid carbon dioxide is used to achieve those temperatures where cooling is necessary. Heating is by means of an electric element.

(3.2) Temperature Measurement and Control.

Sample temperature is determined by a temperature-controlled oven. However, because the sample is contained within a brass cavity with rather restricted airflow, it is found that up to an hour is required for the sample temperature to reach the temperature of the oven, a time which was unacceptably long considering the number of measurements that were to be made. Also, the long temperature equilibration time would require large quantities of expensive coolant for temperatures below room temperature, and would result in excessive evaporation at

the higher temperatures. In addition, measurements in the vicinity of the freezing point of a mixture of liquids are difficult because, in spite of constant temperature, the dielectric constant changes slowly. This phenomenon is thought to be due to ice-crystal formation causing changes in the proportions of frozen and liquid materials.

Because of the above problems, a dynamic method is required whereby constant cooling or heating are maintained while making measurements of dielectric constant at appropriate temperatures. Unfortunately it is impossible to make simultaneous temperature and dielectric measurements because of the perturbing effect of the temperature measuring device. It is therefore necessary to use the following steps to obtain the required data: (a) A cooling and heating procedure which gives the desired range of temperatures is established. (b) Using this procedure, measurements of temperature vs. time are made. (c) Using an identical procedure, measurements of dielectric constant vs. time are made. (d) Removing time from the two sets of measurements, curves of dielectric constant vs. temperature are plotted.

Although three replications of temperature vs. time measurements, and six replications of dielectric constant vs. time measurements are performed, for each sample, only about half the time is required for this technique as

compared to the point-by-point method. The repeatability of the temperature vs. time measurements indicates that the heating and cooling rates for given oven settings are within ±3%, thus justifying this temperature measurement procedure.

Separate temperature vs. time curves for each sample are necessary because the specific heat, latent heat and freezing point of different samples varies considerably. This is only so in the range -60° to +23°C. Tests revealed that for the higher temperatures, differences are less than ±5% and only one set of temperature vs. time curves are used for all samples.

Temperature measurements are performed by passing a thermocouple through one of the slots in the cavity and immersing it halfway into the sample. For measurements below room temperature, the oven is set at -80°C and temperature readings are taken every minute for 11 minutes as the sample cools down from room temperature. After 11 minutes, the oven is reset to +40°C and readings are again taken every minute for a further 23 minutes. These times are chosen to give a minimum sample temperature of about -60°C and a maximum of about +30°C. Equilibration at the low temperature is not attempted in order to conserve coolant. For measurements above room temperature, readings are taken every minute for 16 minutes with an oven setting of +200°C.

Identical procedures are adopted during the dielectric measurements, with thermocouple removed from the sample. Cross-correlation of the temperature and dielectric data is achieved by the use of forms of the type shown in table 3.1. Except for the region around the freezing point, where different degrees of super-cooling sometimes occurred, overall temperature measurement accuracy is ±5%.

Substance	Temp. °C	ϵ'	ϵ''
(1) distilled water	20	78.0	11.0
(2) 40% water, 60% methanol	20	46.0	17.0
(3) methanol	20	22.0	13.0
(4) 10% acetone, 20% methanol 70% benzene	20	7.3	1.6
(5) 6% methanol, 94% benzene	23	2.98	0.18
(6) monochlorobenzene	23	5.54	0.67
(7) ethyl acetate	23	6.4	0.34

TABLE 3.2 The Calibration Liquids

(3.3) Calibration Procedure.

In order to calibrate the cavity, a number of standard solutions were made (38). These solutions and their

dielectric properties are detailed in table 3.1.

Using these values and the measured values of attenuation and frequency shift, as read on the power meter and the 10-turn potentiometer, a set of calculation graphs are constructed (38). Figure 3.3 shows ϵ' vs. frequency shift, and is constructed by simply plotting the appropriate values. Figure 3.4 and 3.5 are constructed in conjunction with one another. Measured values of attenuation are first plotted on figure 3.5 along with their corresponding values of ϵ''. A reference line of slope $m=(\log 100-\log 10)/(30-10)=0.05$ (all logs are to the base 10) (see equation 2.2) is drawn for each plotted point in figure 3.5, and its equivalent value at an attenuation of 25 dB (i.e. $\epsilon''(25)$) is found. This value is transferred to figure 3.4 where it is plotted against $\log(\epsilon'-1)$. Using the values of $\epsilon''(25)$ for any desired ϵ', the other sloping lines of figure 3.5 can now be drawn parallel to the reference line. Graphical determination of ϵ' and ϵ'' from measured values of frequency shift and attenuation then comprises the following steps:

(1) Using the frequency shift, enter figure 3.3 and obtain ϵ'.
(2) With this value of ϵ', the corresponding $\epsilon''(25)$ is found from figure 3.4.
(3) Using $\epsilon''(25)$ and the measured attenuation, ϵ'' is then found using figure 3.3.

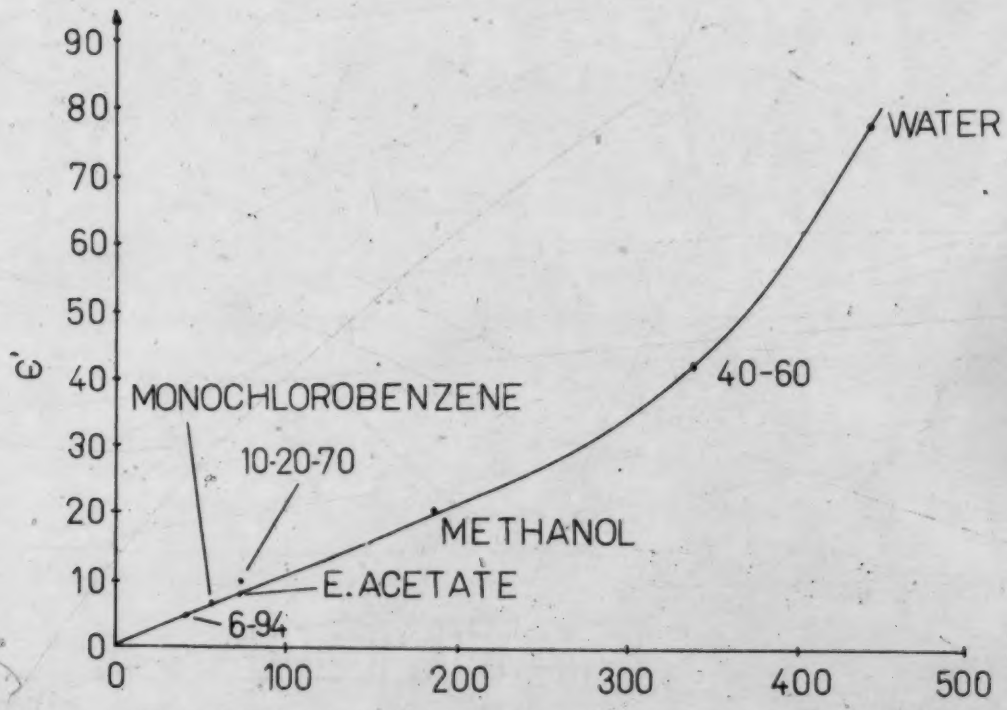

FIGURE 3.3 ε' VS. FREQUENCY SHIFT (10-TURN POT)

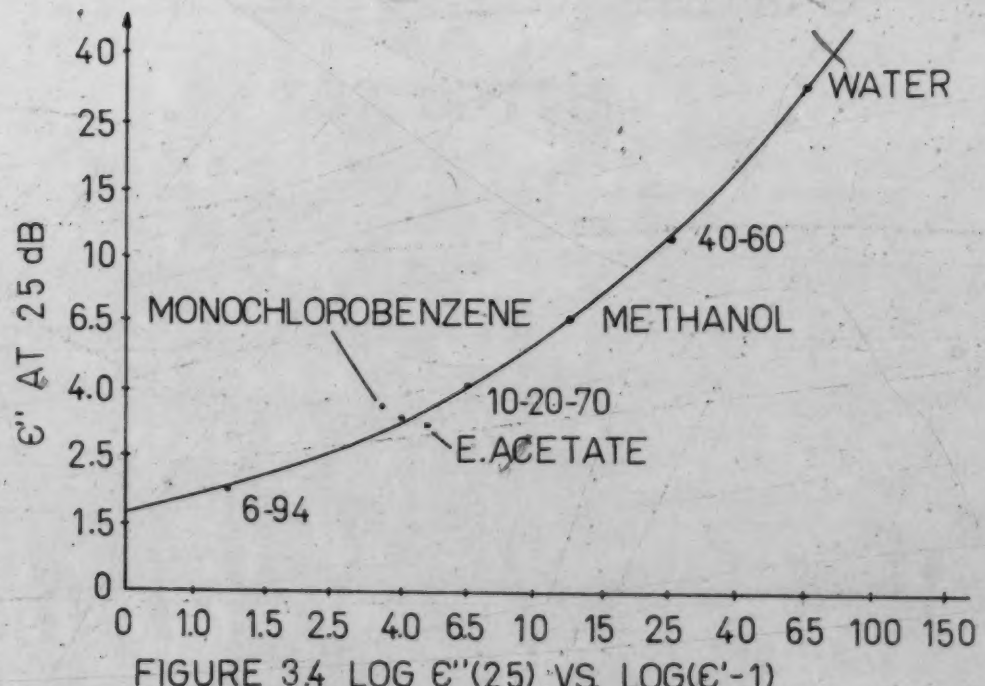

FIGURE 3.4 LOG ε''(25) VS. LOG(ε'-1)

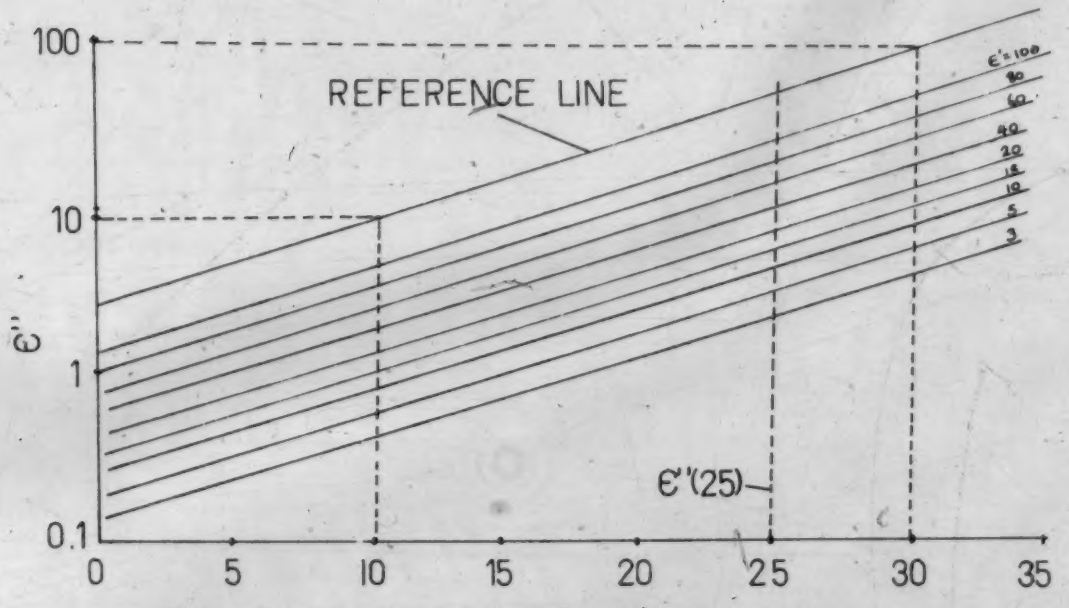

FIGURE 3.5 ε'' VS. ATTENUATION (dB)

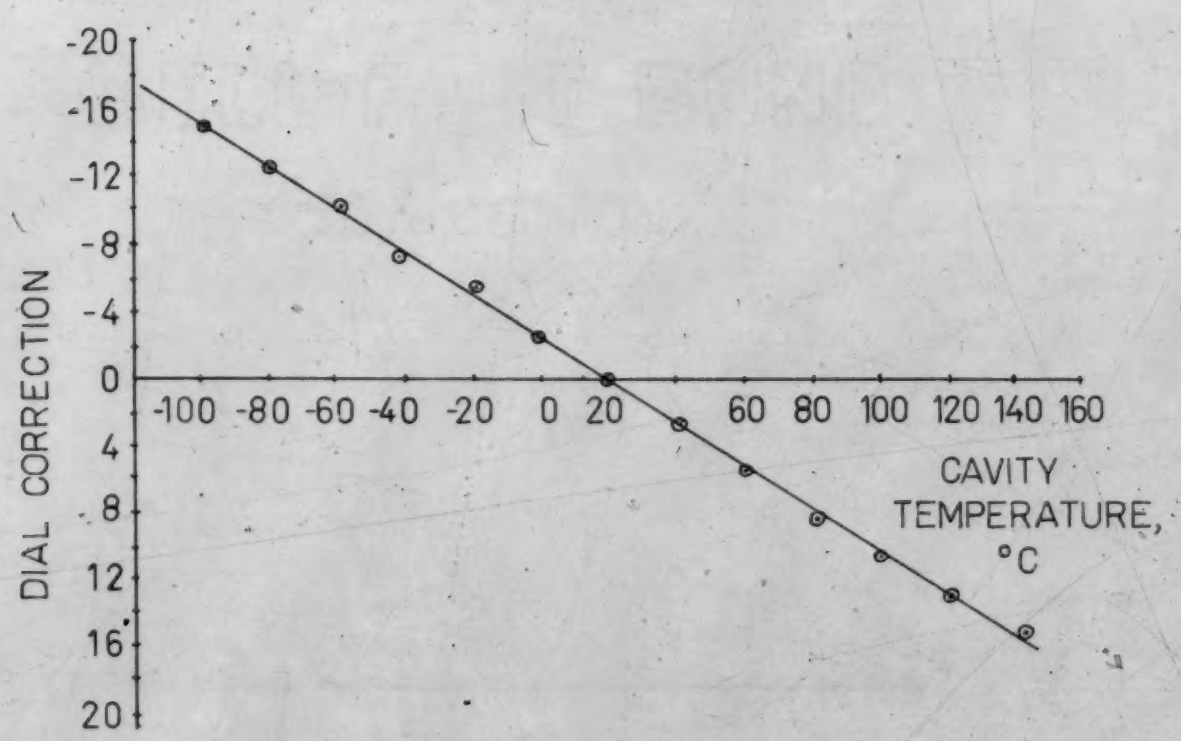

FIGURE 3.6 DIAL CORRECTION VS. TEMPERATURE

This procedure is very tedious in view of the fact that these operations have to be repeated three times for each point to be plotted in order to give values for the mean and standard deviation. To facilitate the calculations for the many points required, computer programs to perform the above operations were therefore written. These are described in detail in section 3.9.

(3.4) Corrections for cavity expansion and contraction.

The resonant frequency of a cavity is primarily dependent on its dimensions, and, being made of metal, the cavity dimensions are subject to variation with changes of temperature. In a situation where the parameter being measured is frequency shift, the temperature at which the loaded and unloaded resonant frequency is measured is not important, provided it is the same in both cases. However, in the present application, situations arise where the unloaded measurements are made at room temperature, while the loaded measurements are made at temperatures in the range -60°C to +100°C. To compensate for the resulting dimensional changes, appropriate corrections as shown in figure 3.6 are applied. This curve is obtained by measuring unloaded frequency as read on the ten-turn pot while subjecting the cavity to the heating and cooling procedure of section 3.2. Because sample and cavity temperature differ, cooling or heating time is again used as the common

element to correlate correction values with measurements. Though sample temperatures at these times are different for different solutions, the effect of the samples on cavity temperature is negligible, and the same correction curve applies to all measurements.

(3.5) Measurement Procedure.

There are three different experimental procedures. These are:

(1) Varying temperature measurements from room temperature to -60°C.
(2) Varying temperature measurements from room temperature to +100°C.
(3) Varying concentration measurements at several fixed temperatures.

The experimental procedure for each type is slightly different, and will be described below.

(3.6) Varying temperature measurements (-60°C to +20°C).

For each different solution, three temperature calibration runs are performed in the manner described in section 3.2. Teflon sample tubes are used for distilled

water and 1% DMSO, and quartz glass tubes are used in all other cases. Each run uses a different, newly mixed, sample. The mean temperatures obtained are entered in the appropriate column of a table like that shown in table 3.1. Appropriate correction values for frequency shift are also entered in the table. With the thermocouple removed from the cavity, and with an empty sample tube in place, the signal source is adjusted for maximum transmission through the cavity. The signal level is then adjusted to give a convenient reading on the power meter (usually +10dBm), and the zero set control on the frequency deviation meter is adjusted for balance with the 10-turn pot set to zero. With a newly mixed sample in place, the 11 minute cooling and 26 minute heating cycle is started. At one-minute intervals, the signal source frequency is adjusted for maximum transmission and the values of frequency shift and attenuation are recorded on the table. To ensure readings exactly on the minute, frequency adjustment is started shortly before the minute, with the reading being taken at the appropriate moment. Because rates of change are slow, the error attributable to this source is negligible. The procedure is repeated for 6 different newly-mixed samples. The samples are newly mixed to reduce the possibility of evaporation, which would cause an increase in the DMSO concentration, the latter being less volatile than water. Sets of 6 measurements are chosen as a compromise between obtaining reasonable values of standard deviation and

available time.

(3.7) Varying temperature measurements (+20°C to +100°C).

The measurements above room temperature are performed in the same way as in section 3.6, except that only one set of temperature vs. time measurements are made. Differences between the behaviour of different liquids is negligible as confirmed by temperature measurements on different samples. At these higher temperatures, some evaporation occurs, but in the relatively short measurement time involved, the expansion of the liquid, which in any case rules out the possibility of a cover, is more important. The overflow of the expanded liquid collected in the conical tube support, and it was thought that this might lead to inaccurate results. However, tests revealed that this is not the case, probably because the electric field at the ends of the tubes is very small. Similarly, removal of small amounts of liquid from the tubes did not affect the measured dielectric constant. The density change caused by liquid expansion always occurs for heated liquids so does not affect the results.

(3.8) Varying concentration measurements.

Varying concentration measurements at room temperature

(23°C) only require obtaining balance with the ten-turn pot with and without a sample. In the case of the 5°C and 50°C measurements, however, a set of 11 tubes containing solutions of 0-100% in 10% steps are placed in the oven along with the cavity. After an equilibration time of about 1 hour at the desired temperature, the equipment is balanced in the usual manner, the oven opened, and the empty tube substituted for one of the 11 samples. After a further 10 to 15 minutes equilibration time, the appropriate measurements are made, and then the process is repeated for the second sample. After one measurement on each sample, the equipment is again balanced, and a second measurement made on each sample. At this point, a new set of samples is prepared, and the process repeated. In this way, six measurements are obtained at each percentage concentration. In the case of the 50°C measurements, the tubes are sealed with tape to reduce evaporation during the four hour period in the oven. To allow for expansion, the tubes were not completely filled at room temperature. There was no observed evaporation at 5°C.

(3.9) Data Reduction.

Computer programs were written in FORTRAN for data processing; these are listed in appendix A and only briefly described here. Three programs are used in the data reduction process. Two programs are for data analysis and

one is a plotting program which graphs the values of ϵ', ϵ'' and loss tangent vs. temperature. The plotting routine is a simple modification of a library program.

The two analytical programs are a calibration routine and a routine to convert the measured values of frequency shift and attenuation to values of ϵ' and ϵ''. Their function is described below.

(1) Calibration routine: This program is called CALCOEFF, its purpose being to calculate the regression coefficients for the curves of figures 3.3 and 3.4. In order to achieve this, the program takes the measured values of frequency shift and attenuation, six of each in this case, and calculates a mean, an upperbound and a lowerbound. Combining these values with the known calibration values of ϵ' and ϵ'' results in 3 sets of coefficients for the curves of ϵ' vs. frequency shift and another 3 sets for the curves of $\log(\epsilon'-1)$ vs. $\log\epsilon''$(25). The coefficients are obtained using a bicubic spline fit of the measured data. Figures 3.7 and 3.8 compare the measured data with the curves calculated from the spline fit for each of the two cases. These regression coefficients apply to the frequency shift data as obtained with the measuring system of figure 3.1. They can be used with any frequency measuring system by relating data from such a system to figure 3.2, although this would only apply to the particular cavity used here.

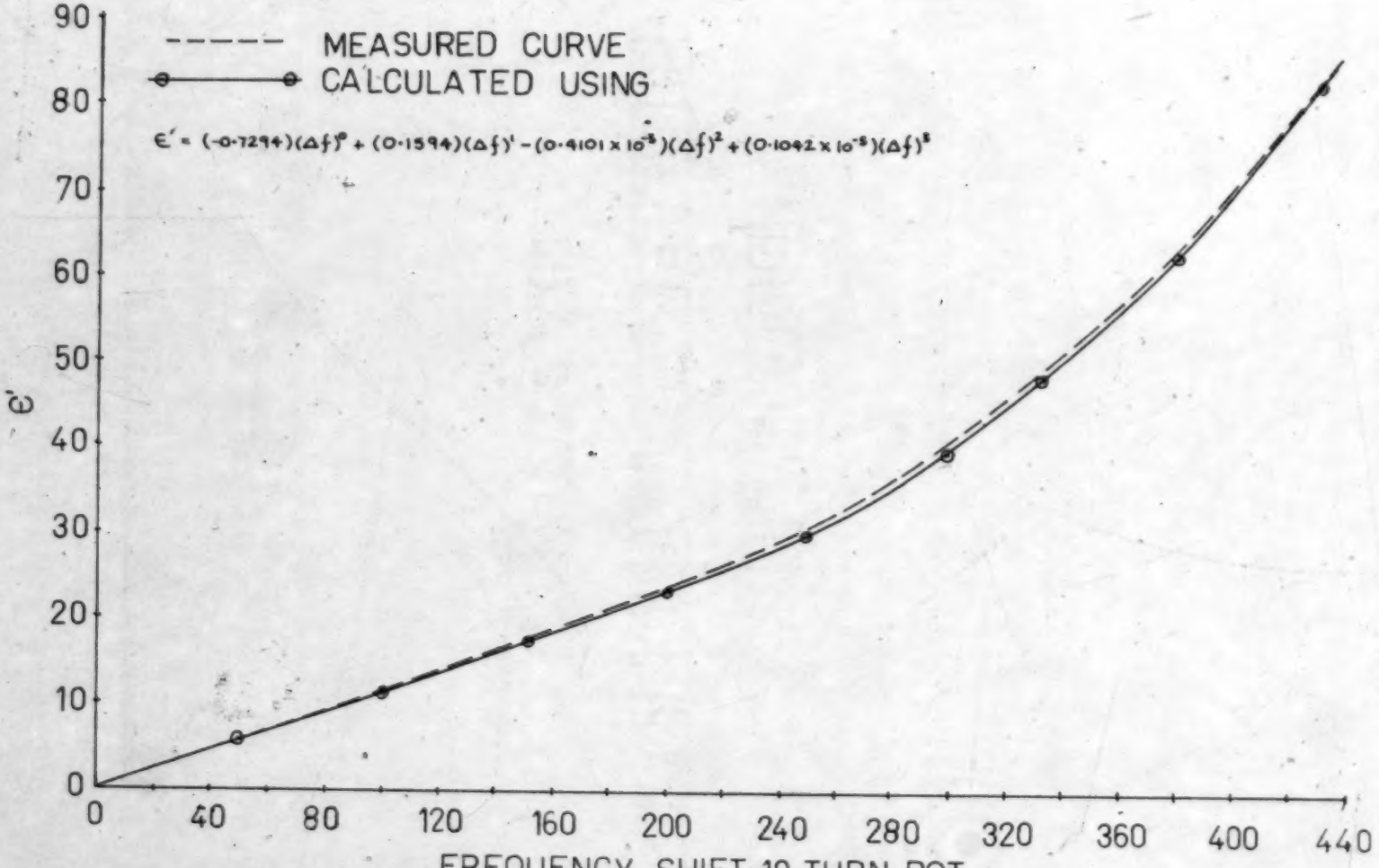

FIGURE 3.7 ϵ' VS. FREQ. SHIFT AS MEASURED AND CALCULATED

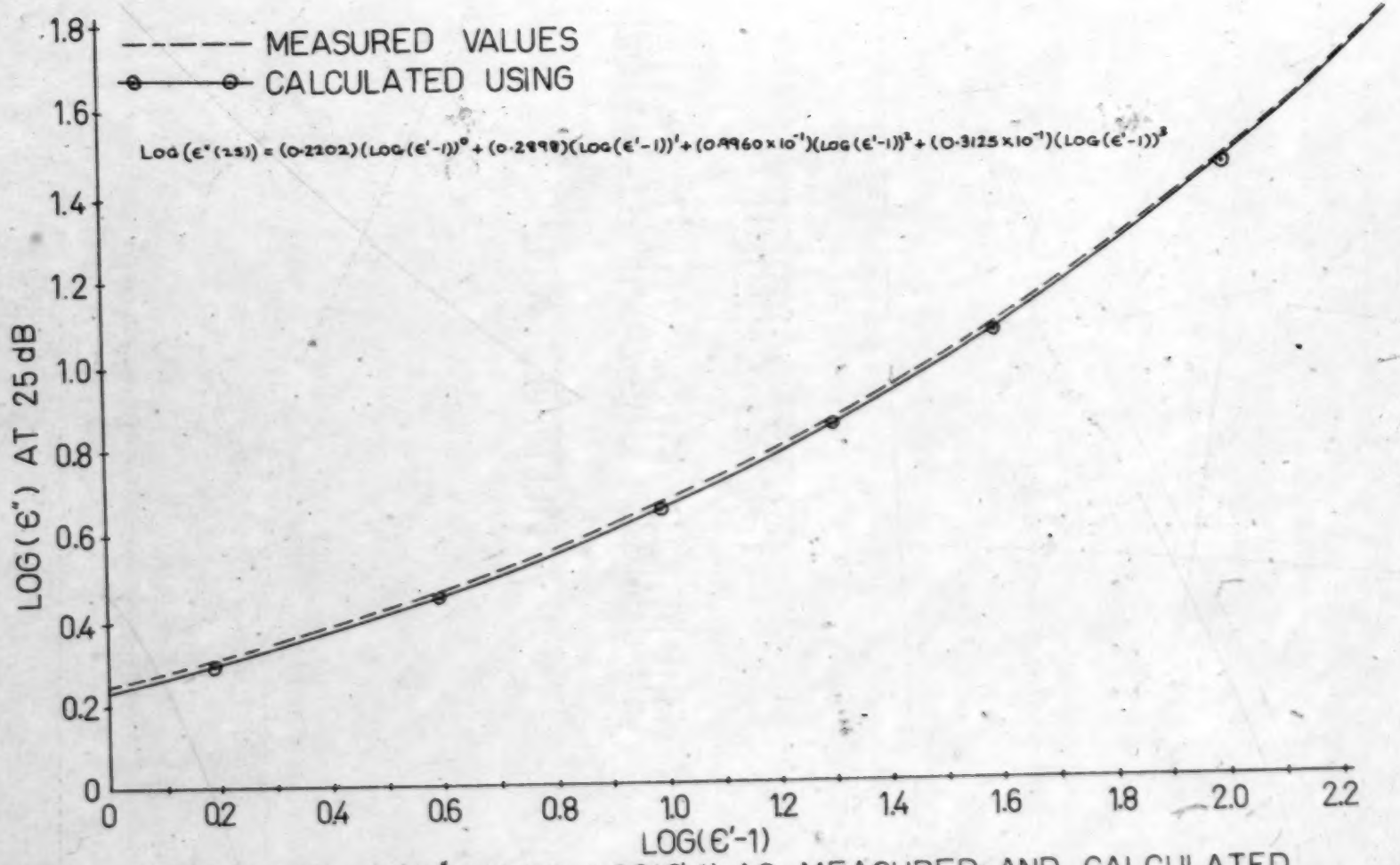

FIGURE 3.8 LOG(ε'(25)) VS. LOG(ε'-1) AS MEASURED AND CALCULATED

(2) Calculation of dielectric values: This program is called CALCULATE and its purpose is to obtain values of ϵ' and ϵ'' from measurements of frequency shift and attenuation on unknown liquids. Although the temperature and concentration at which the measurements are made does not enter directly into the calculations, these values are also carried by the program to enable the appropriate printouts to be made.

The program CALCULATE executes the following steps:

(a) Read the temperature or concentration with the corresponding frequency shift and attenuation. In this case, 6 values are read each time.

(b) Using these values and the three sets of regression coefficients for figure 3.7, three values of ϵ' are calculated at each value of temperature or concentration. These values represent the mean and upper and lower bounds of ϵ' for that point.

(c) Using the calculated values of ϵ', and the regression coefficients of figure 3.8, three values of ϵ'' are obtained. Again, these values represent the mean, upper and lower bounds.

(d) The mean, upper and lower bounds of ϵ'' are now calculated from:

$$\epsilon'' = \text{alog}(AT/20+\log\epsilon''(25)-1.25) \quad \ldots\ldots(3.1)$$

where AT is the attenuation. This equation is a mathematical representation of figure 3.3.

(e) For each temperature or concentration, print out the three values of ϵ' and the three values of ϵ''.

The program is written so that it will accommodate any specified number of different temperatures or concentrations, and any specified number (two or more) of repeated measurements. The accuracy of the algorithm was checked by obtaining values for selected points using the graphical technique, and comparing these values with the corresponding computed values. There was never more than 1-2% variation, which is easily attributable to the inaccuracies of the graphical technique and the spline fit.

Chapter 4. Results of the Dielectric Measurements.

(4.1) Presentation

In the course of the dielectric measurements, a considerable amount of data was obtained and a brief discussion concerning data presentation follows.

Curves of ϵ' and ϵ'' are presented for distilled water and for 1%, 5%, 10%, 20%, 70% and 100% DMSO. These comprise figures 4.1 to 4.14. All the curves in this group are drawn with the same axes to facilitate comparison. Parts of the curves for distilled water are shown dotted on those for each of the other solutions to further help comparisons of the behaviour of the different liquids.

In each case, the error bars represent one standard deviation as computed on the basis of 6 separately measured values. Some error bars have been omitted, particularly those in the vicinity of the freezing point. The reason for this is that the rapid changes encountered in this region cause small uncertainties in temperature to become large uncertainties in dielectric properties, resulting in large and confusing error bars. In addition, super-cooling effects result in erratic and unpredictable behaviour in the freezing zone.

A further problem encountered was that the curves for dielectric properties obtained during cooling differed somewhat from those obtained during heating. The reason for this is that, as the freezing point is approached from temperatures either above or below, reasonable homogeneity is maintained in the sample. However, after passing the freezing point, a mixture of solid and liquid is established because the liquid does not instantaneously freeze throughout, due to latent heat requirements. The dielectric properties of this mixture of phases are ill-defined and certainly different to those of the homogenous material. Therefore, to avoid confusion on the graphs, only points obtained during the approach to the change of phase are plotted (i.e. points above the freezing point during cooling, and points below the freezing point during heating). In some instances where super-cooling is involved, this policy necessitated interpolation between adjacent values in order to obtain a value right at the freezing point for the cooling curve. This point is then connected to the value for the same temperature as obtained during heating. Errors in the immediate vicinity of the phase change are of the order of ±50%, and caution must be exercised in interpreting the dielectric behaviour at this point. For the rest of the curves, the error is less than 10%.

The second group of curves shows the behaviour of the

dielectric properties of water and a 5% (w/w) solution of dextran. These comprise figures 4.15 and 4.14. The axes in this case are different to figures 4.1 to 4.14, hence the repeated curves for water as a standard of comparison. A maximum temperature of 40°C is used here because dextran is primarily used in applications at temperatures below this value. The comments made above with regard to the first group also apply.

The third group of curves comprise dielectric values for 10% DMSO and solutions of 10% DMSO with 0.1% NaCl, 1.0% NaCl and 5% dextran (w/w). These are figures 4.17 and 4.18. Again, the axes are different from those of the first group, and so 10% DMSO is repeated for comparison purposes. Previous comments with regard to maximum temperature also apply here.

The fourth and final group of curves, figures 4.19-4.21, comprises measurements made for different concentrations of DMSO at various fixed temperatures. In this instance, values of the loss-tangent are also plotted for reasons made clear in section 4.2. Loss-tangent values were not considered necessary in the first three groups.

(4.2) Comparison with Literature for Distilled Water.

In order to ascertain the accuracy of the measurement

technique, and also for purposes of comparison, dielectric measurements on distilled water in the temperature range from -60°C to +100°C were made. The results of these measurements along with those of von Hippel (40) are presented in figures 4.1 and 4.2. For both ϵ' and ϵ'', ±1% agreement is indicated except at high temperatures for ϵ' and in the immediate vicinity of the freezing point for ϵ'', where the deviation is approximately ±10%. This suggests that the technique employed in the present work provides results which are consistent with those in the literature. In this context, it should be pointed out that for very low loss materials such as ice from distilled water, the values of ϵ'' are not expected to be accurate unless the calibration curves are adjusted for the presence of the sample holding tube. The values presented in appendix D for ice are therefore not accurate, but represent the minimum resolution of the calibration curves as obtained in Chapter 3. The dielectric loss for ice is too small to appear in figure 4.2, and in the case of the other mixtures, losses in this region are higher, and an accuracy of better than ±10% is expected. In addition, very high loss materials (loss tangent>3) introduce considerable attenuation and this leads to measurement difficulties because the attenuation readings are close to the noise level, and accurate tuning for cavity resonance is difficult. This explains the larger error in the vicinity of the freezing point.

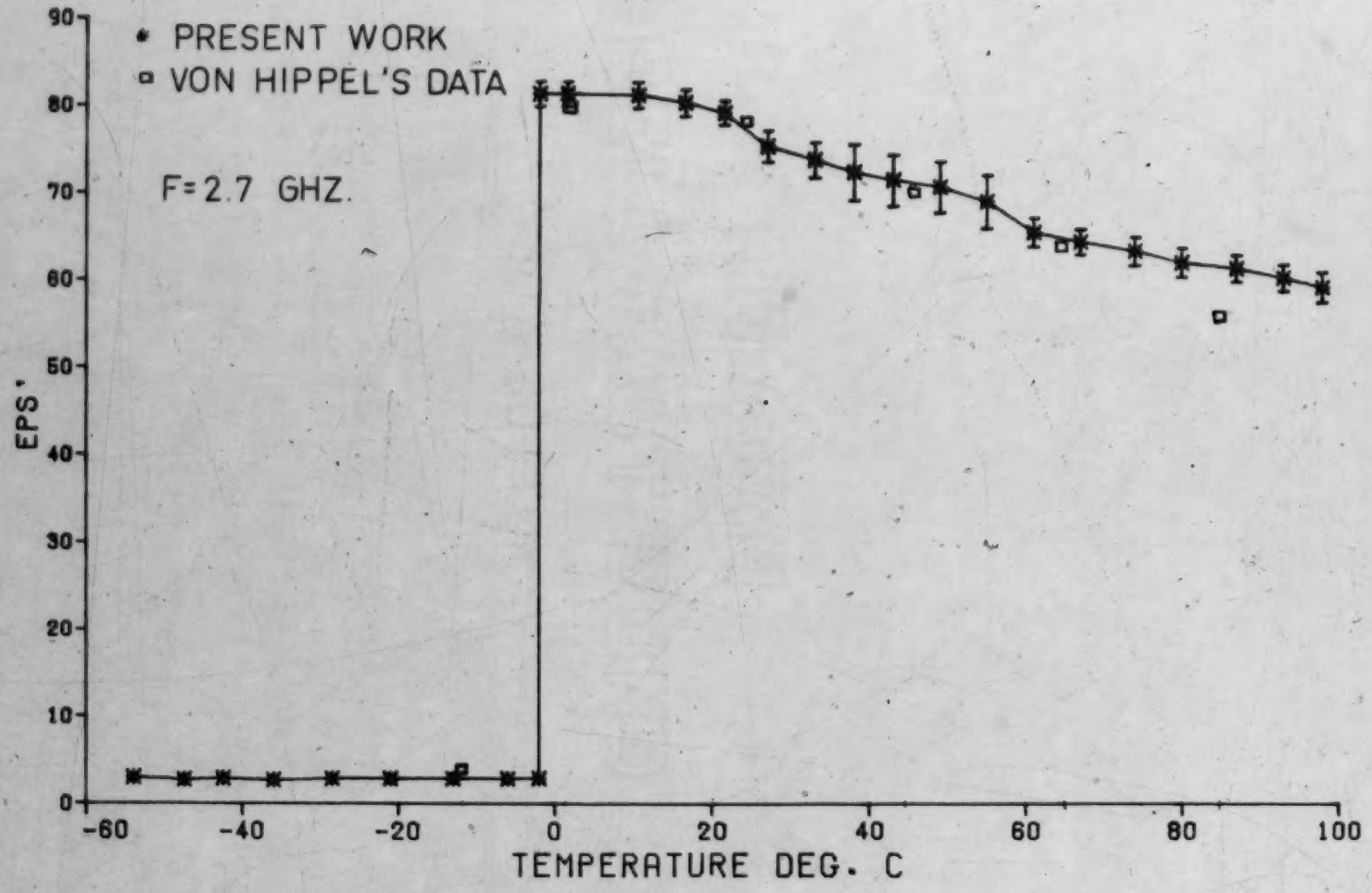

FIG.4.1 EPS' VS. TEMPERATURE FOR DISTILLED WATER

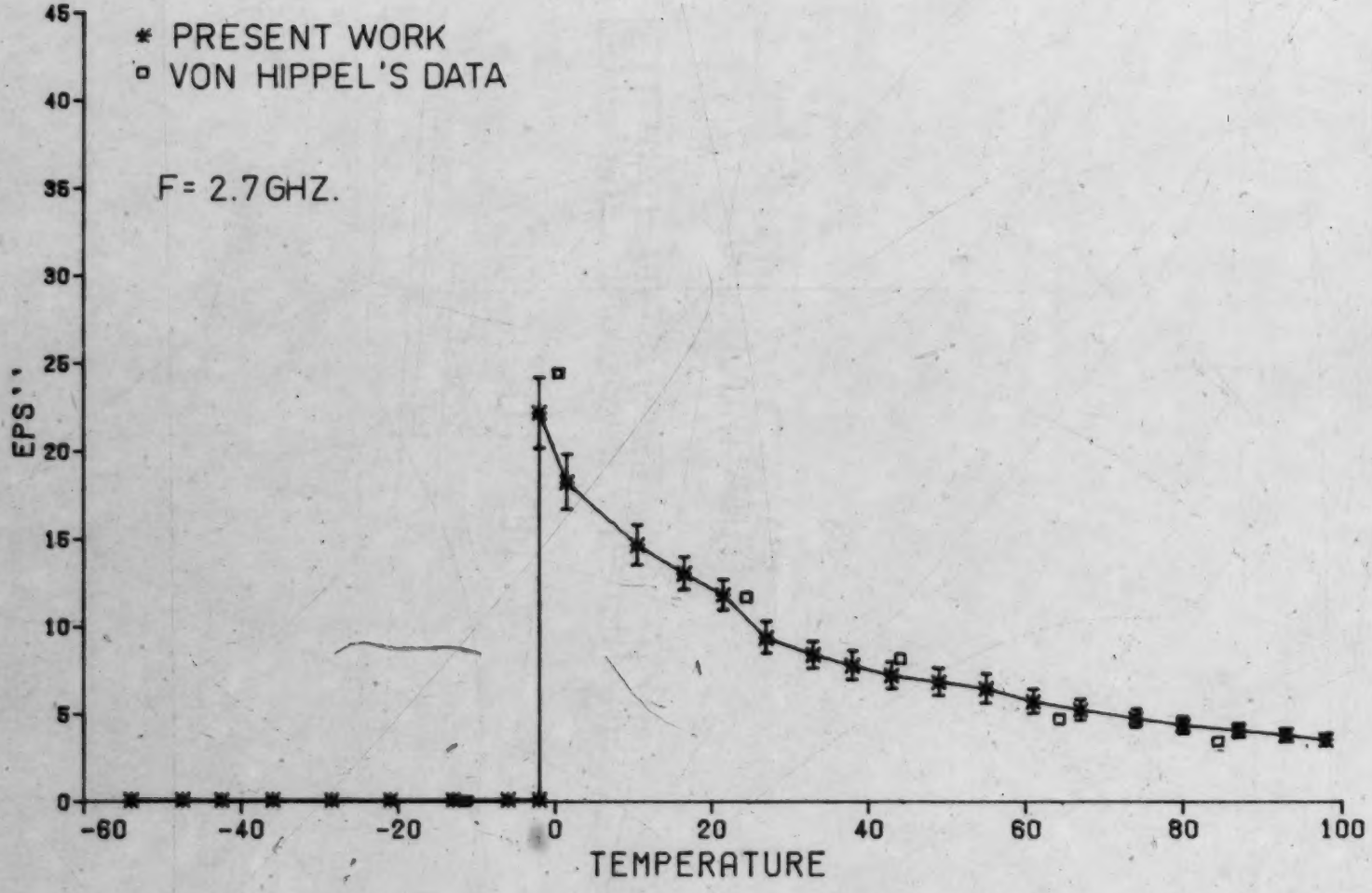

FIG.4.2 EPS'' VS. TEMPERATURE FOR DISTILLED WATER

(4.3) Measurements on Various Concentrations.

Moving now to the results obtained for the first group of measurements, it is seen that the behaviour above the freezing point of ϵ' for all solutions except those of 70% and 100% DMSO is very similar to that of water. The freezing point for any DMSO solution can be established by reference to the phase diagram of figure 4.22 (41). In the case of ϵ'', the behaviour is again similar but with generally higher losses for the DMSO solutions. For all solutions excepting 70% DMSO, the values of both ϵ' and ϵ'' decrease with increasing temperature above the freezing point. In the case of ϵ' for 70% and 100% DMSO, there is a considerable variation from the corresponding values for water, although the behaviour with temperature is similar. ϵ'' for 70% DMSO shows a broad peak around 23°C, a fact which will be discussed in more detail below. For the solutions on which measurements were made, the maximum loss occurred in the case of 20% DMSO at a temperature just above the freezing point. This can be explained by consideration of the fact that liquids have what might be considered an instantaneous structure (42) comprising, in the present case, hydrogen bonded molecules. The proportion of bonded molecules at any instant increases as the temperature is lowered towards the freezing point, and so the molecular forces impeding the dipole orientation dominate, and the dipoles become less able to follow the changes in applied electric field. Hence,

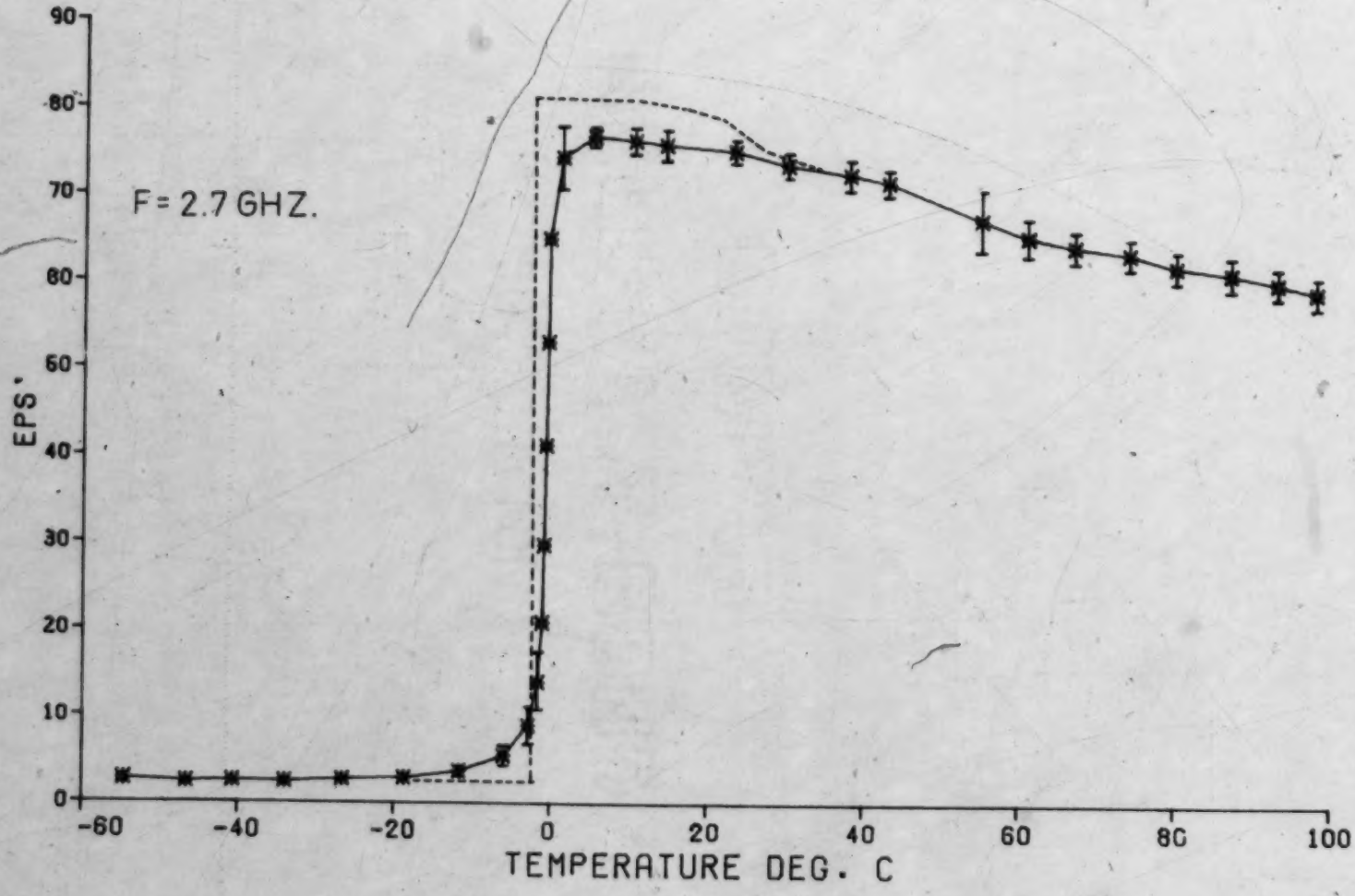

FIG.4.3 EPS' VS. TEMPERATURE FOR 1% DMSO IN WATER

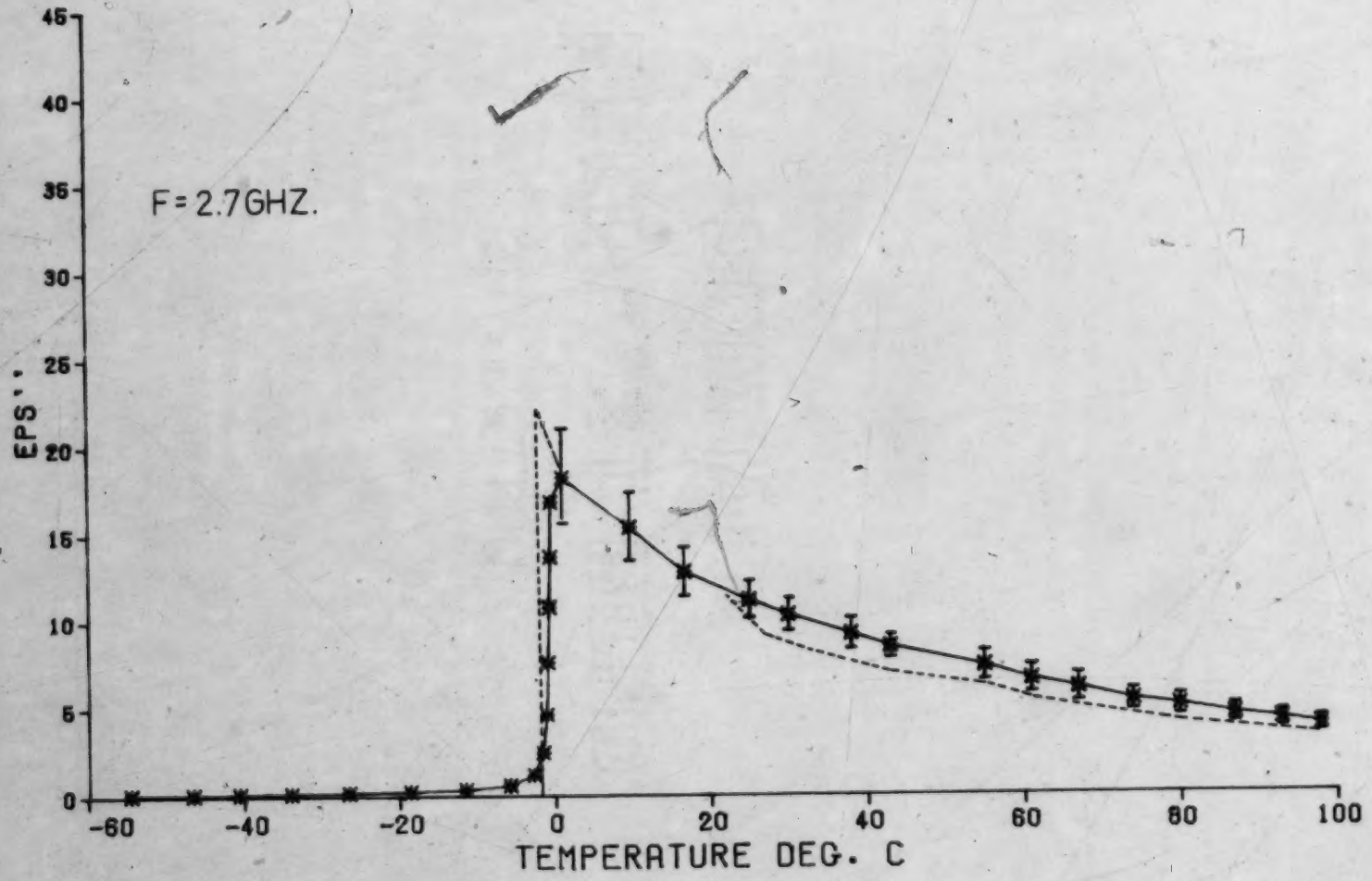

FIG.4.4 EPS'' VS. TEMPERATURE FOR 1% DMSO IN WATER

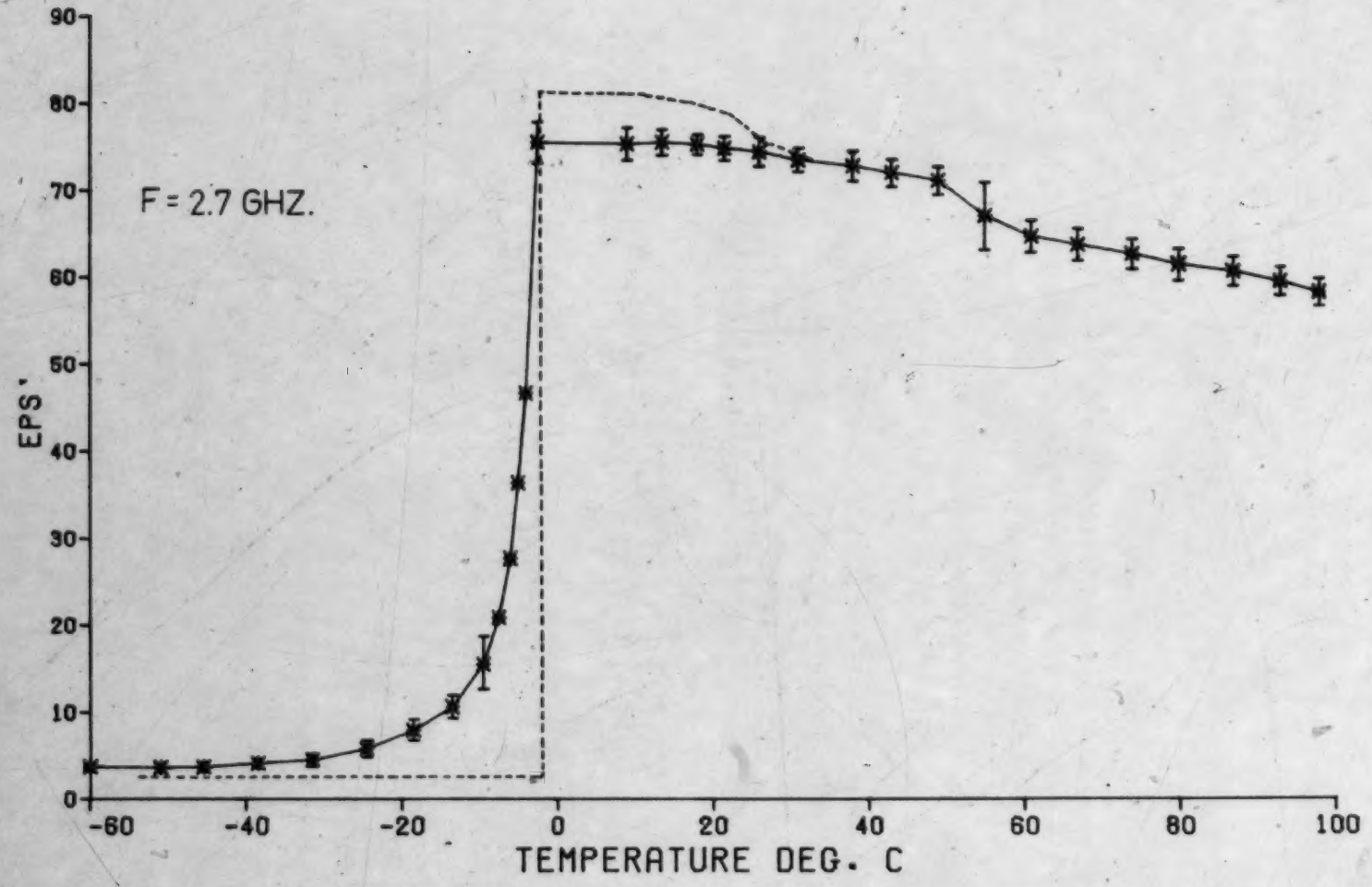

FIG.4.5 EPS' VS. TEMPERATURE FOR 5% DMSO IN WATER

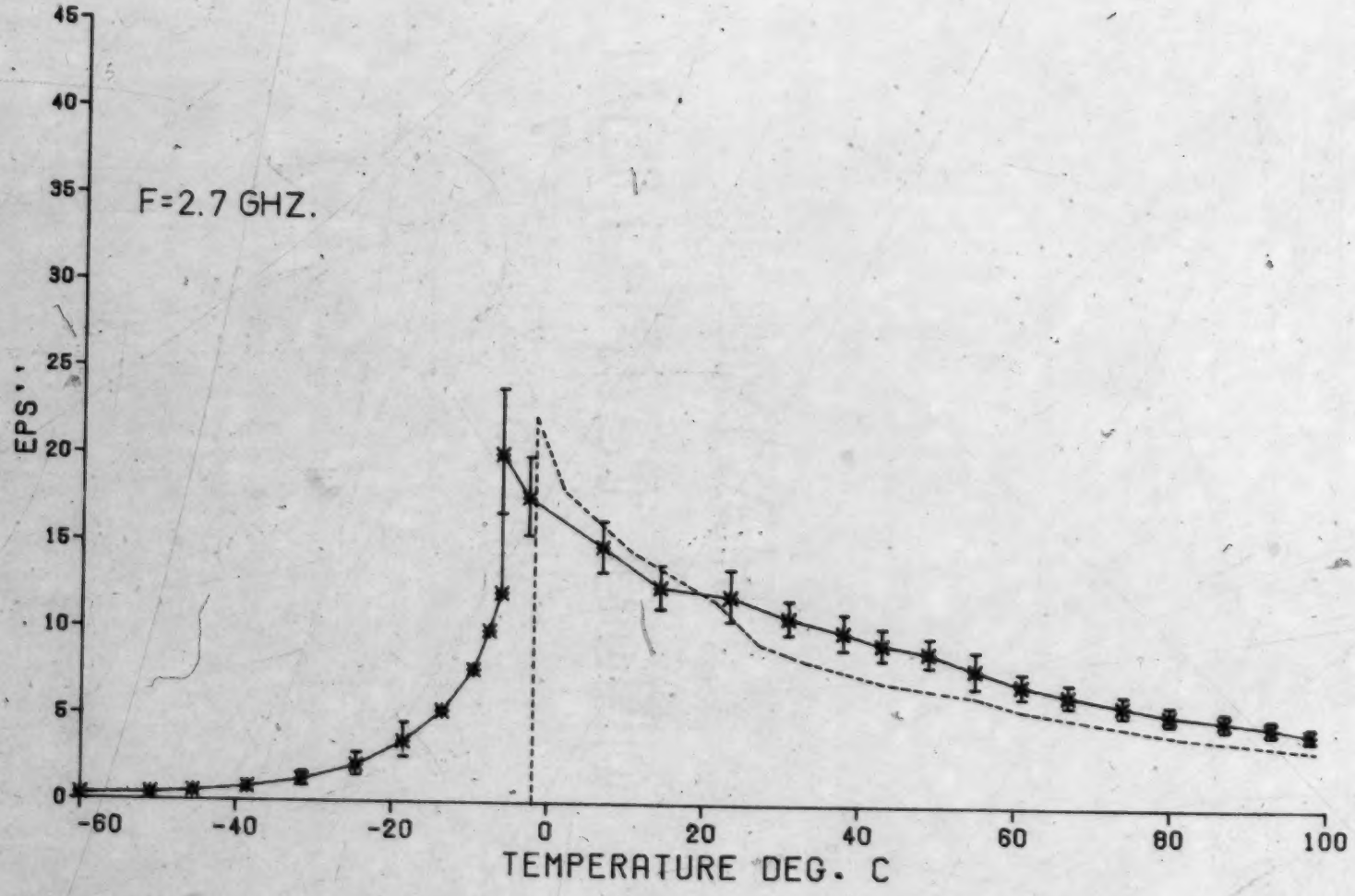

FIG.4.6 EPS'' VS. TEMPERATURE FOR 5% DMSO IN WATER

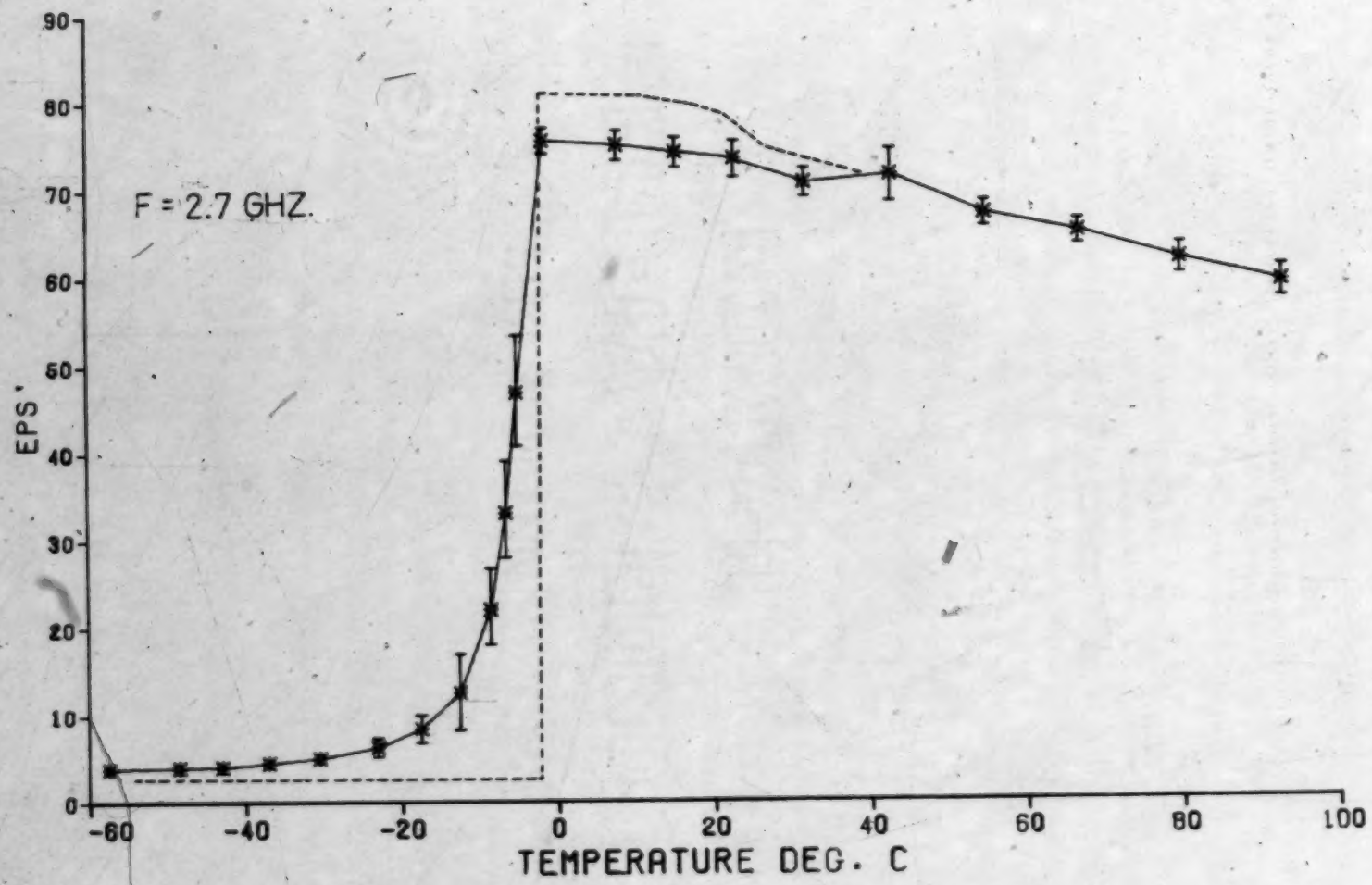

FIG.4.7 EPS' VS. TEMPERATURE FOR 10% DMSO IN WATER

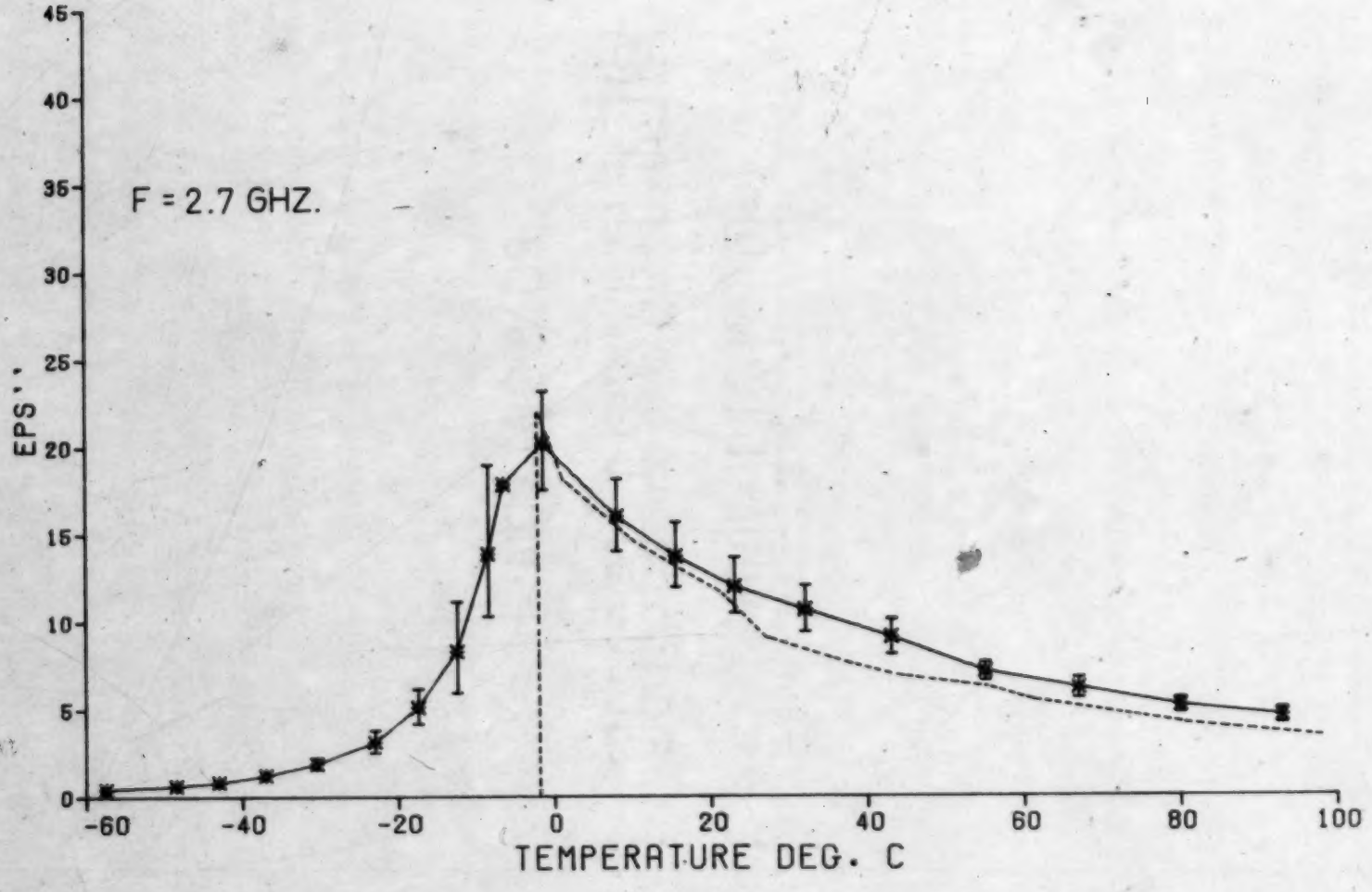

FIG. 4.8 EPS'' VS. TEMPERATURE FOR 10% DMSO IN WATER

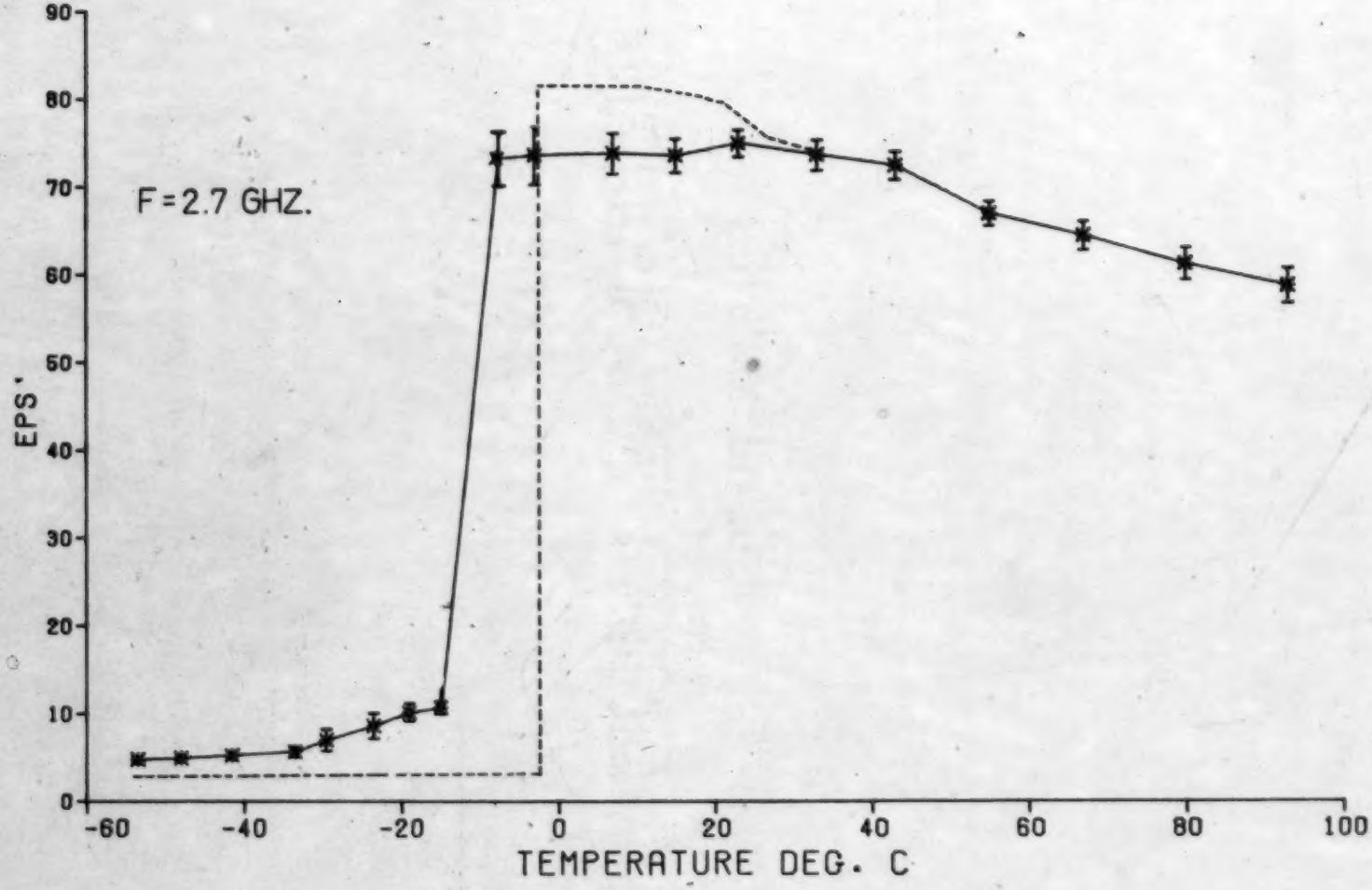

FIG. 4.9 EPS' VS. TEMPERATURE FOR 20% DMSO IN WATER

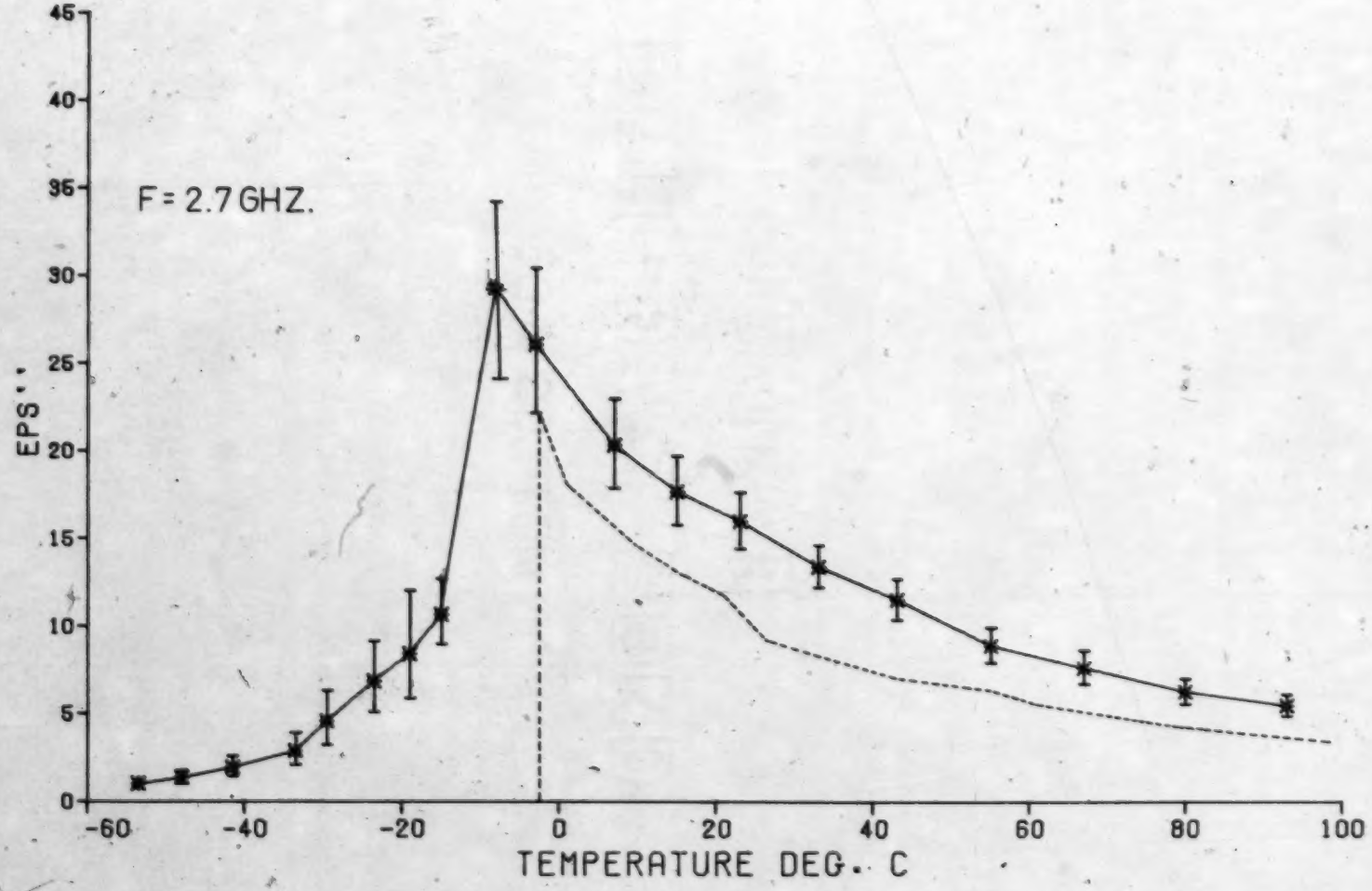

FIG. 4.10 EPS'' VS. TEMPERATURE FOR 20% DMSO IN WATER

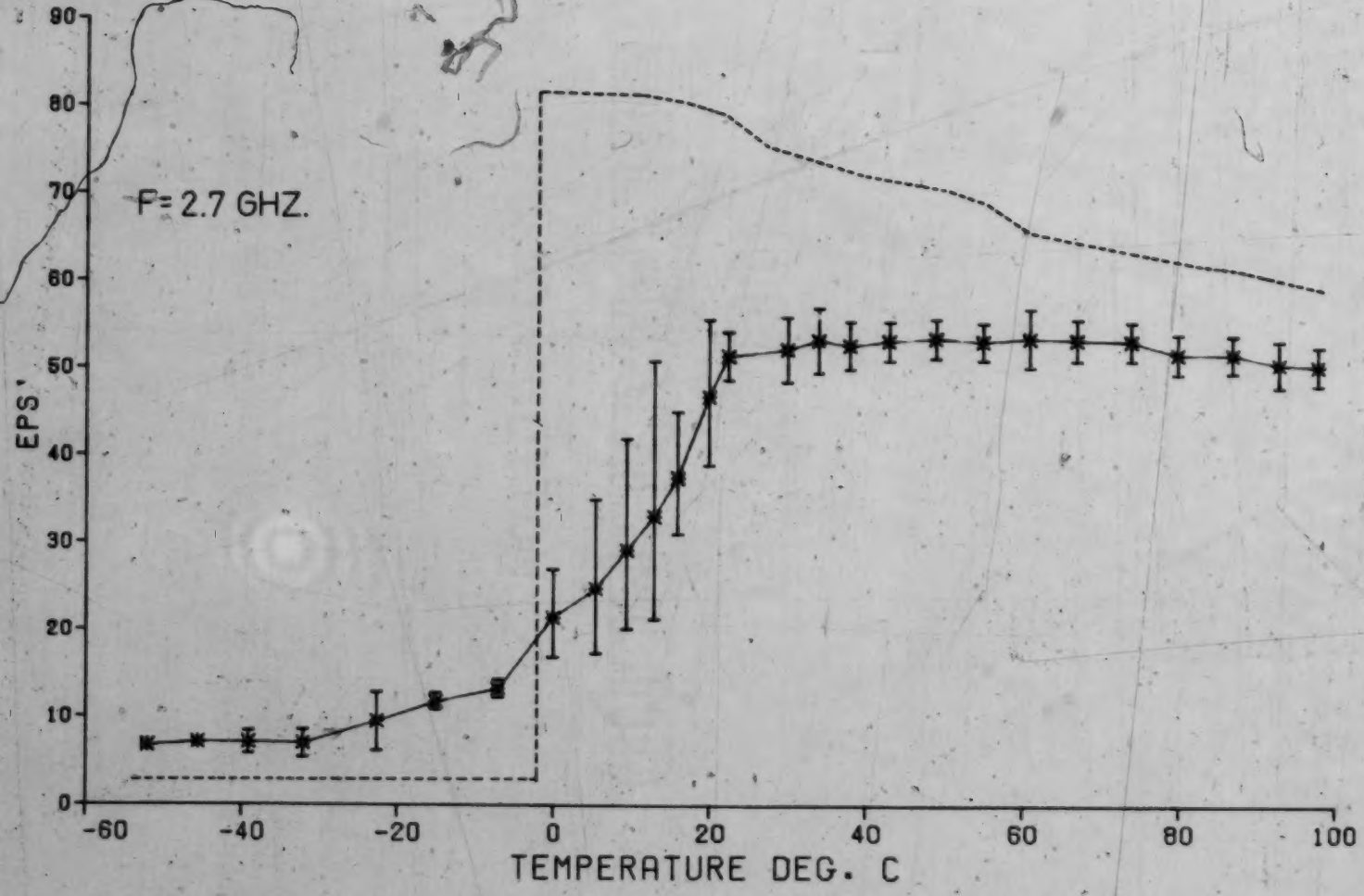

FIG. 4.11 EPS' VS. TEMPERATURE FOR 70% DMSO IN WATER

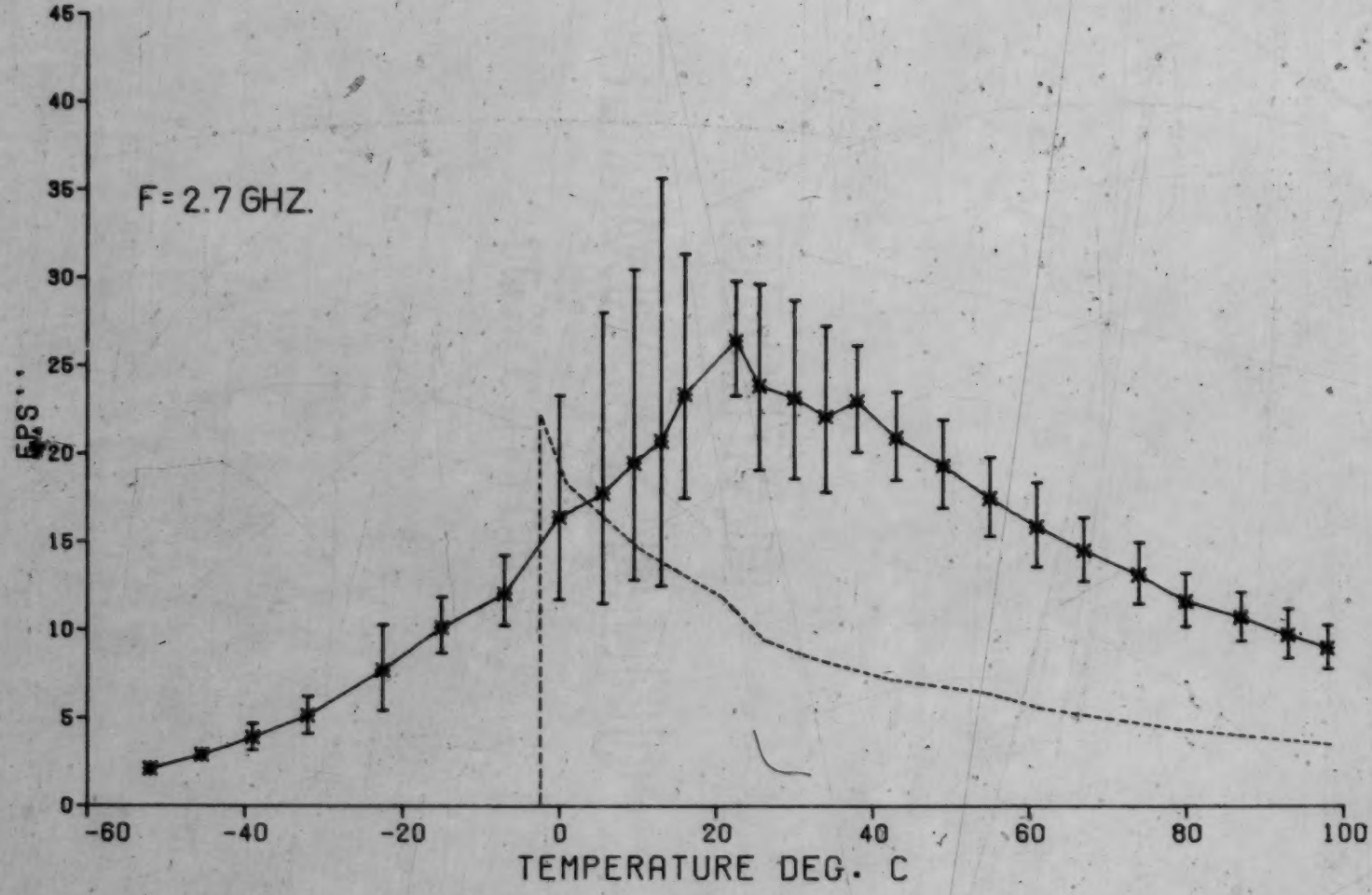

FIG. 4.12 EPS'' VS. TEMPERATURE FOR 70% DMSO IN WATER

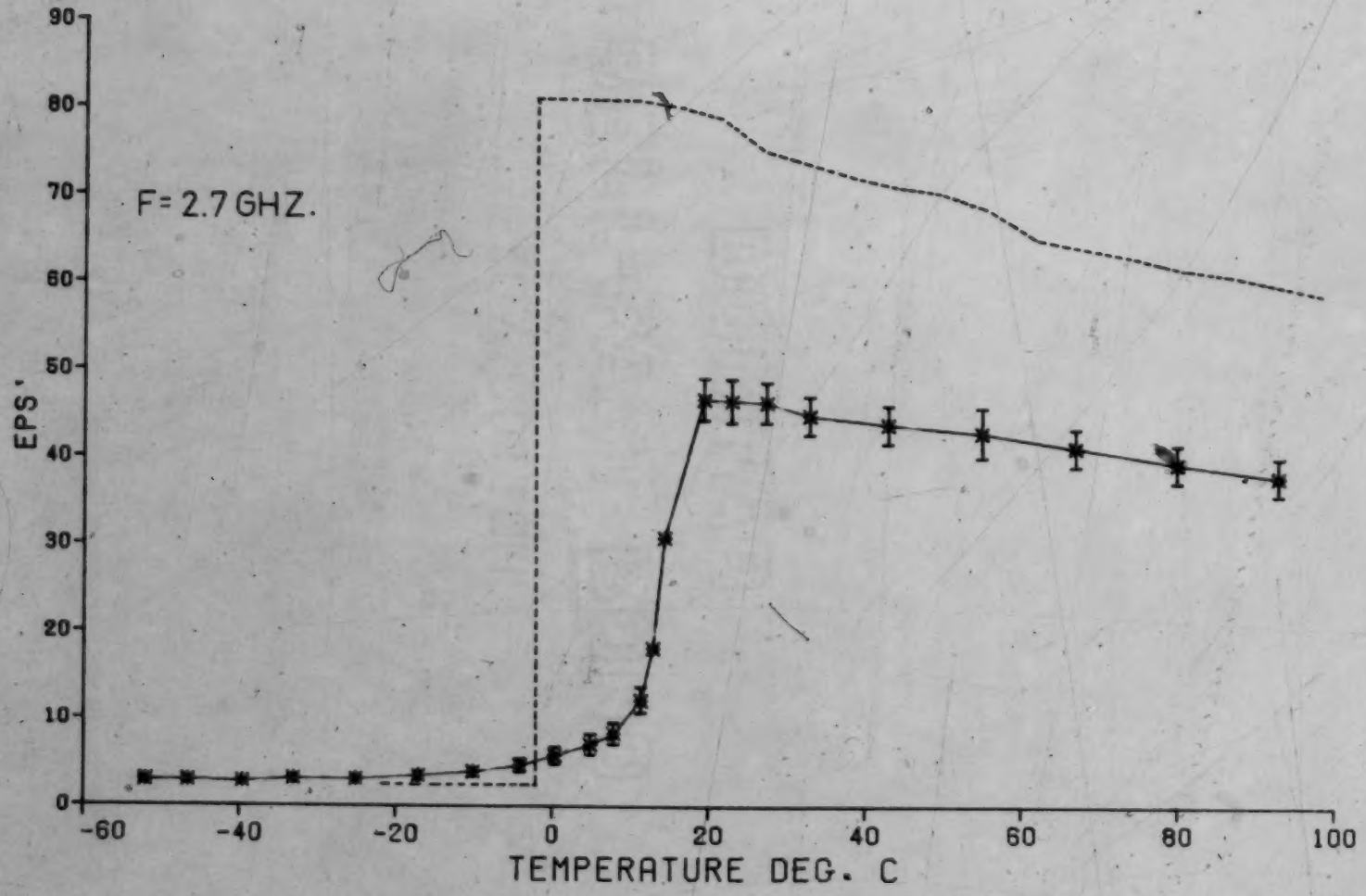

FIG. 4.13 EPS' VS. TEMPERATURE FOR 100% DMSO

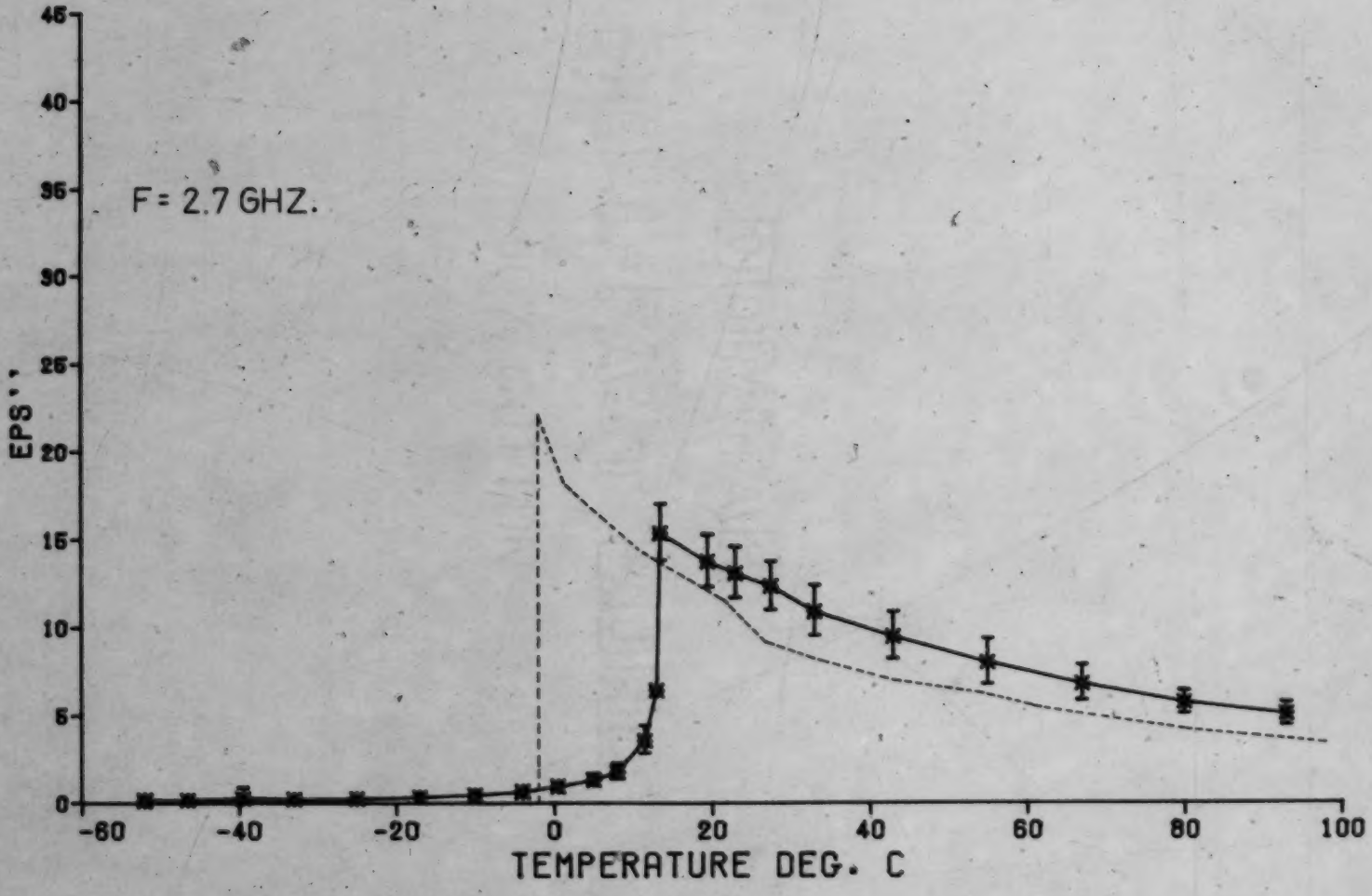

FIG. 4.14 EPS'' VS. TEMPERATURE FOR 100% DMSO

an increasing phase-lag between the field and the dipole orientation develops, and losses (i.e. ϵ'') increase.

In all cases, except for 70% DMSO, a fairly abrupt change in both ϵ' and ϵ'' is evident at the freezing point. This may also be the case for 70% DMSO, but the freezing temperature of -72°C was below the measurement range. These abrupt changes are associated with the phase change at which the continuously changing instantaneous structure of the liquid becomes a rigid solid. The effect of this is to reduce the relaxation frequency. For instance, the Cole-Cole plot for ice (43) (figure 4.23) shows that the relaxation frequency of this material is about 3.0 Khz as compared to 18 Ghz for water (figure 4.24)(43). At frequencies around 3 Ghz, as used in the present measurements, ϵ'' for ice is very small and $\epsilon' \approx 3.2$ and shows very little temperature dependence for the range of temperatures considered here. In the case of the DMSO mixtures, however, losses are considerably increased over those of ice, even in the case of 1% DMSO. In addition, the change in the dielectric properties as the freezing point is approached from below is relatively gradual. These phenomena suggest that hydrogen bonding between the water and the DMSO is taking place, thereby reducing the relaxation frequency of the bound water, and therefore increasing ϵ''. This also occurs in other situations, for instance, where water molecules form bonds to the cellulose in wood (44). The cryobiological

implications of these results will be discussed in section 4.3.

(4.4) Comparison of Cole-Cole Plots for Water and DMSO.

The fact that ϵ'' decreases with increasing temperature above the freezing point suggests that the measuring frequency is below the relaxation frequency for all the concentrations considered in this group, except for 70% DMSO (figure 4.12). For the liquid phase, this can be explained by reference to figure 4.24 which is a Cole-Cole plot for water and for DMSO drawn on the basis of literature data (16,17,43), and some of the present measurements. It is evident from this figure that the relaxation frequency for water is in the vicinity of 18 Ghz, and that for DMSO is in the vicinity of 9 Ghz. For measurements at frequencies below the relaxation frequency, decreases in both ϵ' and ϵ'' with increasing temperature would therefore be expected. This corresponds to moving from curve A to curve B.

This point is further clarified by reference to figure 4.25 (40). Here it can be seen that the relaxation frequency increases with increasing temperature. Considering a measurement at frequency f_b below the relaxation frequency, it is clear that a drop in value from ϵ''_{b1} to ϵ''_{b2} would be expected for a temperature increase from T_1 to T_2. On the other hand, for a measurement well above the relaxation

frequency, such as f_a, an increase from ϵ''_{a1} to ϵ''_{a2} is expected for an increase in temperature. From this discussion, it is apparent that a peak in the value of ϵ'' as the temperature is varied would suggest that the measuring frequency was in fact the relaxation frequency at the temperature of the peak.

(4.5) Relaxation in a 70% Solution of DMSO in Water.

Further consideration of figure 4.24 suggests that increasing the DMSO concentration up to 70% is analagous to increasing the measurement frequency or reducing the relaxation frequency of the solution. Increasing the concentration from 70% to 100% has the same effect as increasing temperature, and from the above discussion, this has the effect of increasing the relaxation frequency of the solution. It would therefore be expected that a 70% mixture of DMSO would have the minimum relaxation frequency of any aqueous solution of DMSO.

This implies that the hydrogen bonding between the DMSO and the water molecules reaches a maximum for the eutectic mixture (i.e. approximately 70% DMSO). Szmant (14) has noted several other effects that occur for the eutectic mixture, and he indicates that the addition of DMSO to water increases the organization of water up to concentrations of 0.33 mole fraction DMSO (i.e. 66%). The composition of the

liquid is then DMSO.$2H_2O$.

Referring to figure 4.12, a definite peak in the temperature curve of ϵ'' occurs in the vicinity of 23°C. This leads to the conclusion that the relaxation frequency for 70% DMSO at 23°C is at the frequency at which this measurement was made (i.e. 2750 Mhz). Because of the large error-bars in the vicinity of the peak (due to a large attenuation through the cavity), the exact position of the peak is ill-defined. In addition, the freezing point of 100% DMSO is at 18°C, only 5°C below this temperature, and so the values at temperatures below the maximum may be due to some partial freezing phenomenon in the liquid. The even larger error-bars in this region tend to support this possibility because partially frozen solutions are characteristically ill-defined as to their composition. On the other hand, the fact that ϵ'' for other concentrations continues to increase right down to the freezing point reinforces the conclusion that the 70% solution does exhibit a minimum relaxation frequency.

(4.6) <u>5% Dextran Solution.</u>

Figures 4.15 and 4.16 are plots of the temperature behaviour of a 5% (w/w) solution of dextran. Dextran is one of a class of high molecular weight cryoprotective agents. The results show that the effects of dextran on the

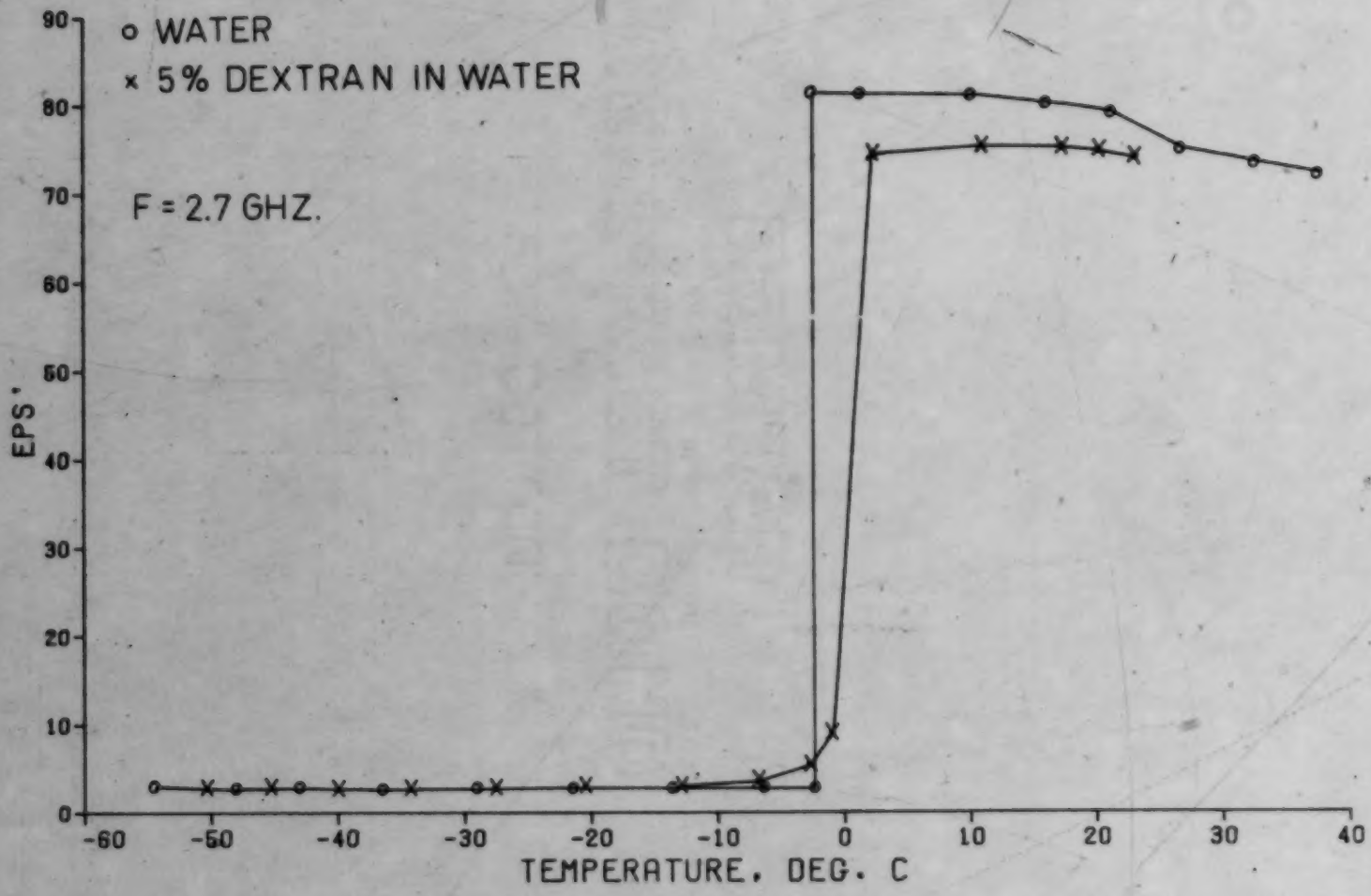

FIG. 4.15 EPS' FOR WATER AND 5% DEXTRAN

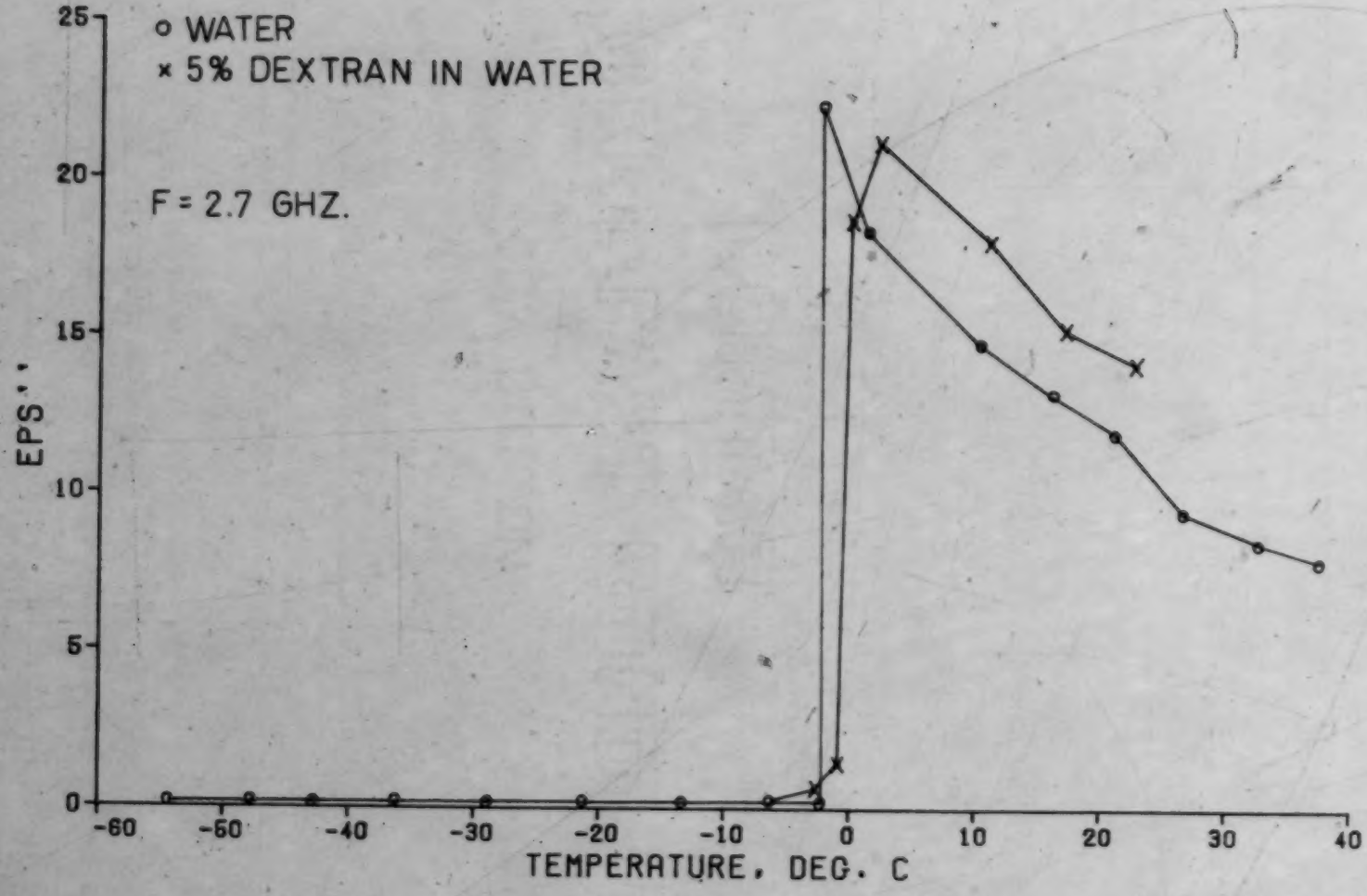

FIG. 4.16 EPS'' FOR WATER AND 5% DEXTRAN

dielectric constant are minimal, although the solution is slightly more lossy than water above the freezing point, and the transition below the freezing point is not quite as abrupt. Below this transition region, the solution behaves very similarly to pure water, suggesting that the macromolecules have little effect on the ice structure. Because of the large size of the molecules, it is likely that more significant effects would be apparent at lower frequencies, as has been indicated on proteins and other biomolecules (43).

(4.7) 10% DMSO and Various Additives.

Figures 4.17 and 4.18 are the results of measurements on solutions of 10% DMSO and mixtures of 10% DMSO with either 0.1% NaCl, 1.0% NaCl or 5% dextran (w/w). Most biological solutions contain ionic components and so the NaCl was added to give some indication of the effect of an ionic component on the dielectric properties. As can be seen from the results, the only significant effect is the addition of 1% NaCl to the 10% DMSO, and it is only ε'' above the freezing point that is affected in this case. 1% NaCl is close to the widely used physiological saline solution of 0.9% NaCl, and was chosen for this reason. The increase in conductivity resulting from the addition of the NaCl accounts for the increase in ε'' as observed in figure 4.18.

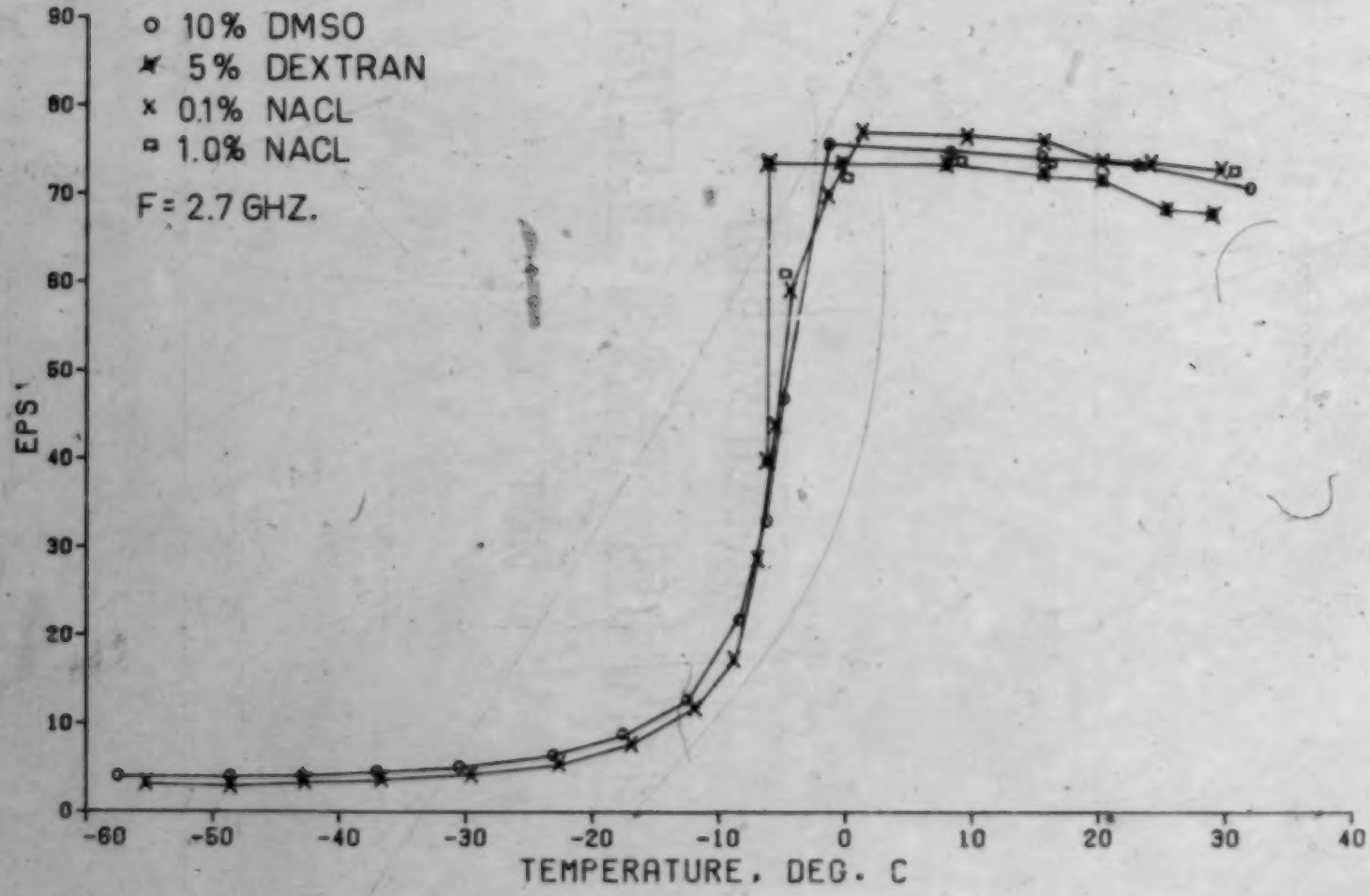

FIG. 4.17 EPS' FOR VARIOUS COMPOUNDS IN WATER

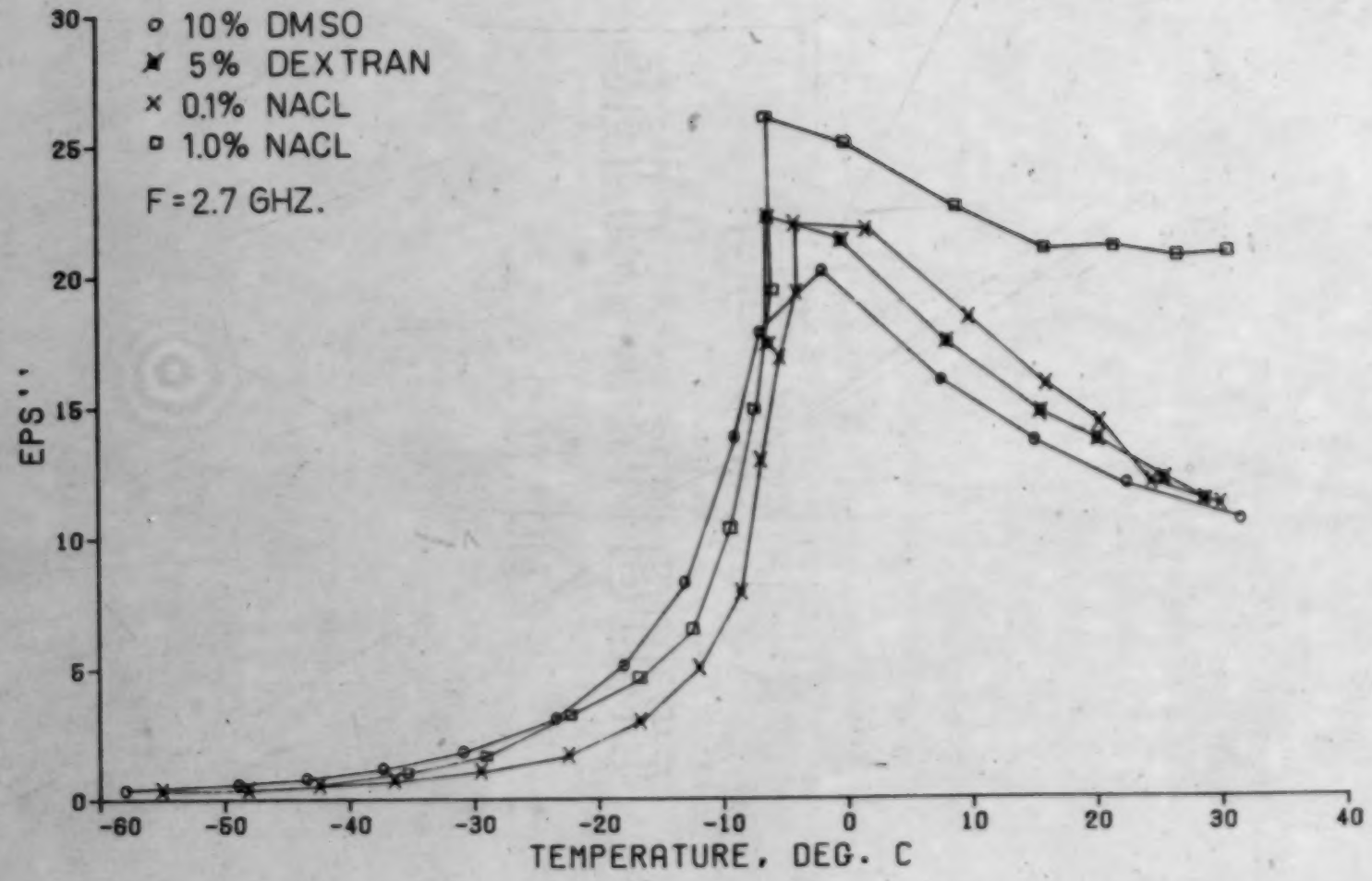

FIG. 4.18 EPS'' FOR VARIOUS COMPOUNDS IN DMSO

(4.8) Behaviour of ϵ' with Concentration.

The final group of curves comprises figures 4.19, 4.20 and 4.21. In these, the dielectric properties, including the loss tangent, are plotted against the DMSO concentration for three different temperatures. Figure 4.19 shows that the behavior of ϵ' at 23°C and 50°C is as one would expect on the basis of linear mixing, that is, with the values decreasing linearly from those of water to those of pure DMSO. The curve for 5°C (figure 4.19), however, has a minimum value at 70% DMSO. This is consistent with the curve of figure 4.11. The abrupt change at about 90% DMSO is due to higher concentrations having freezing points above 5°C. The reason for the minimum in the value of ϵ' at 5°C can be explained by reference to figure 4.26, which is a typical Debye curve of the behaviour of a dielectric. Previous results indicated that DMSO at a concentration of 70% has a minimum relaxation frequency, $f_\flat$. Therefore, at 70%, measurements are being made in the vicinity of point f on figure 4.26, with a resultant value of $\epsilon'_\flat$. For any other concentration, however, the relaxation frequency is higher which is analagous to being in the region to the left of $f_\flat$ such that $f<f_\flat$. For any point in this region, the value of ϵ' will be greater than $\epsilon'_\flat$ and so one would expect $\epsilon'_\flat$ to be the minimum value. The fact that this is so for all the concentrations in figure 4.19, except those below the freezing point, confirms the earlier results that a 70% DMSO

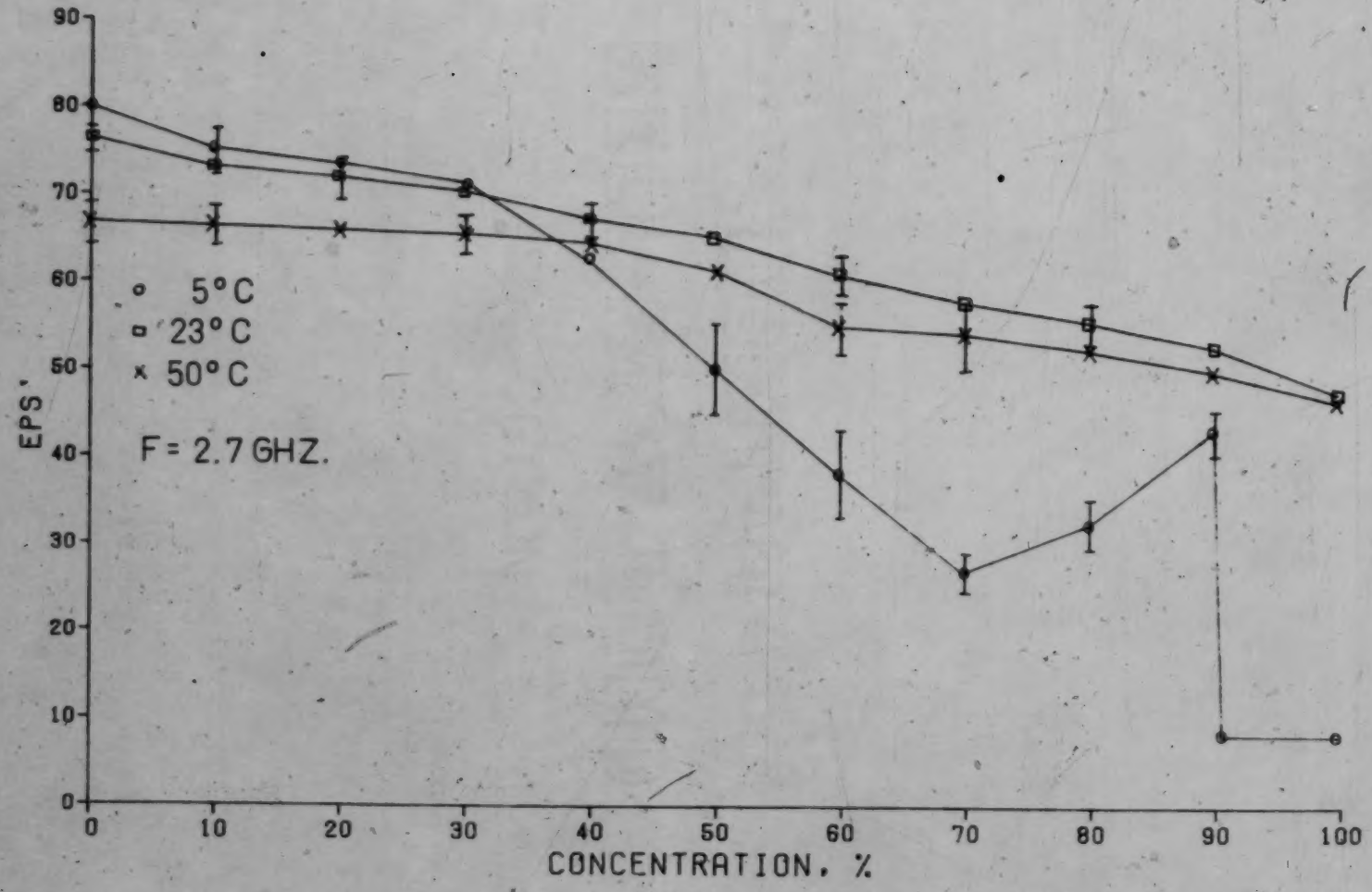

FIG. 4.19 EPS' FOR DMSO AT VARIOUS TEMPERATURES

solution has the minimum relaxation frequency, and that this frequency is of the order of 3 Ghz.

(4.9) Behaviour of ϵ'' with Concentration.

Turning now to figure 4.20, we see that ϵ'' goes through a maximum at about 40% DMSO, for a temperature of 5°C, but has maxima at 70% for 23°C and at about 50% for 50°C. Reference to appendix D shows that the high losses in the vicinity of the maxima of these curves results in large standard deviations and so the exact locations of the maxima are hard to determine. However, where comparison is possible with the earlier curves, the data is consistent. The trend towards increasing losses with decreasing temperature and increasing DMSO concentration is maintained throughout except in the vicinity of 70% DMSO where the behaviour is consistent with a dispersion region. Figure 4.21 is a plot of the loss tangent vs concentration, and for all temperatures plotted, it shows maxima in the vicinity of 70% DMSO. This can be explained by considering the definition of loss tangent (ϵ''/ϵ'). Figure 4.26 shows that ϵ''/ϵ' could go through a maximum in the vicinity of f_D, though this would depend on the behaviour of ϵ' in this region.

(4.10) Biological Implications of the Results.

The results are now examined with a view to the effects

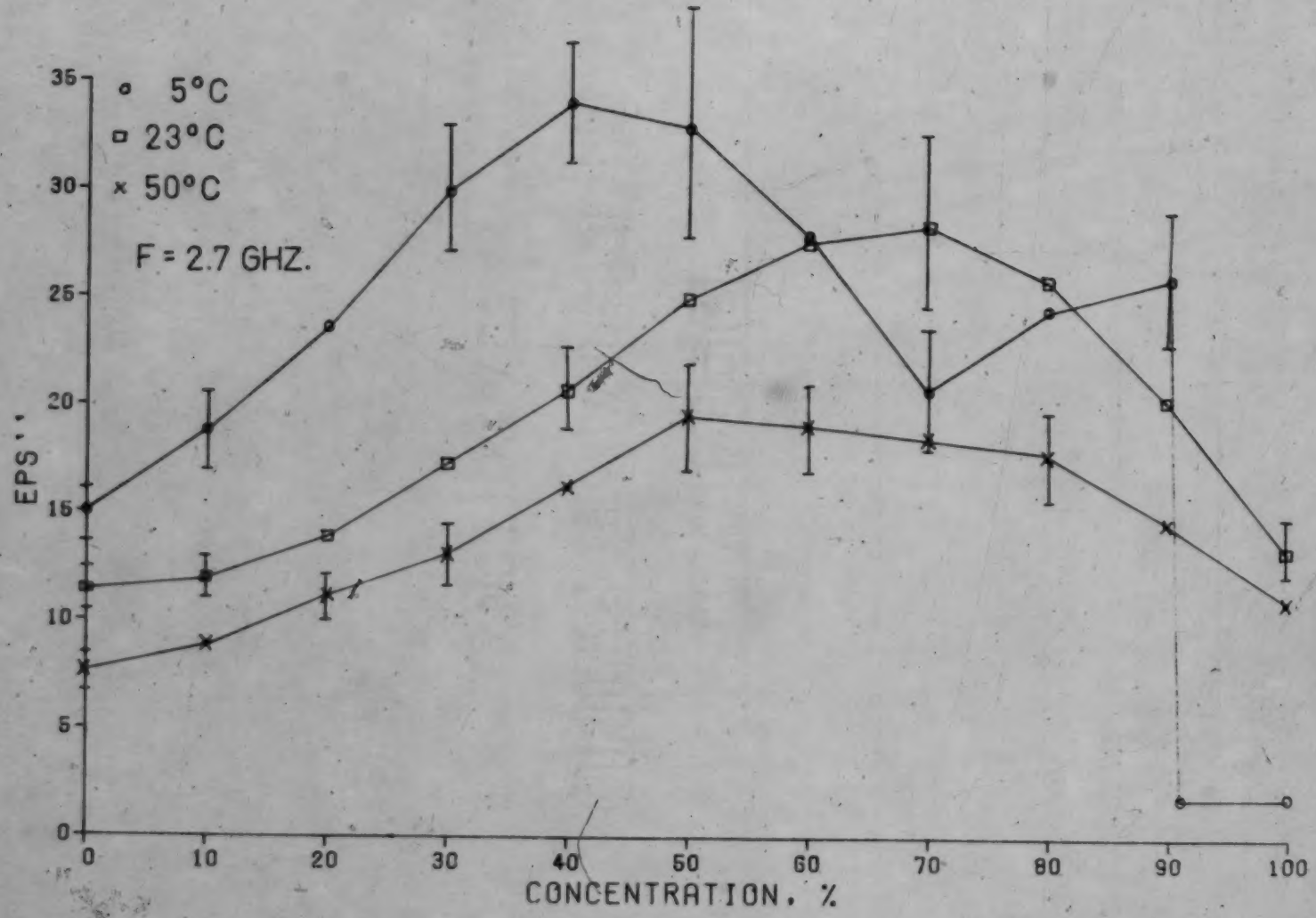

FIG. 420 EPS'' FOR DMSO AT VARIOUS TEMPERATURES

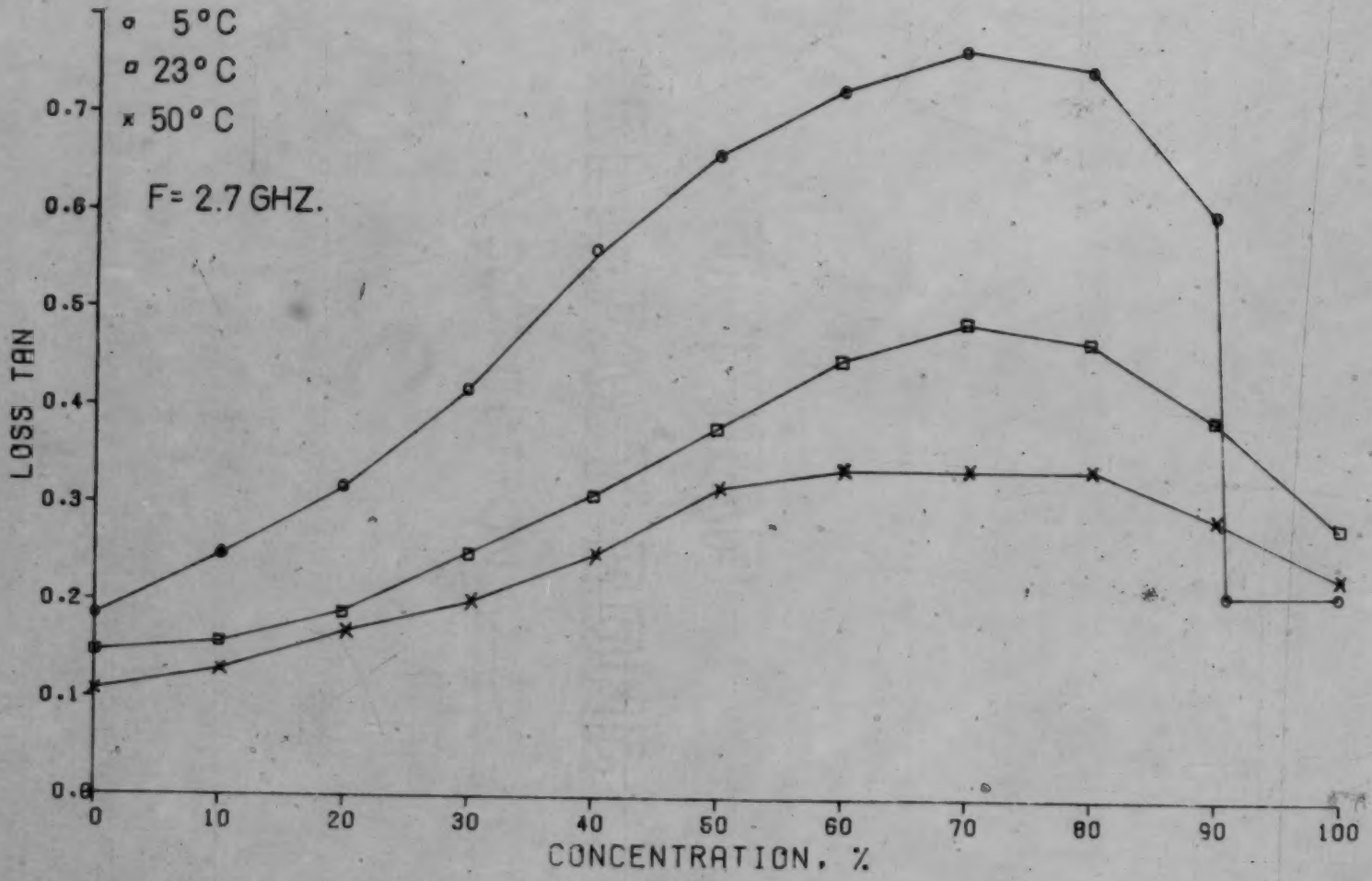

FIG 4.21 LOSS TAN FOR DMSO AT VARIOUS TEMPERATURES

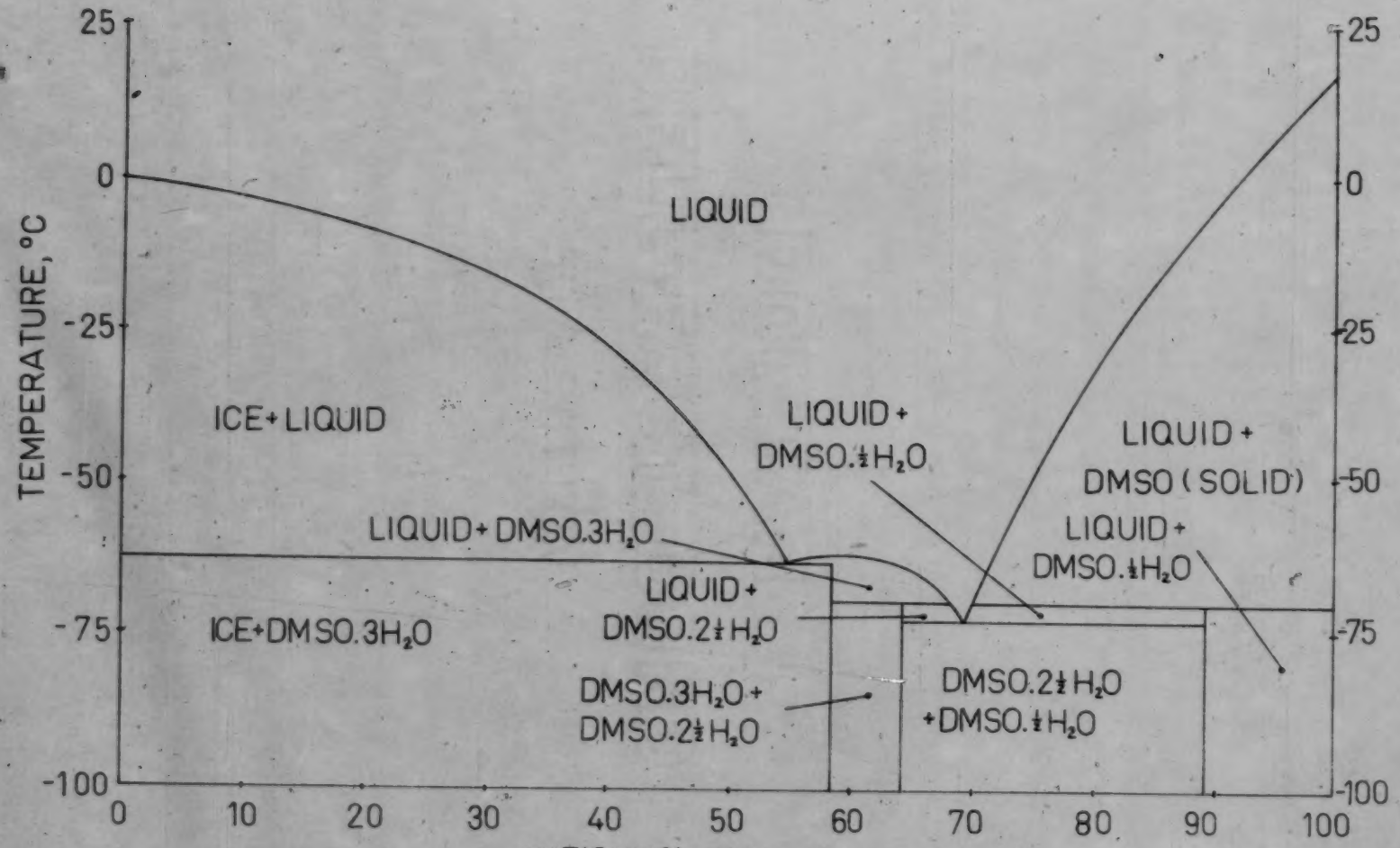

FIGURE 4.22 THE BINARY H_2O DMSO SYSTEM

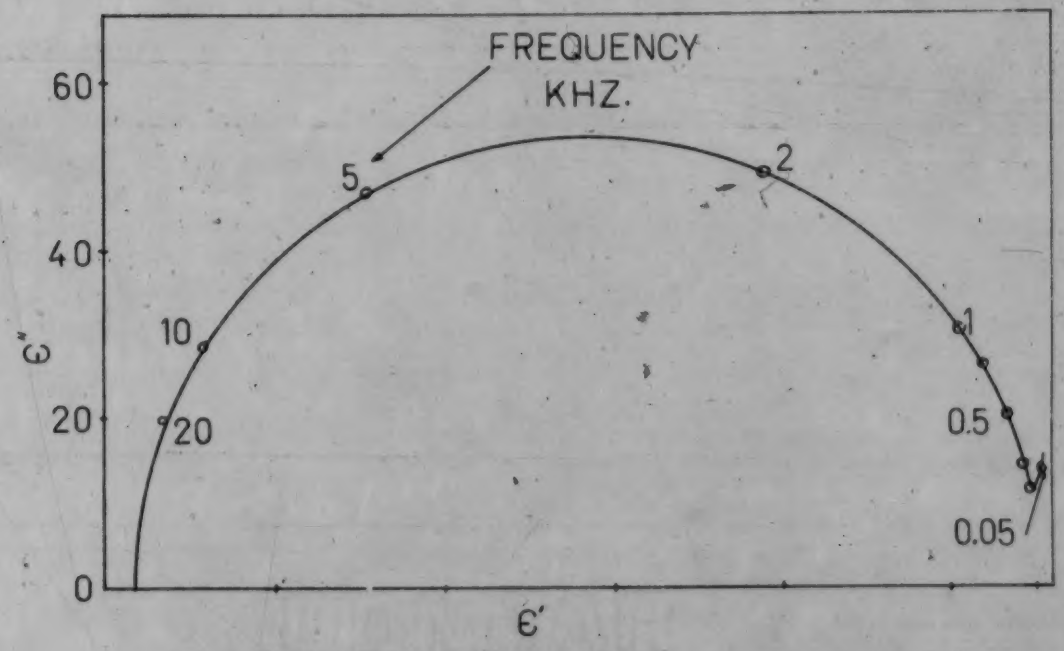

FIGURE 4.23 COLE-COLE PLOT FOR ICE AT -10.9 °C

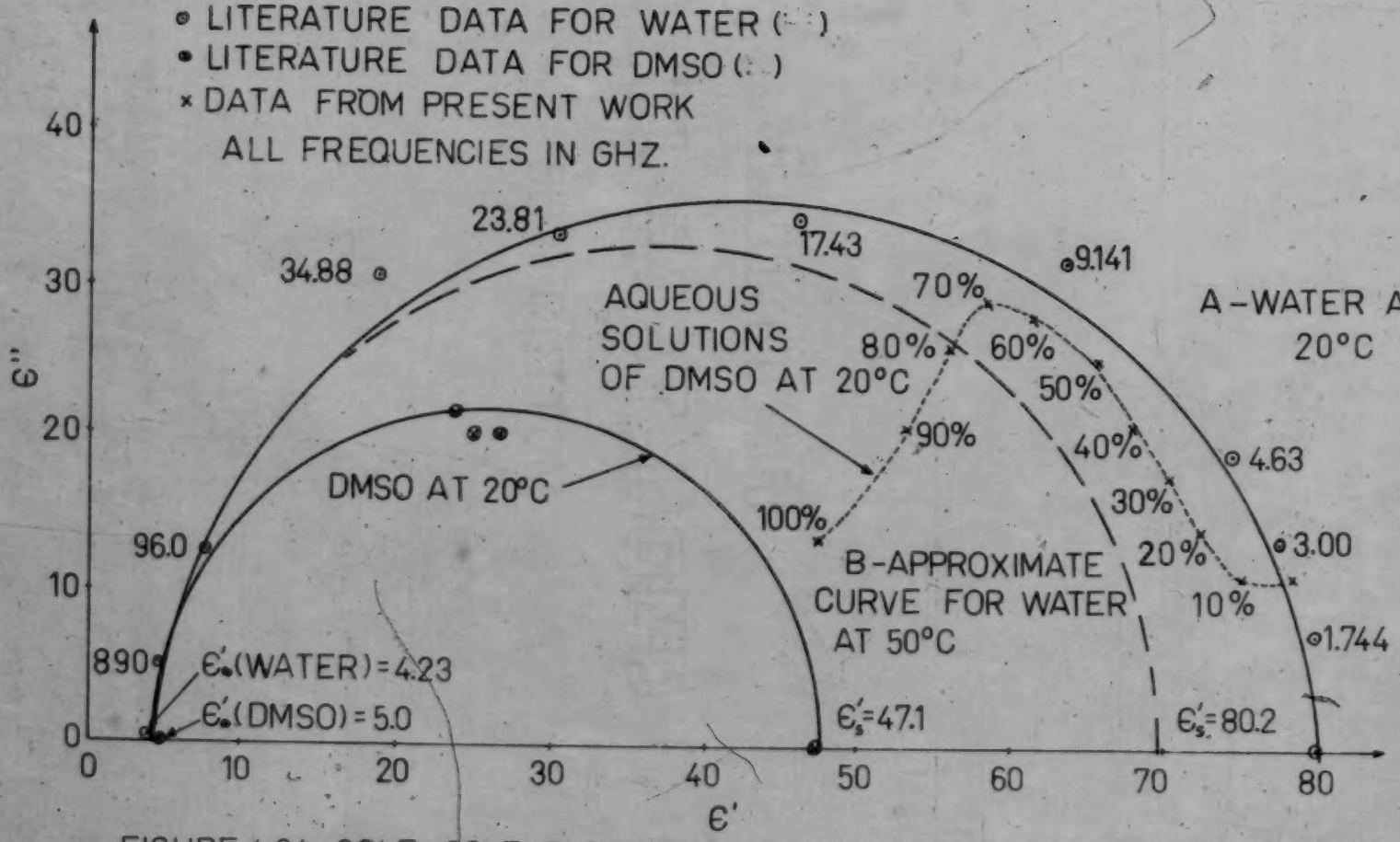

FIGURE 4.24 COLE-COLE PLOTS FOR SOLUTIONS OF WATER AND DMSO

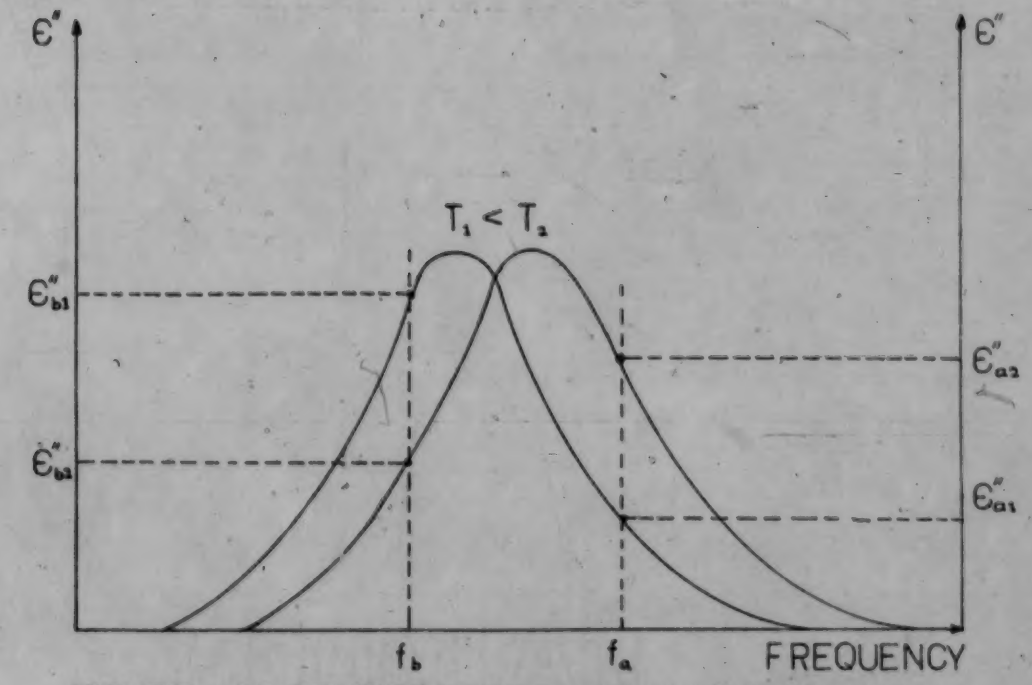

FIGURE 4.25 TEMPEARTURE BEHAVIOUR OF THE RELAXATION FREQUENCY

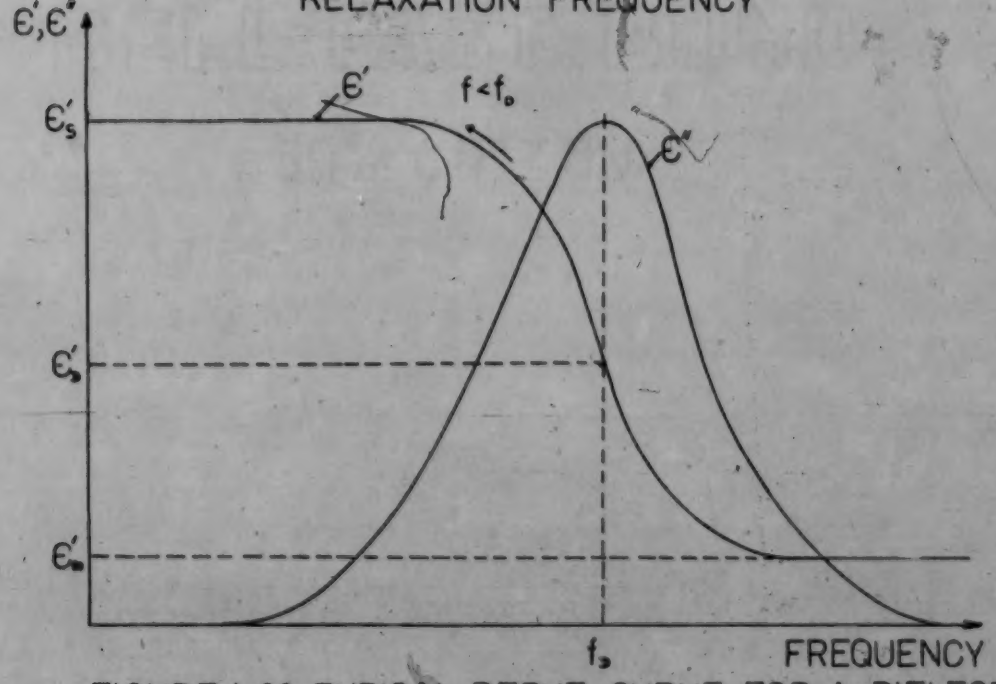

FIGURE 4.26 TYPICAL DEBYE CURVE FOR A DIELECTRIC WITH A SINGLE RELATION FREQENCY

of microwave heating of biological materials containing the solutions as cryoprotective agents. As the results have indicated, the dielectric loss of frozen materials is considerably less than it would be at room temperature. This is generally true of all frozen materials containing water, and, specifically, of biological tissue. In cryobiological applications, the biomaterials to be heated are initially in the frozen state, and so the expected dielectric loss is small. This is in direct conflict with the requirements of rapid heating, and any means of increasing the dielectric loss at low temperatures is useful. From figures 4.3 to 4.12, it is clear that the addition of DMSO increases the losses at low temperatures. In general, the higher the percentage of DMSO, the higher the increase in the losses.

One of the important areas of current cryobiological research is in establishing the most effective cryoprotective agent. With regard to DMSO, various concentrations have been employed, usually in the range 1-10%. However, Pegg (45) has used apparatus in which the concentration is increased up to 70% as cooling proceeds. Aside from the cryoprotective properties, the question of toxicity arises, and concentrations above about 15-20% are usually considered to be toxic (15). However, reducing the temperature allows the use of higher concentrations, hence the technique of Pegg (45) is acceptable.

Referring again to figures 4.3 to 4.12, it appears that maximum enhancement of low temperature heating would occur with 70% DMSO. This is only practical when the concentration is increased with decreasing temperature, and so for the more usual application where a single concentration is used, a limiting concentration of 10% is indicated. Reasonable enhancement of the dielectric loss does occur at this concentration.

As has been pointed out earlier, the critical range in tissue freezing and recovery is between -60°C and +10°C. Therefore, it is in this range that the possibility of rapid heating is most important, and so the low losses at temperatures below -60°C do not constitute a serious disadvantage. It may therefore be concluded that the addition of DMSO is beneficial to tissue heating at low temperatures, and that higher concentrations of DMSO provide progressively more enhancement.

Another important question in microwave heating in cryobiology is that of heating uniformity, and the dielectric measurement results are now examined in this light. Consider a homogenous body which is at the same temperature throughout. The body is placed in a microwave field and heating is begun. It is inevitable that some non-uniformity of field distribution will exist, and this will cause different areas to heat at different rates. From the

results presented in the curves, and from other dielectric data on frozen biological materials (46), it is clear that the warmer the material, the higher the loss and therefore the more energy it will absorb. This will tend to increase the non-uniformity of temperature distribution, perhaps to the extent that temperature gradients are able to cause damage. This effect becomes more pronounced for those solutions in which the change in dielectric constant is more abrupt. Heat conduction effects are of course a moderating influence but non-uniformities will still arise.

The dielectric properties of perfused biological materials are heavily dependent on the presence of the perfusate if this is DMSO (22). This means that the above behaviour will certainly be influenced by the properties of the DMSO solutions. It is reasonable to suppose that those solutions exhibiting the most abrupt changes in dielectric properties would cause the greatest non-uniformity of heating. In this category are water and the 1% solution of DMSO. Although not directly related to the present discusssion, the solution containing dextran also exhibits an abrupt change which suggests that cryoprotective agents of this type are less suitable than DMSO-based agents from the standpoint of microwave heating. On the other hand, those solutions containing higher percentages of DMSO (≥5%) show increasingly gradual transitions in the vicinity of the freezing point, and their use is therefore suggested from

considerations of heating uniformity.

(4.11) Concluding Remarks.

In conclusion, then, DMSO solutions up to a concentration of about 70% (eutectic mixture), exhibit relaxation frequencies which fall from approximately 18 Ghz for pure water to about 3 Ghz for 70% DMSO. As the concentration is increased above 70%, the relaxation frequency increases to about 9 Ghz for pure DMSO. Of the solutions measured, the most lossy was a 40% solution at 5°C, ϵ'' in this case being approximately 34. Of the other additives tested, only 1% NaCl had any appreciable effect, and then only on ϵ'' at temperatures above the freezing point.

From a biolgical viewpoint, considerations of microwave heating rate and uniformity dictate the use of the highest possible concentration of DMSO permitted by considerations of cryoprotective action and toxicity. The technique of Pegg (45) where the DMSO concentration at low temperatures is high is certainly attractive from a heating standpoint. The implications of the results of the dielectric measurements on DMSO solutions underline the importance of a knowledge of the dielectric properties of cryoprotective agents when microwave heating is used.

Chapter 5. Electromagnetic Field Modelling.

(5.1) A Review of Some Existing Techniques.

The recent proliferation of high power microwave devices has aggravated the problems of electromagnetic 'pollution', but has also made new heating techniques available to the biomedical engineer. The effects of microwaves on living tissue have thus become a question of some importance, and the accurate determination of the electromagnetic fields within arbitrary-shaped inhomogeneous dielectric scatterers is a problem which is basic to this question. Broadly speaking, two approaches are available for the solution of this problem. These are: (a) direct or indirect measurement of the fields and (b) mathematical determination of the fields based on solutions to Maxwell's equations.

Some of the methods that have been used in the first category include:

(1) The use of probes or loops to measure the electromagnetic fields at particular points. Because the presence of a metallic probe would considerably perturb the fields, non-metallic probes using liquid crystals to measure the heating effect of the field have been developed (47). Information is transferred from the probe to the measuring equipment using optic fibres to minimise field perturbation.

(2) The use of thin sheets of lossy material with which liquid crystals are in thermal contact. Colour photographs of the sheets after a period of heating can then be interpreted as electromagnetic field distributions (48).
(3) Observation of the re-radiation from a diode implanted in the scatterer, which is in an electromagnetic field (49).
(4) The use of colour thermovision on sectioned phantom scatterers to determine the heating distribution, from which the field distribution can be inferred (50,51).

Though some of these methods have proved very effective, they are not as flexible as mathematical methods because of hardware requirements, and because of difficulties involved when measurements are to be made on biological tissues. For these reasons, it was decided to adopt a mathematical approach towards modelling the heating of frozen organs in a microwave field.

In the past several years, a considerable number of mathematical field modelling techniques have appeared, and Bates (52) recently reviewed existing methods. For simple scatterers such as spheres, cylinders and cubes, analytical solutions which can often be obtained by separation of variables, are available. However, for the more complicated scatterers encountered in cryobiology, one must resort to a numerical method if an accurate model is to be constructed. Three classes of model exist. These are:

(1) Transmission models: In these, assumptions about the reflection and refraction of the impinging waves are made, and the amount of energy absorbed in finite elements of the scatterer is calculated as the electromagnetic wave propagates towards the interior of the scatterer. The shape of the scatterer is limited to fairly simple cases, but different dielectric properties can be assigned to different regions. Typical of this type of model is that of Nykvist (28), which models the heating of a meat roast in a microwave oven, where energy is approaching from many different directions.

(2) Frequency Domain Models: Most of the models appearing in the literature fall into this class, and the methods are based on the assumption of an $\exp(j2\pi ft)$ time dependence in the fundamental Maxwell's equations. A set of linear equations for either field variables or field expansion coefficients is derived, and then solved with a suitable matrix inversion scheme. Representative models of this type are those due to Shapiro (53) and Durney (54). In these models, the scatterers are restricted in shape and apply to a multi-layered sphere and a prolate spheroid respectively. The solution of a set of integral equations, as presented by Livesay (55) also falls into this category, but it is applicable to arbitrary-shaped bodies. The disadvantage of this method is that it would require the inversion of a very large matrix if it were applied to a large scatterer with fine structural details, as is the case in many biological

applications.

(3) Time-domain Methods: These methods treat the irradiation of the scatterer as an initial value problem, considering propagation of waves from a source which is turned on at time t=0. A solution of a finite-difference analog of the time-dependent Maxwell's equations is obtained on a lattice of points including the scatterer. A good example of this technique was presented by Yee (56), being later extended to biological materials by Taflove (31,57). This method appeared to be the most suitable and was the one finally chosen for the heating studies performed in the present work.

(5.2) Reasons for Choice of the Method Used.

For reasons outlined in Chapter 6, it was decided to investigate microwave heating of canine kidneys under conditions of plane wave illumination. These organs have a complex structure with many fine details, and so the method chosen would have to be able to model these details with reasonable accuracy. In the model finally adopted, details down to $\lambda_m/20$ were incorporated (λ_m=minimum wavelength). The possibility of approximating the kidney to various regular shapes such as spheres, cylinders and oblate spheroids was considered, but the resulting internal structure could not have had this degree of detail and still maintain the regularity and symmetry demanded by the models

intended for these shapes. The inclusion of the small details in the model thus ruled out the first category and, excepting Livesay's model (55), the second category discussed above. Several factors influenced the choice of Taflove's model over that of Livesay. They are:

(1) The accuracy of Livesay's model depends on the size of the scatterer in relation to the wavelength, which is not the case with Taflove's model.

(2) To implement Livesay's model, the scatterer would have to be sub-divided into N sub-volumes and three coefficients would have to be calculated for each sub-volume. A numerical integration technique would probably be necessary for each of these calculations. The resulting 3Nx3N matrix would then have to be inverted to obtain the required solution. On the basis of data presented in Chapter 6, and assuming a maximum sub-volume size of one quarter of the minimum wavelength encountered, approximately 100 sub-volumes are required. Thus, a 300x300 matrix would have to be inverted. Although not prohibitive, this is a problem of some magnitude and would have no advantage over Taflove's method in this regard.

(3) A possible future extension of Taflove's method to non-plane wave irradiation of a scatterer surrounded by conducting walls (i.e. a microwave oven) appears to be a reasonable possibility (see Chapter 7). This would allow even more realistic modelling of microwave-heated materials.

(5.3) Description of the Method Chosen.

As mentioned above, the method chosen is a time-domain approach which treats the irradiation of the scatterer as an initial value problem. At time t=0, a plane wave of frequency f is assumed to be turned on. The propagation of waves from this source is simulated by solving a finite difference analog of the time dependent Maxwell's equations on a lattice of points including the scatterer. Time stepping is continued until the sinusoidal steady-state is achieved at each point. The field envelope, or maximum absolute value during the final half-wave cycle of time-stepping is taken as the magnitude of the phasor of the steady state field. The following description is based on that presented by Yee (56) and extended by Taflove (31,57).

(5.4) The Yee Algorithm.

In the MKS system, with μ, ϵ and σ time independent, Maxwell's equations in the rectangular co-ordinate system (x,y,z) can be represented as follows:

$$\frac{\partial H_x}{\partial t} = \frac{1}{\mu}\left(\frac{\partial E_y}{\partial z} - \frac{\partial E_z}{\partial y}\right) \quad \cdots\cdots 5.1a$$

$$\frac{\partial H_y}{\partial t} = \frac{1}{\mu}\left(\frac{\partial E_z}{\partial x} - \frac{\partial E_x}{\partial z}\right) \quad \cdots\cdots 5.1b$$

$$\frac{\partial H_z}{\partial t} = \frac{1}{\mu}\left(\frac{\partial E_x}{\partial y} - \frac{\partial E_y}{\partial x}\right) \quad \cdots\cdots 5.1c$$

$$\frac{\partial E_x}{\partial t} = \frac{1}{\epsilon}\left(\frac{\partial H_z}{\partial y} - \frac{\partial H_y}{\partial z} - \sigma E_x\right) \quad \ldots\ldots 5.1d$$

$$\frac{\partial E_y}{\partial t} = \frac{1}{\epsilon}\left(\frac{\partial H_x}{\partial z} - \frac{\partial H_z}{\partial x} - \sigma E_y\right) \quad \ldots\ldots 5.1e$$

$$\frac{\partial E_z}{\partial t} = \frac{1}{\epsilon}\left(\frac{\partial H_y}{\partial x} - \frac{\partial H_x}{\partial y} - \sigma E_z\right) \quad \ldots\ldots 5.1f$$

At this point, a set of finite difference equations following Yee's (Y3) notation are introduced. A space lattice point is denoted as:

$$(i,j,k) = (i\delta, j\delta, k\delta) \quad \ldots\ldots (5.2)$$

and any function of space and time as:

$$F^n(i,j,k) = F(i\delta, j\delta, k\delta, n\delta t) \quad \ldots\ldots (5.3)$$

where $\delta = \delta x = \delta y = \delta z$ is the space increment and δt is the time increment. Yee uses finite difference expressions for the space and time derivatives that are both simply programmed and second order accurate in δ and δt. They are:

$$\frac{\partial F^n(i,j,k)}{\partial x} = \frac{F^n(i+\frac{1}{2},j,k) - F^n(i-\frac{1}{2},j,k)}{\delta} + O(\delta^2) \quad \ldots\ldots 5.4$$

$$\frac{\partial F^n(i,j,k)}{\partial t} = \frac{F^{n+\frac{1}{2}}(i,j,k) - F^{n-\frac{1}{2}}(i,j,k)}{\delta t} + O(\delta t^2) \quad \ldots\ldots 5.5$$

In order to achieve the accuracy of 5.4, and to realise all the space derivatives of 5.1a - 5.1f, the components of $\bar{E}$ and $\bar{H}$ are positioned about a unit cell of the lattice as shown in figure 5.1. To achieve the accuracy of 5.5, $\bar{E}$ and $\bar{H}$

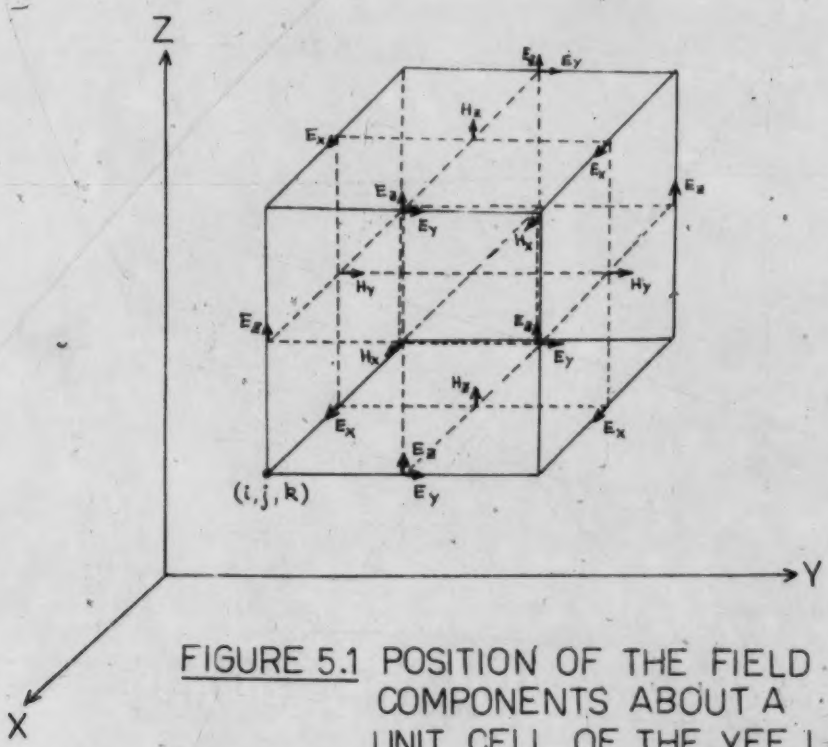

FIGURE 5.1 POSITION OF THE FIELD COMPONENTS ABOUT A UNIT CELL OF THE YEE LATTICE

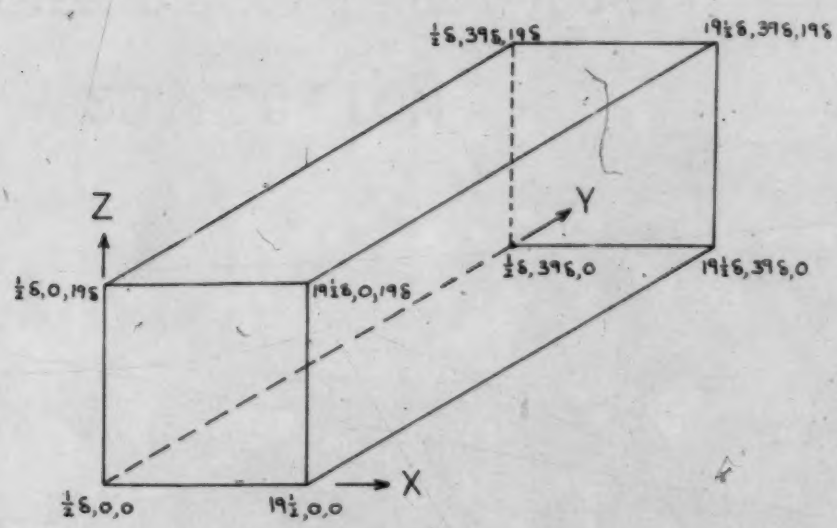

FIGURE 5.2 LATTICE USED TO TEST THE PROGRAM ON A SPHERE

are evaluated at alternate half-time steps. These assumptions lead to the following set of finite difference equations for 5.1a - 5.1f (56):

$$H_x^{n+\frac{1}{2}}(i,j+\tfrac{1}{2},k+\tfrac{1}{2}) = H_x^{n-\frac{1}{2}}(i,j+\tfrac{1}{2},k+\tfrac{1}{2}) + \frac{\delta t}{\mu(i,j+\frac{1}{2},k+\frac{1}{2})\delta}\left\{\begin{matrix} E_y^n(i,j+\frac{1}{2},k+1) - E_y^n(i,j+\frac{1}{2},k) + \\ E_z^n(i,j,k+\frac{1}{2}) - E_z^n(i,j+1,k+\frac{1}{2}) \end{matrix}\right\} \quad \cdots 5.6a$$

$$H_y^{n+\frac{1}{2}}(i+\tfrac{1}{2},j,k+\tfrac{1}{2}) = H_y^{n-\frac{1}{2}}(i+\tfrac{1}{2},j,k+\tfrac{1}{2}) + \frac{\delta t}{\mu(i+\frac{1}{2},j,k+\frac{1}{2})\delta}\left\{\begin{matrix} E_z^n(i+1,j,k+\frac{1}{2}) - E_z^n(i,j,k+\frac{1}{2}) + \\ E_x^n(i+\frac{1}{2},j,k) - E_x^n(i+\frac{1}{2},j,k+1) \end{matrix}\right\} \quad \cdots 5.6b$$

$$H_z^{n+\frac{1}{2}}(i+\tfrac{1}{2},j+\tfrac{1}{2},k) = H_z^{n-\frac{1}{2}}(i+\tfrac{1}{2},j+\tfrac{1}{2},k) + \frac{\delta t}{\mu(i+\frac{1}{2},j+\frac{1}{2},k)\delta}\left\{\begin{matrix} E_x^n(i+\frac{1}{2},j+1,k) - E_x^n(i+\frac{1}{2},j,k) + \\ E_y^n(i,j+\frac{1}{2},k) - E_y^n(i+1,j+\frac{1}{2},k) \end{matrix}\right\} \quad \cdots 5.6c$$

$$E_x^{n+1}(i+\tfrac{1}{2},j,k) = \left\{1 - \frac{\sigma(i+\frac{1}{2},j,k)\,\delta t}{\epsilon(i+\frac{1}{2},j,k)}\right\} E_x^n(i+\tfrac{1}{2},j,k) \quad \cdots 5.6d$$
$$+ \frac{\delta t}{\epsilon(i+\frac{1}{2},j,k)\delta}\left\{\begin{matrix} H_z^{n+\frac{1}{2}}(i+\frac{1}{2},j+\frac{1}{2},k) - H_z^{n+\frac{1}{2}}(i+\frac{1}{2},j-\frac{1}{2},k) + \\ H_y^{n+\frac{1}{2}}(i+\frac{1}{2},j,k-\frac{1}{2}) - H_y^{n+\frac{1}{2}}(i+\frac{1}{2},j,k+\frac{1}{2}) \end{matrix}\right\}$$

$$E_y^{n+1}(i,j+\tfrac{1}{2},k) = \left\{1 - \frac{\sigma(i,j+\frac{1}{2},k)\,\delta t}{\epsilon(i,j+\frac{1}{2},k)}\right\} E_y^n(i,j+\tfrac{1}{2},k) \quad \cdots 5.6e$$
$$+ \frac{\delta t}{\epsilon(i,j+\frac{1}{2},k)\delta}\left\{\begin{matrix} H_x^{n+\frac{1}{2}}(i,j+\frac{1}{2},k+\frac{1}{2}) - H_x^{n+\frac{1}{2}}(i,j+\frac{1}{2},k-\frac{1}{2}) + \\ H_z^{n+\frac{1}{2}}(i-\frac{1}{2},j+\frac{1}{2},k) - H_z^{n+\frac{1}{2}}(i+\frac{1}{2},j+\frac{1}{2},k) \end{matrix}\right\}$$

$$E_z^{n+1}(i,j,k+\tfrac{1}{2}) = \left\{1 - \frac{\sigma(i,j,k+\frac{1}{2})\,\delta t}{\epsilon(i,j,k+\frac{1}{2})}\right\} E_z^n(i,j,k+\tfrac{1}{2}) \quad \cdots 5.6f$$
$$+ \frac{\delta t}{\epsilon(i,j,k+\frac{1}{2})\delta}\left\{\begin{matrix} H_y^{n+\frac{1}{2}}(i+\frac{1}{2},j,k+\frac{1}{2}) - H_y^{n+\frac{1}{2}}(i-\frac{1}{2},j,k+\frac{1}{2}) + \\ H_x^{n+\frac{1}{2}}(i,j-\frac{1}{2},k+\frac{1}{2}) - H_x^{n+\frac{1}{2}}(i,j+\frac{1}{2},k+\frac{1}{2}) \end{matrix}\right\}$$

The assumption that $\delta t/\mu(i,j,k)\delta$ is constant for all i,j,k of the lattice is now made, and the following constants are defined:

$$R = \delta t/\epsilon_0 \quad \cdots\cdots 5.7a$$

$$R_a = \delta t^2/(\delta^2 \mu_0 \epsilon_0) \quad \cdots\cdots 5.7b$$

$$R_b = \delta t/\mu_0 \delta \quad \cdots\cdots 5.7c$$

$$C_a(m) = 1.0 - R\sigma(m)/\epsilon_r(m) \quad \cdots\cdots 5.7d$$

$$C_b(m) = R_a/\epsilon_r(m) \quad \cdots\cdots 5.7e$$

where m is a tissue type integer (simply an integer assigned to a given type of tissue). The proportional electric field vector is defined as:

$$\tilde{E} = R_b E \quad \cdots\cdots 7.8$$

and so equations 5.7a -5.7e and 5.8 allow 5.6a to be re-written as follows:

$$H_x^{n+\frac{1}{2}}(i,j+\tfrac{1}{2},k+\tfrac{1}{2}) = H_x^{n-\frac{1}{2}}(i,j+\tfrac{1}{2},k+\tfrac{1}{2}) + \tilde{E}_y^n(i,j+\tfrac{1}{2},k+1) - E_y^n(i,j+\tfrac{1}{2},k) + \tilde{E}_y^n(i,j,k+\tfrac{1}{2}) - E_z^n(i,j+1,k+\tfrac{1}{2}) \quad \cdots\cdots 5.9a$$

5.6b and 5.6c can be written in a similar way. In the same way, 5.6d can be written as follows:

$$m = \text{media}(i+\tfrac{1}{2},j,k) \quad \cdots\cdots 5.10a$$

$$\tilde{E}_x^{n+1}(i+\tfrac{1}{2},j,k) = C_a(m)\,\tilde{E}_x^{n}(i+\tfrac{1}{2},j,k) + C_b(m)\left[H_z^{n+\frac{1}{2}}(i+\tfrac{1}{2},j+\tfrac{1}{2},k) - H_z^{n+\frac{1}{2}}(i+\tfrac{1}{2},j-\tfrac{1}{2},k) + H_y^{n+\frac{1}{2}}(i+\tfrac{1}{2},j,k-\tfrac{1}{2}) - H_y^{n+\frac{1}{2}}(i+\tfrac{1}{2},j,k+\tfrac{1}{2})\right] \quad \ldots\ldots 5.10b$$

5.6e and 5.6f can be written in a similar way.

(5.5) Lattice Truncation Conditions.

A basic problem with any finite difference solution of Maxwell's equations is the treatment of the field vector components at the lattice truncation. Because of limited computer storage, the lattice cannot cover a sufficiently large portion of space so that the scattered wave at the lattice truncation might be closely approximated. Necessarily, the lattice must terminate close to the scatterer in a region where the nature of the scattered wave is unknown.

Proper truncation of the lattice requires that any outgoing wave disappear at the lattice boundary without reflection during the continuous time-stepping of the algorithm. Improper truncation results in error for all time steps after the boundary wave reflections return to the vicinity of the scatterer. One possible truncation condition is to set the field components at each truncation point to zero for all time steps. This situation is similar to that resulting if a conductor were present at that point, and would result in reflections. This is known as a "hard"

truncation condition.

In the free-space situation being modelled here, the hard truncation condition is inadequate, and a "soft" truncation has been developed. One possibility for a soft truncation is to assign linearly increasing values of conductivity near the lattice boundaries, thereby absorbing the outgoing wave. For small reflection, however, this would require absorption over approximately 1 wavelength, which is intolerable from the point of view of computer storage. In addition, wavefront distortion for waves propagating parallel to the lattice boundary would be undesirable.

To overcome this problem, a soft lattice truncation which relates the field values at the lattice boundaries to those 1δ or 2δ within the boundary was developed. An exact condition is available for a one-dimensional lattice, since all waves would arrive perpendicularly at the lattice boundary. However, in the 2- or 3-dimensional case, one or several waves at differing angles of incidence could be arriving simultaneously, and no exact condition is available for this situation. Taflove (57) discusses this at length for the 1- and 2-dimensional cases, and only the 3-dimensional case will be dealt with here.

A typical lattice is shown in figure 5.2. This lattice was used to test the program on a sphere, as described in

section 5.9. From the basic time step relation of the algorithm:

$$2c\delta t = \delta \quad \ldots\ldots 5.11$$

That is, it takes two time steps for a wave in air to cross between two adjacent lattice points. The integer constant,

$$\ell(m) = 2\lambda(1)/\lambda(m) \quad \ldots\ldots 5.12$$

is defined as the number of time steps required to propagate between adjacent lattice points in tissue type m. (1) is the wavelength in air, and (m) is the wavelength in tissue type m. Further, the stored field vectors

$$\hat{\tilde{E}} = \tilde{E}^{n-\ell(m)}(i,j,k) \quad \ldots\ldots 5.13a$$

$$\hat{H} = \hat{H}^{n-\ell(m)}(i,j,k) \quad \ldots\ldots 5.13b$$

are defined. For the lattice plane x=1/2 (see figure 5.2), the truncation is given by:

$$H_y^n(\tfrac{1}{2},j,k+\tfrac{1}{2}) = [\hat{H}_y(\tfrac{3}{2},j,k-\tfrac{1}{2}) + \hat{H}_y(\tfrac{3}{2},j,k+\tfrac{1}{2}) + H_y(\tfrac{3}{2},j,k+\tfrac{3}{2})]/3 \quad \ldots\ldots 5.14a$$

which in effect takes the mean of the H-field values at the point, and its two adjacent lattice points as existed 1 time steps before, and assigns that value to the lattice truncation point. Similarly, the other lattice truncation conditions are:

For plane x=1/2 .

$$H_z^n(\tfrac{1}{2},j+\tfrac{1}{2},k) = [\hat{H}_z(\tfrac{3}{2},j+\tfrac{1}{2},k-1) + \hat{H}_z(\tfrac{3}{2},j+\tfrac{1}{2},k) +$$

$$+ H_z\left(\tfrac{3}{2}, j+\tfrac{1}{2}, k+1\right)] / 3 \quad \ldots\ldots \text{5.14 b}$$

For plane y=0.

$$\tilde{E}_x^n\left(i+\tfrac{1}{2}, 0, k\right) = \tilde{E}_x^{n-2}\left(i+\tfrac{1}{2}, 1, k\right) \quad \ldots\ldots \text{5.14c}$$

$$\tilde{E}_z^n\left(i, 39, k+\tfrac{1}{2}\right) = \hat{E}_z\left(i, 38, k+\tfrac{1}{2}\right) \quad \ldots\ldots \text{5.14d}$$

For plane y=39 .

$$\tilde{E}_x^n\left(i+\tfrac{1}{2}, 39, k\right) = \hat{E}_x\left(i+\tfrac{1}{2}, 38, k\right) \quad \ldots\ldots \text{5.14e}$$

$$\tilde{E}_z^n\left(i, 39, k+\tfrac{1}{2}\right) = \hat{E}_z\left(i, 38, k+\tfrac{1}{2}\right) \quad \ldots\ldots \text{5.14f}$$

For plane z=0.

$$\tilde{E}_x^n\left(i+\tfrac{1}{2}, j, 0\right) = [\hat{\tilde{E}}_x\left(i-\tfrac{1}{2}, j, 1\right) + \hat{\tilde{E}}_x\left(i+\tfrac{1}{2}, j, 1\right) + \hat{\tilde{E}}_x\left(i+\tfrac{3}{2}, j, 1\right)] / 3 \quad \ldots\ldots \text{5.14g}$$

$$\tilde{E}_x^n\left(i, j+\tfrac{1}{2}, 0\right) = [\hat{\tilde{E}}_y\left(i-1, j+\tfrac{1}{2}, 1\right) + \hat{\tilde{E}}_y\left(i, j+\tfrac{1}{2}, 1\right) + \hat{\tilde{E}}_y\left(i+1, j+\tfrac{1}{2}, 1\right)] / 3 \quad \ldots\ldots \text{5.14h}$$

(5.6) The Symmetry Conditions.

If even symmetry of the scatterer about one or two planes can be assumed, an important saving in computer time and memory space can be realised. In the case of the canine kidney, symmetry about two planes is assumed (see Chapter 6). An incident plane wave having components E and H is assumed and so the following symmetry conditions can be defined.

$$H_y^n\left(27\tfrac{1}{2}, j, k+\tfrac{1}{2}\right) = H_z^n\left(27\tfrac{1}{2}, j+\tfrac{1}{2}, k\right) = 0 \quad \ldots\ldots \text{5.15a}$$

$$\tilde{E}_x^n\left(i+\tfrac{1}{2}, j, 15\right) = \tilde{E}_y^n\left(i, j+\tfrac{1}{2}, 19\right) = 0 \quad \ldots\ldots \text{5.15b}$$

(5.7) The Plane Wave Source Condition.

The simulation of a continuous sinusoidal plane wave source is now considered. One possibility would be to vary the electric field along the points of one endface in the appropriate manner, but this would represent a "hard" truncation condition for any scattered waves, and so cause undesirable reflections. Alternatively, a sinusoidal variation can be superimposed on the existing field at the points in a plane imbedded 2 or 3 into the lattice from one endface. This allows reflections to pass through the source and be truncated in the manner described above. This condition simulates a plane wave originating at infinity and a reflected wave returning to infinity without further interaction. The appropriate equation defining this type of source is:

$$\tilde{E}^{n}_{3}(i,3,k+\tfrac{1}{2}) \leftarrow 1000\, R_b \sin(2\pi f n\delta t) + \tilde{E}^{n}_{3}(i,3,k+\tfrac{1}{2}) \quad \ldots\ldots 5.16$$

This defines an impinging field with an E component being developed at plane 3δ.

(5.8) Stability Criterion.

Taflove (57) derives the stability criterion for the algorithm, and arrives at the following result:

$$v_{max}\,\delta t \leq \left(\frac{1}{\delta x^2} + \frac{1}{\delta y^2} + \frac{1}{\delta z^2}\right)^{-\frac{1}{2}} \quad \ldots\ldots 5.17$$

where v_{max} is the maximum phase velocity expected within the

model. For a 3-dimensional lattice this reduces to:

$$\delta t \leq \frac{\delta}{c\sqrt{3}} = 0.577 \frac{\delta}{c} \quad \ldots\ldots 5.18$$

This criterion applies for an infinite lattice, and so it is not strictly correct when lattice truncation conditions are included. In effect, this limits the number of time steps for which the program can be run before the presence of the instabilities becomes apparent. For convenience, a choice of $t=\delta/2c$ was made in the program, and no instabilities were encountered for up to three input cycles. Approximately 1.5 cycles are sufficient to establish steady state conditions, as was verified by printouts at 1, 2 and 3 cycles.

(5.9) Computer Program.

A computer program based on the solution of equations 5.9 to 5.16 was obtained from Taflove, and was re-written to allow it to be employed for the present problem. A listing of the new program is given in appendix B. Input data to the program includes a listing of the dielectric properties encountered at each point in a lattice of points containing the scatterer. The means by which this is done is detailed in Chapter 6.

Before running the program with kidney data, it was run

for a dielectric sphere for which an alternate solution, using the summed-series technique of Stratton (32), was available. Figure 5.2 details the lattice into which 1/4 of a sphere was incorporated, and the parameters for which the program was run were $\epsilon' = 4.0$, $\sigma = 0$, magnitude of incident $E_z = 1000$, f = 2.5 Ghz, $\delta = \lambda_m/20 = 0.3$ cm, $\delta t = 5$ psec and envelope observation was for $460 \leq n \leq 500$, where n is the number of time steps. For a three dimensional program, there is additional flexibility in specifying the dielectric parameters in the free space region outside the scatterer. The finite difference equation for E_z (equation 5.10d) requires that $\sigma(1)=0$, where $\sigma(1)$ is the conductivity of the surrounding medium. This assures that there is no attenuation of the incident wave. For the finite difference equations of E_x and E_y (equations 5.10b and 5.10c), however, a small value of $\sigma(1)$ can be assumed for the x and y directions without affecting the propagation of the incident wave, or the diffracted wave within the scatterer. This assumption results in the attenuation of the E_x and E_y components of the exterior diffracted wave, and thus reduces z-directed wave reflections at the lattice truncations. This further aid to stability was implemented by setting $\sigma(1)=0.1$ mho/m for equation 5.10d and 5.10c, and setting $\sigma(1)=0$ for equation 5.10d. The technique could also be applied by creating an H-field loss to be used in equations 5.9a, 5.9b and 5.9c. Judicious use of this type of anisotropy provides additional control over program stability.

(5.10) Comparison of "Exact" and Time-domain Solutions.

Figure 5.3 compares the results of the program with those obtained by the exact summed series technique. It is noted that the computed solution locates the positons of the peaks and nulls of the electric field with a maximum error of $\pm\delta$, or about ±3% of the diameter of the scatterer. The magnitude of each peak is determined with a maximum error of ±10%. This leads to the conclusion that the accuracy should be sufficient to allow the useful solution of the fields within most biological scatterers.

(5.11) Calculation of Absorbed Power.

Since the program generates a large amount of data, modifications to provide results printed out in the same form as the lattice data were made to facilitate point-by-point comparison. Of primary importance in a microwave heating study is the amount of power deposited at each point in the scatterer. Because of uncertainties in the dielectric parameters, and to allow a compact printout, it was felt that a heating index in the range 0-9 would provide adequate information at this stage. The power absorbed in a dielectric medium is given by:

$$P = \frac{\sigma}{2} (|E|)^2 \ W/m^3 \quad \cdots\cdots 5.19$$

For calculation purposes, the program assumes an incident

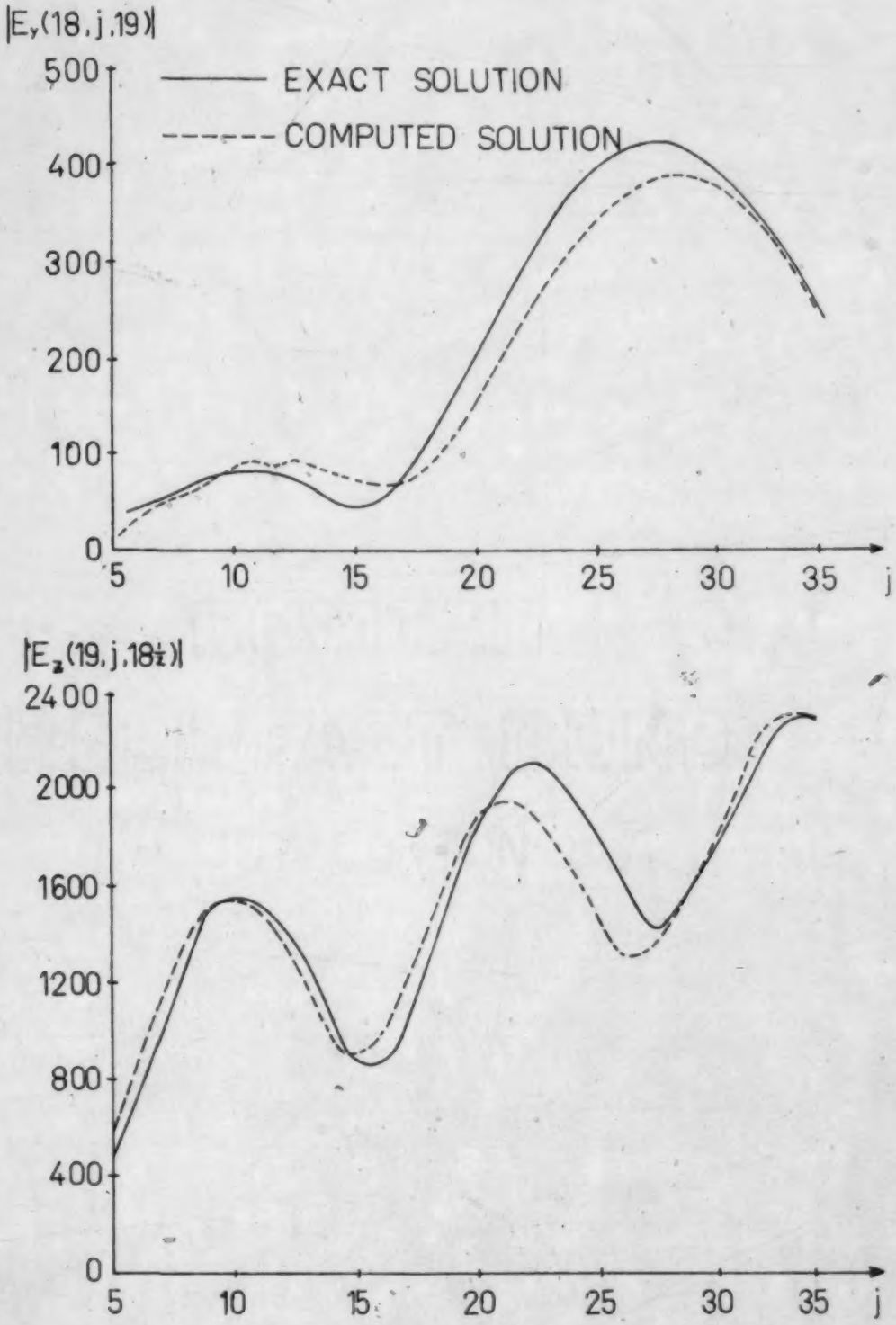

FIGURE 5.3 ELECTRIC FIELDS WITHIN A DIELECTRIC SPHERE

electric field, E_{inc}, of 1000 v/m. Normalising the dissipated power to a unit incident electric field, the following is obtained:

$$P_N = \frac{\sigma}{2}\left(\frac{|E|}{|E_{inc}|}\right)^2 \quad W/m^3 \quad \ldots\ldots 5.20$$

The whole lattice is now scanned for the maximum value, P_{Nmax} of P_N, and a heating index such that $P_{Nmax} = 9$ is defined as follows:

$$HI = \frac{P_N}{P_{Nmax}} \cdot 9 \quad \ldots\ldots 5.21$$

This value is printed out in the same form as the dielectric media lattice. The program also prints out the value of P_{Nmax} so that the power dissipated at any point can be calculated from:

$$P_D = \frac{HI \cdot P_{Nmax}}{9} \cdot 2\eta_0 P_{inc} \quad W/m^3 \quad \ldots\ldots 5.22$$

where P_{inc} is the incident power density in W/m^2 and is the impedance of free space.

Chapter 6. The kidney model

(6.1) Modelling of Heating Processes.

Numerical modelling of microwave heating can be divided into two problems. The first of these is calculating the fields within the body at each point, and the second is solving the heat diffusion equations for temperature distribution based on the energy absorbed at each point. The solution to the first problem depends on the dielectric properties of the body at each space point. These properties depend on the temperature at these points. For the second problem, a knowledge of the thermal properties at each point of the body is necessary. In a situation where the range of temperatures is small, temperature invariance of the dielectric and thermal properties can be assumed, and a final steady state temperature distribution can be calculated by solving both problems. However, when a wide range of temperatures is involved, changes in the dielectric and thermal properties have to be considered. The problem is further complicated by changes of state.

In the present study, microwave heating of a canine kidney is examined, and temperatures between -20° and +20°C are considered. Large changes in dielectric properties as well as a change of state are encountered in this range. One possible solution would be to divide this range into a

number of steps of, say, 10°C, all properties being considered invariant throughout the step. Considering a model with a homogeneous temperature distribution at the lowest temperature, heating could continue until the temperature of some point of the model had been raised by 10°C. Based on the new temperature distribution, a second model of the distribution of dielectric properties could be derived and the process repeated. At the change of state of any point, a negative heating term could be introduced to account for the latent heat of fusion.

Two problems arise with this approach. The first is that the second and subsequent models would be different for each new set of parameters being tested. A system where the new model is automatically derived could no doubt be devised, but the processing time, which is already quite long just for solving the field distribution problem, would become quite unreasonable. In view of these considerations, it is decided to limit the calculations to finding the heating function for various homogeneously distributed temperatures. Notwithstanding these limitations, several valuable conclusions arise, as described in section 6.4.

(6.2) Reasons for Choice of the Canine Kidney.

There are several reasons why it was decided to model heating of the canine kidney. These are:

(1) Because kidneys are one of the more commonly transplanted organs there is considerable interest in their long-term storage. This has led to substantial research on the preservation of this particular organ, much of the reported work being on canine kidneys. In particular, the work of Rajotte (11) on the microwave rewarming of canine kidneys provides a valuable source of data for comparison with the model.

(2) From a modelling point of view, the physical size of the canine kidney is attractive because a fairly detailed model is possible without excessive computer storage requirements. (see section 6.3).

(3) Unlike some organs, the kidney contains several different tissue types, and this better serves to demonstrate the flexibility of the model chosen. In addition reasonable estimates of the dielectric properties of the various tissue types can be made from data available in the literature.

(6.3) Modelling the Kidney.

The first step in producing a reasonable model of the kidney was to establish appropriate planes of symmetry. Figure 6.1 shows dorsal and transverse views of a canine kidney, with typical dimensions of the organ. There are two planes of symmetry, these being the dorsal and the transverse planes. By considering radiation along the axis

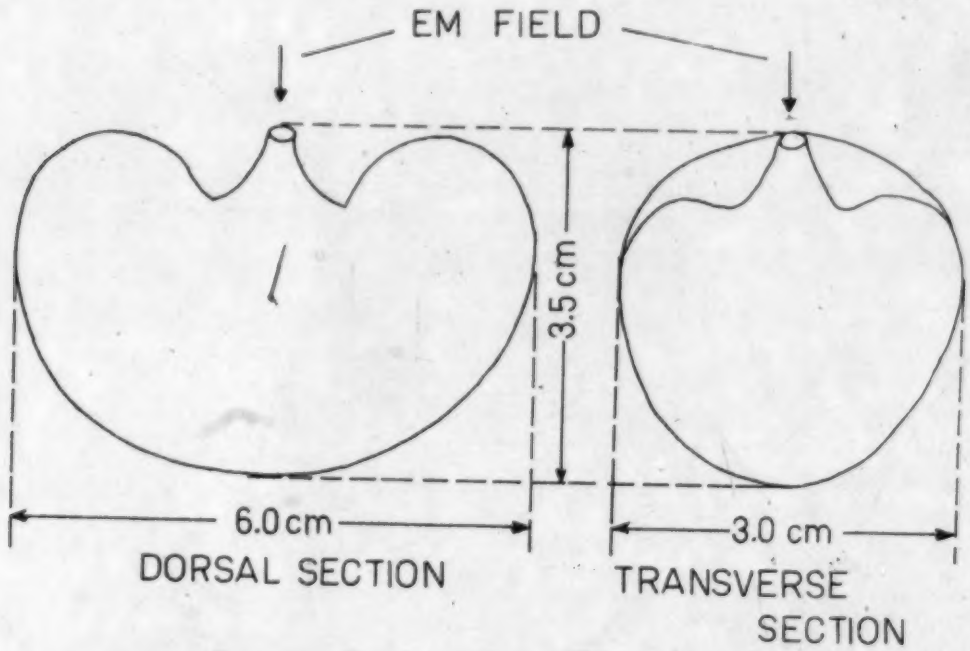

FIGURE 6.1 DORSAL AND TRANSVERSE VIEWS, WITH DIMENSIONS, OF THE CANINE KIDNEY

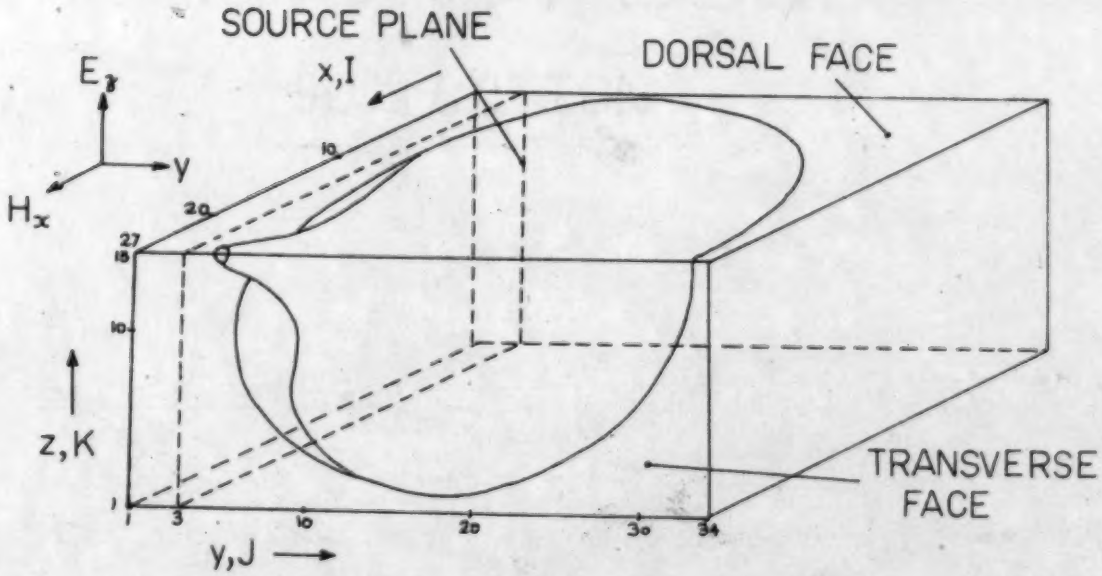

FIGURE 6.2 ARRANGEMENT OF THE LATTICE AROUND THE KIDNEY

indicated on the diagram it is possible to divide the kidney into 4 symmetrical pieces, thus effecting a four times saving in computer storage. The internal structure of the kidney is also approximately symmetrical about the above planes and so this configuration was the one selected. An additional advantage of this choice of symmetry is that radiation from above constitutes a different case from that of radiation from below, and so the same model can easily be used to examine radiation from the two directions.

Having established the planes of symmetry, the next step is to superimpose a lattice of points on the scatterer (kidney). Experience with the test program for a spherical scatterer, as described in Chapter 5, suggested that approximately 14000 lattice points would be reasonable from both CPU time and storage space considerations. Typical CPU time for this number of points was about 4.5 minutes with about 800 Kbytes of storage being used. Although 3 Mbytes of storage was available, the cost of each run of the program was very sensitive to this factor, and it was decided to limit the number of lattice points at this stage. According to the stability criteria discussed in Chapter 5, the spacing of the lattice points must satisfy the following relationship if algorithm stability is to be assured:

$$\delta \leq \frac{1}{20} \lambda_m \approx \frac{1}{20} \cdot \frac{\lambda_o}{\sqrt{\epsilon'_m}} \quad \ldots\ldots 6.1$$

where λ_o is the free space wavelength, λ_m is the minimum wavelength in the scatterer and ϵ'_m is the maximum dielectric constant encountered within the scatterer. Ideally, the model should hold for the highest dielectric constant which would be encountered, in this case, probably that of water (≈80). This gives a δ (at 2.5 Ghz) of:

$$\delta = \frac{1}{2o} \cdot \frac{12.00}{\sqrt{80}} = 0.67 \text{ mm} \quad \cdots\cdots 6.2$$

Considering the dimensions of figures 6.1 and 6.2, the following number of points results (all dimensions in mm):

$$N = \frac{15}{0.67} \times \frac{30}{0.67} \times \frac{35}{0.67} \approx 50{,}000 \text{ pts.} \quad \cdots\cdots 6.3$$

This would require considerably more funds than were available, and so the maximum value used for ϵ' will have to be restricted. In practice, this means that the model will have to be restricted to lower temperatures, where the value of ϵ' is lower. Nevertheless, valuable information can still be obtained. A consideration of the required lengths of the various axes as dictated by the dimensions of the scatterer leads to the following for the number of points along each axis:

$$N_x = \frac{15}{\delta} + 3 \quad \cdots\cdots 6.4$$

$$N_y = \frac{30}{\delta} + 3 \quad \cdots\cdots 6.5$$

} 2 extra lattice spaces are allowed at the edges of the scatterer.

$$N_y = \frac{35}{\delta} + 6 \cdots 66 \Big\}$$ 5 extra spaces are allowed at the end for wave launching.

This allows calculation of the total number of points, and since it was decided to limit these to approximately 14000, the lattice spacing can be found:

$$N = N_x \cdot N_y \cdot N_z = \left(\frac{15}{\delta} + 3\right)\left(\frac{30}{\delta} + 3\right)\left(\frac{35}{\delta} + 6\right) \approx 14{,}000 \quad \cdots 6.7$$

Setting $k = 1/\delta$, and dividing through by 1000:

$$k^3 + 4.71\,k^2 + 7.14\,k - 890 \approx 0 \quad \cdots 6.8$$

i.e. $k \approx 8$ and $\delta \approx 1.25$ mm.

This allows a maximum ε' of 23 at 2.5 Ghz, or values of ε' up to 80 to a frequency of approximately 1.3 Ghz. Assuming that $\delta = 1.25$mm, the following distribution of lattice points is obtained:

$$N_x = 15; \quad N_y = 34; \quad N_z = 27; \quad N = 13770$$

For programming convenience, an extra point was alotted to each of N_x and N_z for a total of 15232 points. Although somewhat higher than 14000, this figure was acceptable. Figure 6.2 shows how the lattice is arranged around the scatterer. The components of the impinging plane wave which is generated at plane J = 3 are also shown.

Having established the arrangement of the kidney within

the lattice, it is now necessary to establish the internal details. To minimise the number of pages of data printout, it was decided to construct 15 planes (K = 1 to K = 15) of 27x34 (IxJ) points. This necessitated visualising the kidney structure at each plane. To aid in this procedure, figures 6.3, and 6.4 were obtained from standard texts of canine anatomy (58,59). Using these drawings, and designating the different tissue types as indicated below, the set of planes of figure 6.5(1) to 6.5(15) were drawn. The bracketed number refers to the plane number. The tissue types are:

1 - medium external to scatterer, in this case, air.
2 - cortex
3 - medulla.
4 - renal sinus (fat).
5 - renal pelvis (connected to ureter).

Although figures 6.3 and 6.4 do not make the disposition of the renal sinus clear, Evans (58) describes it as "surrounding the renal pelvis", and this is how it is considered here. Many details are too small to appear on the 1.25mm lattice. This includes the vascular structure, comprising, among other things, the artery and vein leading to the kidney. Although these are in the same size range as the ureter, the latter becomes the relatively large renal pelvis within the kidney, while the vascular structure becomes progressively smaller as it evolves into the

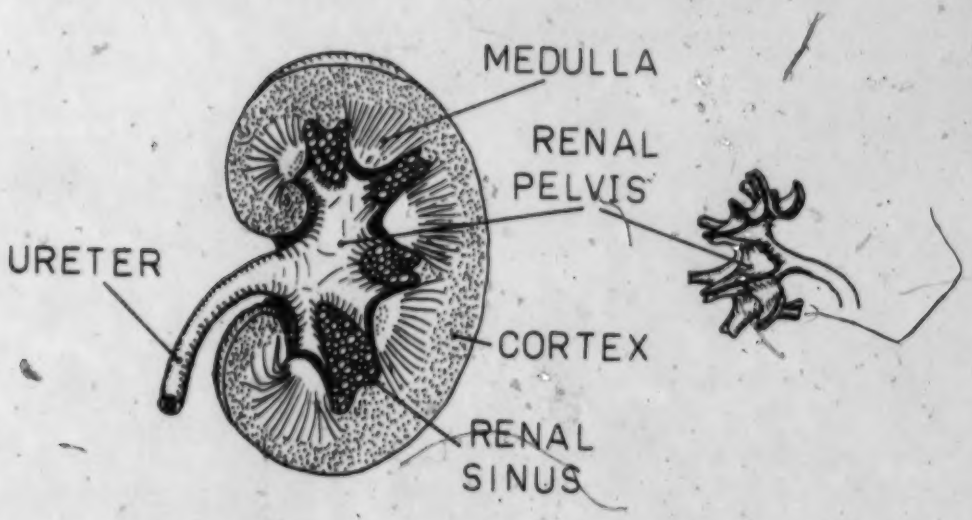

FIGURE 6.3 DORSAL SECTION OF KIDNEY AND CAST OF PELVIS

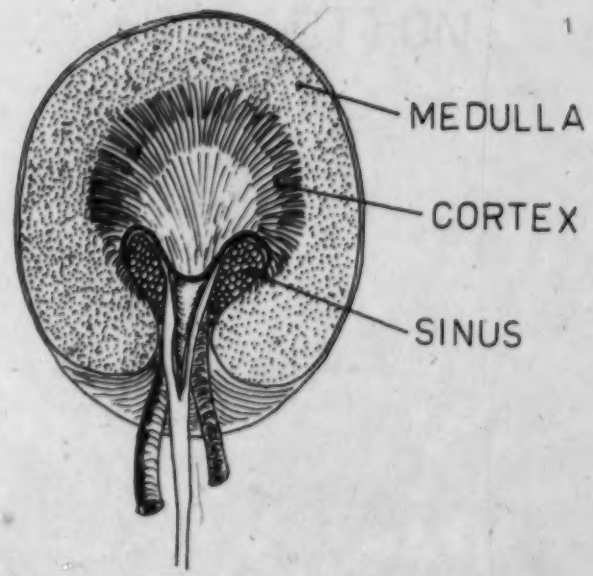

FIGURE 6.4 TRANSVERSE SECTION

FIGURE 6.5(1-15)

The 15 planes of the dielectric media lattice. The media are:

(1) Air

(2) Cortex

(3) Medulla

(4) Renal Sinus

(5) Renal Pelvis

Note: The labelling of the I planes is somewhat unusual and is as follows:

On figures	1	2	3	.....					1	1	1	.....								2	2	2				
									0	1	2									5	6	7				
Corresponds to	1	2	3	.....				10	11	12	.....								25	26	27					

DIELECTRIC MEDIA LATTICE

PLANE K = 1

J	I = 1	2	3	4	5	6	7	8	9	10	11	12	13	14	15	16	17	18	19	20	21	22	23	24	25	26	27
34	1	1	1	1	1	1	1	1	1	1	1	1	1	1	1	1	1	1	1	1	1	1	1	1	1	1	1
33	1	1	1	1	1	1	1	1	1	1	1	1	1	1	1	1	1	1	1	1	1	1	1	1	1	1	1
32	1	1	1	1	1	1	1	1	1	1	1	1	1	1	1	1	1	1	1	1	1	1	1	1	1	1	1
31	1	1	1	1	1	1	1	1	1	1	1	1	1	1	1	1	1	1	1	1	1	1	1	1	1	1	1
30	1	1	1	1	1	1	1	1	1	1	1	1	1	1	1	1	1	1	1	1	1	1	1	1	1	1	1
29	1	1	1	1	1	1	1	1	1	1	1	1	1	1	1	1	1	1	1	1	1	1	1	1	1	1	1
28	1	1	1	1	1	1	1	1	1	1	1	1	1	1	1	1	1	1	1	1	1	1	1	1	1	1	1
27	1	1	1	1	1	1	1	1	1	1	1	1	1	1	1	1	1	1	1	1	1	1	1	1	1	1	1
26	1	1	1	1	1	1	1	1	1	1	1	1	1	1	1	1	1	1	1	1	1	1	1	1	1	1	1
25	1	1	1	1	1	1	1	1	1	1	1	1	1	1	1	1	1	1	1	1	1	1	1	1	1	1	1
24	1	1	1	1	1	1	1	1	1	1	1	1	1	1	1	1	1	1	1	1	1	1	1	1	1	1	1
23	1	1	1	1	1	1	1	1	1	1	1	1	1	1	1	1	1	1	1	1	1	1	1	1	1	1	1
22	1	1	1	1	1	1	1	1	1	1	1	1	1	1	1	1	1	1	1	1	1	1	1	1	1	1	1
21	1	1	1	1	1	1	1	1	1	1	1	1	1	1	1	1	1	1	1	1	1	1	1	1	1	1	1
20	1	1	1	1	1	1	1	1	1	1	1	1	1	1	1	1	1	1	1	1	1	1	1	1	1	1	1
19	1	1	1	1	1	1	1	1	1	1	1	1	1	1	1	1	1	1	1	1	1	1	1	1	1	1	1
18	1	1	1	1	1	1	1	1	1	1	1	1	1	1	1	1	1	1	1	1	1	1	1	1	1	1	1
17	1	1	1	1	1	1	1	1	1	1	1	1	1	1	1	1	1	1	1	1	1	1	1	1	1	1	1
16	1	1	1	1	1	1	1	1	1	1	1	1	1	1	1	1	1	1	1	1	1	1	1	1	1	1	1
15	1	1	1	1	1	1	1	1	1	1	1	1	1	1	1	1	1	1	1	1	1	1	1	1	1	1	1
14	1	1	1	1	1	1	1	1	1	1	1	1	1	1	1	1	1	1	1	1	1	1	1	1	1	1	1
13	1	1	1	1	1	1	1	1	1	1	1	1	1	1	1	1	1	1	1	1	1	1	1	1	1	1	1
12	1	1	1	1	1	1	1	1	1	1	1	1	1	1	1	1	1	1	1	1	1	1	1	1	1	1	1
11	1	1	1	1	1	1	1	1	1	1	1	1	1	1	1	1	1	1	1	1	1	1	1	1	1	1	1
10	1	1	1	1	1	1	1	1	1	1	1	1	1	1	1	1	1	1	1	1	1	1	1	1	1	1	1
9	1	1	1	1	1	1	1	1	1	1	1	1	1	1	1	1	1	1	1	1	1	1	1	1	1	1	1
8	1	1	1	1	1	1	1	1	1	1	1	1	1	1	1	1	1	1	1	1	1	1	1	1	1	1	1
7	1	1	1	1	1	1	1	1	1	1	1	1	1	1	1	1	1	1	1	1	1	1	1	1	1	1	1
6	1	1	1	1	1	1	1	1	1	1	1	1	1	1	1	1	1	1	1	1	1	1	1	1	1	1	1
5	1	1	1	1	1	1	1	1	1	1	1	1	1	1	1	1	1	1	1	1	1	1	1	1	1	1	1
4	1	1	1	1	1	1	1	1	1	1	1	1	1	1	1	1	1	1	1	1	1	1	1	1	1	1	1
3	1	1	1	1	1	1	1	1	1	1	1	1	1	1	1	1	1	1	1	1	1	1	1	1	1	1	1
2	1	1	1	1	1	1	1	1	1	1	1	1	1	1	1	1	1	1	1	1	1	1	1	1	1	1	1
1	1	1	1	1	1	1	1	1	1	1	1	1	1	1	1	1	1	1	1	1	1	1	1	1	1	1	1

DIELECTRIC MEDIA LATTICE

PLANE K = 2

J																											
34	1	1	1	1	1	1	1	1	1	1	1	1	1	1	1	1	1	1	1	1	1	1	1	1	1	1	1
33	1	1	1	1	1	1	1	1	1	1	1	1	1	1	1	1	1	1	1	1	1	1	1	1	1	1	1
32	1	1	1	1	1	1	1	1	1	1	1	1	1	1	1	1	1	1	1	1	1	1	1	1	1	1	1
31	1	1	1	1	1	1	1	1	1	1	1	1	1	1	1	1	1	1	1	1	1	1	1	1	1	1	1
30	1	1	1	1	1	1	1	1	1	1	1	1	1	1	1	1	1	1	1	1	1	1	1	1	1	1	1
29	1	1	1	1	1	1	1	1	1	1	1	1	1	1	1	1	1	1	1	1	1	1	1	1	1	1	1
28	1	1	1	1	1	1	1	1	1	1	1	1	1	1	1	1	1	1	1	1	1	1	1	1	1	1	1
27	1	1	1	1	1	1	1	1	1	1	1	1	1	1	1	1	1	1	1	1	1	1	1	1	1	1	1
26	1	1	1	1	1	1	1	1	1	1	1	1	1	1	1	1	1	1	1	1	1	1	1	1	1	1	1
25	1	1	1	1	1	1	1	1	1	1	1	1	1	1	1	1	1	1	1	1	1	1	1	1	1	1	1
24	1	1	1	1	1	1	1	1	1	1	1	1	1	1	1	1	1	1	1	1	1	1	1	1	1	1	1
23	1	1	1	1	1	1	1	1	1	1	1	1	1	1	1	1	1	1	1	1	1	1	1	1	1	1	1
22	1	1	1	1	1	1	1	1	1	1	1	1	1	1	1	1	1	1	1	1	1	1	1	1	1	1	1
21	1	1	1	1	1	1	1	1	1	1	1	1	1	1	1	1	1	1	1	1	1	1	1	1	1	1	1
20	1	1	1	1	1	1	1	1	1	1	1	1	1	1	1	1	1	1	1	1	1	1	1	1	1	1	1
19	1	1	1	1	1	1	1	1	1	1	1	1	1	1	1	1	1	1	1	1	1	1	1	1	1	1	1
18	1	1	1	1	1	1	1	1	1	1	1	1	1	1	1	1	1	1	1	1	1	1	1	1	1	1	1
17	1	1	1	1	1	1	1	1	1	1	1	1	1	1	1	1	1	1	1	1	1	1	1	1	1	1	1
16	1	1	1	1	1	1	1	1	1	1	1	1	1	1	1	1	1	1	1	1	1	1	1	1	1	1	1
15	1	1	1	1	1	1	1	1	1	1	1	1	1	1	1	1	1	1	1	1	1	1	1	1	1	1	1
14	1	1	1	1	1	1	1	1	1	1	1	1	1	1	1	1	1	1	1	1	1	1	1	1	1	1	1
13	1	1	1	1	1	1	1	1	1	1	1	1	1	1	1	1	1	1	1	1	1	1	1	1	1	1	1
12	1	1	1	1	1	1	1	1	1	1	1	1	1	1	1	1	1	1	1	1	1	1	1	1	1	1	1
11	1	1	1	1	1	1	1	1	1	1	1	1	1	1	1	1	1	1	1	1	1	1	1	1	1	1	1
10	1	1	1	1	1	1	1	1	1	1	1	1	1	1	1	1	1	1	1	1	1	1	1	1	1	1	1
9	1	1	1	1	1	1	1	1	1	1	1	1	1	1	1	1	1	1	1	1	1	1	1	1	1	1	1
8	1	1	1	1	1	1	1	1	1	1	1	1	1	1	1	1	1	1	1	1	1	1	1	1	1	1	1
7	1	1	1	1	1	1	1	1	1	1	1	1	1	1	1	1	1	1	1	1	1	1	1	1	1	1	1
6	1	1	1	1	1	1	1	1	1	1	1	1	1	1	1	1	1	1	1	1	1	1	1	1	1	1	1
5	1	1	1	1	1	1	1	1	1	1	1	1	1	1	1	1	1	1	1	1	1	1	1	1	1	1	1
4	1	1	1	1	1	1	1	1	1	1	1	1	1	1	1	1	1	1	1	1	1	1	1	1	1	1	1
3	1	1	1	1	1	1	1	1	1	1	1	1	1	1	1	1	1	1	1	1	1	1	1	1	1	1	1
2	1	1	1	1	1	1	1	1	1	1	1	1	1	1	1	1	1	1	1	1	1	1	1	1	1	1	1
1	1	1	1	1	1	1	1	1	1	1	1	1	1	1	1	1	1	1	1	1	1	1	1	1	1	1	1

I	1	2	3	4	5	6	7	8	9	10	11	12	13	14	15	16	17	18	19	20	21	22	23	24	25	26	27

DIELECTRIC MEDIA LATTICE

PLANE K = 3

J																										
34	1	1	1	1	1	1	1	1	1	1	1	1	1	1	1	1	1	1	1	1	1	1	1	1	1	1
33	1	1	1	1	1	1	1	1	1	1	1	1	1	1	1	1	1	1	1	1	1	1	1	1	1	1
32	1	1	1	1	1	1	1	1	1	1	1	1	1	1	1	1	1	1	1	1	1	1	1	1	1	1
31	1	1	1	1	1	1	1	1	1	1	1	1	1	1	1	1	1	1	1	1	1	1	1	1	1	1
30	1	1	1	1	1	1	1	1	1	1	1	1	1	1	1	1	1	1	1	1	1	1	1	1	1	1
29	1	1	1	1	1	1	1	1	1	1	1	1	1	1	1	1	1	1	1	1	1	1	1	1	1	1
28	1	1	1	1	1	1	1	1	1	1	1	1	1	1	1	1	1	1	1	1	1	1	1	1	1	1
27	1	1	1	1	1	1	1	1	1	1	1	1	1	1	1	1	1	1	1	1	1	1	1	1	1	1
26	1	1	1	1	1	1	1	1	1	1	1	1	1	1	1	1	1	1	1	1	1	1	1	1	1	1
25	1	1	1	1	1	1	1	1	1	1	1	1	1	1	1	1	1	1	1	1	1	1	1	1	1	1
24	1	1	1	1	1	1	1	1	1	1	1	1	1	1	1	1	1	1	1	1	1	1	1	1	1	1
23	1	1	1	1	1	1	1	1	1	1	1	1	1	1	1	1	1	1	1	1	1	1	1	1	1	1
22	1	1	1	1	1	1	1	1	1	1	1	1	1	1	1	1	1	1	1	1	1	1	1	1	2	2
21	1	1	1	1	1	1	1	1	1	1	1	1	1	1	1	1	1	1	1	1	1	1	2	2	2	2
20	1	1	1	1	1	1	1	1	1	1	1	1	1	1	1	1	1	1	1	1	1	1	2	2	2	2
19	1	1	1	1	1	1	1	1	1	1	1	1	1	1	1	1	1	1	1	1	1	1	1	1	1	1
18	1	1	1	1	1	1	1	1	1	1	1	1	1	1	1	1	1	1	1	1	1	1	1	1	1	1
17	1	1	1	1	1	1	1	1	1	1	1	1	1	1	1	1	1	1	1	1	1	1	1	1	1	1
16	1	1	1	1	1	1	1	1	1	1	1	1	1	1	1	1	1	1	1	1	1	1	1	1	1	1
15	1	1	1	1	1	1	1	1	1	1	1	1	1	1	1	1	1	1	1	1	1	1	1	1	1	1
14	1	1	1	1	1	1	1	1	1	1	1	1	1	1	1	1	1	1	1	1	1	1	1	1	1	1
13	1	1	1	1	1	1	1	1	1	1	1	1	1	1	1	1	1	1	1	1	1	1	1	1	1	1
12	1	1	1	1	1	1	1	1	1	1	1	1	1	1	1	1	1	1	1	1	1	1	1	1	1	1
11	1	1	1	1	1	1	1	1	1	1	1	1	1	1	1	1	1	1	1	1	1	1	1	1	1	1
10	1	1	1	1	1	1	1	1	1	1	1	1	1	1	1	1	1	1	1	1	1	1	1	1	1	1
9	1	1	1	1	1	1	1	1	1	1	1	1	1	1	1	1	1	1	1	1	1	1	1	1	1	1
8	1	1	1	1	1	1	1	1	1	1	1	1	1	1	1	1	1	1	1	1	1	1	1	1	1	1
7	1	1	1	1	1	1	1	1	1	1	1	1	1	1	1	1	1	1	1	1	1	1	1	1	1	1
6	1	1	1	1	1	1	1	1	1	1	1	1	1	1	1	1	1	1	1	1	1	1	1	1	1	1
5	1	1	1	1	1	1	1	1	1	1	1	1	1	1	1	1	1	1	1	1	1	1	1	1	1	1
4	1	1	1	1	1	1	1	1	1	1	1	1	1	1	1	1	1	1	1	1	1	1	1	1	1	1
3	1	1	1	1	1	1	1	1	1	1	1	1	1	1	1	1	1	1	1	1	1	1	1	1	1	1
2	1	1	1	1	1	1	1	1	1	1	1	1	1	1	1	1	1	1	1	1	1	1	1	1	1	1
1	1	1	1	1	1	1	1	1	1	1	1	1	1	1	1	1	1	1	1	1	1	1	1	1	1	1

I	1	2	3	4	5	6	7	8	9	10	11	12	13	14	15	16	17	18	19	20	21	22	23	24	25	26	27

DIELECTRIC MEDIA LATTICE

PLANE K = 4

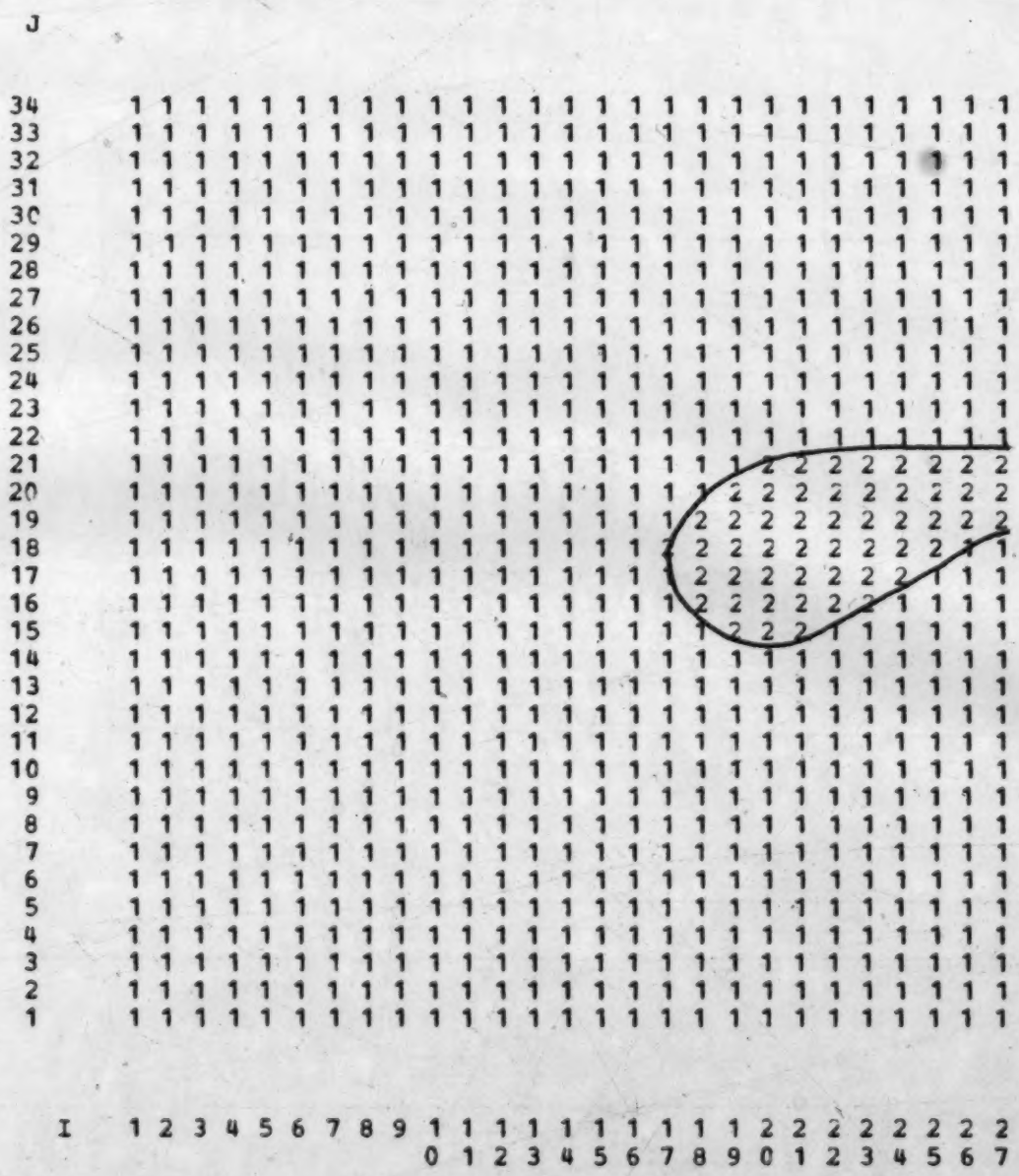

DIELECTRIC MEDIA LATTICE

PLANE K = 5

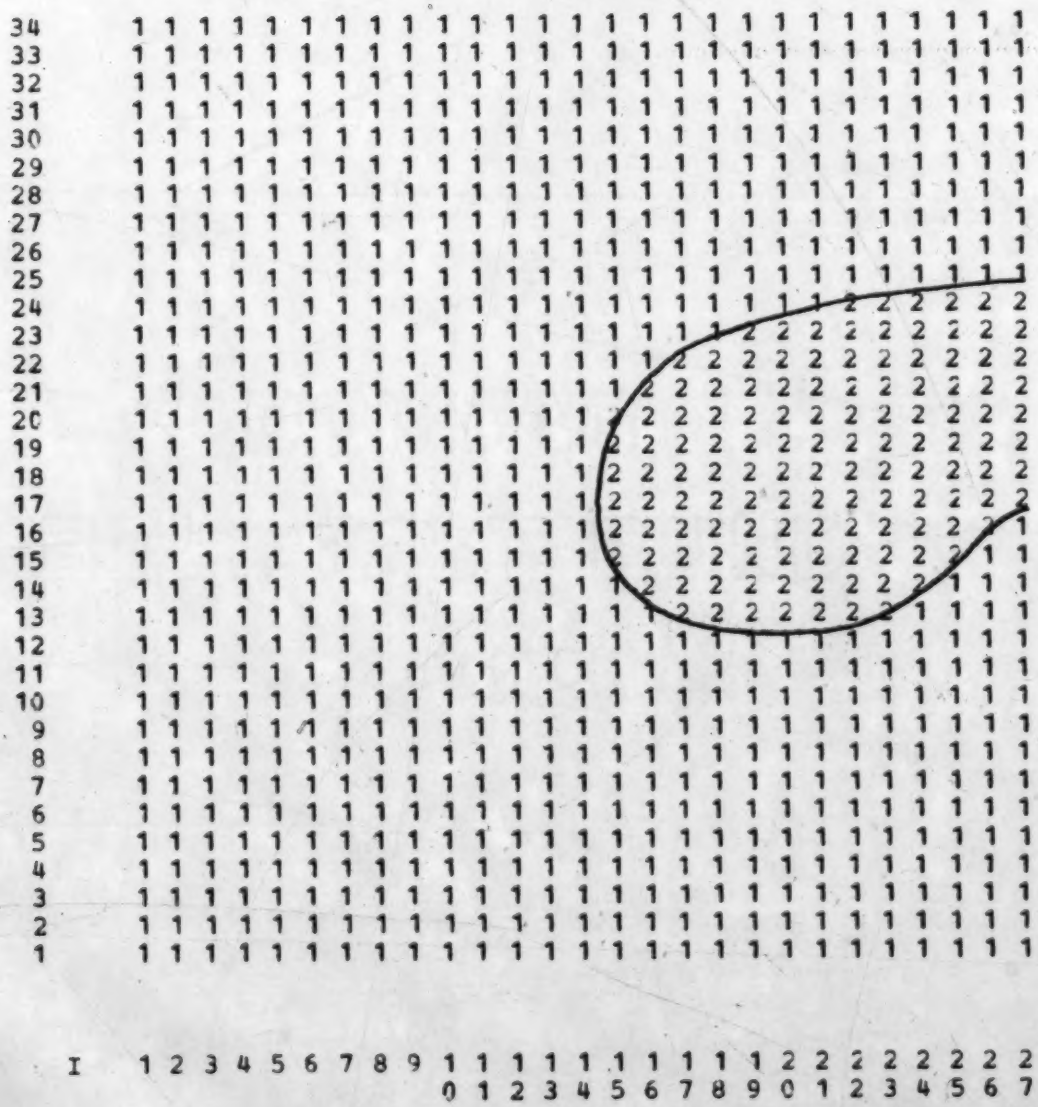

DIELECTRIC MEDIA LATTICE

PLANE K = 6

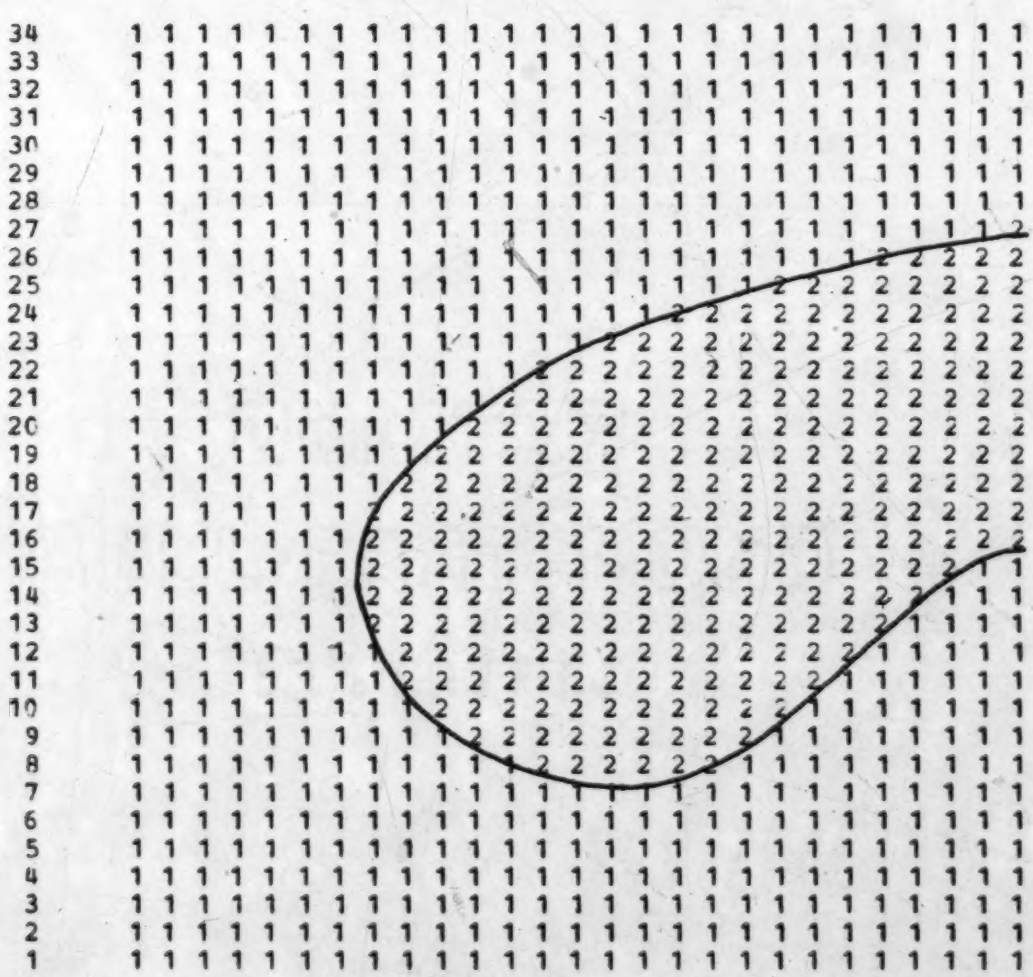

DIELECTRIC MEDIA LATTICE

PLANE K = 7

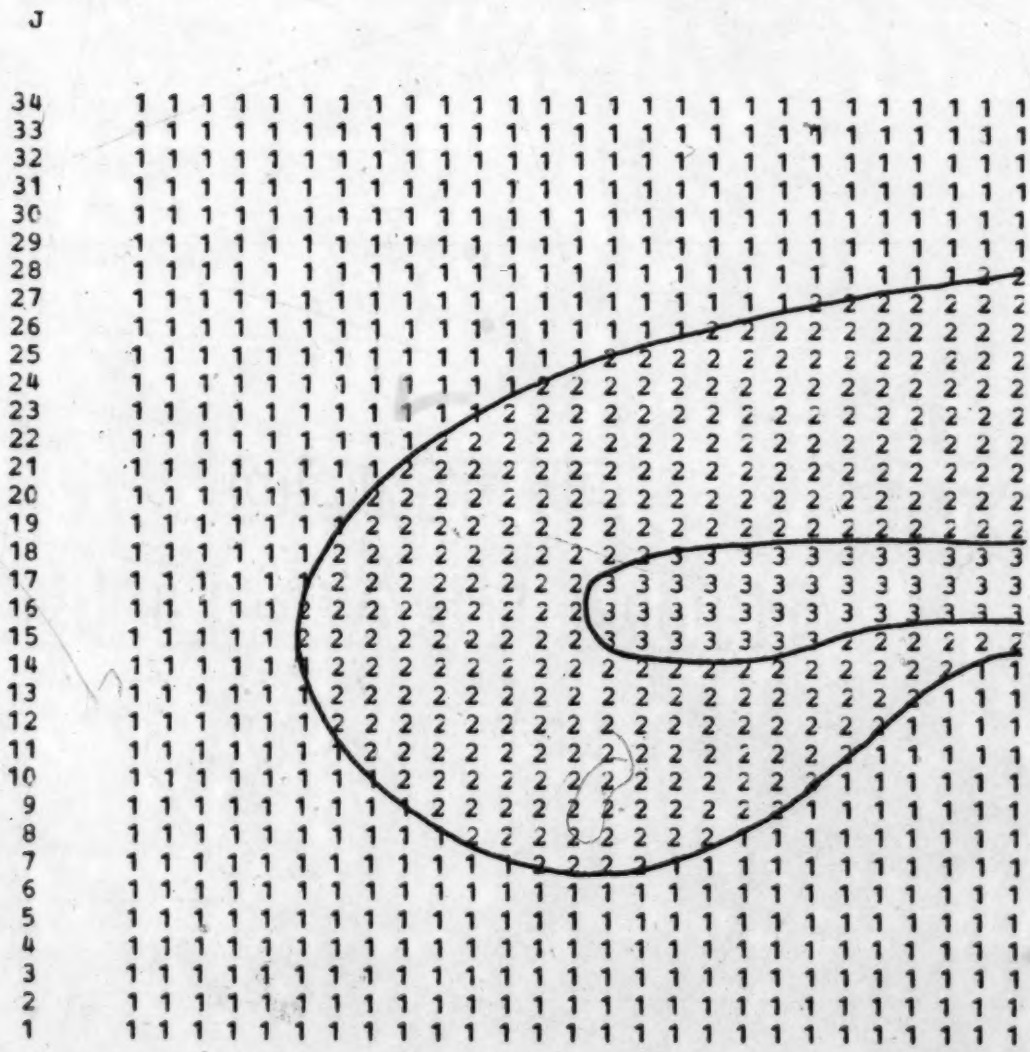

DIELECTRIC MEDIA LATTICE

PLANE K = 8

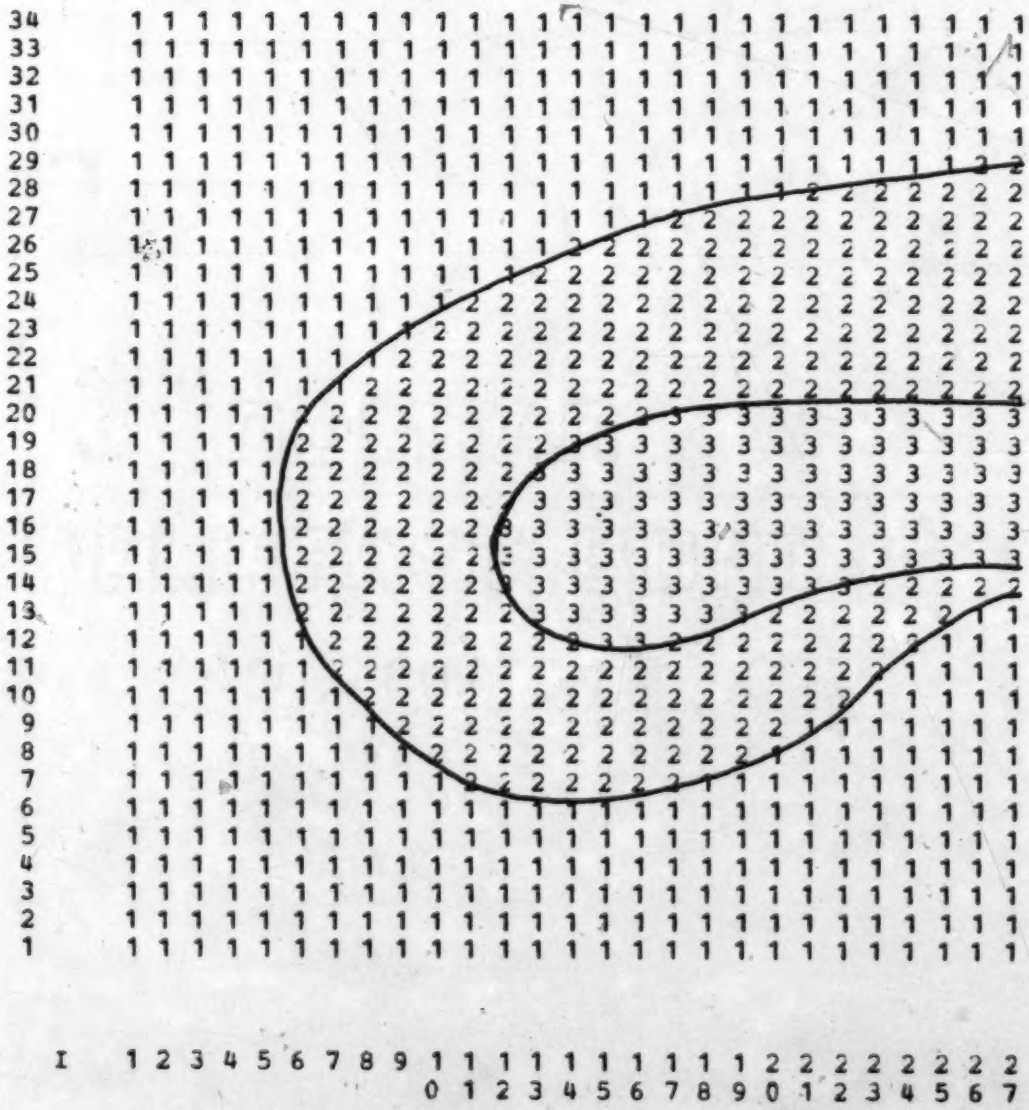

DIELECTRIC MEDIA LATTICE

PLANE K = 9

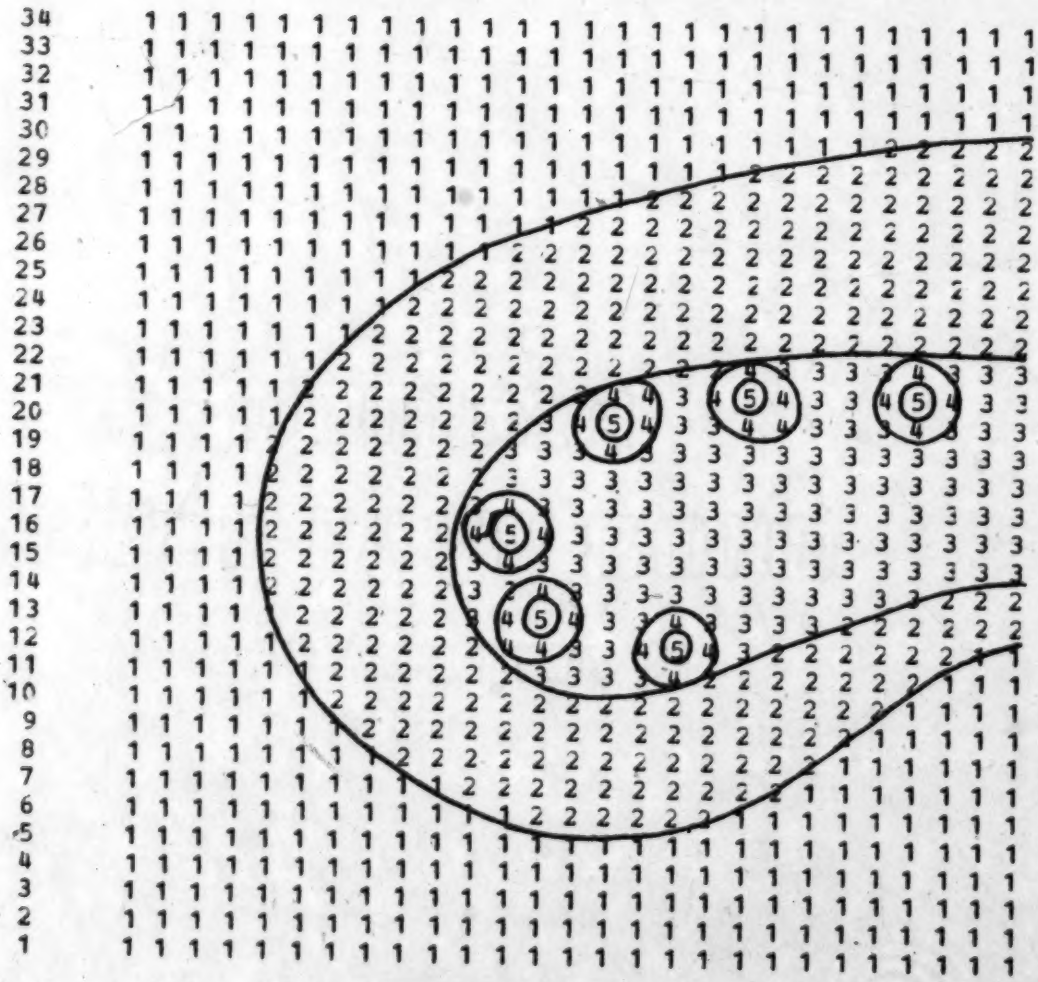

DIELECTRIC MEDIA LATTICE

PLANE K = 10

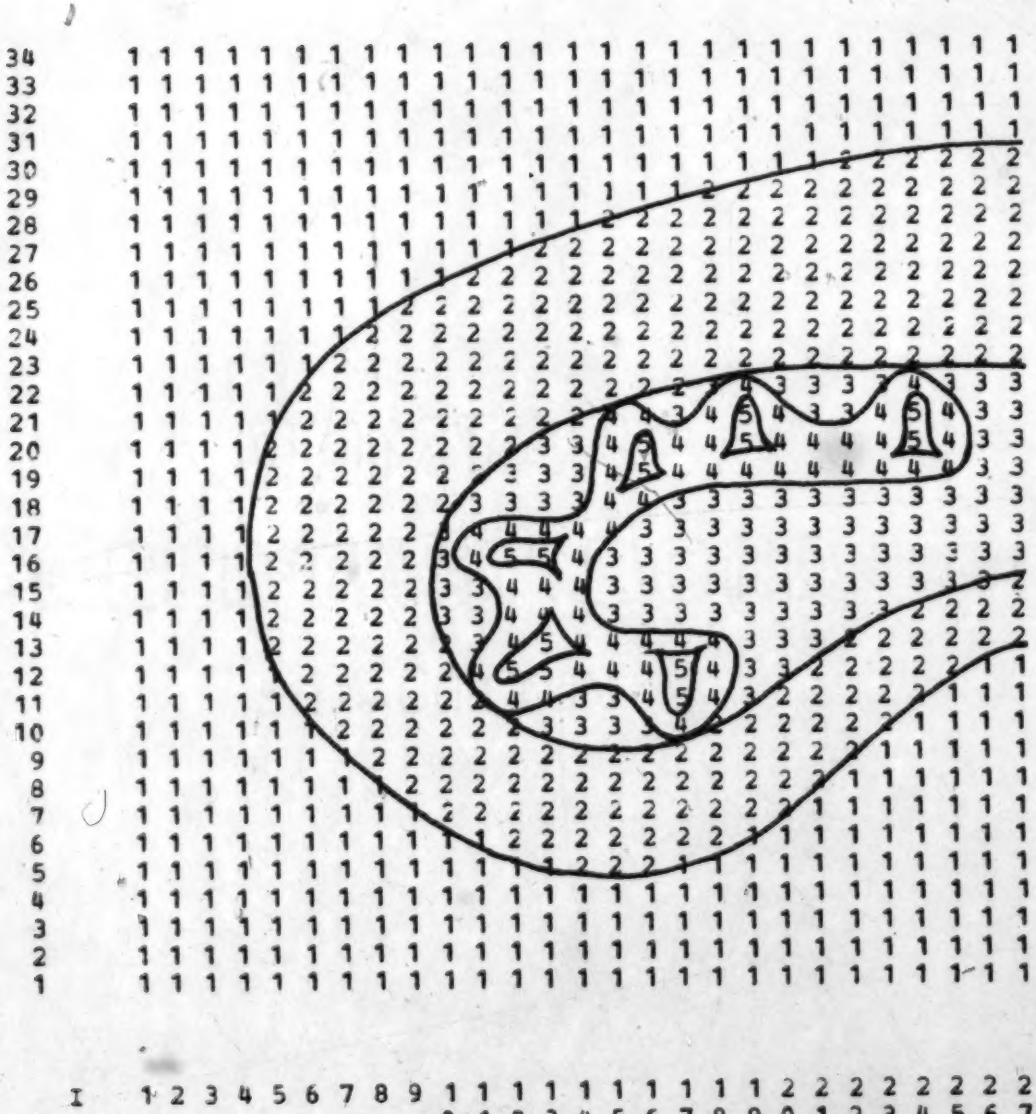

DIELECTRIC MEDIA LATTICE

PLANE K = 11

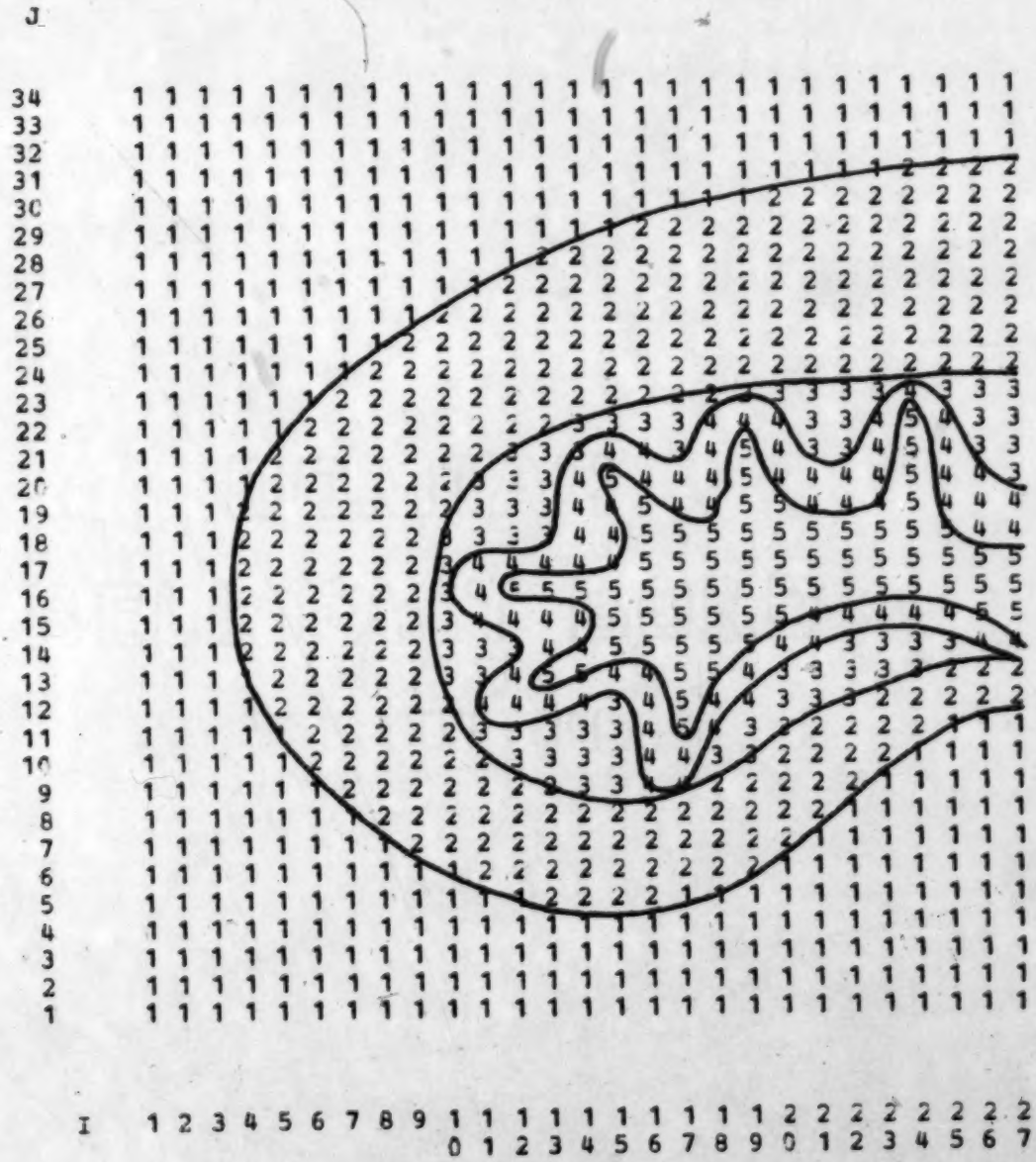

DIELECTRIC MEDIA LATTICE

PLANE K = 12

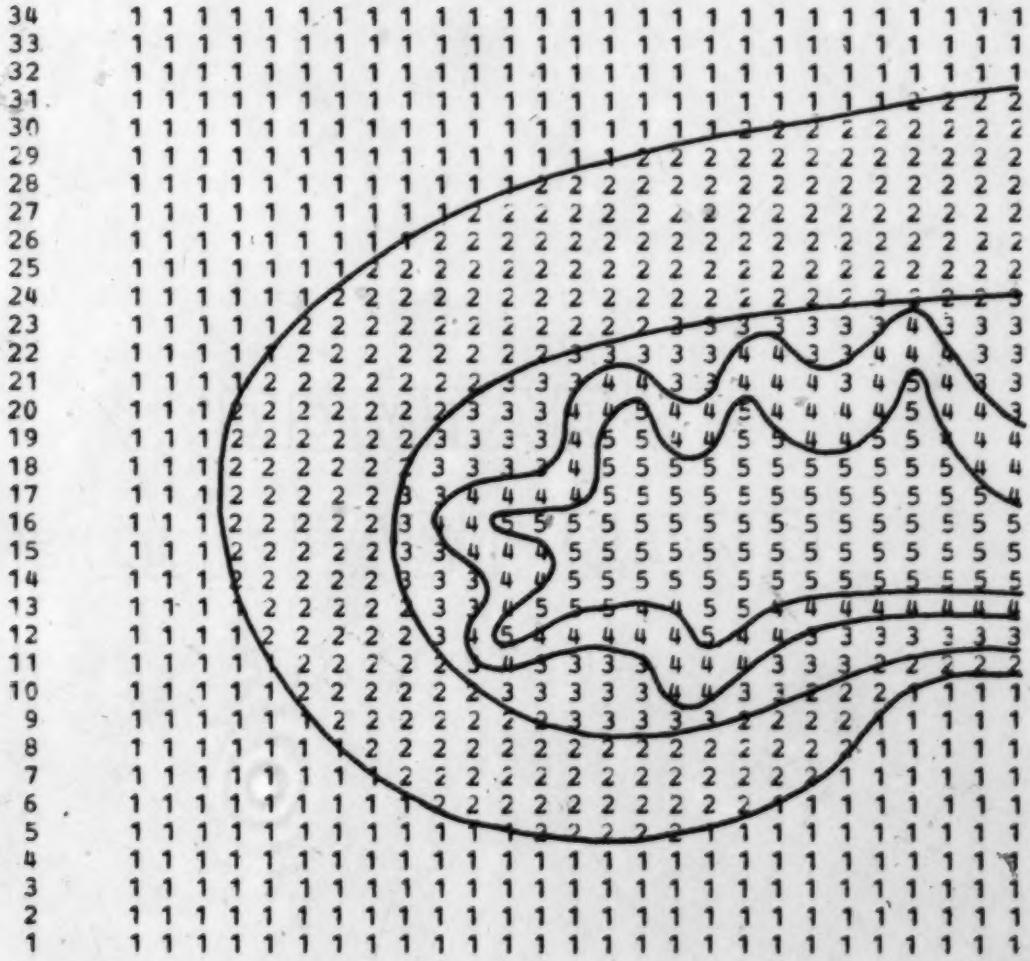

DIELECTRIC MEDIA LATTICE

PLANE K = 13

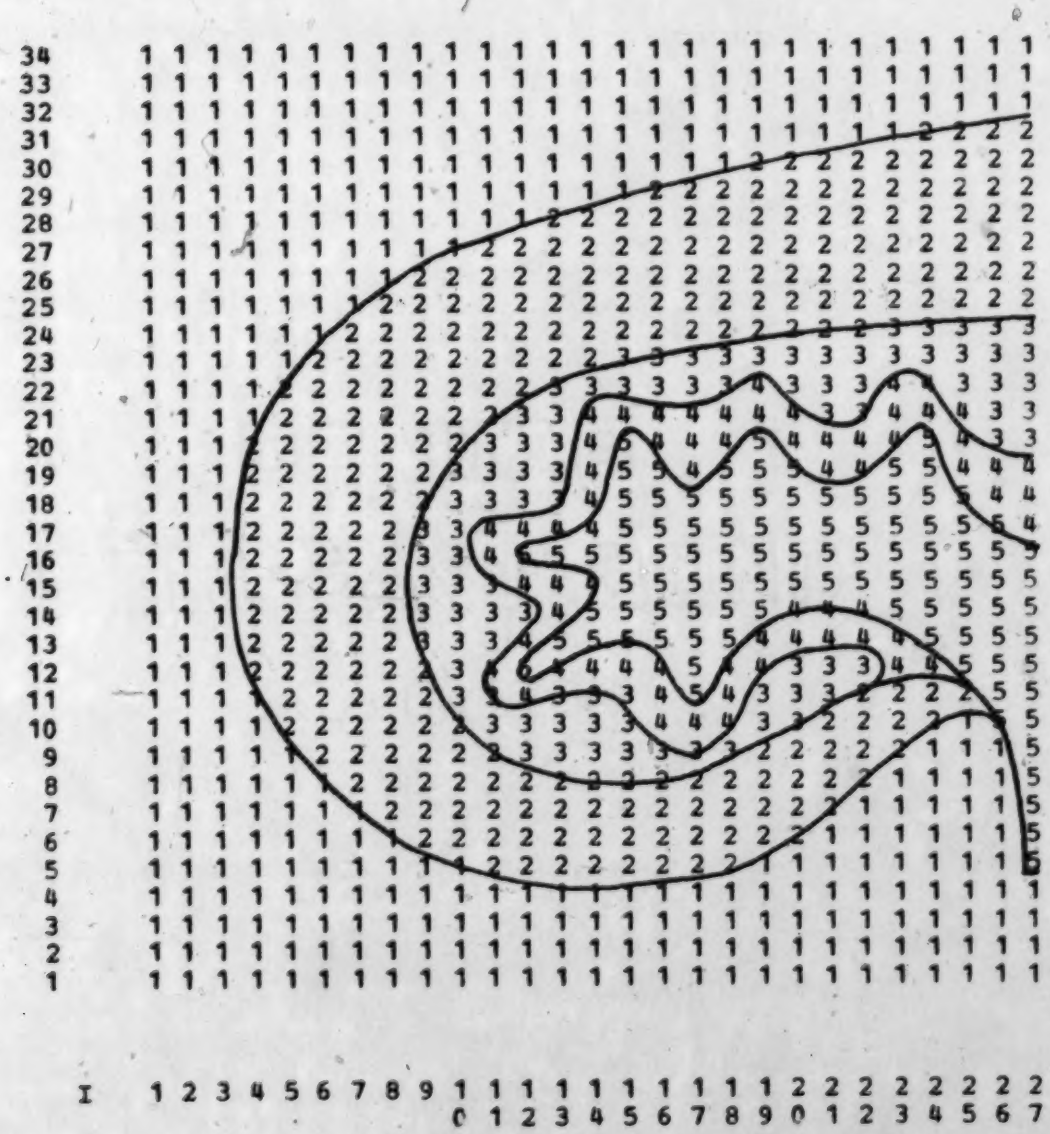

DIELECTRIC MEDIA LATTICE

PLANE K = 14

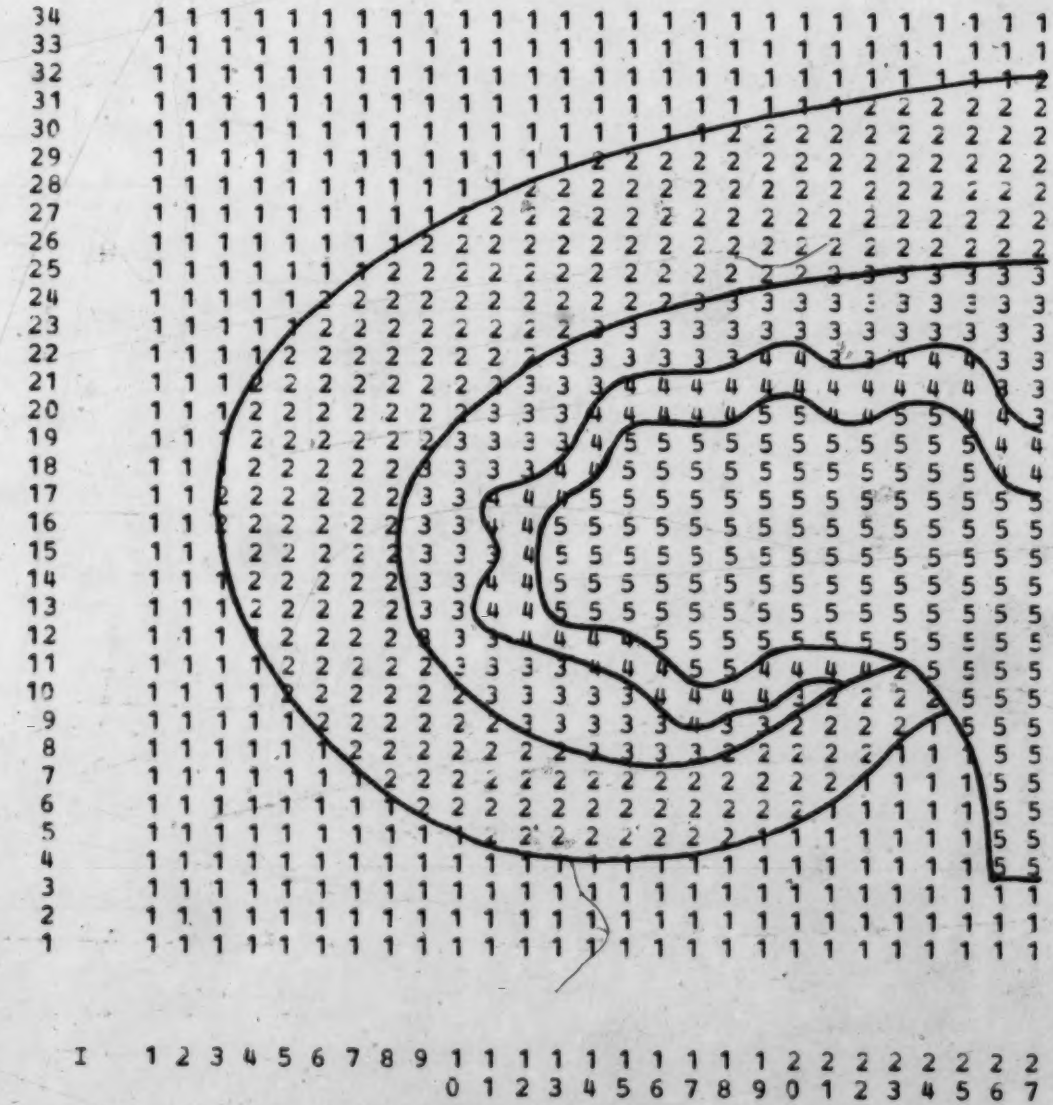

DIELECTRIC MEDIA LATTICE

PLANE K = 15

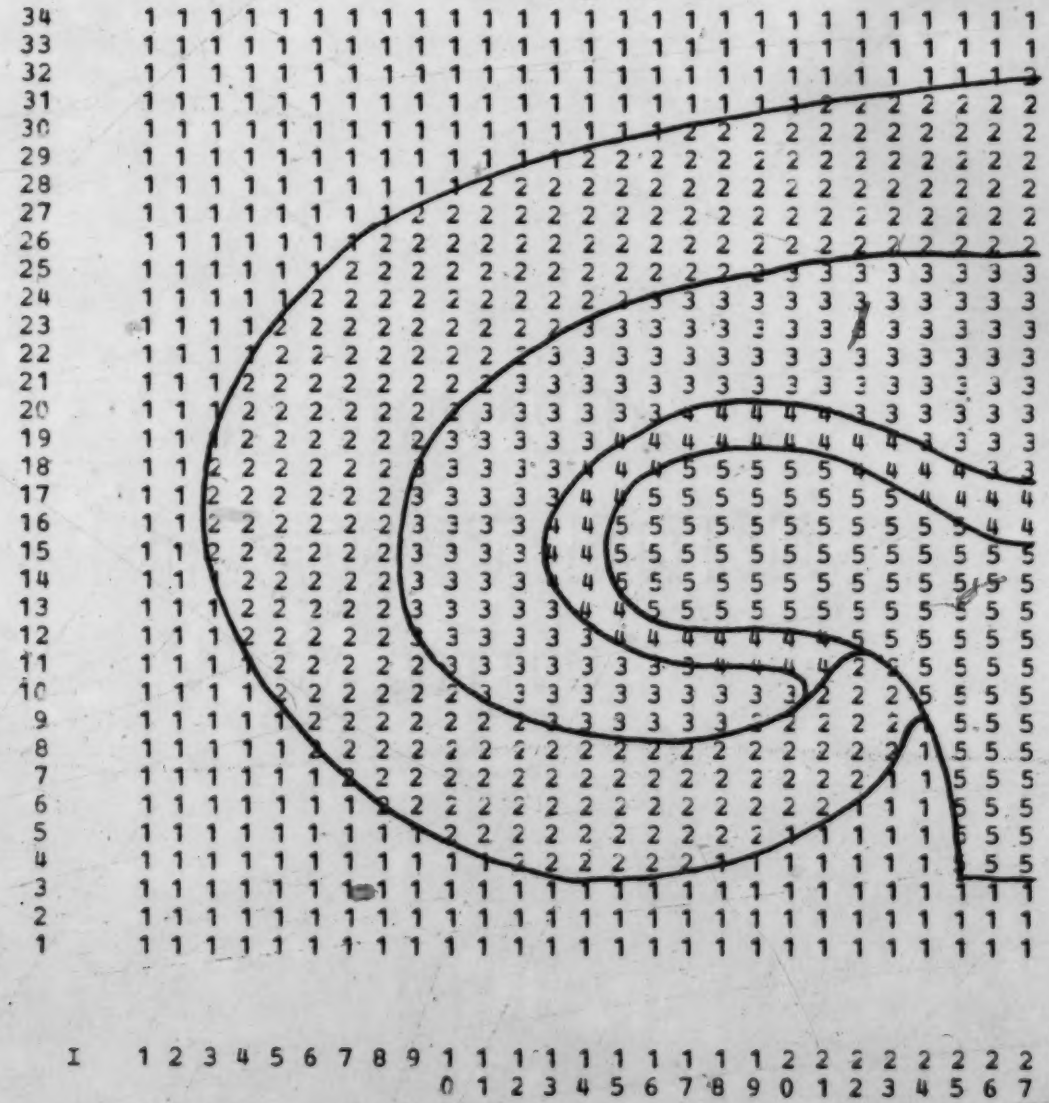

capillary system. Because of the importance of the vascular structure in the perfusion of kidneys during the freezing process, it is hoped that some means will be found to incorporate this structure into the model. The limitation imposed by the exclusion of this structure is that alternative means must be found to account for the presence of the perfusate within the other parts of the kidney. This is done by appropriate choice of dielectric properties.

(6.4) The Dielectric Properties of the Model.

In order to make use of the model, it is necessary to assign dielectric values to the various media. The only known source of data for the properties of DMSO-perfused kidney are the data of Foster et al (22), and this data applies only to media 2 and 3 at 1 Ghz. In addition, the degree of perfusion of the various media is not definitely established. Therefore, estimates based on the existing literature data and assumptions regarding the degree of perfusion of the various media must be made in order to assign suitable values for the model. At this stage, the model can be used to make predictions in two important areas. These are (a) in establishing the amount of energy absorbed by the kidney at low temperatures, thereby allowing some estimates of possible heating rates, and (b) the effect of different parameters on heating uniformity.

It was decided to examine the two above areas in the light of four different parameters. These are:

(1) Illumination frequency: The two ISM bands primarily used for microwave heating are at 915 Mhz and at 2450 Mhz. Illumination frequencies of 1000 and 2500 Mhz were used in the model because much of the existing data pertains to these frequencies.

(2) Cryoprotective Solutions: Most reported studies of the cryopreservation of kidney tissue have used 10% DMSO. For purposes of comparison, it is interesting to examine the effect of a 1% DMSO perfusate as well.

(3) Temperature of model: For reasons outlined earlier, it is difficult to model a continuous heating process, and so it is necessary to choose a particular temperature at which the model is to be tested. At 2500 Mhz, the maximum temperature at which the model can be used is limited by the maximum dielectric constant encountered. To give some idea of how heating patterns would change with temperature, it is interesting to examine the model at different temperatures. The choice of -20°C and -10°C was most reasonable at 2500 Mhz. At 1000 Mhz, there is no temperature limitation, and so, in addition to the choices of -20°C and -10°C, a temperature of +20°C was also selected. The use of the model at temperatures below -20°C was precluded by lack of data.

(4) The kidney state: 4 different kidney states are defined in this case. Foster's measurements (22) and the relevant measurements based on frozen foods and other data, as

presented in tables 6.1, 6.2 and 6.3 were used to obtain appropriate estimates of the dielectric properties of the various media. Table 6.4 shows the properties used in the model as estimated on the basis of the discussion below. The four kidney states are:

(a) No perfusion: This state was chosen for purposes of comparison, and is also useful for examining the effect of the perfusate on the heating rate.

(b) Selective perfusion: Most perfusion studies suggest that the cortex and medulla, which have an extensive vascular system, are well perfused. The pelvis, which contains urine, would certainly undergo some perfusion by virtue of the penetrative properties of DMSO. The renal sinus, on the other hand, is comprised of fat, a medium in which perfusion appears to be minimal. For the present work, a well perfused cortex and medulla, a partially perfused pelvis and an unperfused sinus were selected.

(c) Pelvis completely filled with perfusate: This is an unrealistic assumption from a physiological point of view, but because of the uncertainties of the dielectric properties of urine, it was decided to assume that the pelvis was completely filled with the perfusate, and would therefore be more lossy than assumed in (b). Because some of the tubular structure of the pelvis appears in the model, this condition would also serve to give an indication of the behaviour of the vascular system, which normally also contains perfusate. As previously explained, the vascular

structure does not appear on the model.

If all possible combinations of the above parameters were to be modelled, the program would have to be run 36 times, and even if appropriate funds were available, meaningful analysis of the data would be an enormous task. Therefore, a datum set of parameters was selected from the above possibilities, and selected changes from the datum were made in order to examine the effect of the other parameters. The following set of conditions were chosen as the datum because they represent the situation most likely to be encountered in the real world. The conditions are:

(a) Illumination at 2500 Mhz.

(b) 10% DMSO perfusate. Realistically the perfusate would also contain some ionic components, such as NaCl, but reference to figures 6.17 and 6.18 suggest that these have little effect on the dielectric properties.

(c) A temperature of -20°C. This would be the case with the lowest loss and would be most representative of the low temperature heating rate.

(d) The partially perfused model. This is most consistent with the measurements reported in the literature.

Table 6.4 shows the 8 different sets of parameters to which the model was applied. The dielectric properties assigned to the media in the table were calculated on the

basis of the following assumptions:

(1) The frequency dependence of the cortex and medulla was

Material	ε' / σ	Freq. Mhz.	-20°C	-10°C	+20°C	Ref.
Beef	ε'	900	4.8 *	6.2 *	58.0 *	46
	σ		0.046	0.103	1.226	
	ε'	2700	4.8 *	6.2 *	47.7 *	39
	σ		0.079	0.218	1.863	
Unperfused Kidney	ε'	1000	2.0 *	3.3 *	60.0**	22
	σ		0.002	0.008	1.250	
	ε'	2500	2.0	3.3	50.0	
	σ		0.003	0.017	1.900	
1% Perfused Kidney	ε'	1000	2.1	3.5	60.0	
	σ		0.003	0.011	1.220	
	ε'	2500	2.1	3.5	50.0	
	σ		0.004	0.023	1.86	
10% Perfused Kidney	ε'	1000	3.0 *	5.0 *	60.0 *	22
	σ		0.009	0.035	1.000	
	ε'	2500	3.0	5.0	50.0	
	σ		0.015	0.074	1.520	

Notes: (1) Values marked * are from the literature, and all others are calculated.
(2) Values marked ** are similar to Schwan's (19)

TABLE 6.1 Dielectric Data for Beef and Kidney

assumed to be the same as that of raw beef, for which data at both 1000 Mhz and 2500 Mhz were available, as shown in table 6.1. In addition, the frequency and temperature dependence of perfused and unperfused kidney tissue was assumed to be the same for the small temperature ranges considered. The effect of the perfusate on the tissue properties was assumed to be linear with concentration. The

values marked with an asterisk in table 6.1 are the values measured by the investigators indicated in the reference column, and the other values were derived from these. Referring to table 6.1, note the large difference between the values quoted in the literature for the conductivity of beef and kidney at low temperatures. This is surprising in view of the similarity of their properties at +20°C.

Material	ϵ' / σ	Freq. Mhz.	-20°C	-10°C	+20°C	+37°C	Ref.
Lard (Pig fat)	ϵ'	2500		2.4 *	2.5 *	2.6 *	
	σ			0.006	0.013	0.018	39
Patty Tissue	ϵ'	1000	2.5	2.5	2.5		
	σ		0.008	0.016	0.032		
Patty Tissue	ϵ'	3000	2.5	2.5	2.5		
	σ		0.006	0.012	0.024		

Notes: (1) Values marked * are measured or literature values, the others are calculated.

TABLE 6.2 Dielectric Data for Fat

(2) Literature data for fat varies considerably, and there is not much data available for low temperatures. However, assuming that the temperature and frequency dependence of different fats is the same, the values in table 6.2 were estimated on the assumption that they would behave in the same way as lard, and using the literature values indicated with an asterisk.

Material	ε' / σ	Freq. Mhz.	-20°C	-10°C	+20°C	Ref.
Water	ε'	1000	3.2	3.2 *	79.0 *	43
	σ		0.001	0.001	0.280	
	ε'	2500	3.2	3.2 *	78.0 *	
	σ		0.001	0.001	1.530	
1% DMSO	ε'	1000	2.9	3.8	75.0	
	σ		0.040	0.059	0.290	
	ε'	2700	2.9 *	3.8 *	73.5*	Ch. 6
	σ		0.040	0.059	1.558	
10% DMSO	ε'	1000	7.5	18.5	74.0	
	σ		0.652	1.830	0.380	
	ε'	2700	7.5 *	18.5 *	73.0*	Ch. 6
	σ		0.652	1.830	2.052	

Notes: (1) Values marked * are measured or literature values, the others are calculated.

TABLE 6.3 Dielectric Data for Water and DMSO

(3) The values of table 6.3 are derived on the assumption that the behaviour of DMSO solutions for low concentrations is similar to that of water, both as regards frequency and temperature. This is justified by the results obtained in Chapter 4. Assuming 10% of the volume of the urine in the pelvis is displaced by perfusate, and assuming linear mixing, the values for the pelvis are calculated and shown in table 6.4. It is assumed that the properties of water are similar to those of urine for temperatures of -10°C and -20°C. Again, this is justified by the results of figures 6.17 and 6.18 where an ionic component has little effect on the low temperature dielectric constant. In any case, most of the losses are due to the DMSO.

Cond. #	Freq. Mhz	Per-fusate	Temp. °C	Kidney State	Dielectric Properties	Remarks
1	2500	10% DMSO	-20	Partial per-fusion	1- 1.0,0.005 2- 3.0,0.015 3- 3.0,0.015 4- 2.5,0.006 5- 3.6,0.066	Datum model
2	1000	10% DMSO	-20	Partial per-fusion	1- 1.0,0.005 2- 3.0,0.009 3- 3.0,0.009 4- 2.5,0.008 5- 3.6,0.066	Freq. effect
3	2500	1% DMSO	-20	Partial per-fusion	1- 1.0,0.002 2- 2.1,0.004 3- 2.1,0.004 4- 2.5,0.006 5- 3.1,0.005	Per-fusate effect
4	2500	10% DMSO	-10	Partial per-fusion	1- 1.0,0.005 2- 5.0,0.074 3- 5.0,0.074 4- 2.5,0.012 5- 4.7,0.180	Temp. effect
5	2500	10% DMSO	-20	No per-fusion	1- 1.0,0.001 2- 2.0,0.003 3- 2.0,0.003 4- 2.5,0.006 5- 3.2,0.001	Per-fusion effect
6	2500	10% DMSO	-20	Total pelvic per-fusion	1- 1.0,0.005 2- 3.0,0.015 3- 3.0,0.015 4- 2.5,0.006 5- 7.5,0.650	Effect of lossy pelvis
7	1000	10% DMSO	+20	Partial per-fusion	1- 1.0,0.100 2-60.0,1.000 3-60.0,1.000 4- 2.5,0.032 5-78.0,0.290	Temp. and freq. effect
8	2500	10% DMSO	-10	Partial per-fusion	1- 1.0,0.005 2- 3.0,0.015 3- 3.0,0.015 4- 2.5,0.006 5- 3.6,0.066	Orient-ation effect

TABLE 6.4 Dielectric Properties (ϵ',σ) Used in the Model

(4) The particular choice of the assumed conductivity of air is to keep losses in the air to a minimum in comparison with those of the kidney, and yet to ensure algorithm stability. The values chosen appear in table 6.4.

(6.5) Results Obtained with the Model.

The eight sets of conditions for which the model was run generated 120 pages of data printout and it is obviously impractical to present all of these. It was therefore decided to consider each set of conditions separately and to present only those planes which showed important results. Where appropriate, comparisons between the different sets of conditions are drawn. General conclusions and comparisons with the experimental data of Rajotte (11) are presented in a concluding section.

As explained earlier, the printout is arranged in exactly the same manner as the media lattice input. A digit in the range 0-9 is printed out, and this represents the heating index at each lattice point. The scaling factor to obtain the actual value of power absorbed in W/m^3 at each point is indicated in each case. This value is for unit incident electric field and can be used to obtain the power absorbed for any incident power density by means of equation 7.22.

For all the cases where the incident frequency was 2500 Mhz, the program of appendix B was run for 480 steps with printout at 400 and 480 steps to enable a stability check to be made. No instabilities appeared for any case and only the results obtained after 480 steps are presented here. As a result, the program was run 600 steps in the 1000 Mhz case with only one printout (at 600 steps).

For each case, the dielectric properties are presented in table 6.4. The conditions under which the dielectric properties were obtained are also shown there and will only be repeated where necessary. In labelling the printouts, one figure number at the beginning of each set will be used to represent all the planes within that set, with a bracketed addition to refer to a particular plane within the set, as was done earlier. For instance, the 10th plane in figure 6.6 will be referred to as figure 6.6(10).

(6.6) Condition 1. The Datum Model.

(Figure 6.6(8-11,13,15)

This figure is the printout obtained with the datum model. Plane 8 shows that the dissipation in the medulla and cortex is minimal, and planes 3 to 7, which are not shown, support this observation. The maximum index encountered in any of these planes is 3. In plane 9, an interesting effect becomes evident. Here it is clear that the tubular structure

FIGURE 6.6(8-11,13,15) Datum Model

Set #1: Max. dissipated power = 0.0273 W/m³.

Max. dissipation at plane K = 9.

Frequency = 2500 Mhz.

Perfusate = 10% DMSO.

Temperature = -20°C.

Partial Perfusion.

NORMALISED HEATING INDEX AT TIME STEP 480

PLANE K = 8

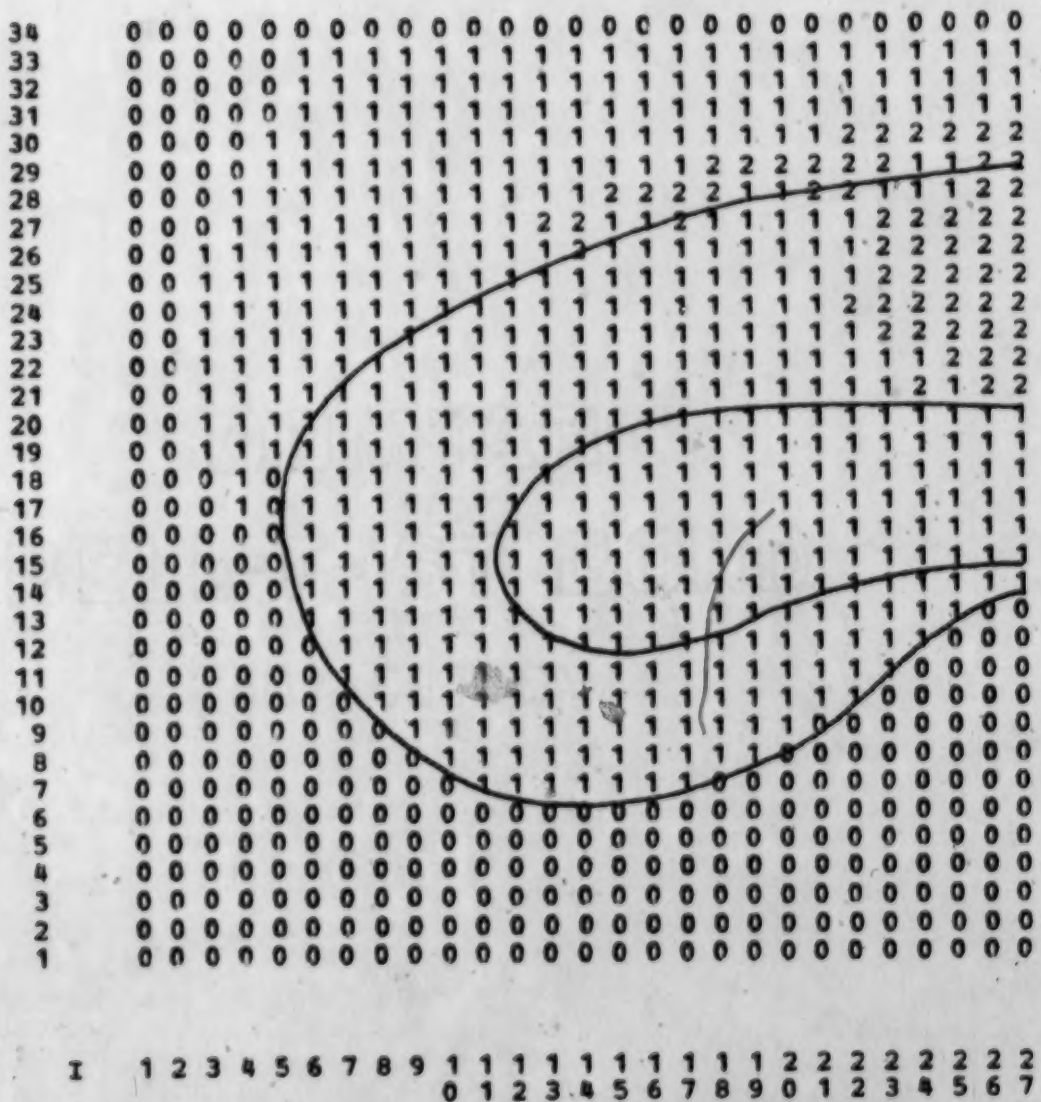

NORMALISED HEATING INDEX AT TIME STEP 480

PLANE K = 9

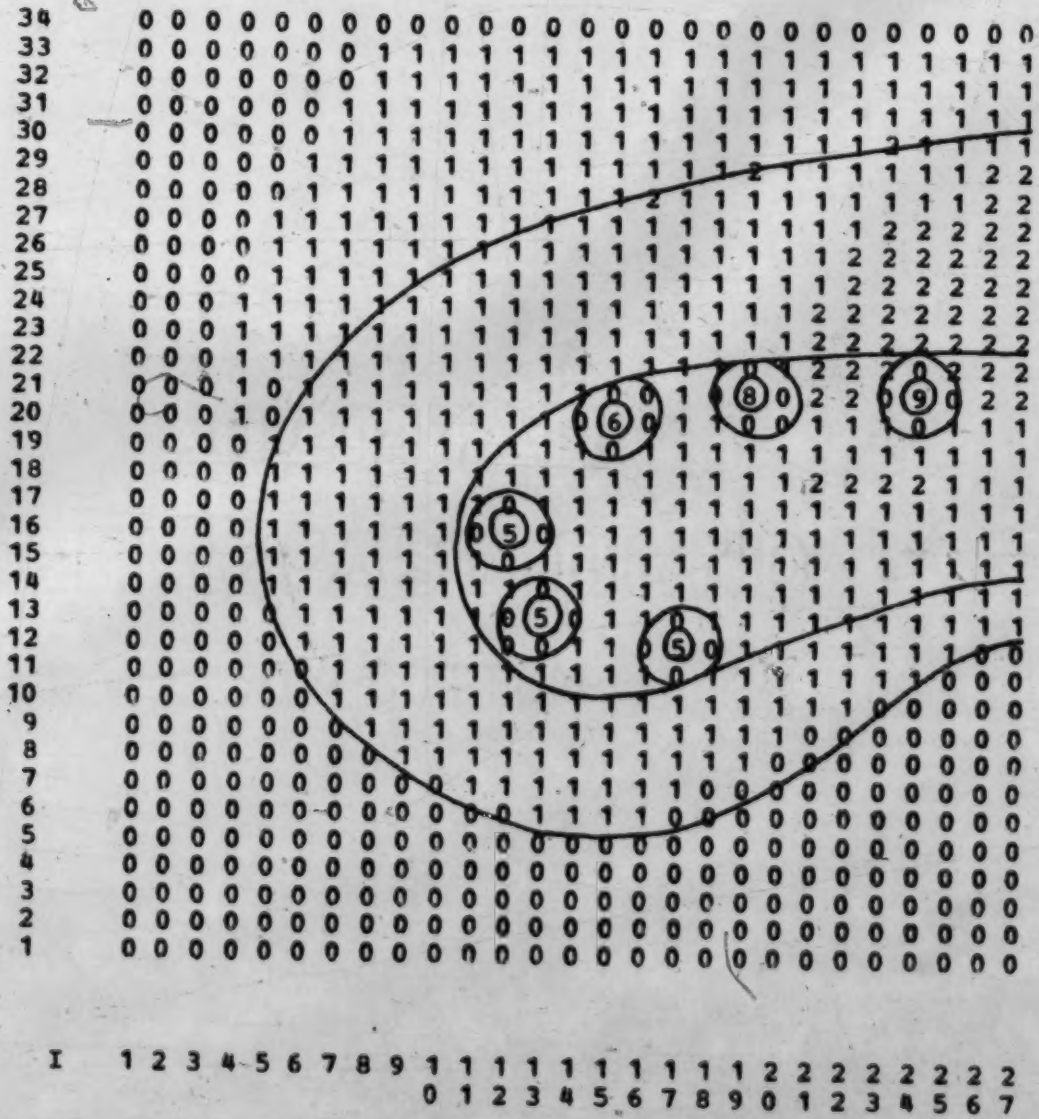

NORMALISED HEATING INDEX AT TIME STEP 480

PLANE K = 10

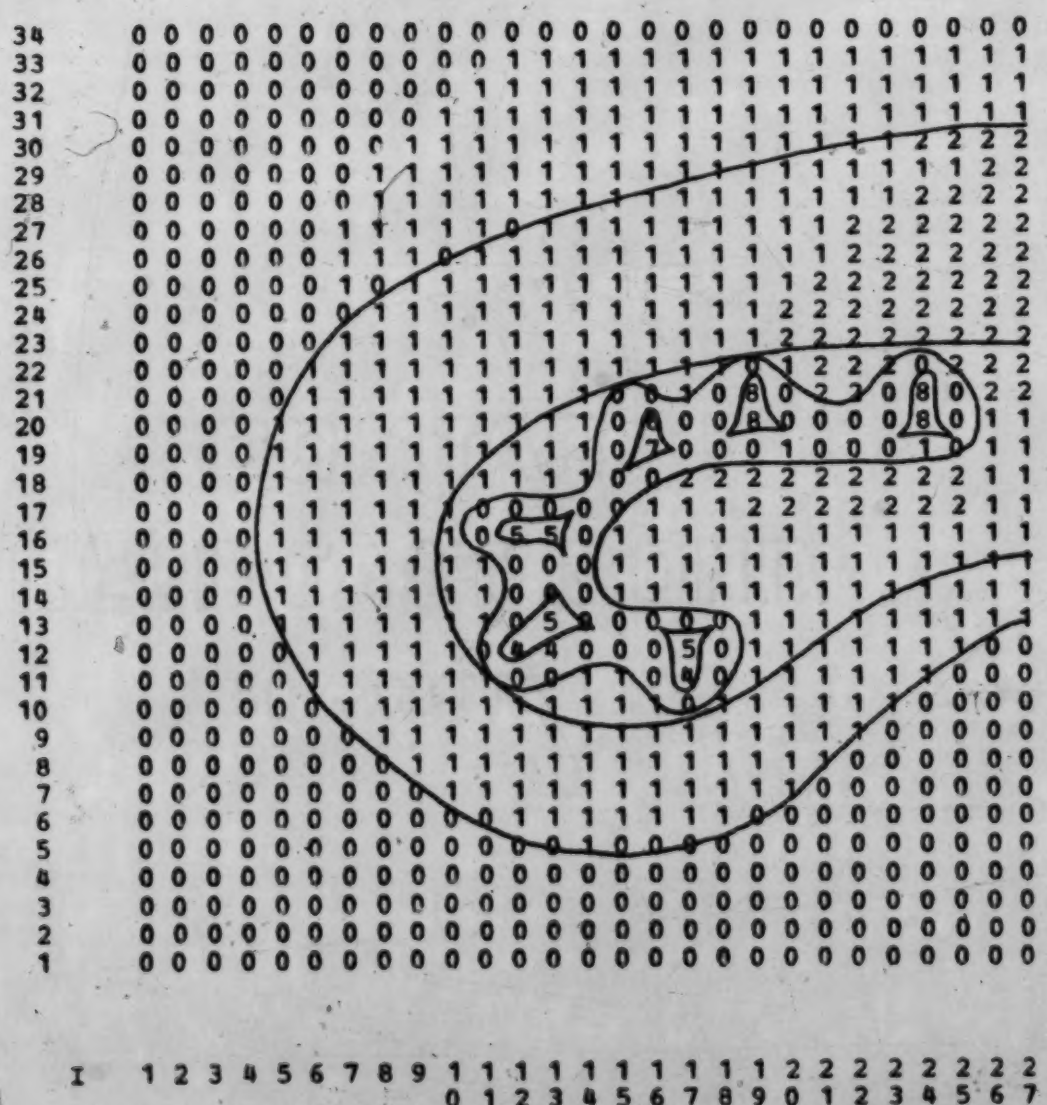

NORMALISED HEATING INDEX AT TIME STEP 480

PLANE K = 11

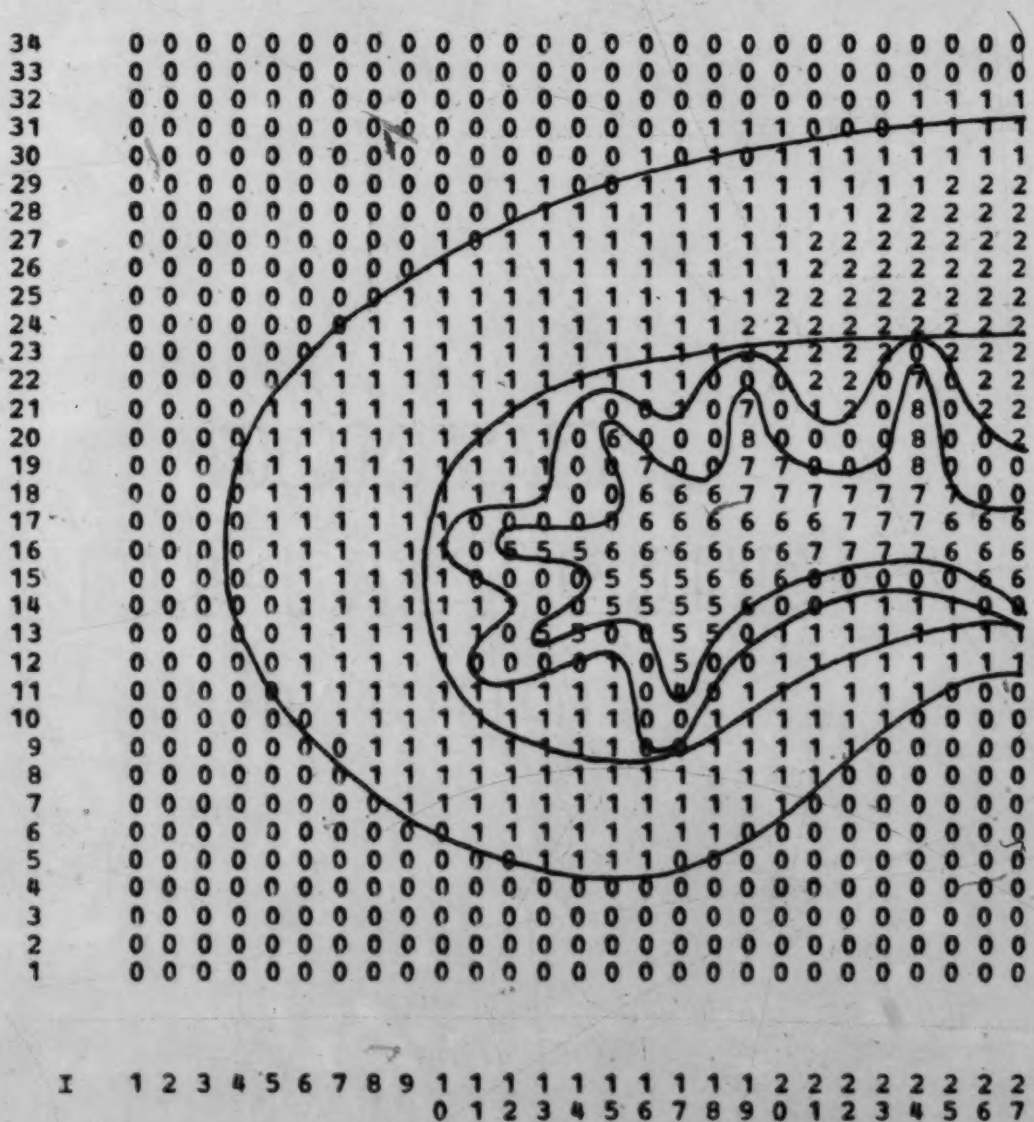

NORMALISED HEATING INDEX AT TIME STEP 480

PLANE K = 13

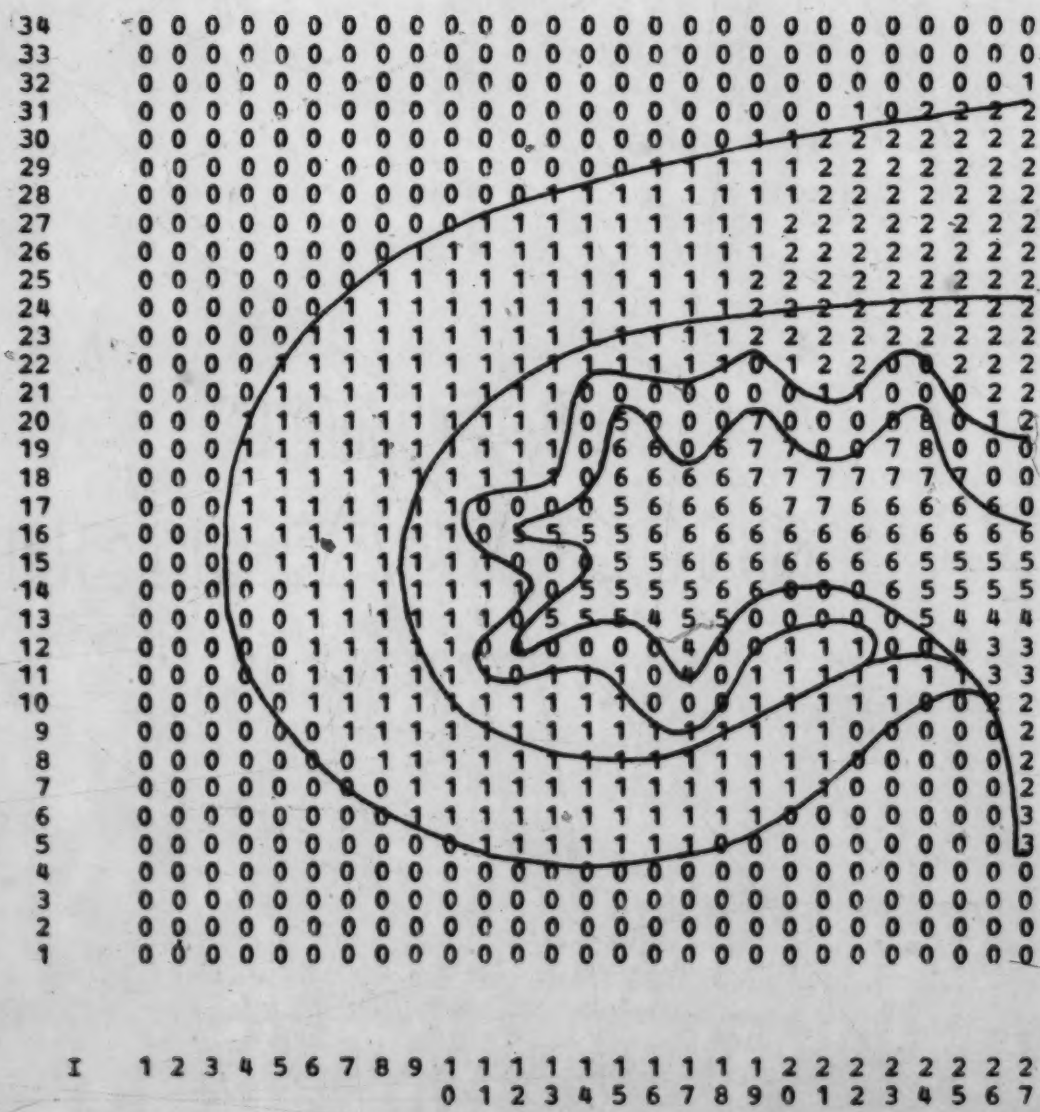

NORMALISED HEATING INDEX AT TIME STEP 480

PLANE K = 15

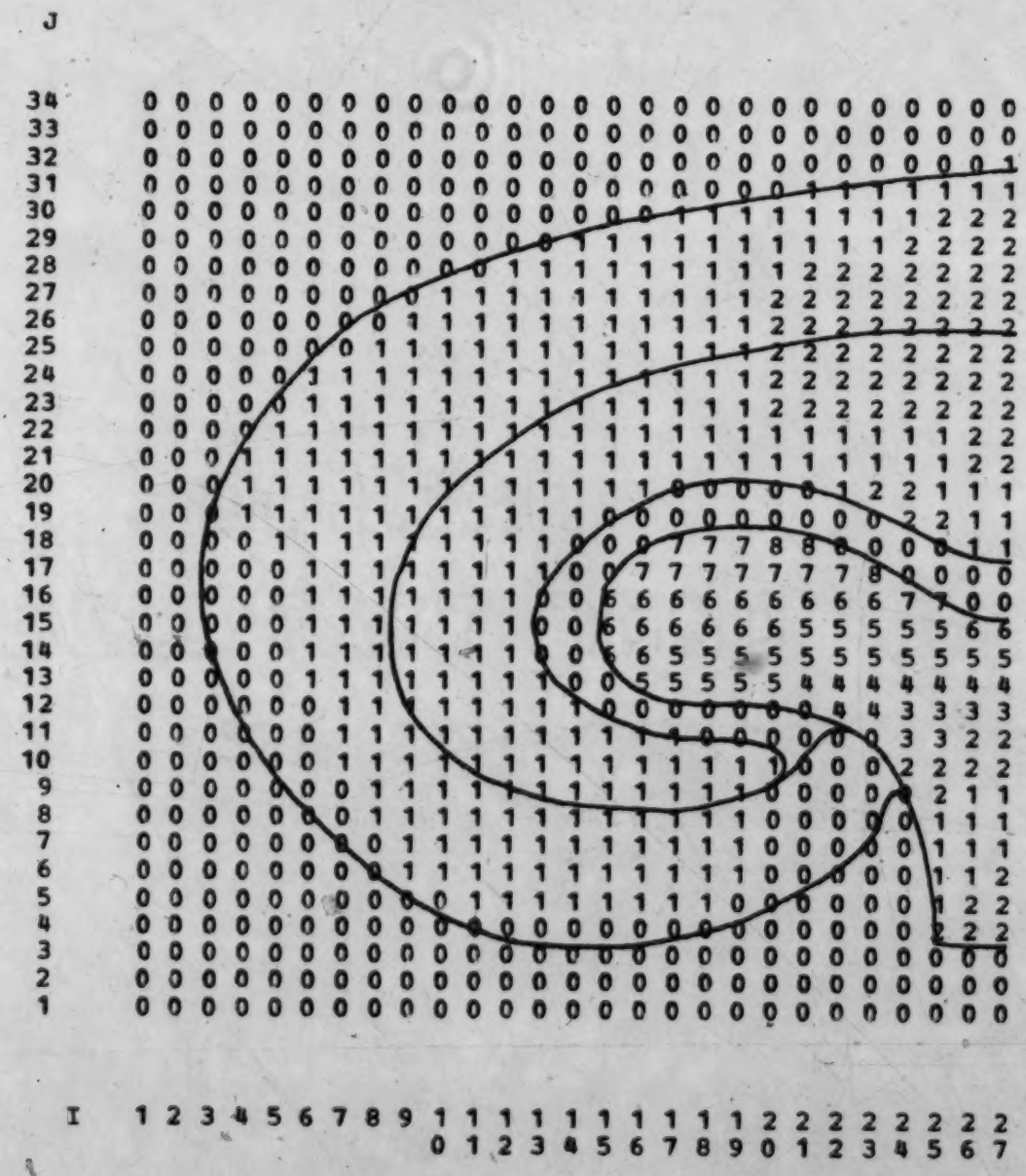

of the ureter is dissipating strongly in contrast to the surrounding fat layer in which no power is being absorbed. This implies that this tubular structure is likely to suffer damage due to heat stress and mechanical stress caused by differential heating. Referring to planes 10,11,13 and 15, it is clear that this effect becomes gradually less pronounced as the tubular structure becomes larger. However, in none of the planes does the fat absorb significant power, and the fat-pelvis interface is always subject to considerable differential heating.

Further reference to planes 10-15 indicates that most of the energy is absorbed by the perfused urine in the pelvis, in spite of the supposedly good perfusion in the cortex and medulla. The best heating in the cortex and medulla occurs on the side away from the impinging wave. The effect of the small loss introduced into the air is seen to be negligible in this case.

(6.7) Condition 2. Effect of Frequency.
(Figure 6.7(8-11,13,15))

The first effect observed in changing the frequency from 2500 Mhz to 1000 Mhz is a drop in the maximum absorbed power from 0.0273 to 0.0117 W/m^3. Again, planes 3-8 (only 8 is shown) in the off axis region of the cortex and medulla show little dissipation. Some loss in the air is evident at

FIGURE 6.7(8-11,13,15) Frequency effect

Set #2: Max. dissipated power = 0.017 W/m^3.

Max. dissipation at plane K = 11.

Frequency = 1000 Mhz.

Perfusate = 10% DMSO.

Temperature = -20°C.

Partial Perfusion.

NORMALISED HEATING INDEX AT TIME STEP 600

PLANE K = 9

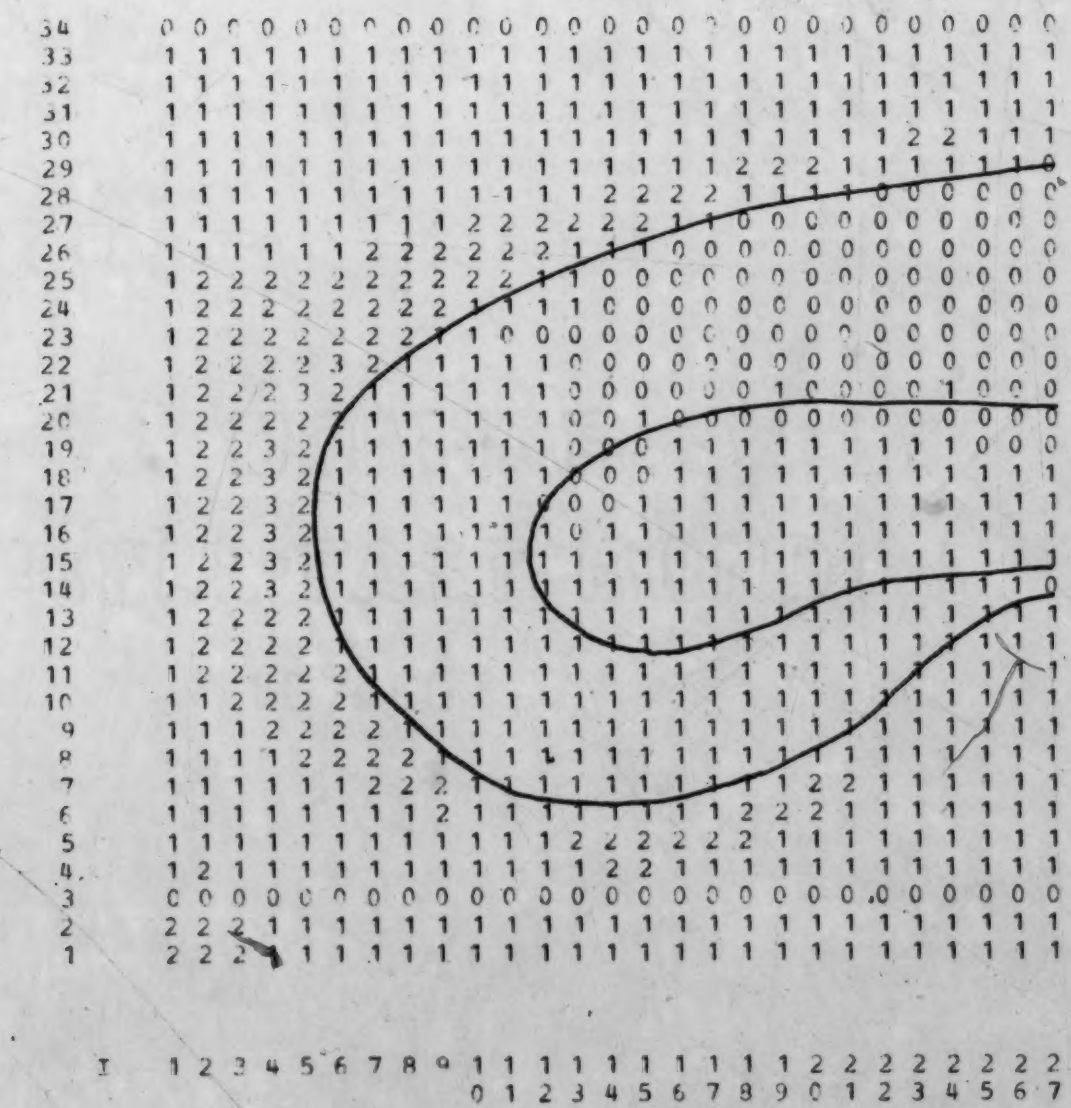

NORMALISED HEATING INDEX AT TIME STEP 600

PLANE K = 9

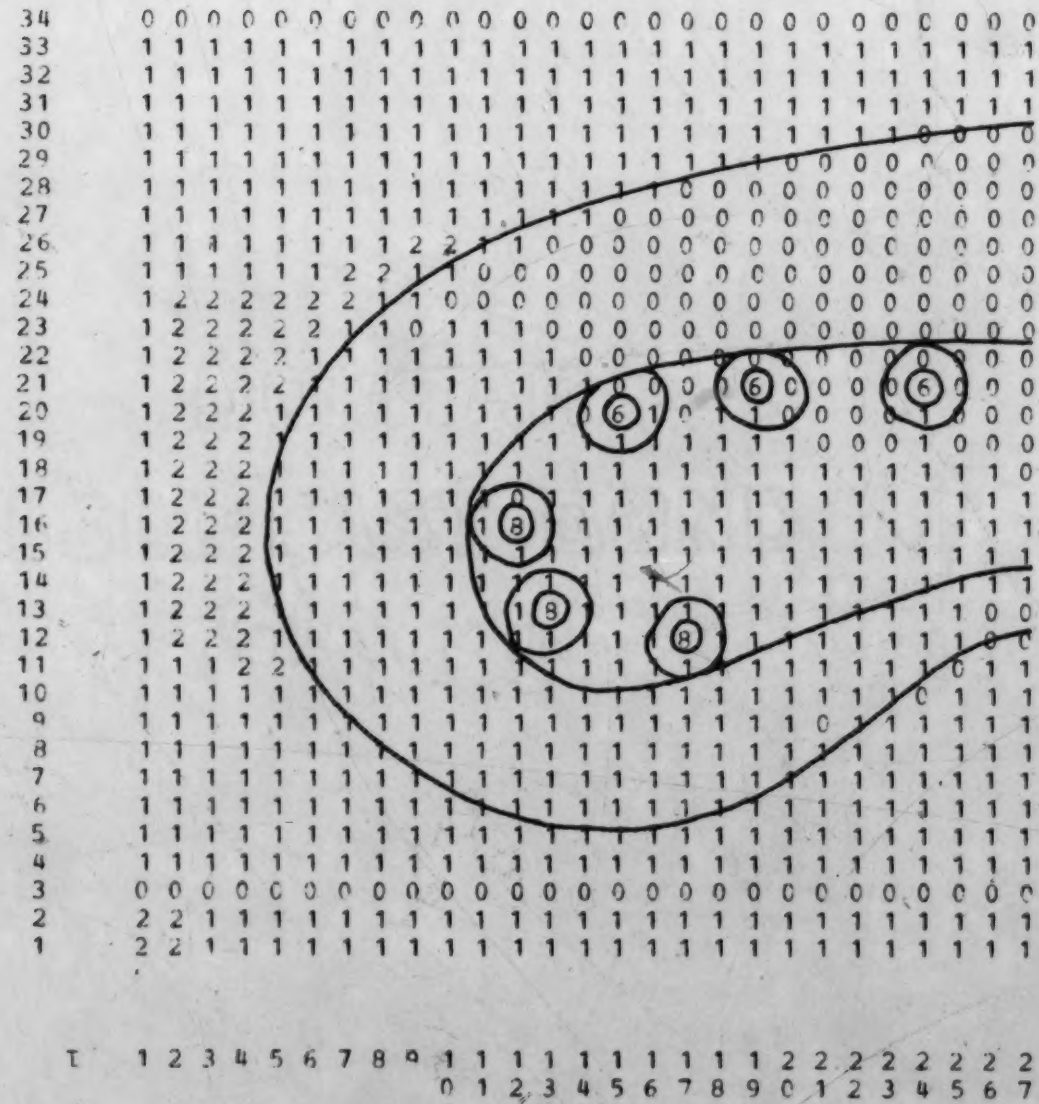

NORMALISED HEATING INDEX AT TIME STEP 600

PLANE K = 10

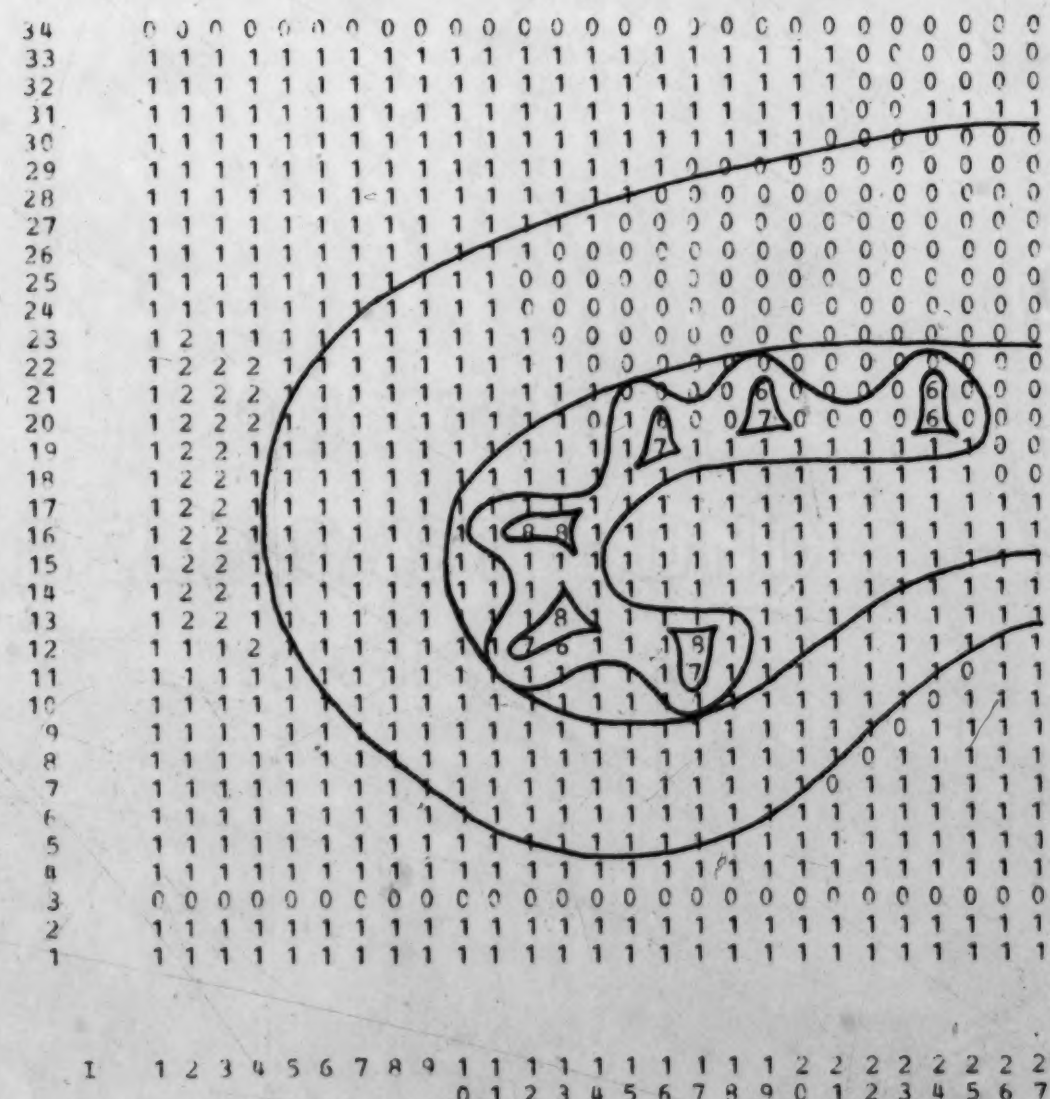

NORMALISED HEATING INDEX AT TIME STEP 600

PLANE K = 11

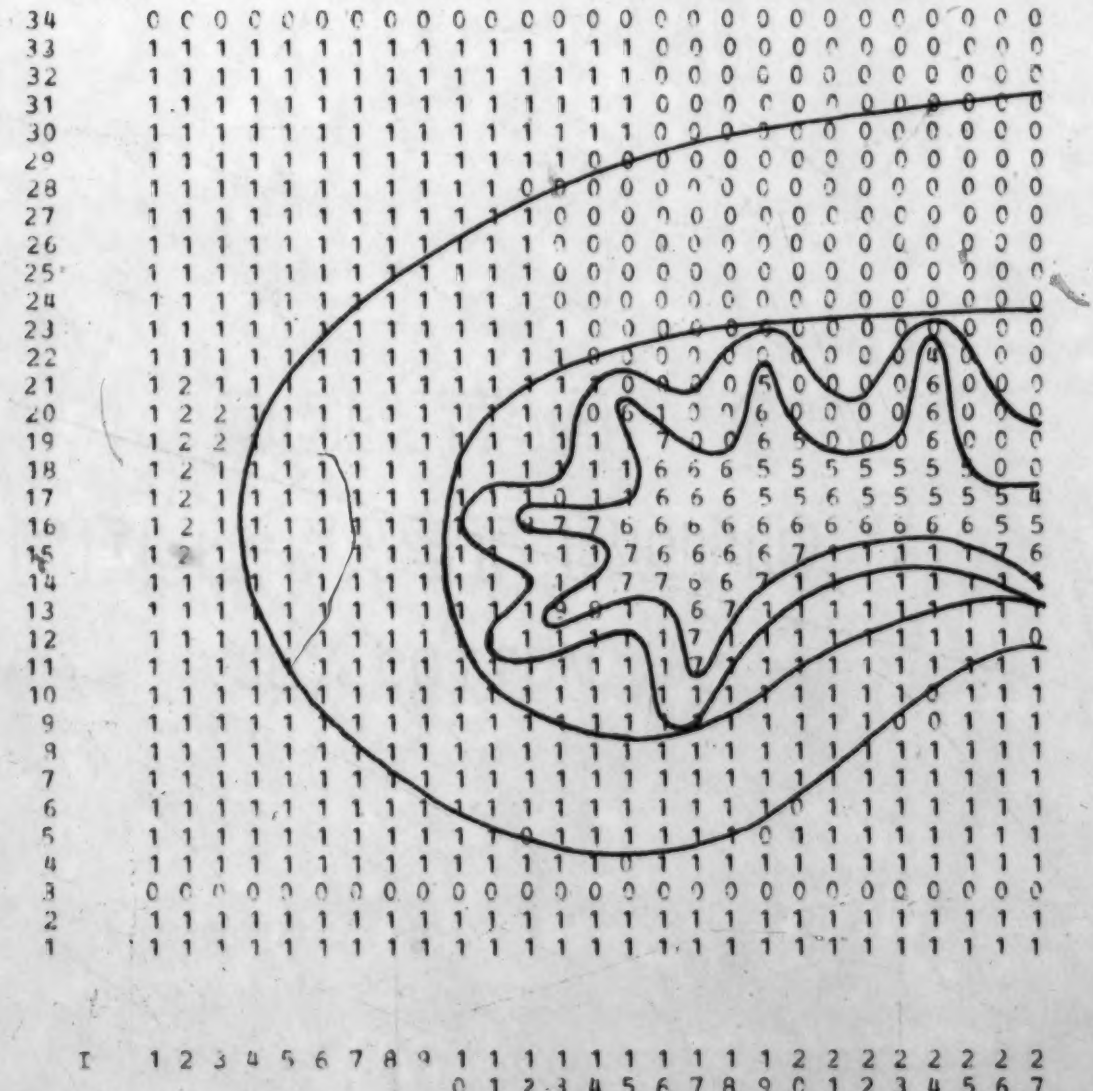

NORMALISED HEATING INDEX AT TIME STEP 600

PLANE K = 13

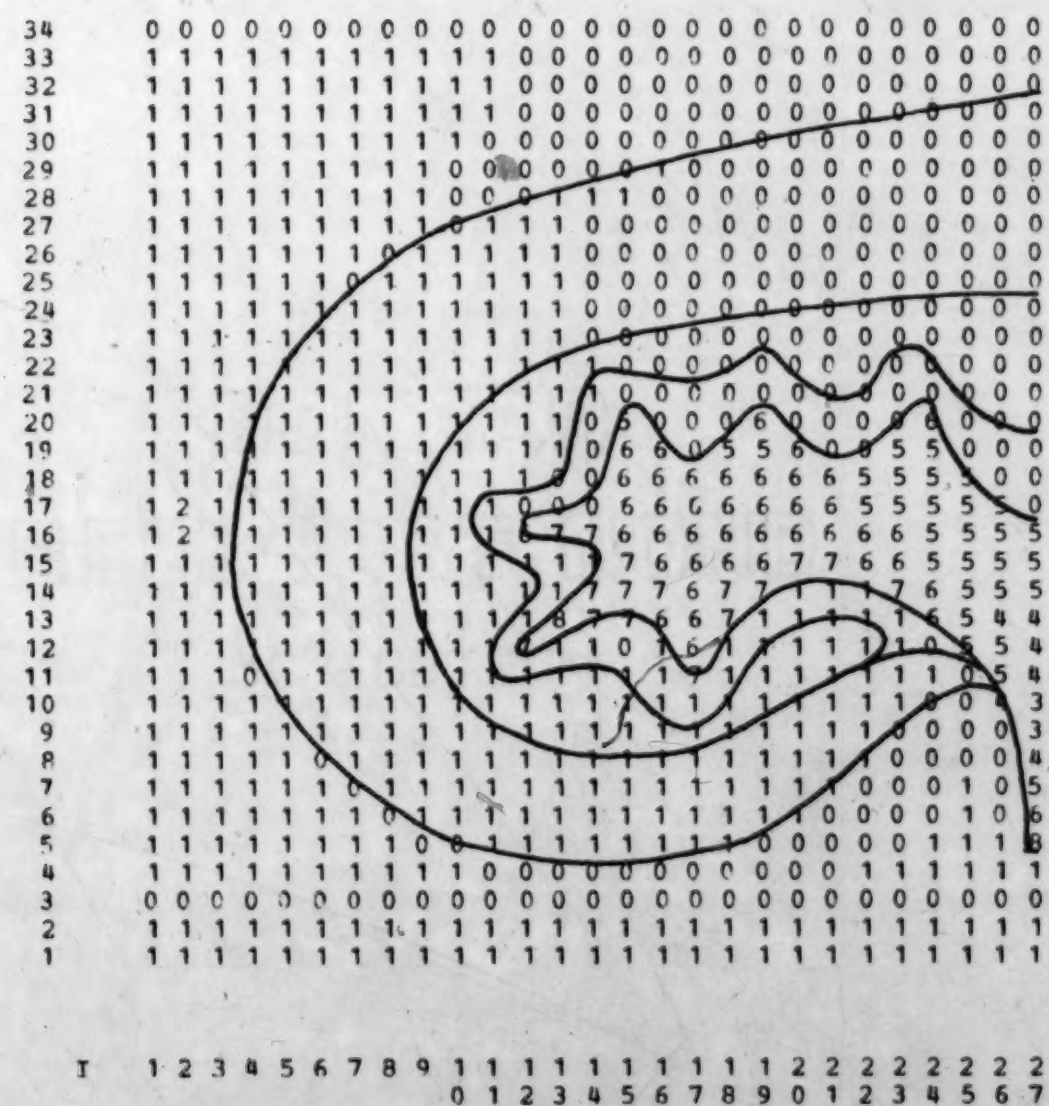

NORMALISED HEATING INDEX AT TIME STEP 600

PLANE K = 15

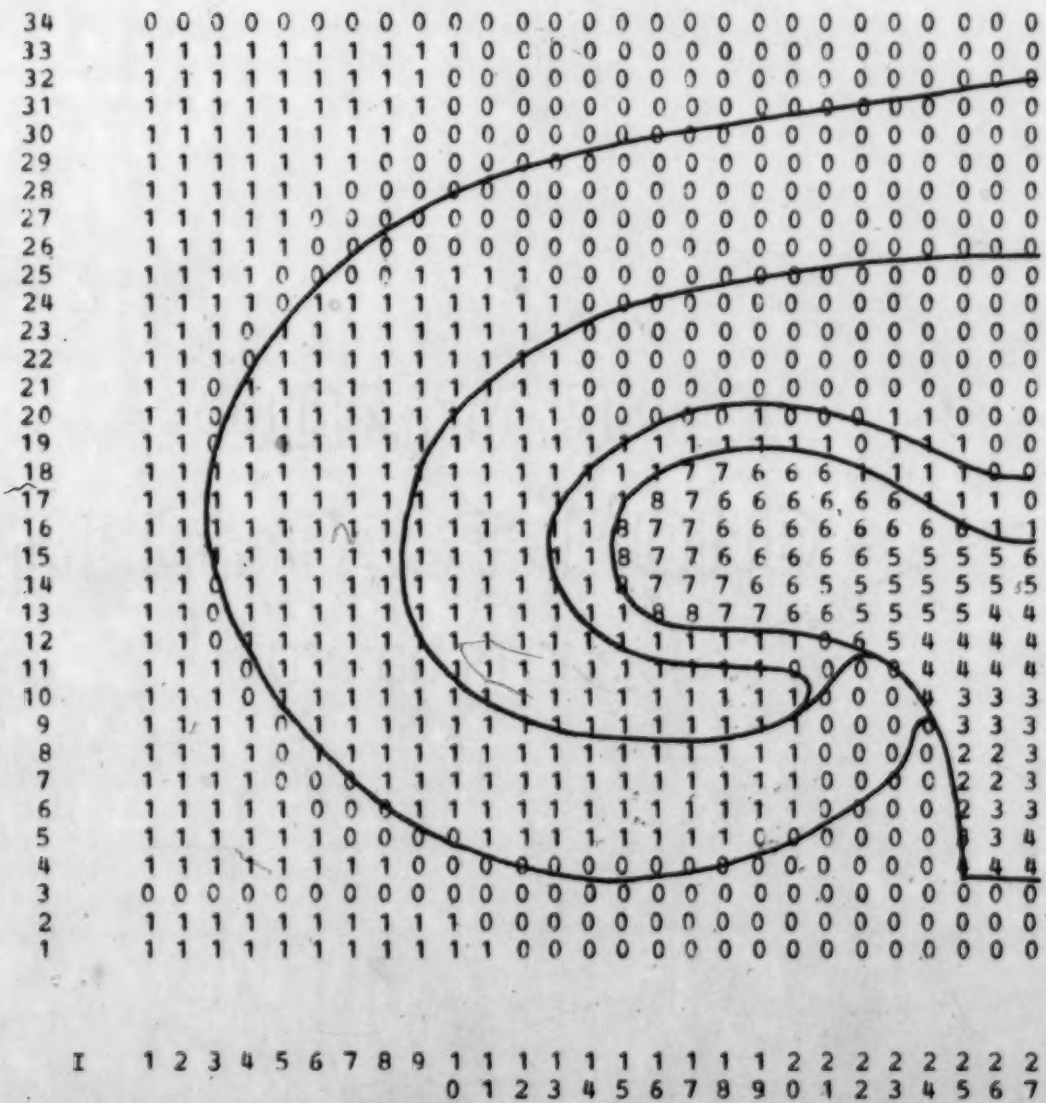

this frequency, but this is due to the artificial loss introduced for stability and only those regions within the kidney should be considered here.

Planes 9,10 and 11 indicate a similar tubule heating effect as was observed for condition 1. Planes 11,13 and 15 show that the pelvic region is again strongly heated with even less heating in the medulla and cortex. At this temperature, the higher frequency (2500 Mhz) appears to give slightly better uniformity and approximately doubles the maximum dissipated power.

(6.8) Condition 3. Effect of Reducing DMSO Concentration. (Figure 6.8(5,8,9,10,12,15))

Again, it is immediately evident that the maximum dissipated power is reduced, in this case by a factor of more than 6. This bears out the prediction made in Chapter 4 with regard to the loss factors of 1% and 10% DMSO. With regard to the heating in the medullla and cortex in this case, it is apparent that a much higher proportion of the energy is absorbed in this region. Planes 3-8 all show reasonably high absorption, with a maximum heating index of 9 in plane 5. Only planes 5 and 8 of this group are shown here. Because it was necessary to set the air loss relatively high in this case, it is clear that some energy is being dissipated in the air, and so, as before, only the

FIGURE 6.8(5,8-10,12,15) Perfusate effect

Set #3: Max. dissipated power = 0.0033 W/m³.

Max. dissipation at plane K = 5.

Frequency = 2500 Mhz.

Perfusate = 1% DMSO.

Temperature = -20°C.

Partial Perfusion.

NORMALISED HEATING INDEX AT TIME STEP 480

PLANE K = 5

J																									
34	0	0	0	0	0	0	0	0	0	0	0	0	0	0	0	0	0	0	0	0	0	0	0	0	0
33	2	3	3	3	3	3	3	3	3	4	4	4	4	4	4	4	4	5	5	5	5	5	5	5	5	5	5
32	2	3	3	3	3	3	3	3	4	4	4	4	4	4	4	4	4	5	5	5	5	5	5	5	5	5	5
31	2	3	3	3	3	3	3	3	4	4	4	4	4	4	4	5	5	5	5	5	5	5	5	5	5	6	6
30	3	3	3	3	3	3	3	4	4	4	4	4	4	4	5	5	5	5	5	5	5	5	6	6	6	6	6
29	3	3	3	3	3	3	3	4	4	4	4	4	4	5	5	5	5	5	5	6	6	6	6	6	6	6	6
28	3	3	3	3	3	3	3	4	4	4	4	4	5	5	5	5	5	6	6	6	6	6	6	6	7	7	7
27	3	3	3	3	3	3	4	4	4	4	4	5	5	5	5	5	6	6	6	6	7	7	7	7	7	7	9
26	3	3	3	3	3	3	4	4	4	4	5	5	5	5	6	6	6	6	6	7	7	7	8	8	8	8	8
25	3	3	3	3	3	4	4	4	4	4	5	5	5	6	6	6	6	6	7	7	7	7	7	7	6	6	6
24	2	3	3	3	3	4	4	4	4	5	5	5	6	6	6	6	7	7	7	6	5	5	5	5	5	5	5
23	2	3	3	3	3	4	4	4	5	5	5	6	6	6	7	7	6	5	6	5	5	4	4	4	4	4	4
22	2	3	3	3	3	4	4	4	5	5	5	6	7	7	6	5	6	5	4	4	4	4	4	4	4	4	4
21	2	3	3	3	3	4	4	4	5	5	6	6	6	6	4	5	4	4	4	5	5	4	5	5	5	5	5
20	2	3	3	3	3	4	4	5	5	6	6	6	6	4	5	4	4	4	4	4	4	4	5	5	5	5	5
19	2	2	3	3	3	4	4	5	5	6	6	6	5	4	5	4	4	4	4	4	4	4	4	4	5	5	5
18	2	2	2	3	3	4	4	5	6	6	5	5	5	4	5	4	4	4	4	4	4	4	4	4	4	4	4
17	2	2	2	3	3	4	4	5	5	5	5	5	5	4	5	4	3	4	4	4	4	4	4	4	4	4	4
16	1	2	2	3	3	4	4	5	5	5	5	5	5	4	4	3	3	4	4	4	4	4	4	4	4	5	3
15	2	2	2	3	3	4	4	5	5	5	5	5	5	4	5	4	3	3	4	4	4	3	4	4	5	3	4
14	2	2	2	3	3	3	4	5	5	5	5	5	4	4	3	4	4	3	3	3	3	3	4	5	3	3	4
13	2	2	2	2	3	3	4	4	4	4	4	4	4	4	4	3	4	4	4	4	4	4	5	3	3	3	3
12	2	2	2	2	3	3	3	4	4	4	4	4	4	4	4	4	4	3	3	3	4	4	3	3	3	3	3
11	2	2	2	2	2	3	3	4	4	4	4	4	4	4	4	4	4	4	4	4	4	4	3	3	3	3	3
10	2	2	2	2	2	2	3	3	4	4	4	4	4	4	4	4	4	4	4	4	4	3	3	3	3	3	3
9	2	2	2	2	2	2	2	3	3	4	4	4	4	4	4	4	4	4	4	4	3	3	3	3	2	2	2
8	2	2	2	2	2	2	2	2	3	3	3	3	4	4	4	4	4	4	3	3	3	2	2	2	2	2	2
7	2	2	2	2	2	2	2	2	2	3	3	3	3	3	3	3	3	3	2	2	2	2	2	2	2	2	2
6	2	2	2	2	2	2	2	2	2	2	2	2	3	3	3	2	2	2	2	2	2	2	2	2	2	2	2
5	2	2	2	2	2	2	2	2	2	2	2	2	2	2	2	2	2	2	2	2	2	2	2	2	2	2	2
4	2	2	2	2	2	2	2	2	2	2	2	2	2	2	2	2	2	2	2	2	2	2	2	2	2	2	2
3	0	0	0	0	0	0	0	0	0	0	0	0	0	0	0	0	0	0	0	0	0	0	0	0	0	0	0
2	2	2	2	2	2	2	2	2	2	2	2	2	2	2	2	2	2	2	2	2	2	1	1	1	1	1	1
1	2	2	2	2	2	2	2	2	2	2	2	2	2	2	2	2	2	2	2	2	2	1	1	1	1	1	1

I	1	2	3	4	5	6	7	8	9	1 0	1 1	1 2	1 3	1 4	1 5	1 6	1 7	1 8	1 9	2 0	2 1	2 2	2 3	2 4	2 5	2 6	2 7

NORMALISED HEATING INDEX AT TIME STEP 480

PLANE K = 8

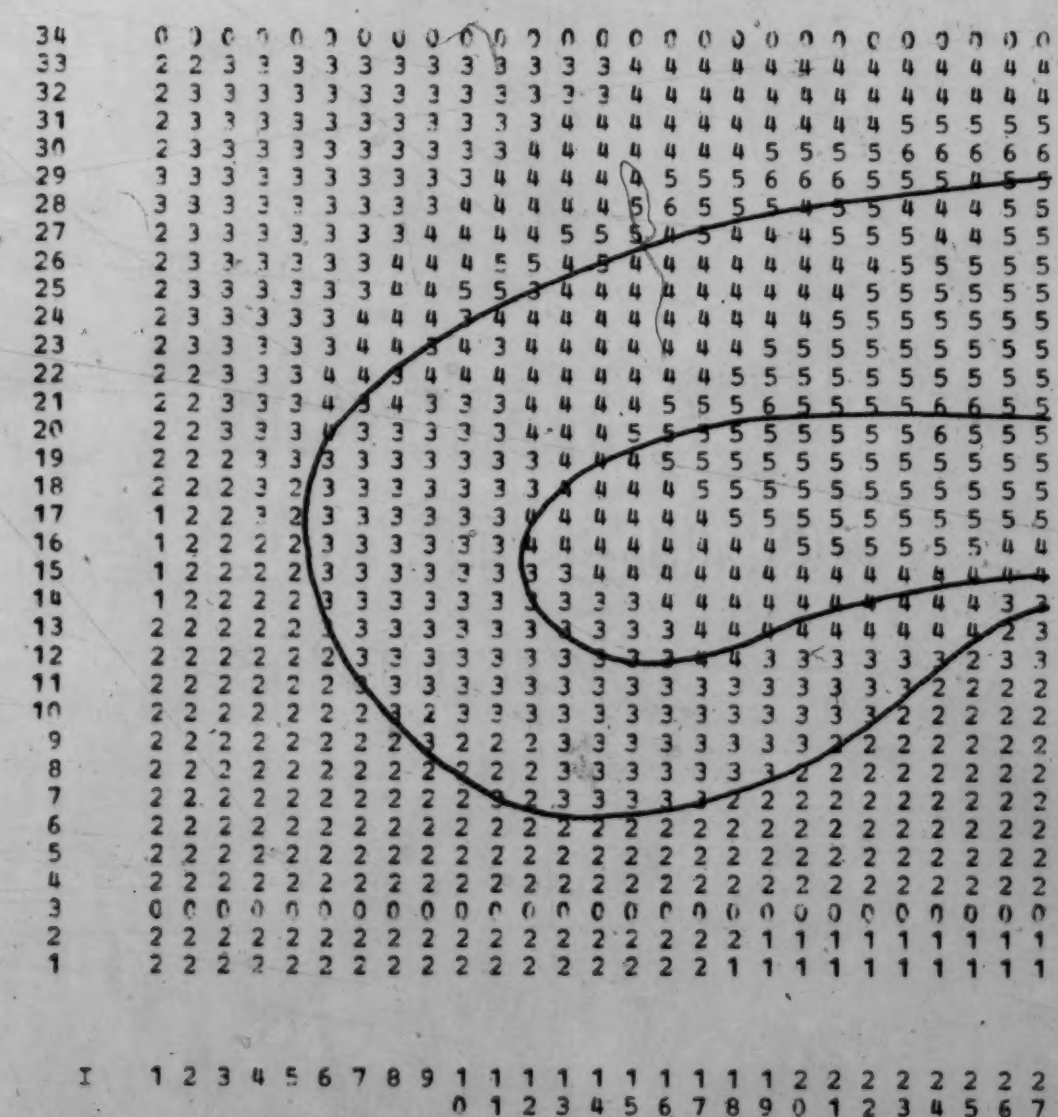

NORMALISED HEATING INDEX AT TIME STEP 480

PLANE K = 9

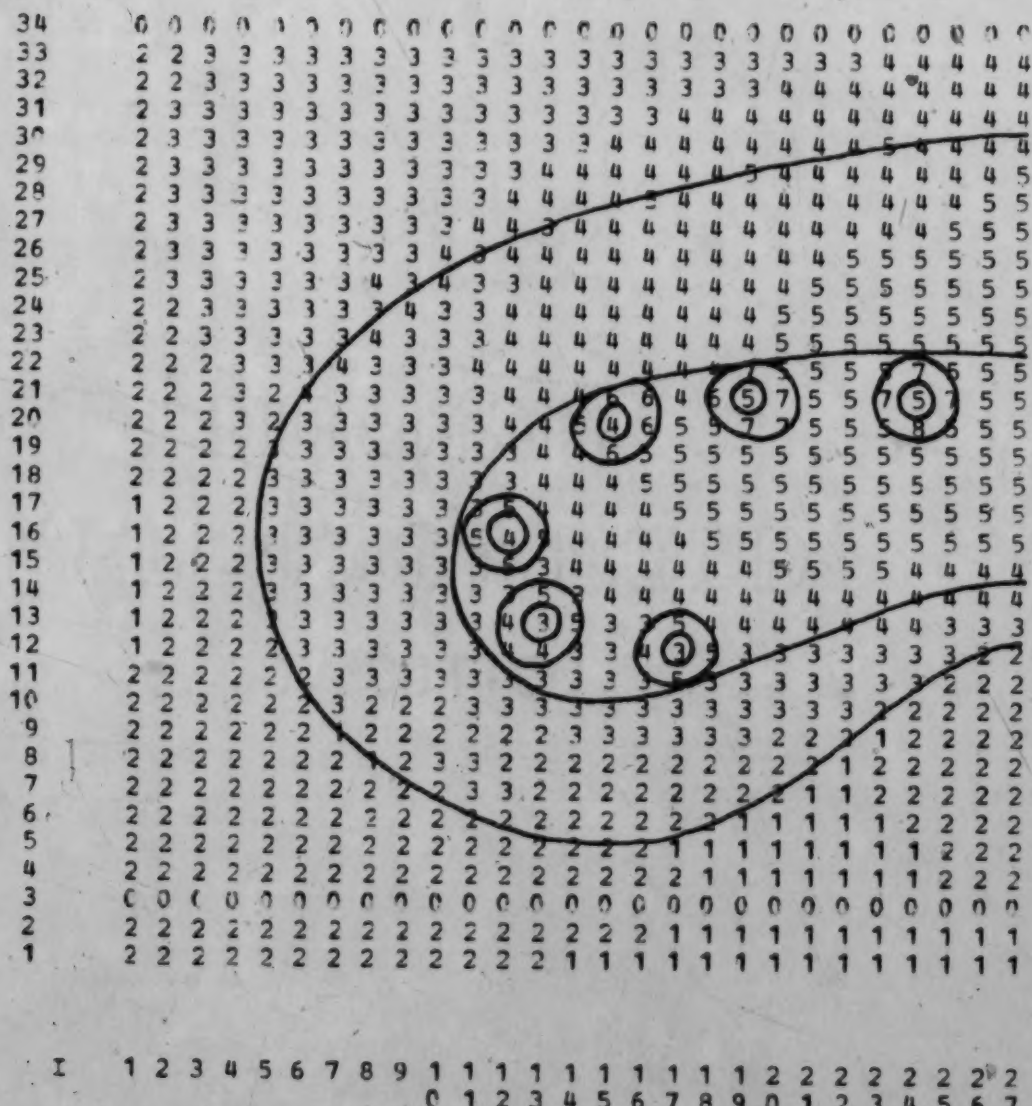

NORMALISED HEATING INDEX AT TIME STEP 480

PLANE K = 10

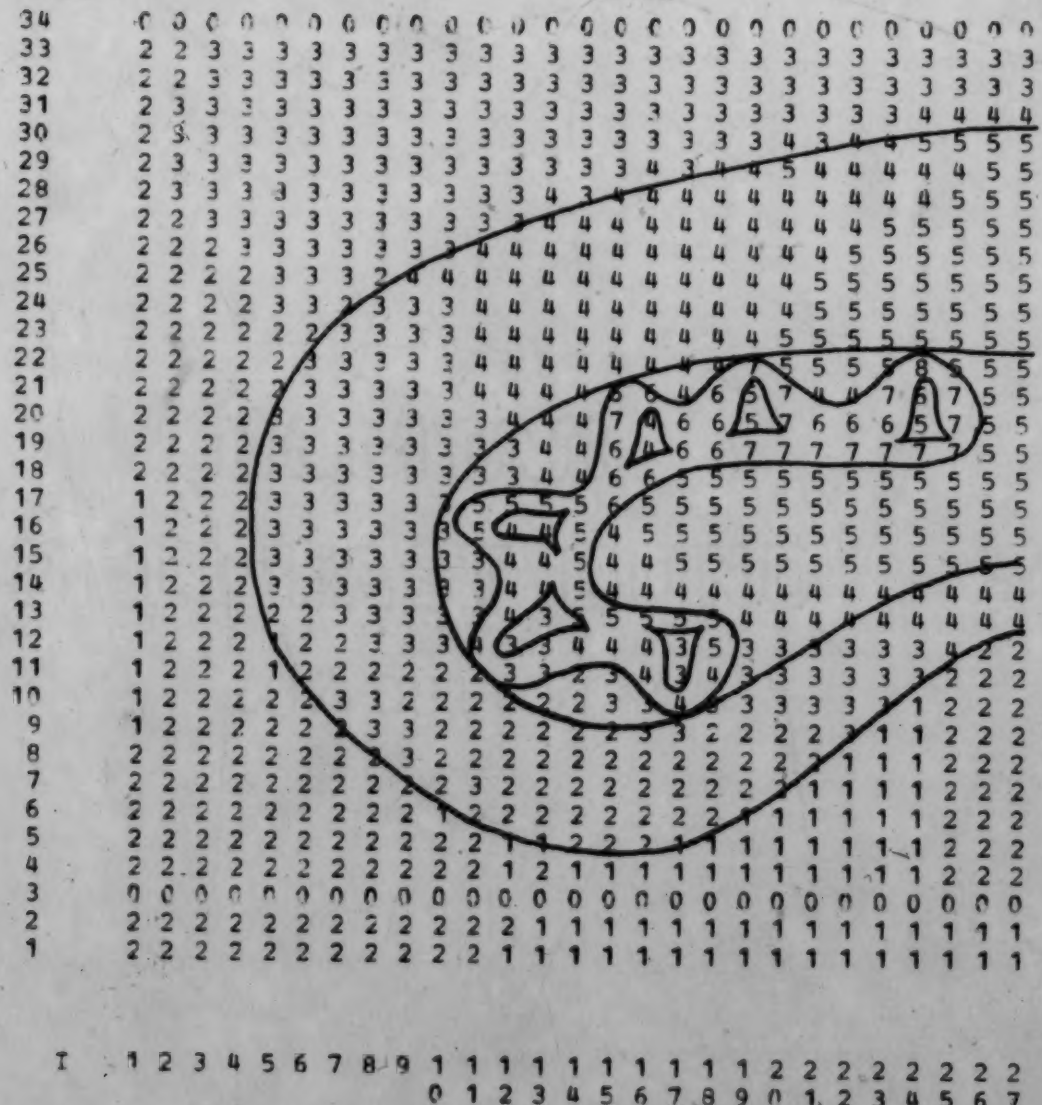

NORMALISED HEATING INDEX AT TIME STEP 480

PLANE K = 12

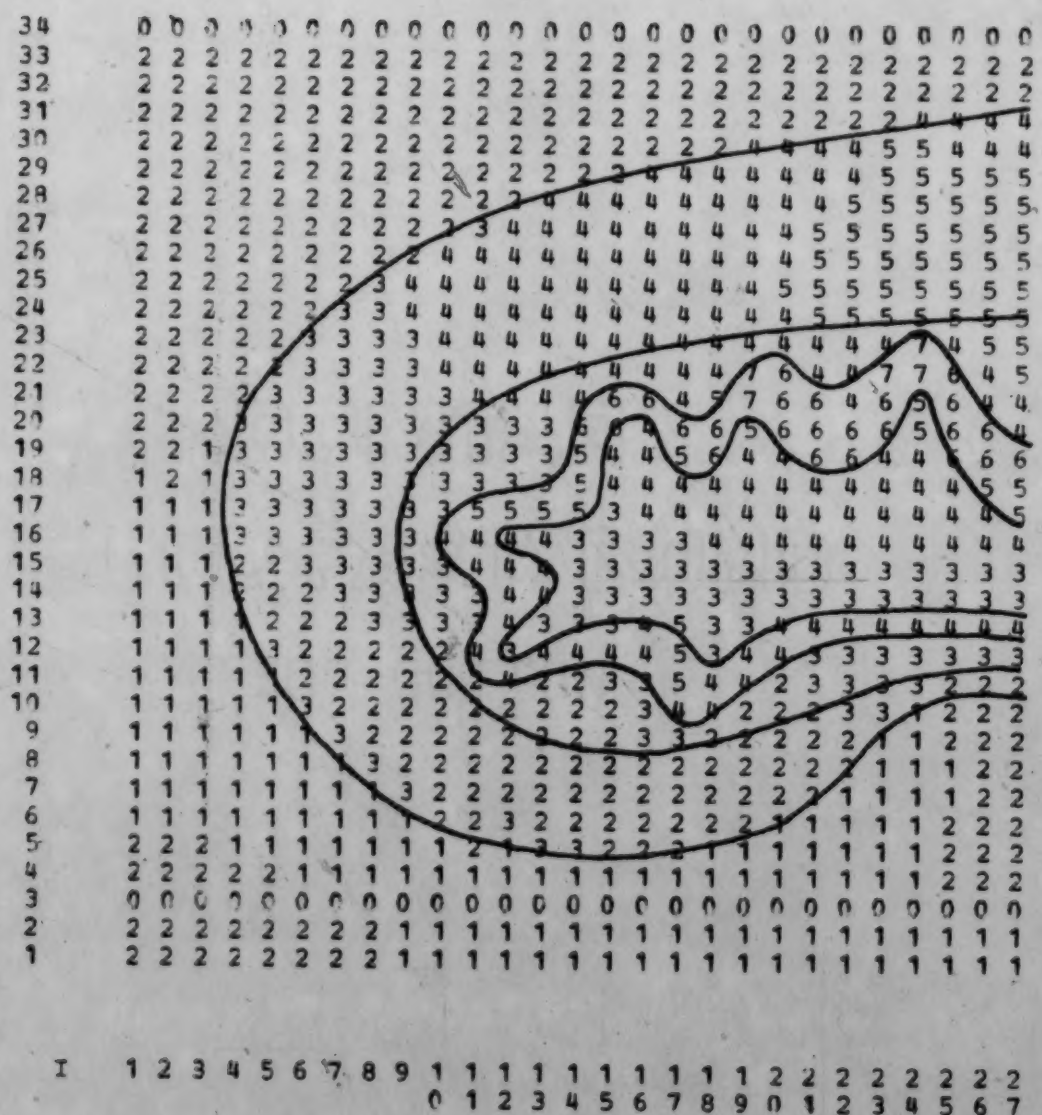

NORMALISED HEATING INDEX AT TIME STEP 480

PLANE K = 15

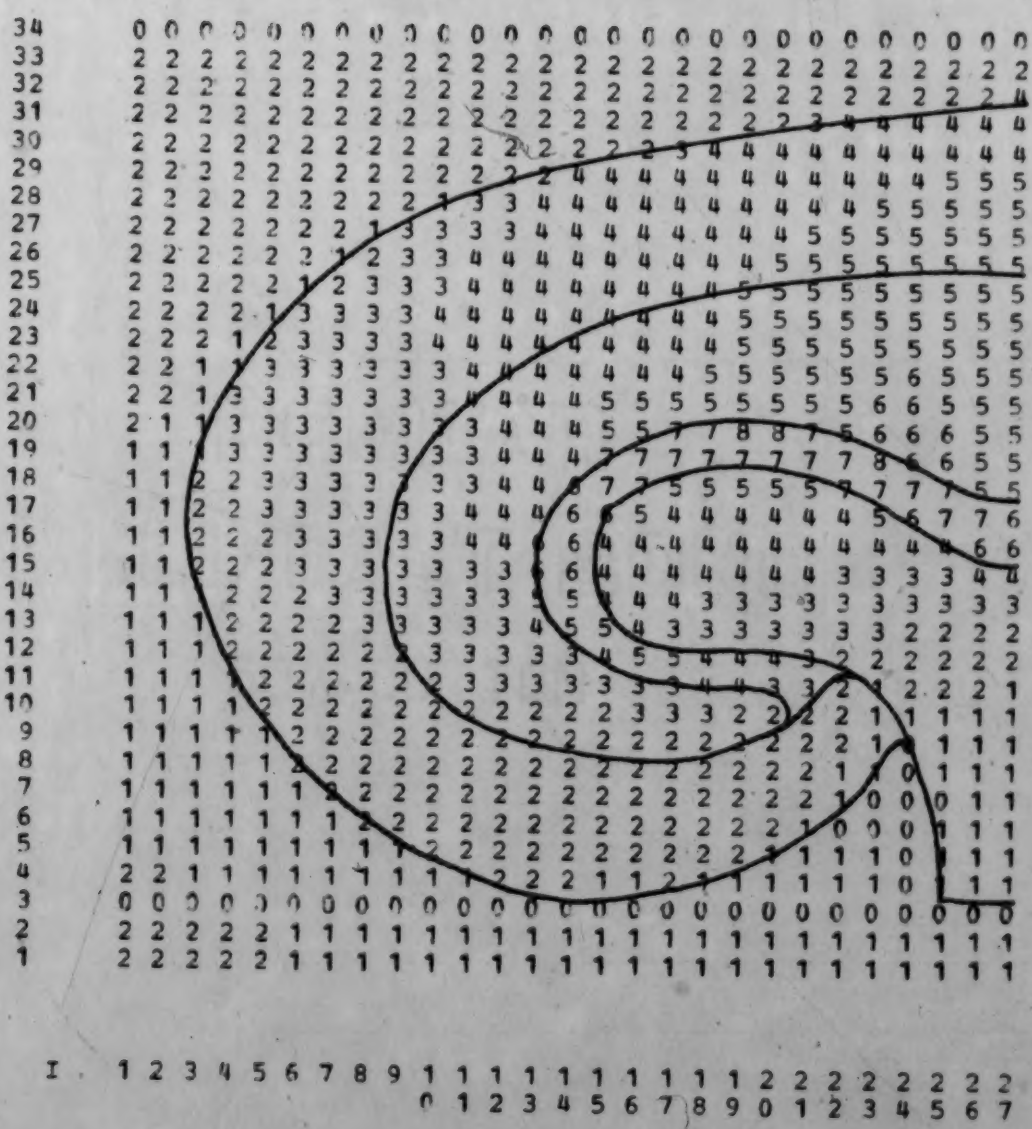

losses within the kidney should be considered.

Although plane 9 does indicate some differential heating, it is the fat layer which is more dissipative in this case. Further, although the highest dissipation is still in the pelvic region, dissipation in the cortex and medulla, as indicated by planes 10,12 and 15, is a much higher percentage of the maximum. A reduction in the DMSO concentration of the perfusate thus appears to have improved uniformity, although it should be remembered that this is at one particular temperature only. The relatively small variations in conductivity in this case suggest that more uniform perfusion at any concentration, thereby resulting in more homogeneous dielectric properties, would certainly enhance heating uniformity.

(6.9) Condition 4, Temperature Effect.

(Figure 6.9(5,8-11,13,15))

In increasing the kidney temperature from -20°C to -10°C, an increase in maximum dissipated power of more than three times from 0.0273 to 0.0920 W/m^3 is observed. Planes 3-8, of which 5 and 8 are representative, suggest that somewhat improved heating in the cortex and medulla has been obtained. Again, the tubular effect at plane 9 is evident, but planes 10-15 suggest that dissipation in the pelvic region is relatively lower and overall uniformity is better.

FIGURE 6.9(5,8-11,13,15) Temperature effect

Set #4: Max. dissipated power = 0.0920 W/m³.

Max. dissipation at plane K = 10.

Frequency = 2500 Mhz.

Perfusate = 10% DMSO.

Temperature = -10°C.

Partial Perfusion.

NORMALISED HEATING INDEX AT TIME STEP 480

PLANE K = 5

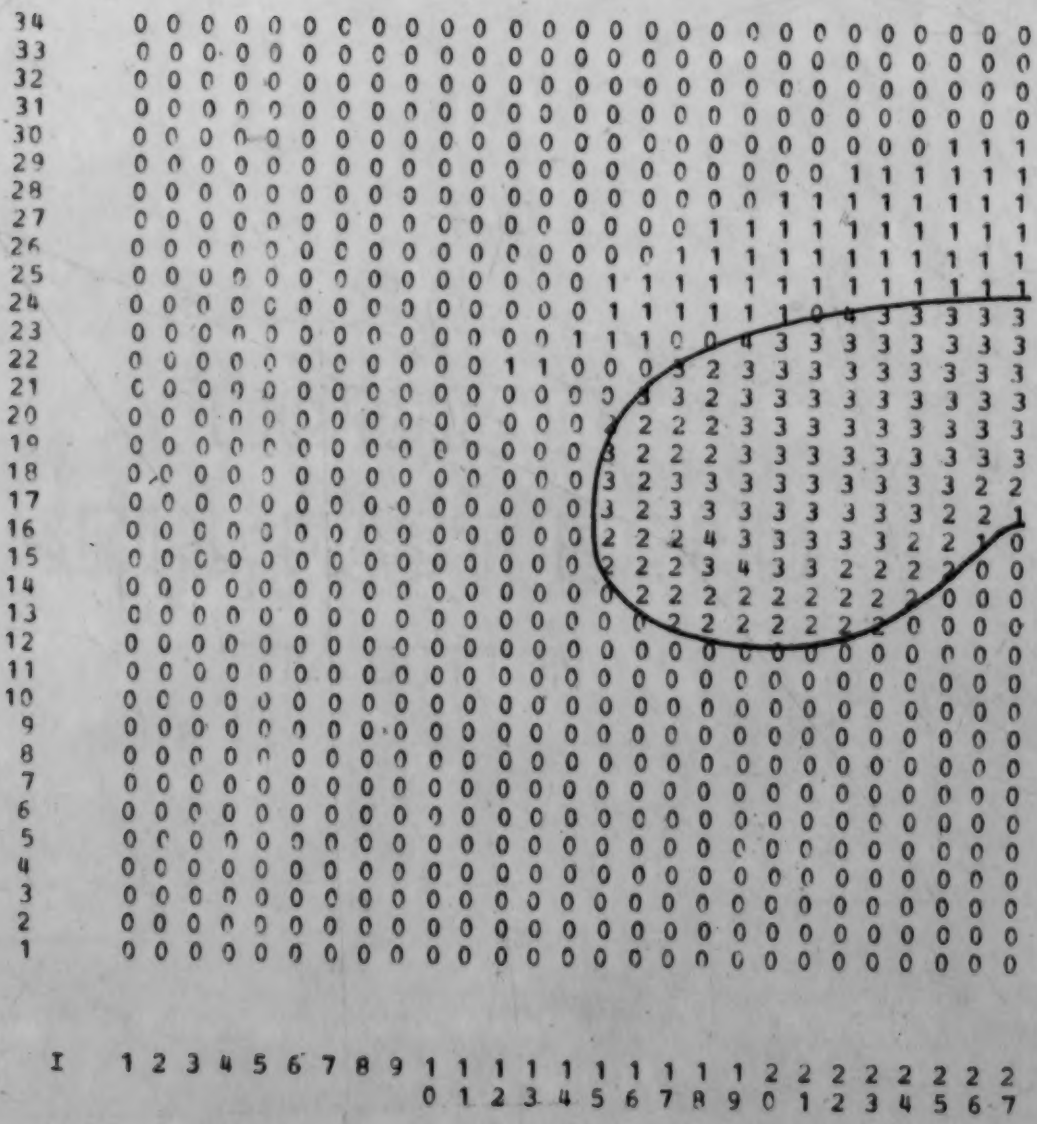

NORMALISED HEATING INDEX AT TIME STEP 480

PLANE K = 8

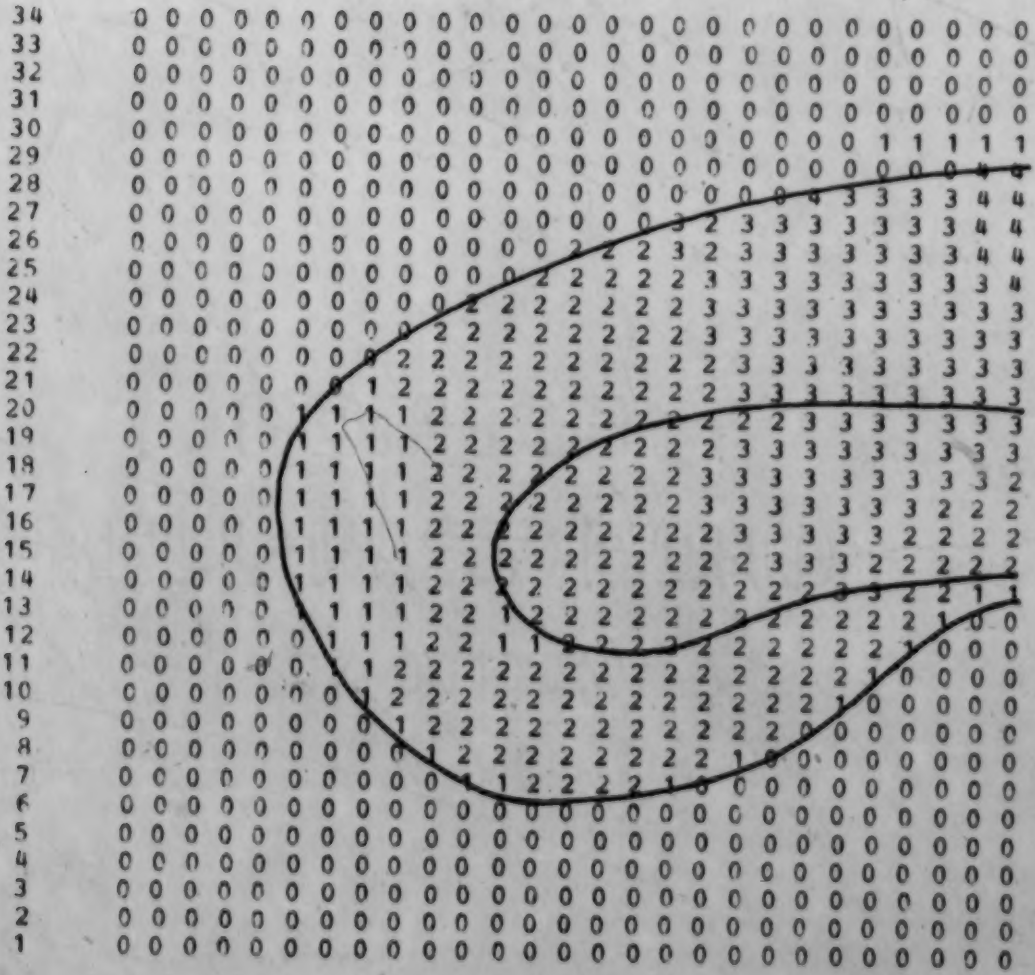

NORMALISED HEATING INDEX AT TIME STEP 480

PLANE K = 9

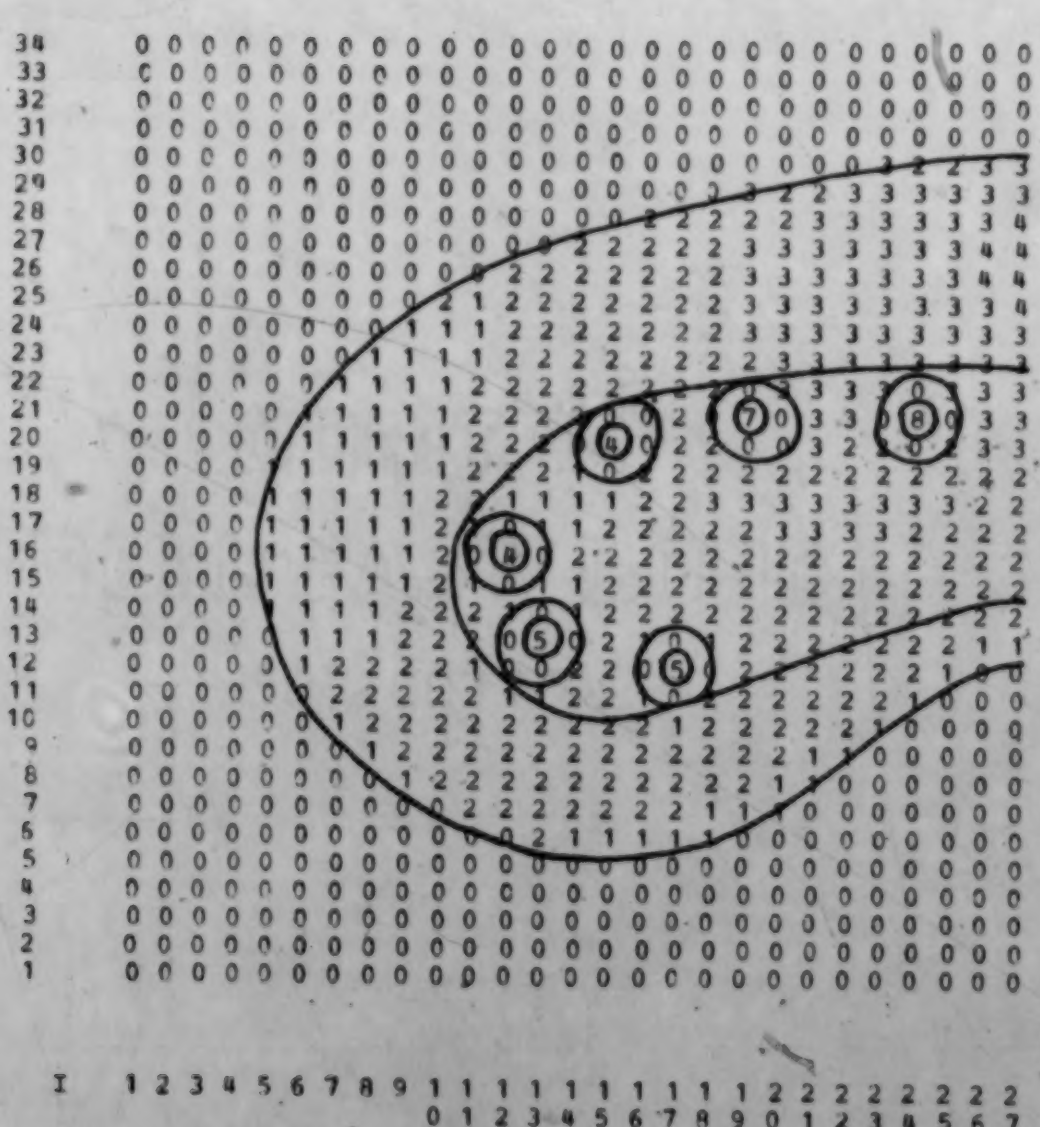

NORMALISED HEATING INDEX AT TIME STEP 480

PLANE K = 10

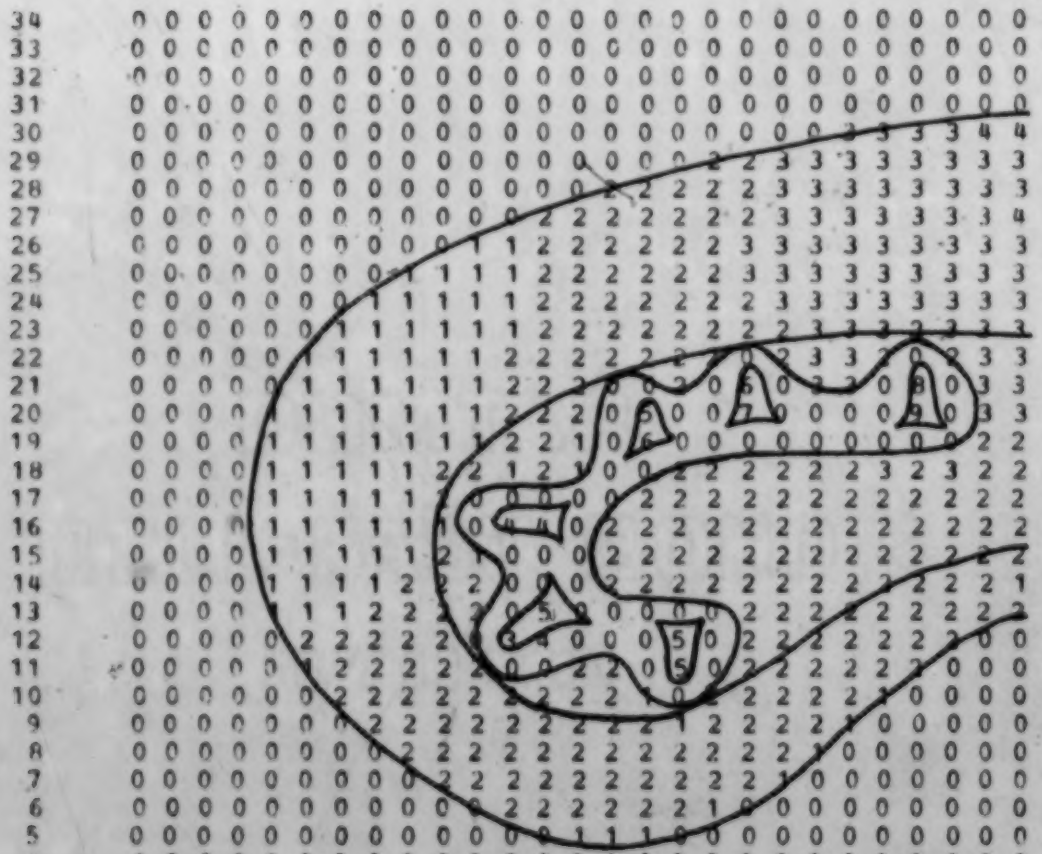

J	I = 1	2	3	4	5	6	7	8	9	10	11	12	13	14	15	16	17	18	19	20	21	22	23	24	25	26	27
34	0	0	0	0	0	0	0	0	0	0	0	0	0	0	0	0	0	0	0	0	0	0	0	0	0	0	0
33	0	0	0	0	0	0	0	0	0	0	0	0	0	0	0	0	0	0	0	0	0	0	0	0	0	0	0
32	0	0	0	0	0	0	0	0	0	0	0	0	0	0	0	0	0	0	0	0	0	0	0	0	0	0	0
31	0	0	0	0	0	0	0	0	0	0	0	0	0	0	0	0	0	0	0	0	0	0	0	0	0	0	0
30	0	0	0	0	0	0	0	0	0	0	0	0	0	0	0	0	0	0	0	0	0	0	0	0	0	0	0
29	0	0	0	0	0	0	0	0	0	0	0	0	0	0	0	0	0	0	0	0	0	0	0	0	0	0	0
28	0	0	0	0	0	0	0	0	0	0	0	0	0	0	0	0	0	0	0	0	0	0	0	0	0	0	0
27	0	0	0	0	0	0	0	0	0	0	0	0	0	0	0	0	0	0	0	0	0	0	0	0	0	0	0
26	0	0	0	0	0	0	0	0	0	0	0	0	0	0	0	0	0	0	0	0	0	0	0	0	0	0	0
25	0	0	0	0	0	0	0	0	0	0	0	0	0	0	0	0	0	0	0	0	0	0	0	0	0	0	0
24	0	0	0	0	0	0	0	0	0	0	0	0	0	0	0	0	0	0	0	0	0	0	0	0	0	0	0
23	0	0	0	0	0	0	0	0	0	0	0	0	0	0	0	0	0	0	0	0	0	0	0	0	0	0	0
22	0	0	0	0	0	0	0	0	0	0	0	0	0	0	0	0	0	0	0	0	0	0	0	0	0	0	0
21	0	0	0	0	0	0	0	0	0	0	0	0	0	0	0	0	0	0	0	0	0	0	0	0	0	0	0
20	0	0	0	0	0	0	0	0	0	0	0	0	0	0	0	0	0	0	0	0	0	0	0	0	0	0	0
19	0	0	0	0	0	0	0	0	0	0	0	0	0	0	0	0	0	0	0	0	0	0	0	0	0	0	0
18	0	0	0	0	0	0	0	0	0	0	0	0	0	0	0	0	0	0	0	0	0	0	0	0	0	0	0
17	0	0	0	0	0	0	0	0	0	0	0	0	0	0	0	0	0	0	0	0	0	0	0	0	0	0	0
16	0	0	0	0	0	0	0	0	0	0	0	0	0	0	0	0	0	0	0	0	0	0	0	0	0	0	0
15	0	0	0	0	0	0	0	0	0	0	0	0	0	0	0	0	0	0	0	0	0	0	0	0	0	0	0
14	0	0	0	0	0	0	0	0	0	0	0	0	0	0	0	0	0	0	0	0	0	0	0	0	0	0	0
13	0	0	0	0	0	0	0	0	0	0	0	0	0	0	0	0	0	0	0	0	0	0	0	0	0	0	0
12	0	0	0	0	0	0	0	0	0	0	0	0	0	0	0	0	0	0	0	0	0	0	0	0	0	0	0
11	0	0	0	0	0	0	0	0	0	0	0	0	0	0	0	0	0	0	0	0	0	0	0	0	0	0	0
10	0	0	0	0	0	0	0	0	0	0	0	0	0	0	0	0	0	0	0	0	0	0	0	0	0	0	0
9	0	0	0	0	0	0	0	0	0	0	0	0	0	0	0	0	0	0	0	0	0	0	0	0	0	0	0
8	0	0	0	0	0	0	0	0	0	0	0	0	0	0	0	0	0	0	0	0	0	0	0	0	0	0	0
7	0	0	0	0	0	0	0	0	0	0	0	0	0	0	0	0	0	0	0	0	0	0	0	0	0	0	0
6	0	0	0	0	0	0	0	0	0	0	0	0	0	0	0	0	0	0	0	0	0	0	0	0	0	0	0
5	0	0	0	0	0	0	0	0	0	0	0	0	0	0	0	0	0	0	0	0	0	0	0	0	0	0	0
4	0	0	0	0	0	0	0	0	0	0	0	0	0	0	0	0	0	0	0	0	0	0	0	0	0	0	0
3	0	0	0	0	0	0	0	0	0	0	0	0	0	0	0	0	0	0	0	0	0	0	0	0	0	0	0
2	0	0	0	0	0	0	0	0	0	0	0	0	0	0	0	0	0	0	0	0	0	0	0	0	0	0	0
1	0	0	0	0	0	0	0	0	0	0	0	0	0	0	0	0	0	0	0	0	0	0	0	0	0	0	0

J	I = 28	29	30	31	32	33	34	35	36	37
34	0	0	0	0	0	0	0	0	0	0
33	0	0	0	0	0	0	0	0	0	0
32	0	0	0	0	0	0	0	0	0	0
31	0	0	0	0	0	0	0	0	0	0
30	4	4	4	4	3	3	3	3	0	0
29	3	3	3	3	3	3	3	3	0	0
28	3	3	3	3	3	3	3	3	0	0
27	4	3	3	3	3	3	3	3	0	0
26	3	3	3	3	3	3	3	3	0	0
25	3	3	3	3	3	3	3	3	0	0
24	3	3	3	3	3	3	3	3	0	0
23	3	3	3	3	3	3	3	3	0	0
22	3	3	3	3	3	3	3	3	0	0
21	3	3	3	3	3	3	3	3	0	0
20	3	3	3	3	3	3	3	3	0	0
19	2	2	2	2	2	2	2	2	0	0
18	2	2	2	2	2	2	2	2	0	0
17	2	2	2	2	2	2	2	2	0	0
16	2	2	2	2	2	2	2	2	0	0
15	2	2	2	2	2	2	2	2	0	0
14	1	2	2	2	2	2	2	2	0	0
13	2	2	2	2	2	2	2	2	0	0
12	0	0	0	0	0	0	0	0	0	0
11	0	0	0	0	0	0	0	0	0	0
10	0	0	0	0	0	0	0	0	0	0
9	0	0	0	0	0	0	0	0	0	0
8	0	0	0	0	0	0	0	0	0	0
7	0	0	0	0	0	0	0	0	0	0
6	0	0	0	0	0	0	0	0	0	0
5	0	0	0	0	0	0	0	0	0	0
4	0	0	0	0	0	0	0	0	0	0
3	0	0	0	0	0	0	0	0	0	0
2	0	0	0	0	0	0	0	0	0	0
1	0	0	0	0	0	0	0	0	0	0

NORMALISED HEATING INDEX AT TIME STEP 480

PLANE K = 11

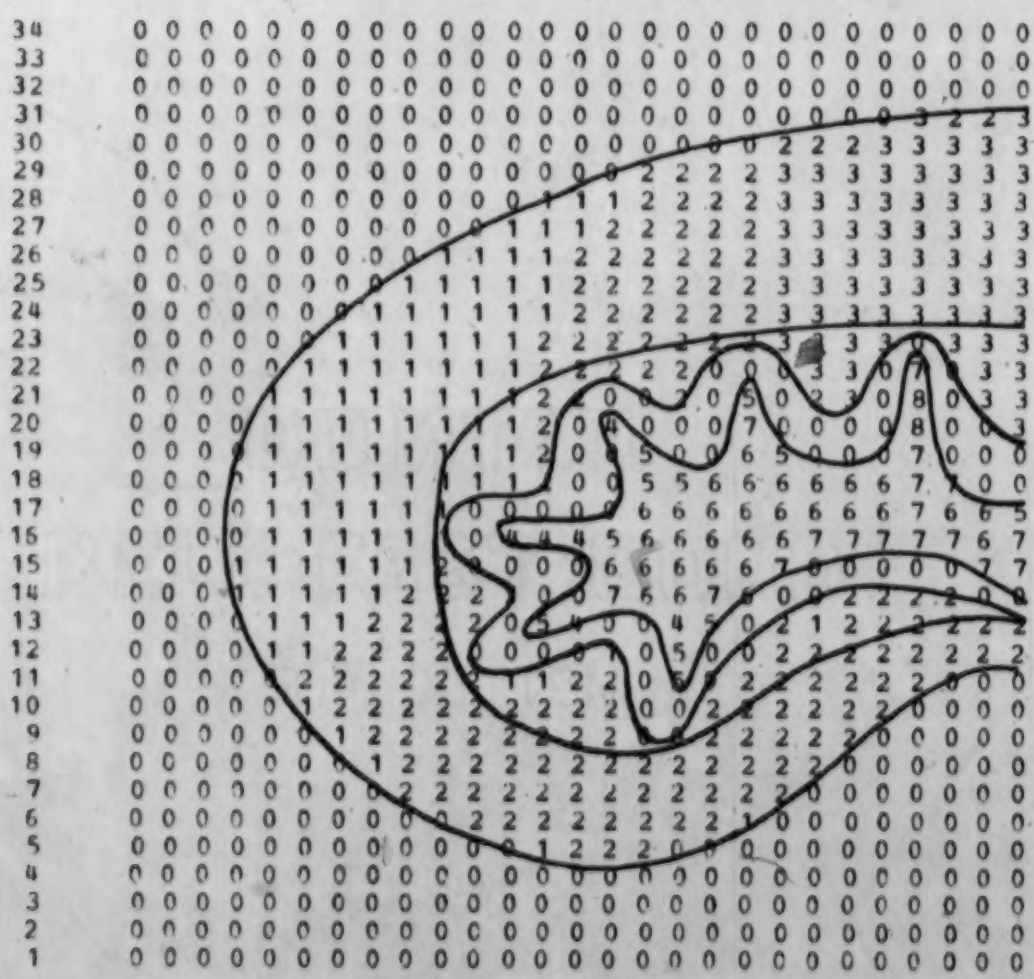

NORMALISED HEATING INDEX AT TIME STEP 480

PLANE K = 13

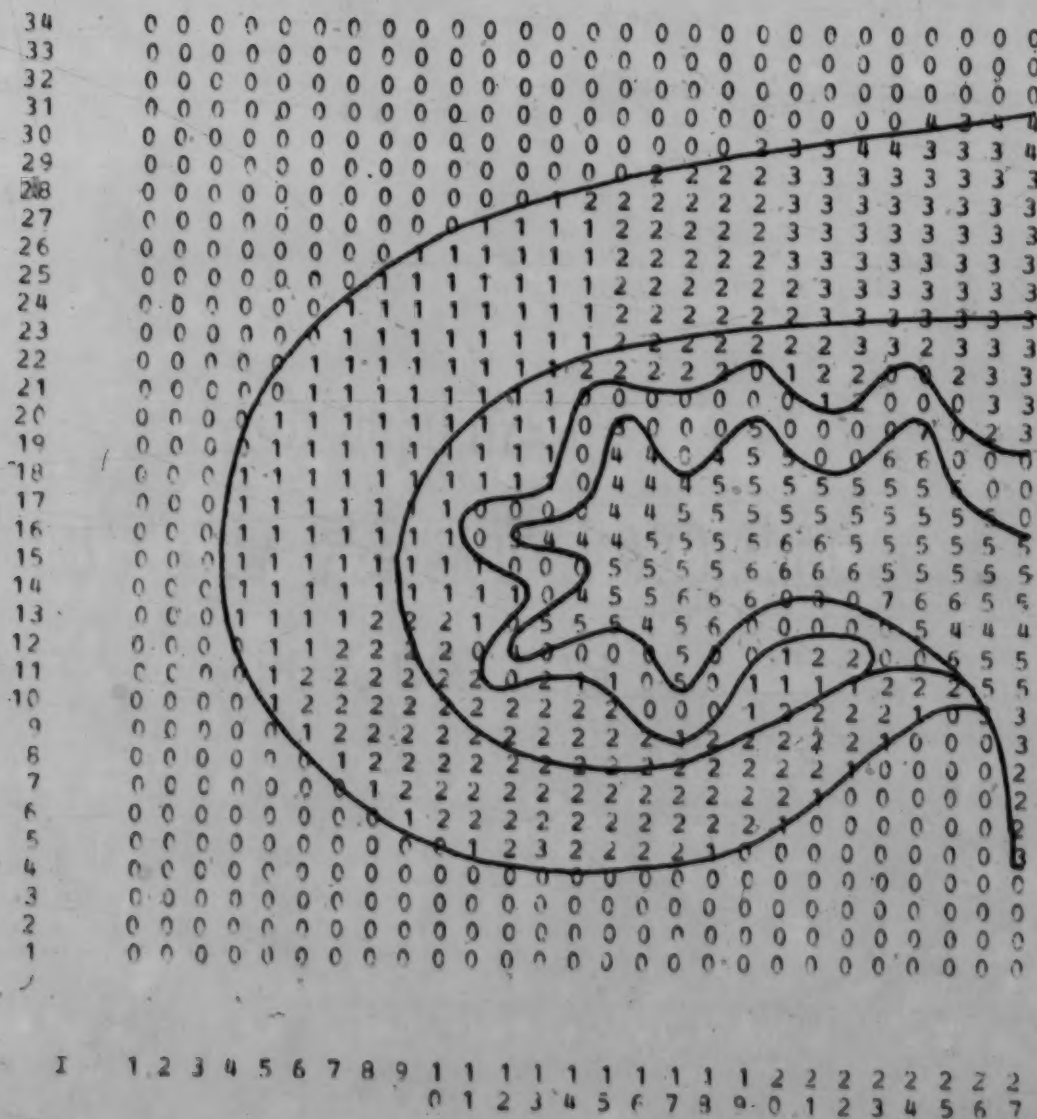

NORMALISED HEATING INDEX AT TIME STEP 480

PLANE K = 15

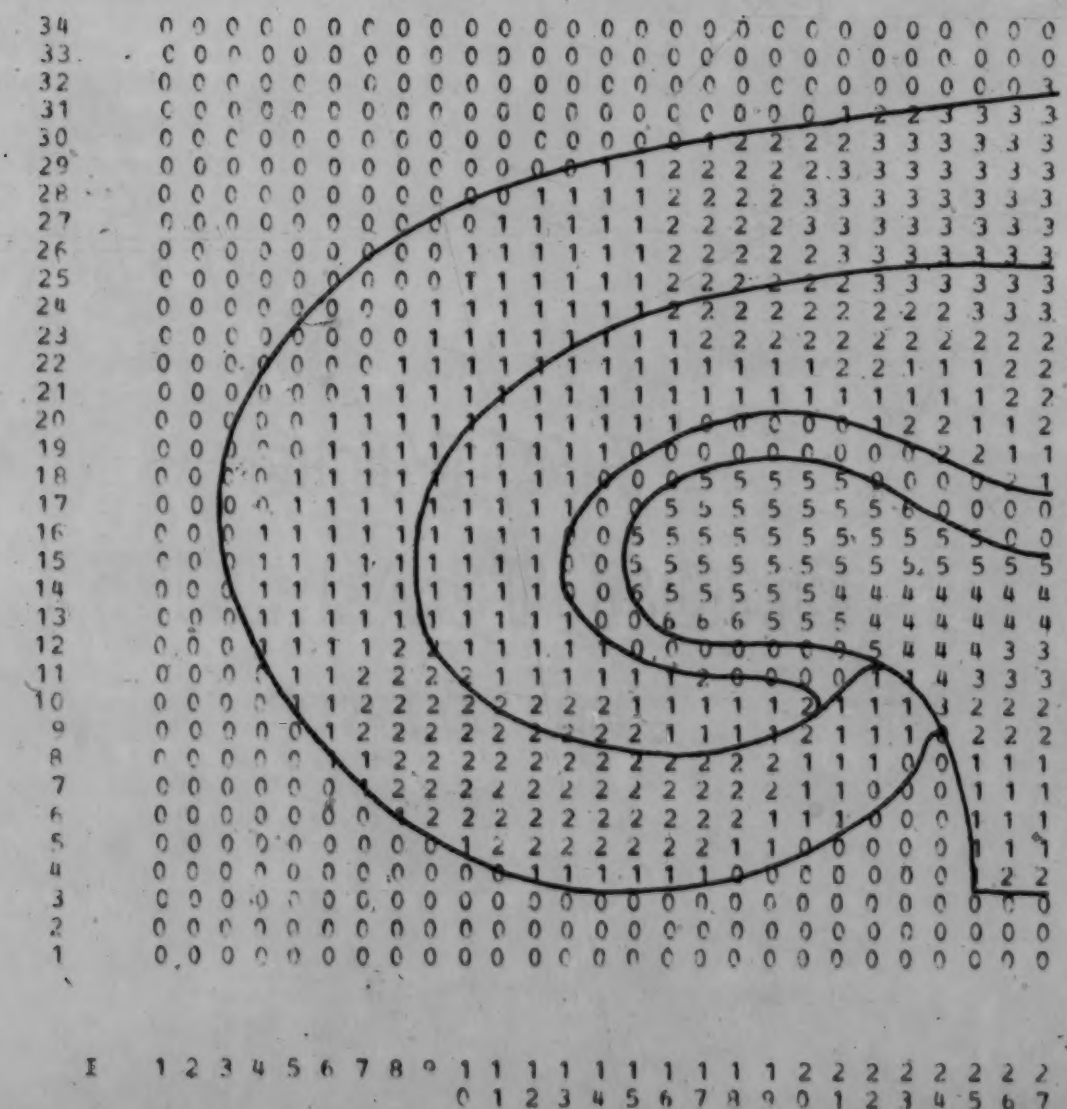

Maximum dissipation occurs in a tubule in plane 10.

Although conclusions are difficult because heating would not be from a uniform temperature in the real case, it seems that a slight improvement in uniformity is obtained as the temperature increases. However, dissipation in the fat layer is still minimal.

(6.10) Condition 5. The Effects of No Perfusion.
(Figure 6.10(5,8,9,11,13,15))

As might be anticipated, the maximum dissipation is considerably reduced, to approximately the same level as for 1% DMSO. Dissipation in the cortex and medulla, of which planes 5 and 8 are representative, is relatively good, and the tubular effect at plane 9 is reversed in that the tubules themselves absorb no power. In contrast to the situation for 1% DMSO, however, it is clear from the representative planes 11,13 and 15 that no dissipation is occurring in the pelvis. In view of the sensitivity of the conductivity of this region to the DMSO concentration, this is not surprising.

(6.11) Condition 6. Total Perfusion of the Pelvis.
(Figure 6.11(9-11,13,15))

In this case, the conductivity of the pelvis is

FIGURE 6.10(5,8,9,11,13,15) Perfusion effect

Set #5: Max. dissipated power = 0.0032 W/m³.

Max. dissipation at plane K = 15.

Frequency = 2500 Mhz.

Perfusate = 10% DMSO.

Temperature = -20°C.

No Perfusion.

NORMALISED HEATING INDEX AT TIME STEP 480.

PLANE K = 5

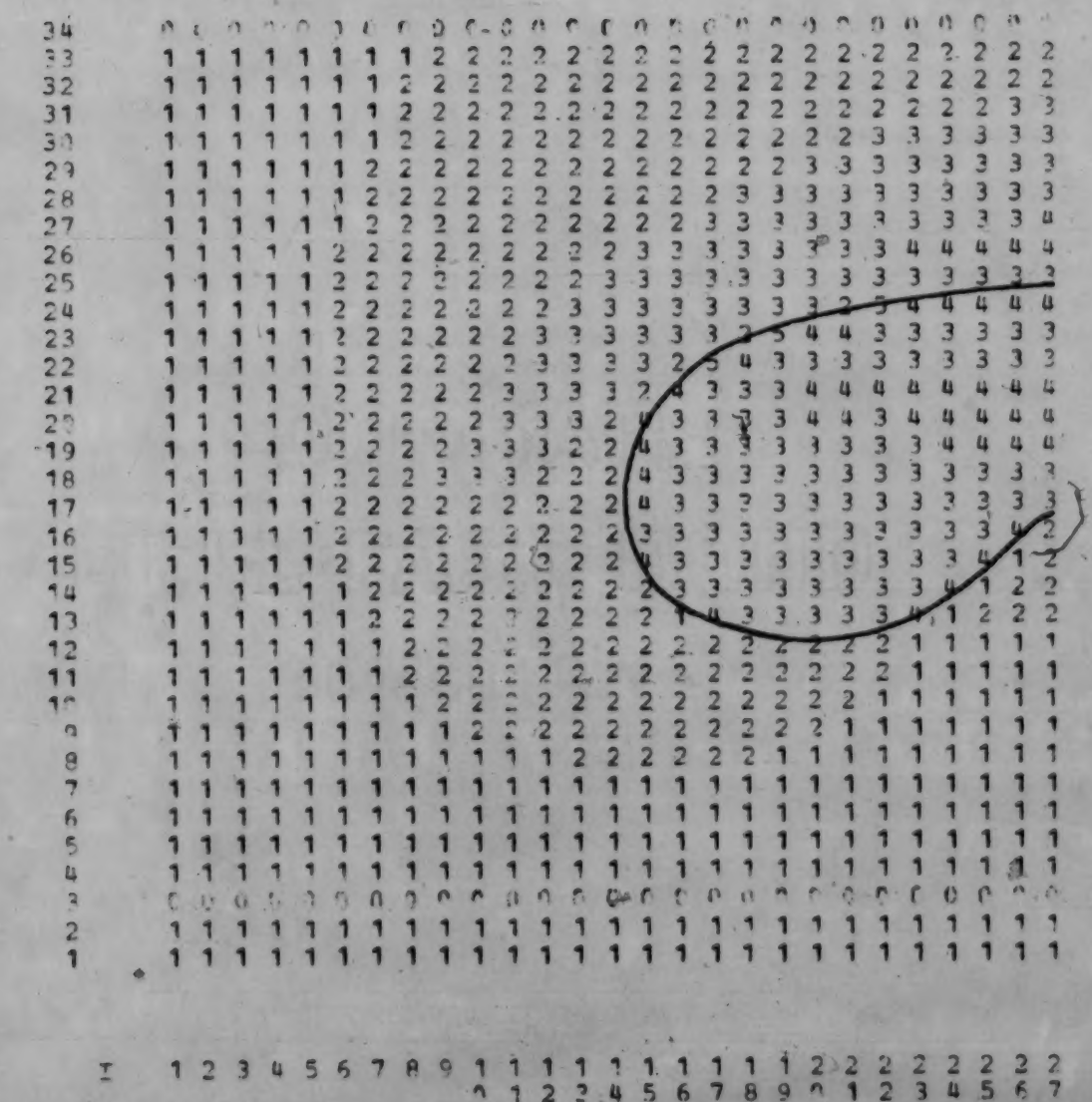

NORMALISED HEATING INDEX AT TIME STEP 48

PLANE K = 8

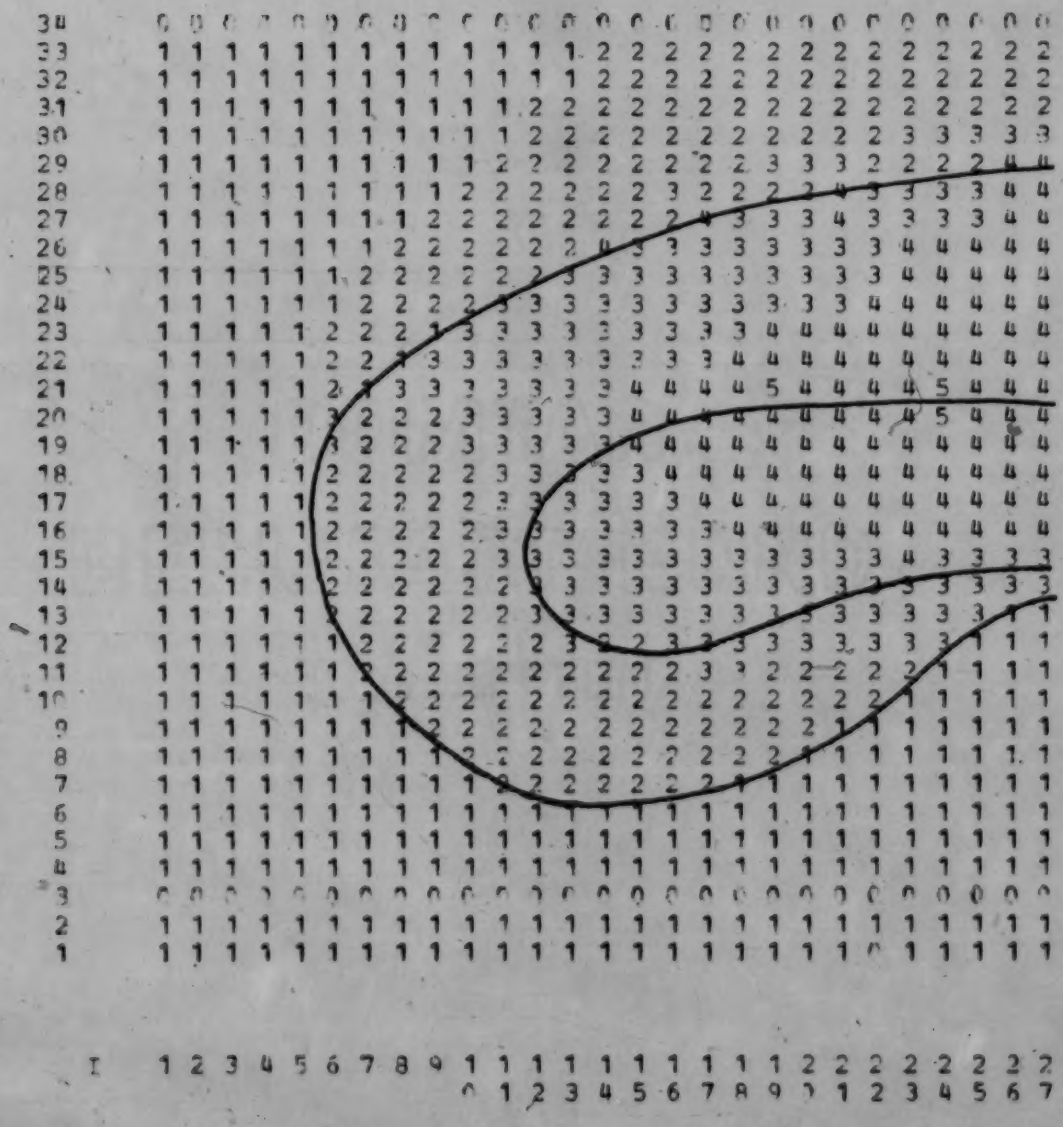

NORMALISED HEATING INDEX AT TIME STEP 480

PLANE K = 9

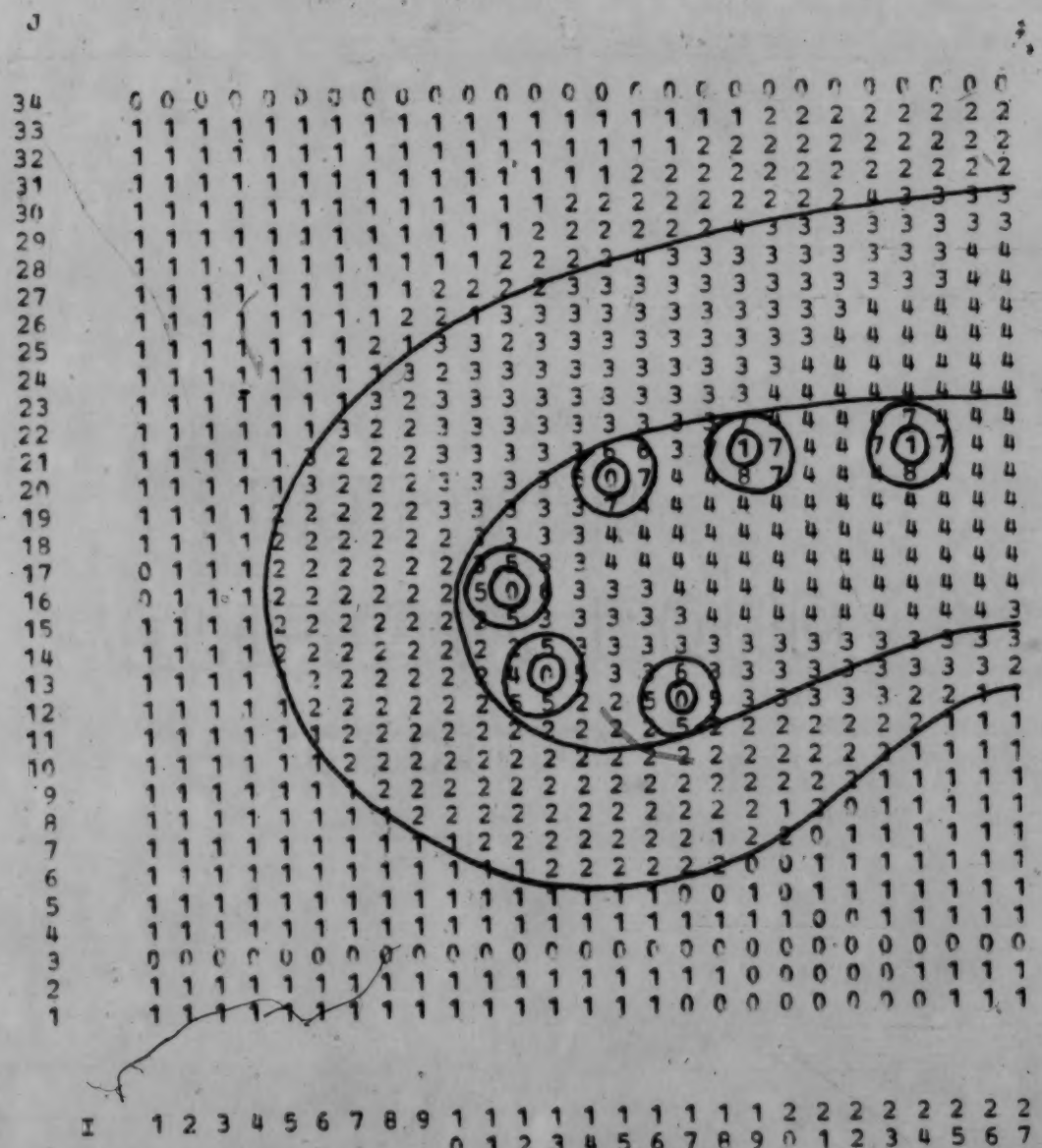

NORMALISED HEATING INDEX AT TIME STEP 480

PLANE K = 11

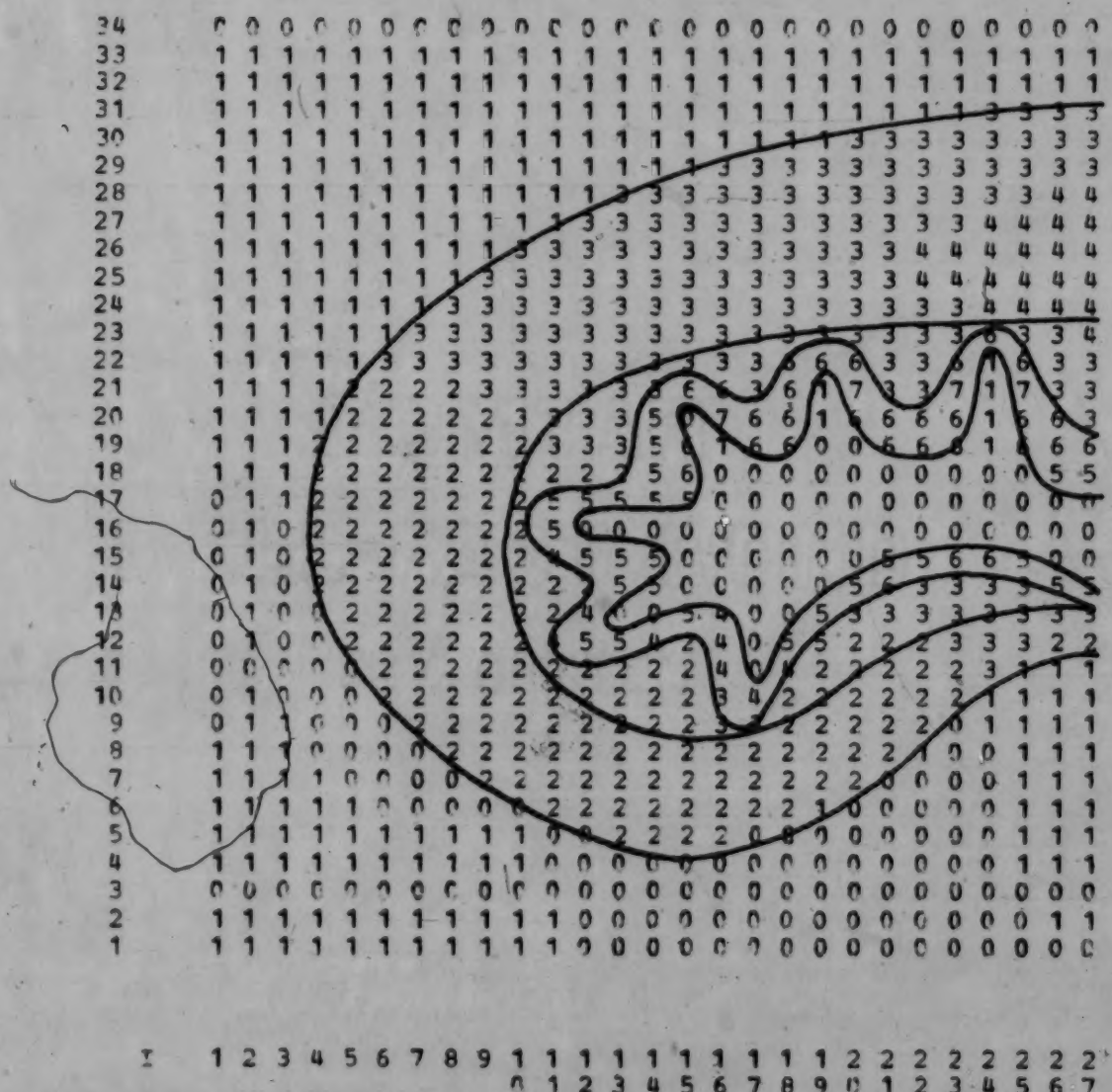

NORMALISED HEATING INDEX AT TIME STEP 480

PLANE K = 13

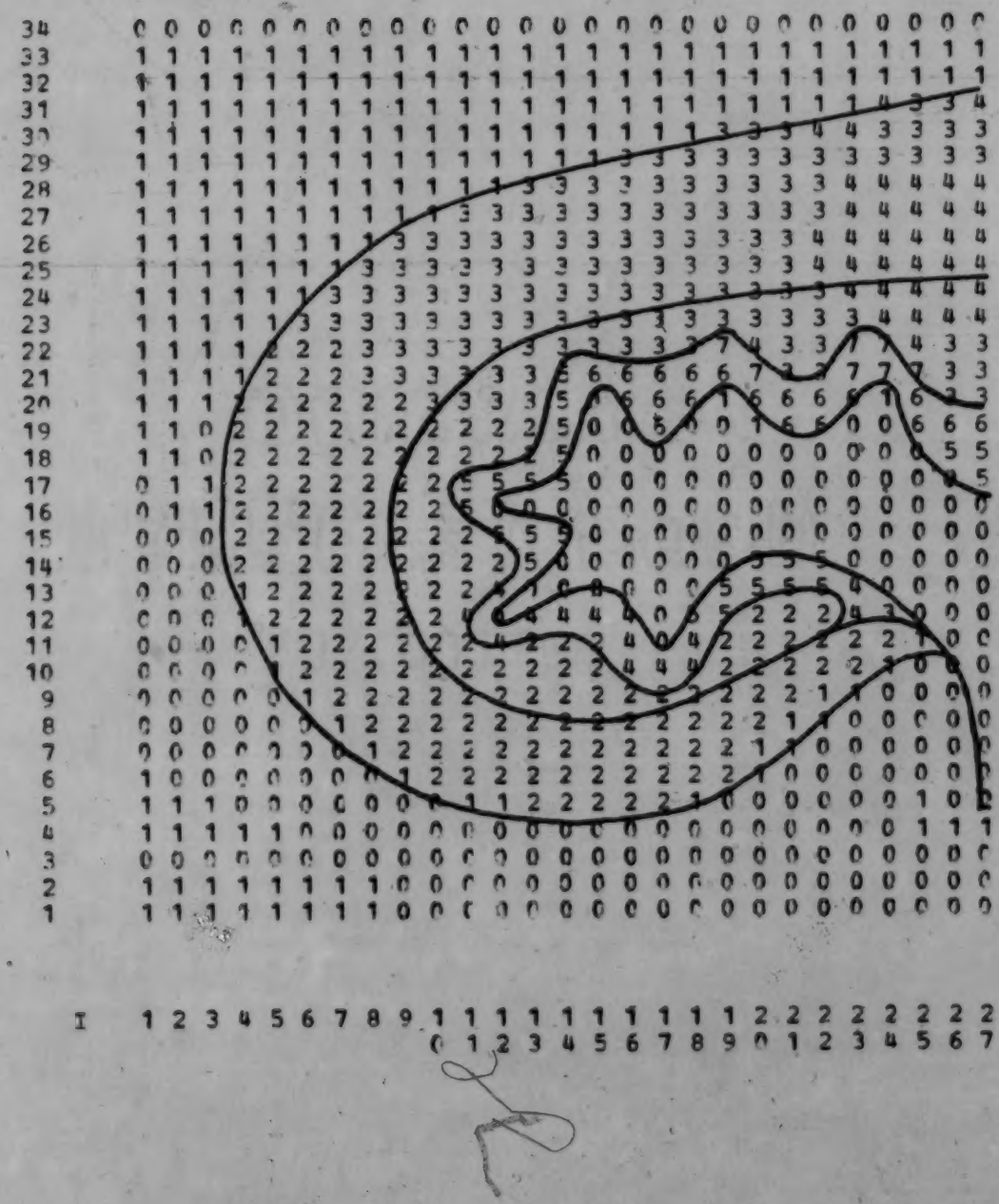

NORMALISED HEATING INDEX AT TIME STEP 480

PLANE K = 15

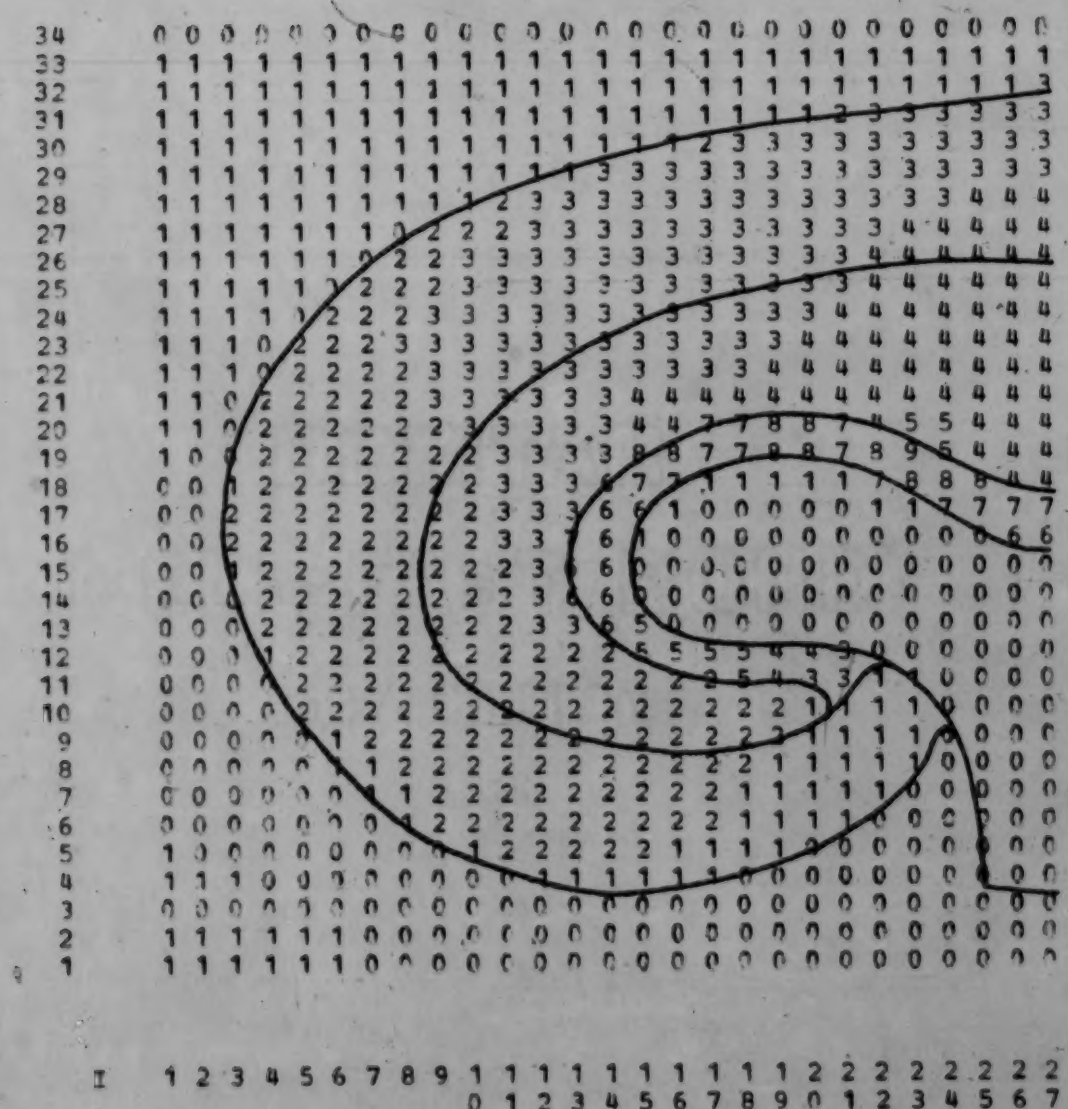

FIGURE 6.11(9-11,13,15) Tubule effect

Set #6: Max. dissipated power = 0.254 W/m³.

Max. dissipation at plane K = 9.

Frequency = .2500 Mhz.

Perfusate = 10% DMSO.

Temperature = -20°C.

Partial Perfusion with 10% DMSO in pelvis.

NORMALISED HEATING INDEX AT TIME STEP 480

PLANE K = 9

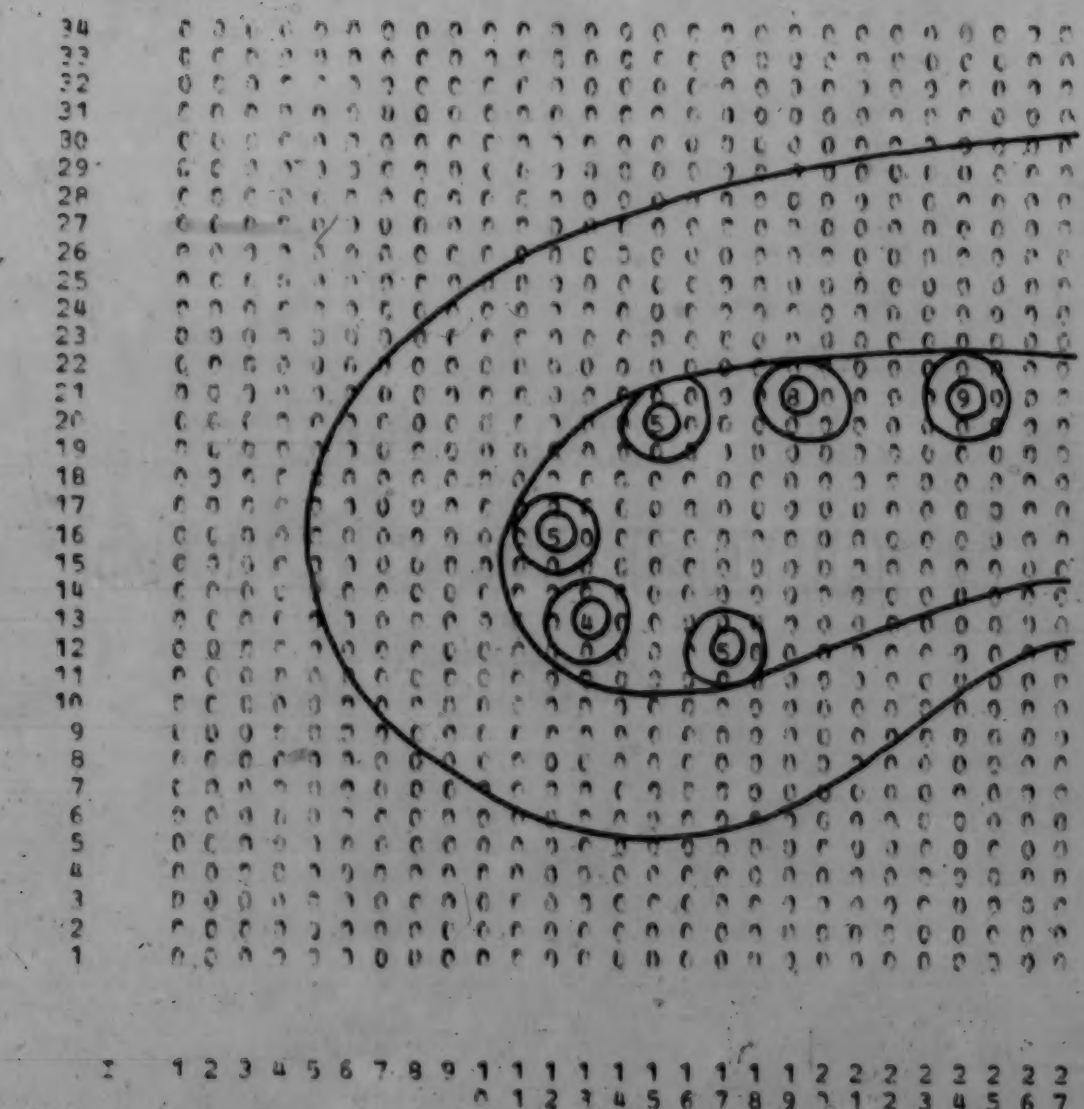

NORMALISED HEATING INDEX AT TIME STEP 480

PLANE K = 10

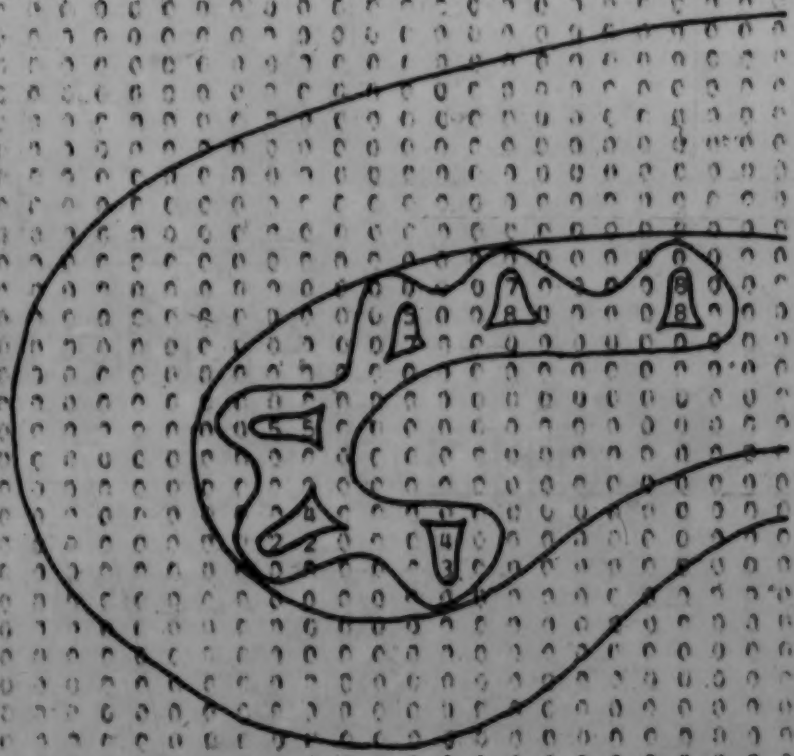

NORMALISED HEATING INDEX AT TIME STEP 480

PLANE K = 11

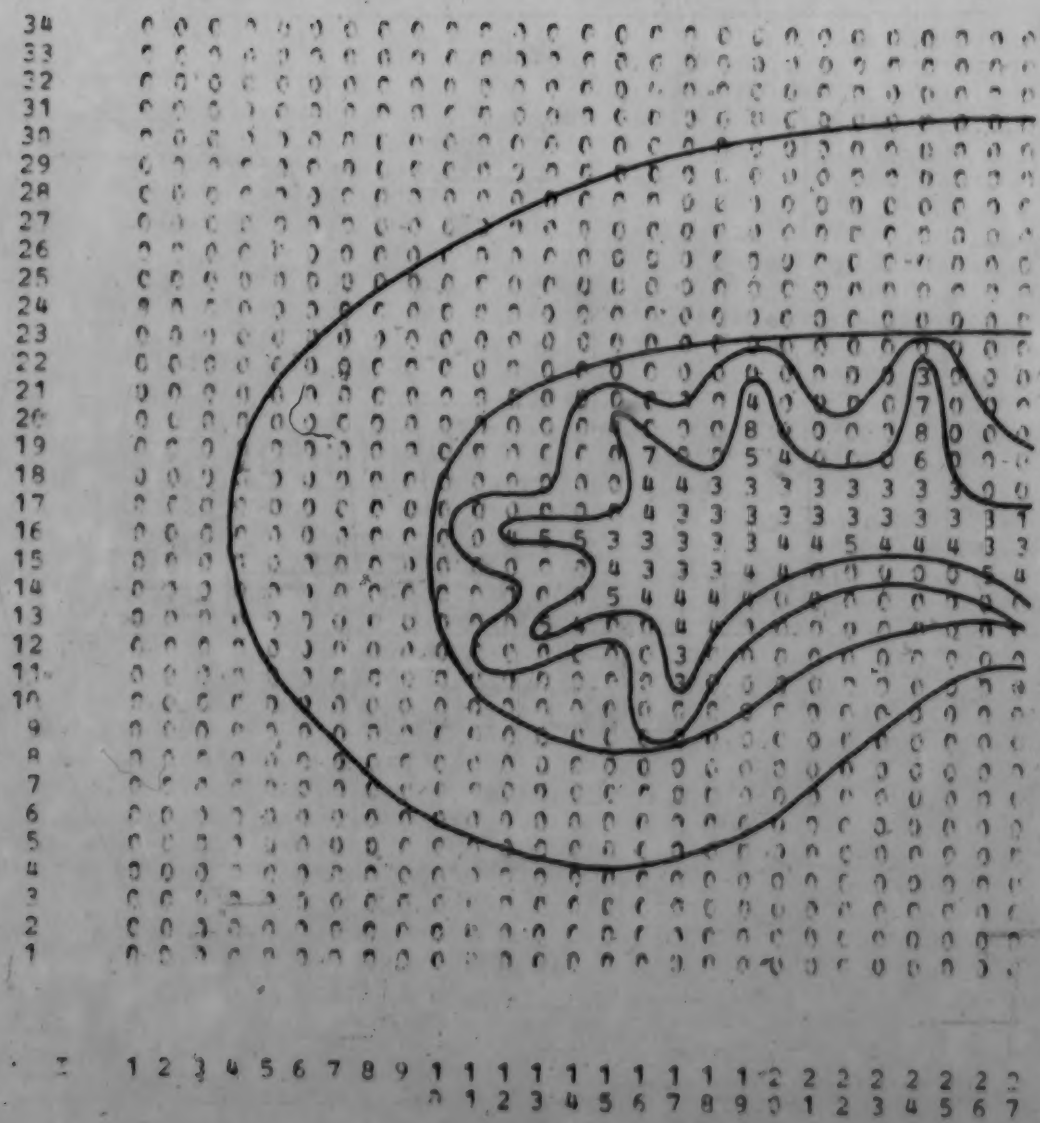

NORMALISED HEATING INDEX AT TIME STEP 480

PLANE K = 13

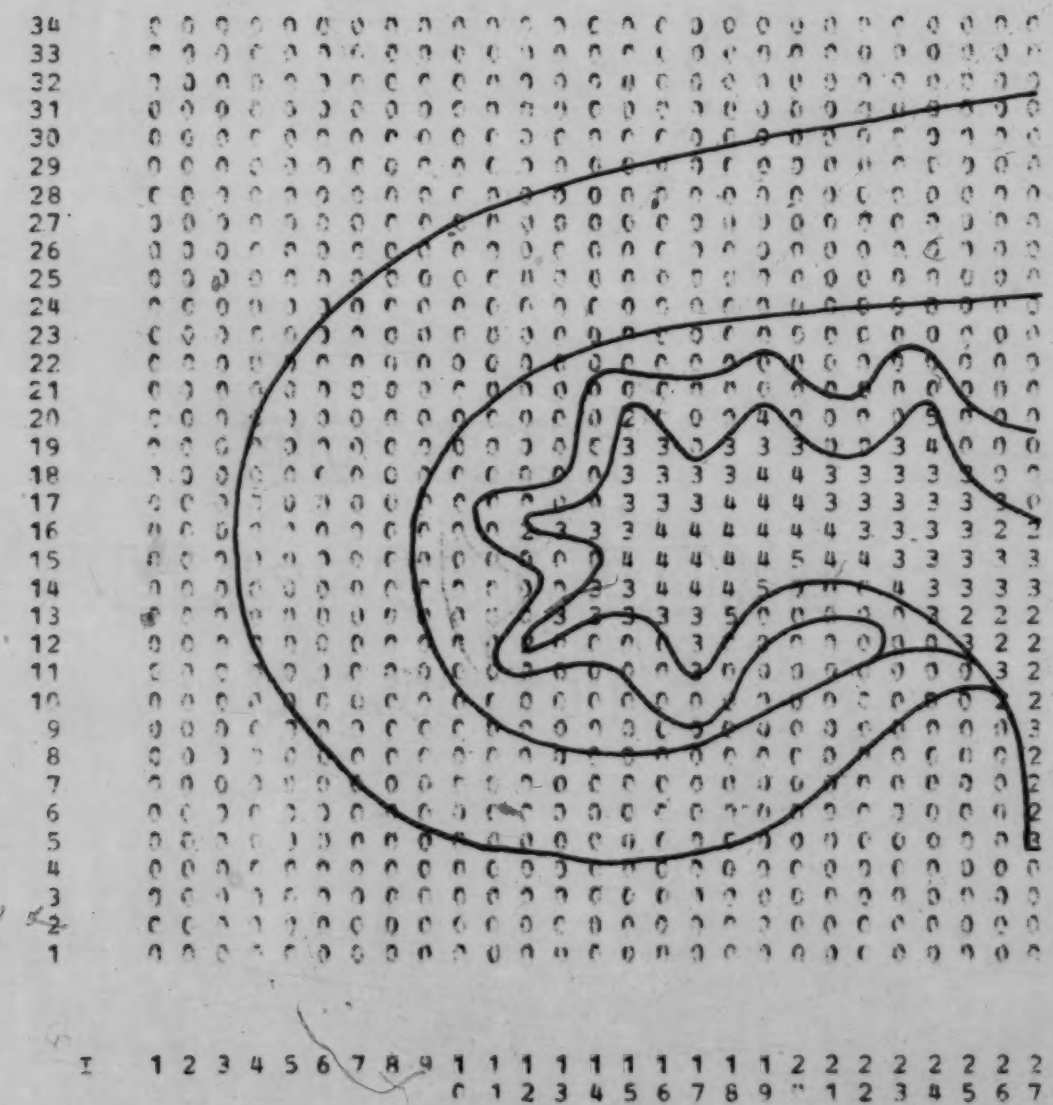

NORMALISED HEATING INDEX AT TIME STEP 480.

PLANE K = 15

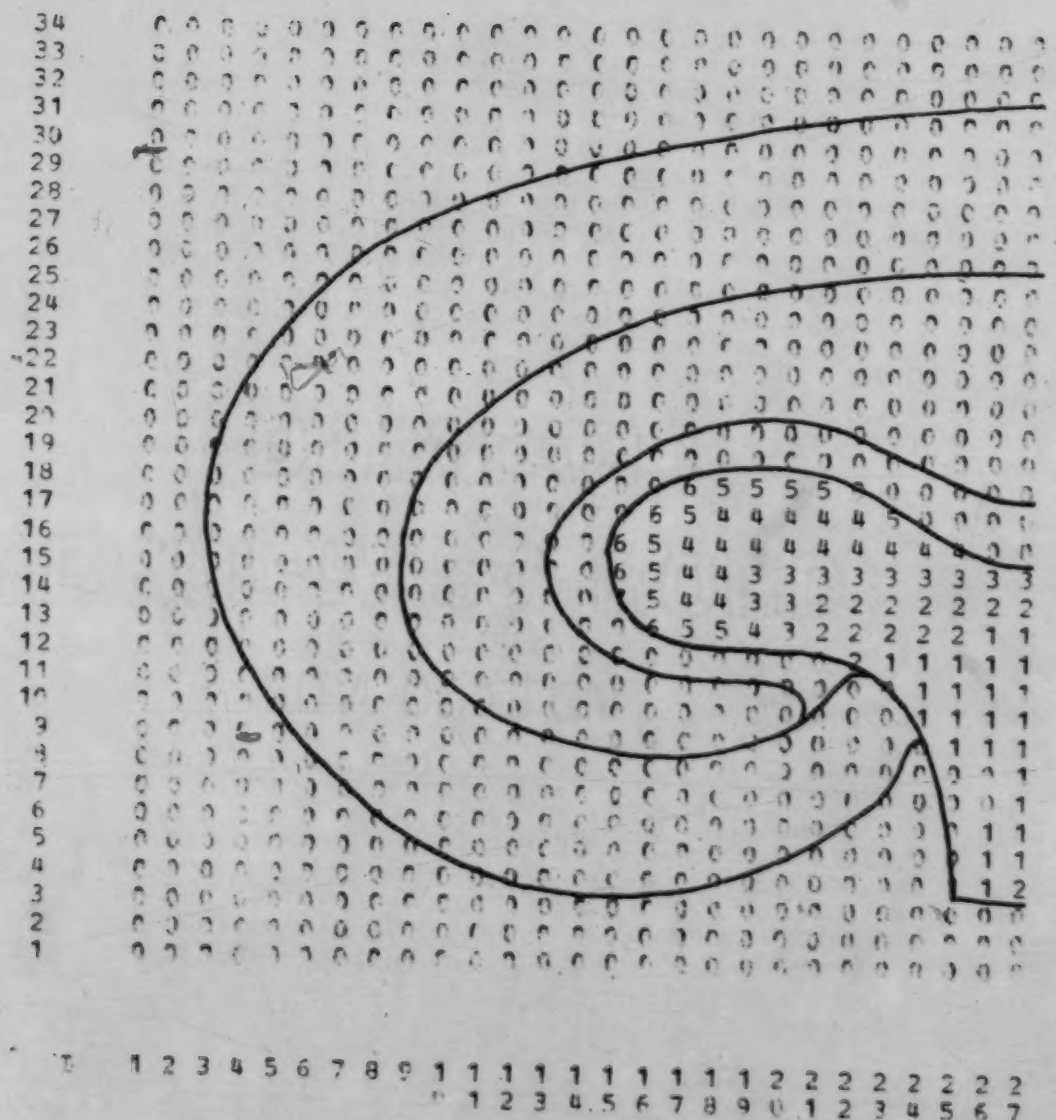

increased to a value representative of total displacement of the urine by the DMSO perfusate. This is interesting for two reasons. The first is that it further indicates the sensitivity of the model to the properties of the pelvic region, and the second is that it suggests what might happen to the vascular system, since this is likely to contain a very high percentage of perfusate, perfusion being through the vascular system.

Plane 9 is the first plane to indicate any dissipation whatsoever, and the value here is very high, and is in the tubular structure. Maximum dissipation is 0.254 W/m^3, a factor of more than 9 times that of the datum model. At this plane, there is no absorbtion anywhere else. Planes 10,11,13 and 15 are representative of the rest of the kidney, and show that all the power is absorbed in the pelvic region. From these results, it is clear that a high content of perfusate in small tubular structures is liable to cause highly non-uniform heating around these structures, with potentially damaging results. This suggests the possibility of a final perfusion step with an appropriate liquid chosen to minimise this effect.

(6.12) Condition 7. 1000 Mhz Heating at 20°C.
(Figure 6.12(5,8,9,11,13,15))

The first interesting point to emerge from this run is

PIGURE 6.12(5,8,9,11,13,15) Temperature effect (1000 Mhz.)

Set #7: Max. dissipated power = 0.115 W/m³.

Max. dissipation at plane K = 10.

Frequency = 1000 Mhz.

Perfusate = 10% DMSO.

Temperature = +20°C.

Partial Perfusion.

NORMALISED HEATING INDEX AT TIME STEP 600

PLANE K = 5

J

34	0	0	0	0	0	0	0	0	0	0	0	0	0	0	0	0	0	0	0	0	0	0	0	0	0
33	1	1	1	1	1	1	1	0	0	0	0	0	0	0	0	0	0	0	0	0	0	0	0	0	0
32	1	1	1	1	1	1	1	1	0	0	0	0	0	0	0	0	0	0	0	0	0	0	0	0	0
31	1	1	1	1	1	1	1	1	1	0	0	0	0	0	0	0	0	0	0	0	0	0	0	0	0
30	1	1	1	1	1	1	1	1	1	1	1	1	1	1	1	0	0	0	0	0	0	0	0	1	1
29	1	1	1	1	1	1	1	1	1	1	1	1	1	1	1	1	1	1	1	1	1	1	1	1	1
28	1	1	1	1	1	1	1	1	1	1	1	1	1	1	1	1	1	1	1	1	1	1	1	1	1
27	1	1	1	1	1	1	1	1	1	1	1	1	1	1	1	1	1	1	1	1	1	1	1	2	2
26	1	1	1	1	1	1	1	1	1	1	1	2	2	1	1	1	1	2	1	1	2	2	2	1	1
25	1	1	1	1	1	1	2	2	2	2	2	2	2	2	2	2	2	2	2	2	2	2	2	2	1
24	1	1	1	1	2	2	2	2	2	2	2	2	2	2	2	2	2	3	2	1	2	3	2	2	2	2	3
23	0	1	1	2	2	2	2	2	2	2	2	2	3	2	3	2	2	2	2	3	4	3	3	3	3	3
22	0	1	1	2	2	2	2	3	3	3	3	4	3	2	2	0	2	2	3	4	4	4	4	4	4	4
21	0	1	2	2	2	3	3	3	3	3	4	3	2	2	0	2	3	3	3	3	3	3	3	3	2	2	2
20	0	1	2	2	3	3	3	3	3	4	3	2	1	0	1	2	3	3	3	3	3	3	3	3	2	2	2
19	0	2	2	2	3	3	4	4	5	4	2	2	1	0	2	2	2	2	3	3	3	3	2	2	2	3	3
18	0	2	2	3	3	4	4	6	4	3	2	2	1	0	2	2	3	2	2	2	2	2	2	2	3	2	1
17	0	2	2	3	4	4	8	5	4	3	2	2	1	0	2	2	3	3	2	2	2	2	2	3	2	1	0
16	0	2	2	3	4	4	7	5	4	3	2	2	1	0	2	2	2	4	3	2	2	3	3	2	1	0	0
15	0	2	2	3	4	4	7	5	4	3	2	2	1	0	1	1	2	2	4	3	3	2	1	1	1	0	0
14	0	2	2	3	4	4	7	5	4	3	3	2	2	1	0	2	1	1	1	1	1	1	1	1	0	1	0
13	1	2	2	3	3	5	8	6	4	4	3	3	2	2	1	0	2	1	1	1	1	1	1	0	1	1	0
12	1	2	2	2	3	4	5	6	5	4	4	3	3	2	2	2	1	1	1	1	1	1	2	1	1	1
11	1	1	2	2	3	4	5	8	6	5	4	4	3	3	3	3	2	2	2	2	2	1	1	1	1	1
10	1	1	2	2	2	3	4	5	8	6	5	5	4	4	4	3	3	3	3	4	3	2	1	1	1	1
9	1	1	2	2	2	3	3	4	5	8	6	6	5	5	4	4	4	4	5	5	3	2	1	1	1	1
8	1	1	2	2	2	2	3	3	4	5	8	7	6	6	6	5	5	6	6	3	2	2	1	1	1	1
7	1	1	2	2	2	2	2	3	3	4	5	5	8	8	7	7	7	8	4	3	2	2	1	1	1	1
6	1	1	2	2	2	2	2	2	3	3	3	4	5	5	4	4	4	3	3	2	2	2	1	1	1	1
5	1	2	2	2	2	2	2	2	2	3	3	3	3	3	3	3	3	3	2	2	2	2	1	1	1	1
4	1	2	2	2	2	2	2	2	2	2	2	2	3	3	3	2	2	2	2	2	2	2	2	1	1	1
3	0	0	0	0	1	1	0	0	1	0	0	0	0	0	0	0	0	0	0	0	0	0	0	0	1	1
2	2	2	2	2	2	2	2	2	2	2	2	2	2	2	2	2	2	2	2	2	2	2	2	1	1	1
1	2	2	2	2	2	2	2	2	2	2	2	2	2	2	2	2	2	2	2	2	2	2	2	1	1	1

I	1	2	3	4	5	6	7	8	9	1 0	1 1	1 2	1 3	1 4	1 5	1 6	1 7	1 8	1 9	2 0	2 1	2 2	2 3	2 4	2 5	2 6	2 7

NORMALISED HEATING INDEX AT TIME STEP 600

PLANE K = 8

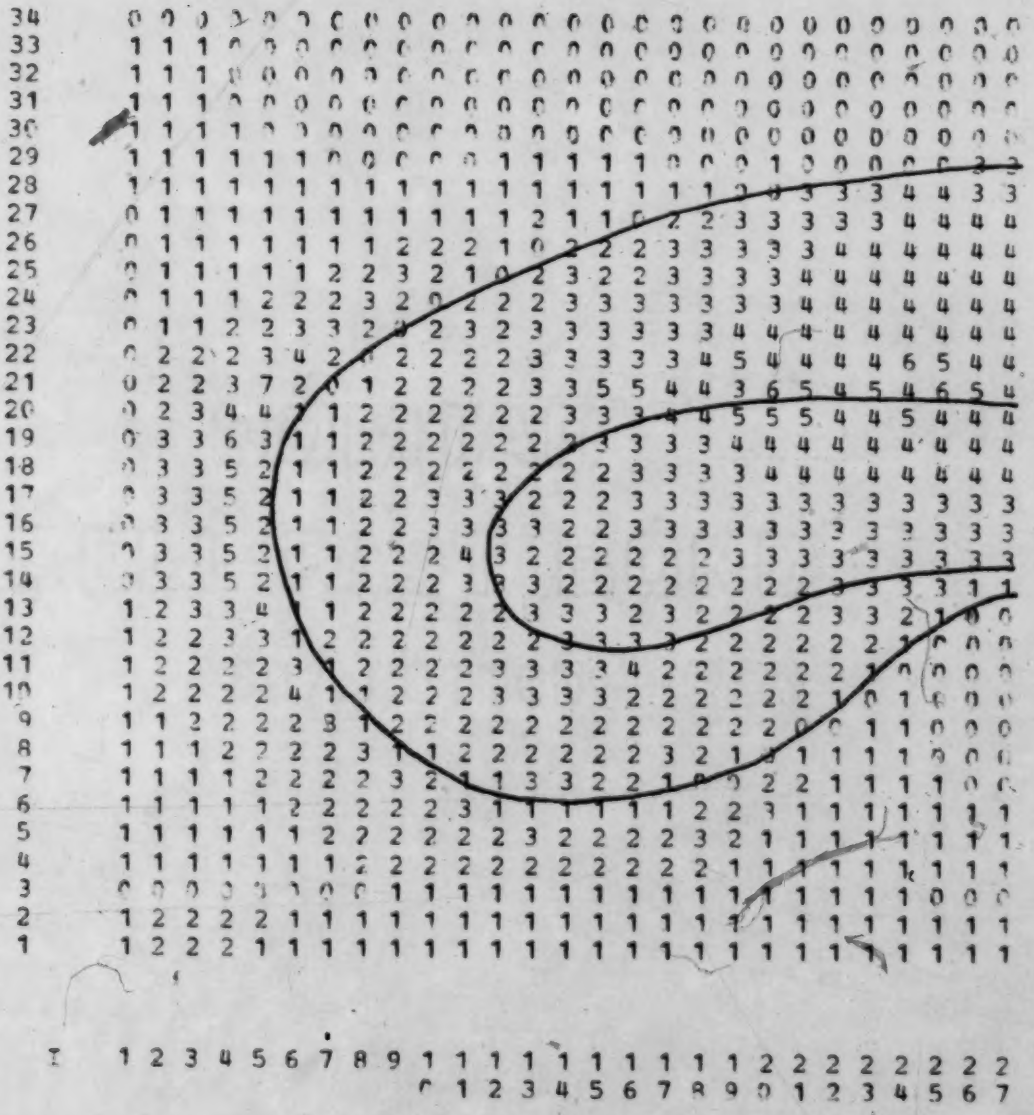

NORMALISED HEATING INDEX AT TIME STEP 600

PLANE K = 9

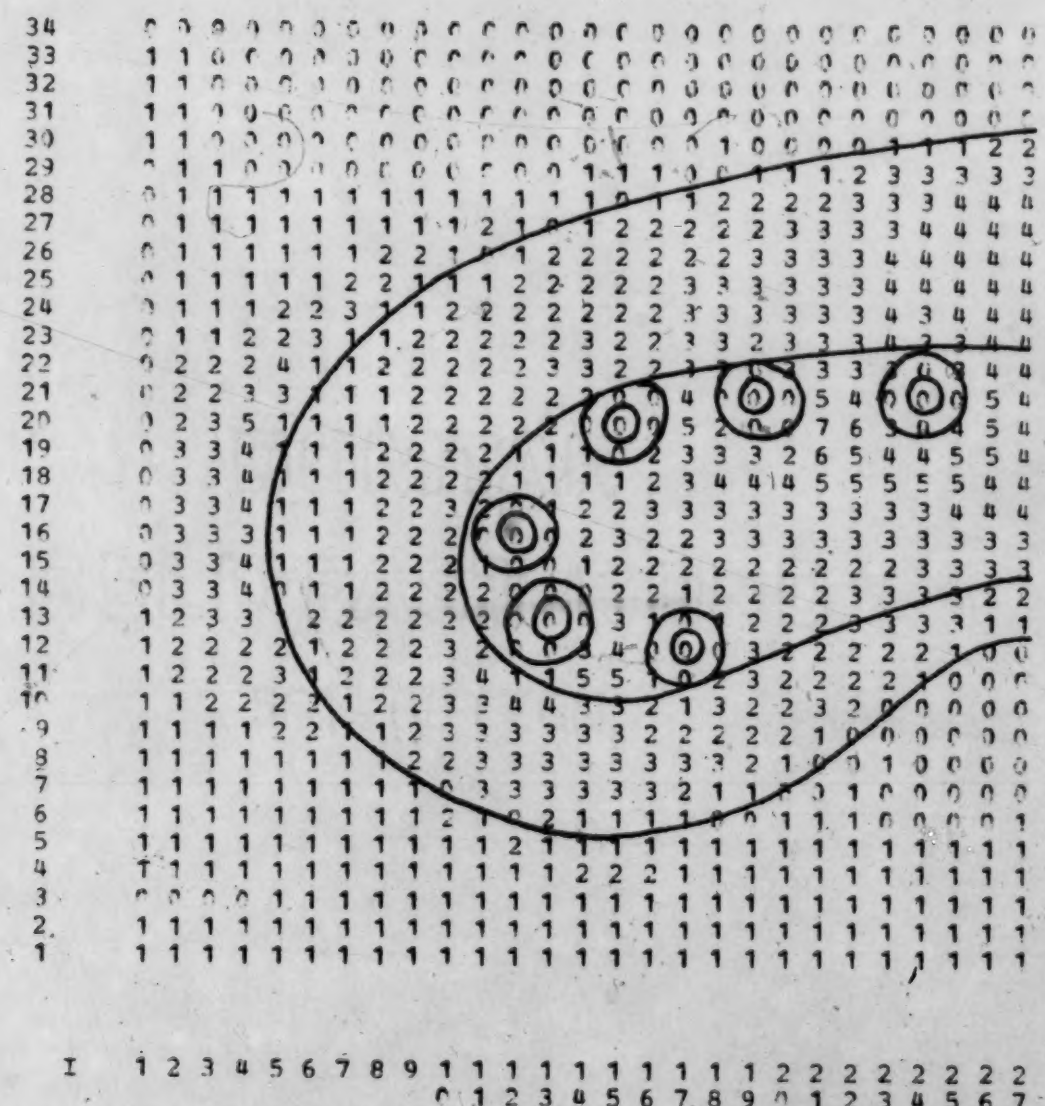

NORMALISED HEATING INDEX AT TIME STEP 600

PLANE K = 11

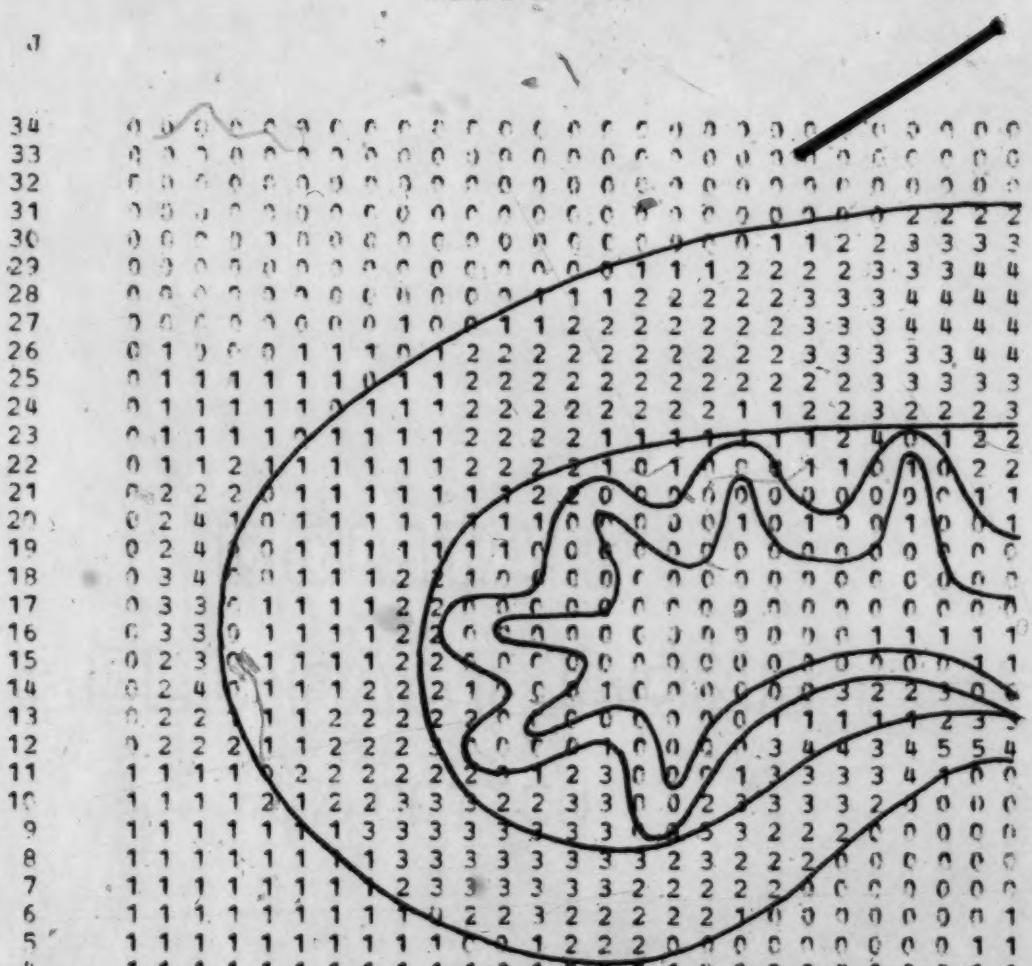

NORMALISED HEATING INDEX AT TIME STEP 600

PLANE K = 13

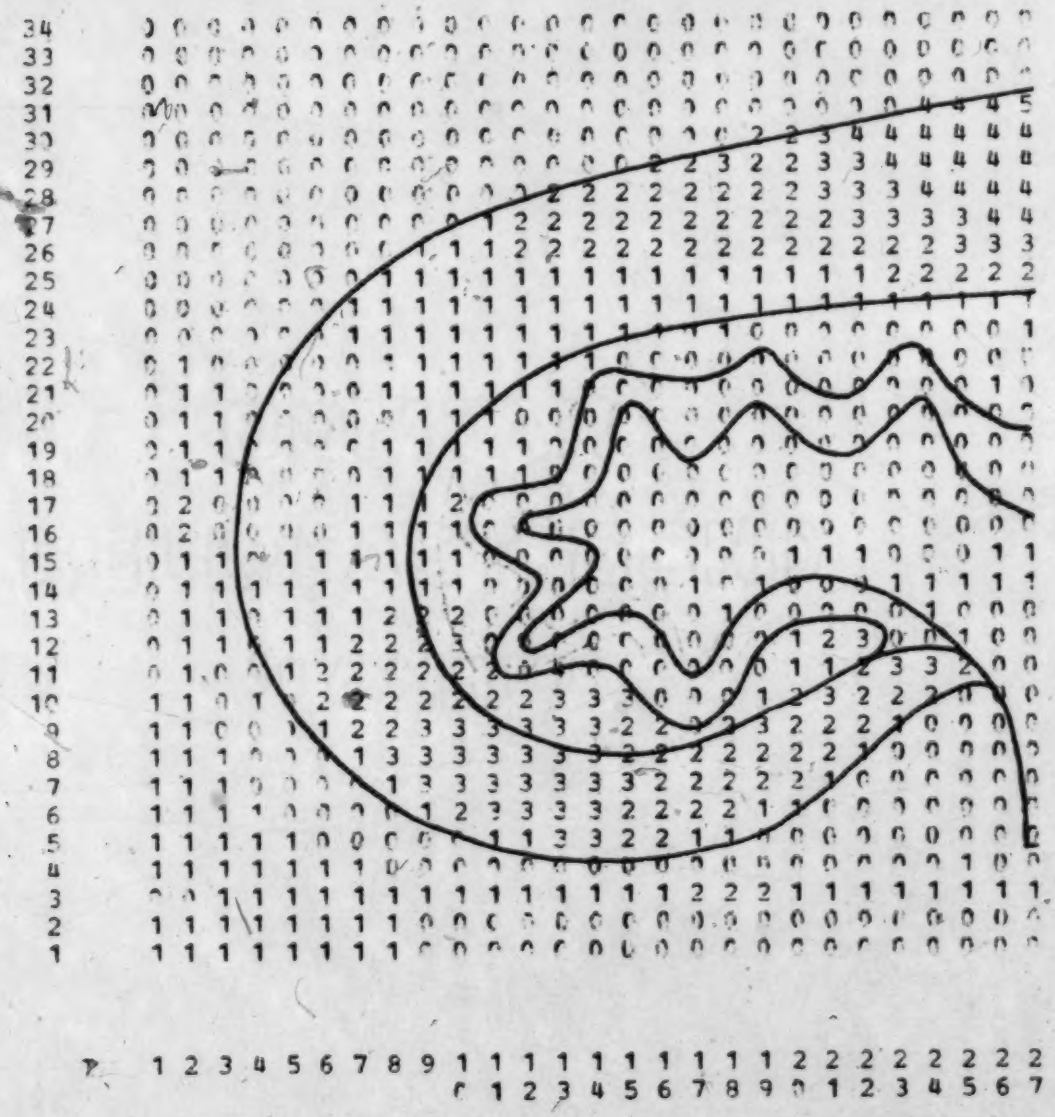

NORMALISED HEATING INDEX AT TIME STEP 600

PLANE K = 15

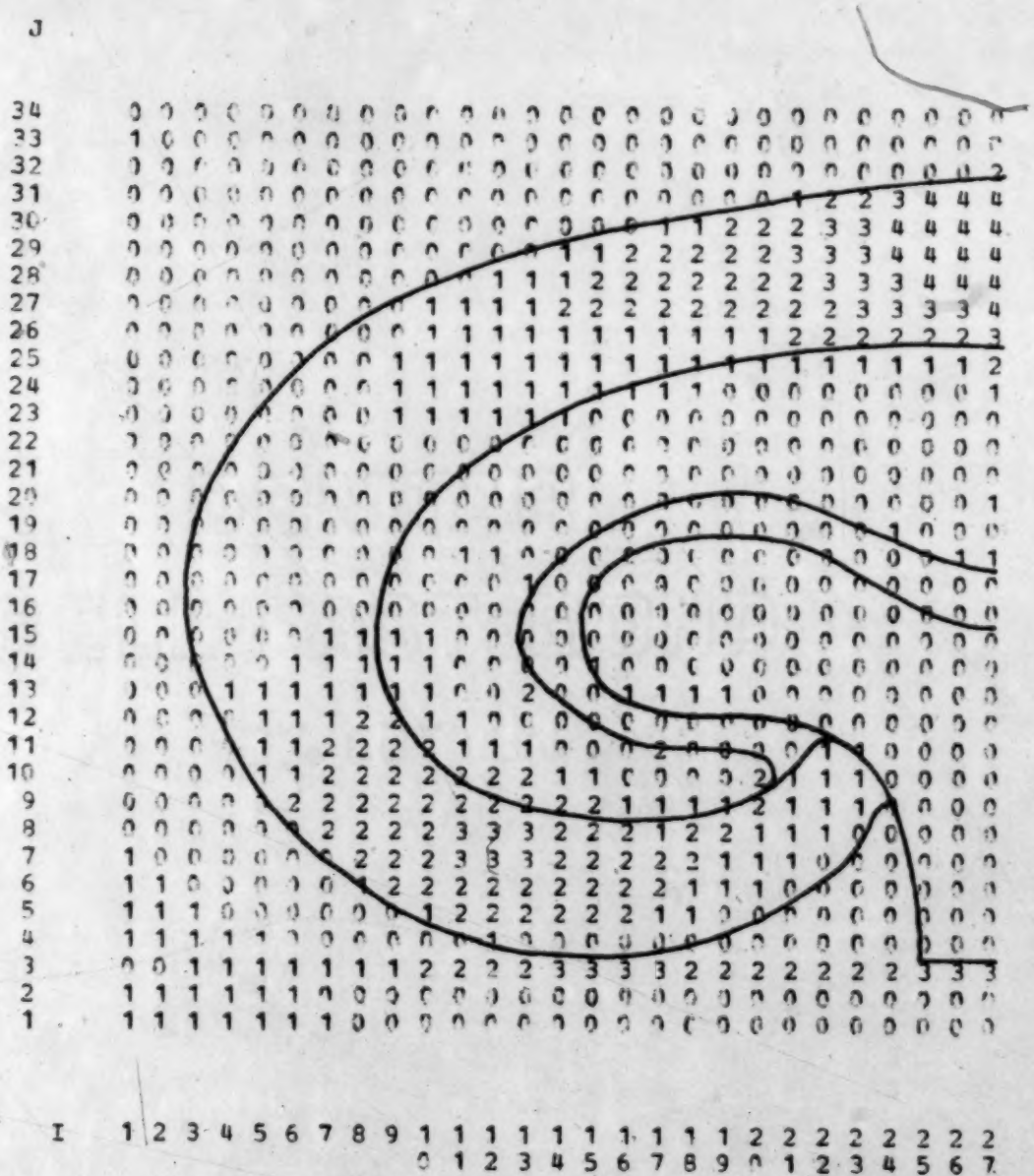

that the maximum dissipation under these conditions is only slightly more than that obtained at -10°C and 2500 Mhz (0.1150 W/m³ as compared with 0.0920 W/m³) This supports the earlier observation that more energy is dissipated at 2500 Mhz, and therefore heating rate is likely to be better at the higher frequency. Planes 3-8, of which planes 5 and 8 are representative indicate reasonable absorption in the off-axis planes of the cortex and medulla. Plane 9 indicates that there is no heating in the tubules or in the fat layer surrounding them. Planes 11,13 and 15 are representative of the axially located planes, and they suggest that very little energy is dissipated in this region, with none at all being dissipated in the pelvis and sinus. This is in contrast to the situation existing in most other models.

(6.13) Condition 8. Reversed Radiation Direction.

No figures are presented for this condition, but results showed that there was little difference in the behaviour of the model for this condition as compared to the datum model. This may not necessarily be true for higher loss conditions, but it does suggest that there is no particular sensitivity to orientation.

(6.14) Comparison with Experimental Results.

Rajotte (11) performed a number of microwave heating

experiments utilising canine kidneys. A brief summary of his experimental conditions and results follows:

(a) Freezing: After rinsing in Baxter's solution, DMSO was added in a two step perfusion process at either 4°C or 25°C. In the first step, 10% DMSO in Ringer's solution was added, and in the second, 20% in the same diluent. Cooling was by liquid nitrogen cooled fluorocarbon perfused through the vascular system. The cooling rate was controlled by the differential temperature between the ureter and the cortex.

(b) Thawing: Thawing was in a multimode cavity at 2450 Mhz. The kidney was immersed in a teflon container of fluorocarbon, which, like teflon, has very low loss at microwave frequencies. After thawing, internal temperature gradients were measured with a thermocouple probe. No gradients were found in the cortex, but cold spots were found in the medulla and pelvic region. Adequate perfusion resulted in temperature gradients of ±10°C but inadequate perfusion gave much larger gradients. Urine remaining in the pelvis caused a large temperature gradient. When the kidney was cut in half, following thawing, it was clearly seen that areas of incomplete perfusion were still frozen.

Direct comparison between the experimental results and those of the model cannot be made due to the entirely different illumination conditions. However, some general comparisons can be made. In the first place, the model confirms that gradients are to be expected if urine remains

in the pelvis. A comparison of conditions 1, 3 and 6 suggests that a lossy pelvic region would strongly dominate the overall dissipation pattern, and it is obviously advantageous to have a fairly low loss material in the pelvic region. This would also aid in reducing the tubular differential heating which was observed in most cases. It is possible that careful adjustment of the loss in this region would provide some control of overall uniformity. Conditions 1,3 and 5 suggest that there may be an optimum DMSO concentration (up to 70%) for a given temperature, and techniques whereby concentration is varied during heating may also provide a means of controlling uniformity.

The model confirms that gradients in the cortex are minimal, although it suggests that heating in this region is not very strong. Rajotte's (11) experimental results do not bear this out, but the fact that heating in this case was in an oven, where radiation impinges from many directions, and was also at temperatures up to 20°C, could explain this discrepancy. Evidence of the effect of temperature is provided by condition 7 where good heating of the cortex and medulla were obtained with little dissipation in the pelvic region. Though the frequency is different, this behaviour is similar to that found by Rajotte (R8).

Further consideration of condition 7 shows that there was little absorption in the pelvic region and tubules for

this run, in spite of the relatively high value of conductivity. These findings agree with Rajotte (11) whose experimental results indicated cold spots in the pelvic region after heating. The model assumed poor perfusion for the pelvic region and so it seems necessary to ensure better perfusion if adequate pelvic heating is to be obtained. This also supports Rajotte, who concluded that the pelvic region was often poorly perfused.

The experimental measurements of temperature gradient were rather coarse, and only took place after the kidney had been thawed. It is therefore very unlikely that the gradients at the fat-pelvis layer would have been observed. Other investigators (53) have found similar gradients in other situations which suggests that those observed in the kidney model do indeed exist.

(6.15) Concluding Remarks.

In conclusion, the model has revealed several important aspects of microwave heating of perfused canine kidney. In the first place, addition of DMSO as perfusate increases the maximum dissipated power, and this would certainly lead to increased heating rates at low temperatures. In this case, more energy was absorbed at 2500 Mhz than at 1000 Mhz.

Secondly, it is clear that uniform perfusion is

essential if uniform heating is to be achieved. This requirement is in conflict with the present methods of perfusion whereby almost pure perfusate is likely to reside in the vascular structure. This results in highly non-uniform heating, especially in those regions which are adjacent to a fatty layer. This condition is further aggravated by the thermal insulation properties of fat (23), which would tend to reduce heat conduction away from the strongly heated areas.

A third important factor that emerges is that overall uniformity is quite dependent on the properties of the pelvic region, and appropriate choice of properties in this region may provide a means of controlling uniformity. The model also suggests that maximum uniformity at a given temperature could be obtained by appropriate choice of DMSO concentration. Unfortunately, adjustment of DMSO concentration in the tissue is difficult, but it could also provide a means of uniformity control. DMSO perfusate for best uniformity at each temperature, and continuous control of concentration may also provide a means of uniformity control.

Finally, the model assumed that there was no perfusion in the sinus, and as a result, almost all of the different conditions modelled indicated sharp gradients in this area. Actual measurements of the perfusion into the sinus would be

useful in checking this result, and means to improve perfusion in this region should be investigated, if indeed it is found to be lacking.

Regarding accuracy, the results obtained with the model would certainly be improved if more accurate estimates of the dielectric properties of the various media were available. However, the conclusions which can be drawn at this stage already demonstrate the utility of the modelling technique. Other improvements which would expand the usefulness of the model are discussed in Chapter 7.

Chapter 7. Suggested Further Research.

(7.1) Dielectric and Thermal Property Measurements.

The application of the numerical model of Chapters 5 and 6 indicated a lack of appropriate data for use in numerical modelling of microwave heating in cryobiology. Extension of the model to considerations of heat conduction will also be hampered by the lack of suitable data for the thermal properties of tissue. In view of the large amount of data required, automated techniques for making thermal and dielectric property measurements are therefore very desirable.

The technique for measuring dielectric constant as employed in Chapter 4 is amenable to automation. The use of a microprocessor is appealing. The processor could adjust the frequency of the source for maximum transmission through the cavity, calculate the frequency shift, note the attenuation, and then, after applying appropriate corrections, calculate the dielectric constant. In conjunction with the temperature calibration curve, the data could immediately be plotted on an x-y plotter to give dielectric constant vs. temperature curves. Extension of the model to other frequencies would require an expansion of the dielectric measurement facility. Because most of the other frequencies of interest from a heating point of view are

lower than 1 Ghz, the use of the time-domain method of Iskander and Stuchly (35) is attractive. Using this technique, a single measurement suffices to give data for a wide range of frequencies.

Regarding thermal properties, experience with frozen foods (23) has suggested that the best approach is to use the enthalpy of the various tissue types. This would provide a measure of the total energy required to raise the temperature of a particular tissue by a given amount. When used in conjunction with thermal conductivity data obtained under identical conditions, enthalpy data would thus allow calculation of the temperature distribution within a body subject to microwave or conductive heating. In addition, if emissivity data were available, the effects of conductive and radiative heating could also be modelled, and the most effective combination could be determined.

(7.2) Numerical Heating Model.

The model described in Chapters 5 and 6 represents a first attempt at modelling microwave heating processes in cryobiology. In the present work, only a heating index for different model parameters was calculated, and general conclusions as to the effect of plane wave radiation were drawn. In an actual heating situation, however, it is the resultant temperature distribution after heating through a

range of temperatures that is important. In addition, plane wave heating is rarely encountered in practice, and application of the model to heating in a microwave oven would be desirable. Increasing the resolution of the kidney lattice to allow incorporation of the vascular structure would also be an important improvement in the model. Finally, extension of the model to an examination of the stresses involved in the heating process is a further possibility.

There are many difficulties involved in modelling a continuous heating process to obtain temperature information. First it would be necessary to develop a program to solve the thermal conduction problem on the same lattice of points as the scatterer, with appropriate temperature dependent thermal properties at each point. Using the results of this program, a new dielectric data lattice would have to be calculated, followed by a new lattice of thermal properties, before the process could be repeated for the next temperature step. As explained before, computer time and storage space are the main limitations to this technique. Other mathematical models could no doubt be developed, but the resulting set of differential equations with variable coefficients would still be difficult to solve.

Discussions with the originator (60) of the modelling

technique used in this work suggested that extension to oven heating is feasible. Introducing a conductive boundary at the edges of the lattice containing the scatterer, or providing appropriate lattice truncation conditions would simulate a scatterer within a conducting cavity. Different types of wave launching structures could also be simulated by assigning appropriate dielectric properties to the points of the scatterer in the vicinity of the coupling area. Again, computer storage is the most serious limitation to application of this model to heating within a microwave oven of reasonable size.

One possible approach towards estimating the stresses involved in the heating process is to use the techniques of Lin (61) who has compared some of the possible mechanisms of microwave auditory effects, as observed by Frey (62). According to Lin's calculations, thermal effects and strictive forces are the primary causes of the auditory effect, and it is reasonable to suppose that these forces will be present during microwave heating, where higher powers, and therefore higher field strengths, are employed. Using the heating model and the appropriate thermal properties, it should be possible to calculate the forces exerted in different parts of the body. It may then be feasible to relate these forces to a threshold for tissue damage, which would in turn set an upper limit to the field strength permissible in a given application.

Conclusion

The results of this work indicate one possible approach to the problem of controlled microwave heating. A system capable of maintaining a constant heating rate within prescribed limits is described and some of the results obtained with the system are presented. Various limitations of the system and some possible improvements are discussed.

Measurements on the dielectric properties of solutions of water and DMSO are described, and the results obtained are presented. A minimum relaxation frequency of 3 Ghz is found for a 70% DMSO solution, the relaxation frequency increasing to 9 Ghz for 100% DMSO and to 18 Ghz for water. The 70% concentration corresponds to the eutectic point of the mixture. The minimum relaxation frequency encountered at this concentration is apparently due to the ocurrence of maximum hydrogen bonding between the water and DMSO molecules. In addition, the presence of DMSO at temperatures below the freezing point is found to increase the losses of the solution, and to reduce the rate of change of ϵ'' with temperature. The cryobiological implications of these results are discussed.

A numerical model to simulate microwave heating of the canine kidney is developed and the model is employed to examine the effect of various parameters on heating rate and

uniformity. It is found that the addition of DMSO to the perfusate enhances the heating rate. The heating uniformity is also sensitive to the DMSO concentration, and it appears that control of the DMSO concentration during heating could provide some measure of control of heating uniformity. In the vicinity of the renal sinus, which absorbs little energy, considerable electric field gradients are found. This is due to the low perfusion assumed for this region, and suggests that ways should be found to improve perfusion in the sinus. The composition of the fluids residing in the renal pelvis is also found to have considerable effect on the heating uniformity. Maximum heating uniformity is found to correspond to maximum uniformity of perfusion. Another phenomenon which the model revealed is that of strong heating of the tubules leading off from the renal pelvis. Although the vascular structure is not represented on the model, it is supposed that similar effects will occur there.

REFERENCES

(1) Andjus, R.K. and J.E. Lovelock, "Re-animation of Rats from Body Temperatures Between 0 deg. C and 1 deg. C by Microwave Diathermy", J. Physiol. (London), 128, 541, (1955).

(2) Kenney, J. and F.D. Ketterer, "Kidney Thawing by Conduction Heating", Cryobiology, 4, Abs. 5, 248, (1955).

(3) Holst, H.I., F.D. Ketterer and H.B. Lehr, "Perfusate and Microwave Radiation Effect on Non-frozen Canine Kidneys", Cryobiology 6, 590, (1970).

(4) Hamilton, R. et al, "Conduction Thawing of Frozen Kidney: An Experimental Technique, abs. 58, 7th Annual Meeting, Soc. for Cryobiology, Cryobiology 6, (1970).

(5) Ketterer, F.D., H.I. Holst and H.B. Lehr, "Progress in Microwave Thawing of Canine Kidneys", abs. 59, 7th Annual Meeting, Soc. for Cryobiology, Cryobiology 6, (1970).

(6) Ketterer, F.D., H.I. Holst and H.B. Lehr, "Improved Viability of Kidneys with Microwave Thawing", abs. 64, 8th Annual Meeting, Soc. for Cryobiology, (1971).

(7) Burns, C.P. and E.C. Burdette, "Multi-Frequency Electromagnetic Thawing of Frozen Kidneys", 1974 IEEE S-MTT, Int. Microwave Symp. Digest for Technical Papers, June 12-14, p 40, (1974).

(8) Rzepecka, M.A., S.S. Stuchly and P.A. Metherall, "A Waveguide Applicator for Irradiation of Samples at

Controlled Temperatures", Proceedings of Microwave Power Symposium, Waterloo, Ontario , editors T.W.R. East and J.D. Ford, IMPI, Edmonton, Canada, pp 30-35, (1975).

(9) Rajotte, R.V., J.B. Dossetor, W.A.G. Voss and C.P. Stiller, "Preservation Studies on Canine Kidneys Recovered from The Deep Frozen State by Microwave Thawing", Proc. IEEE, vol. 62, no 1, pp 76-85, (1974).

(10) Walker, C.M.B., A.H. Huizinga, W.A.G. Voss and W.R. Tinga, "A System for Controlled Microwave Heating of Small Samples", J.M.P. 11(1), pp 29-32, (1976).

(11) Rajotte, R.V., Microwave Thawing of Mammalian Cells and Organs, MSc. Thesis, University of Alberta, Edmonton, Alberta, Canada, 1973.

(12) Mazur, P., "Cryobiology: the Freezing of Systems", Science, 168, pp 939-949, (1970).

(13) Ashwood-Smith, M.J., in DMSO, S.W. Jacob, E.E. Rosenbaum and D.C. Wood, editors, Marcel Dekker, Inc., New York, (1971).

(14) Szmant, H.H., in DMSO, S.W. Jacob, E.E. Rosenbaum and D.C. Wood, editors, Marcel Dekker, Inc., New York, (1971)

(15) Jacob, S.W., E.E. Rosenbaum and D.C. Woods, editors, DMSO, Marcel Dekker, Inc., New York, (1971).

(16) Bourgoin, D., E.Volf and M. Joly, "Mesure de la permittivite complexe relative en ondes cetremetriques de liquides fortement polaires: application a l'eau at

au dimethylsulfoxyde", J. Phys. D: Appl. Phys., vol 5, pp 589-600, (1972).

(17) Doucet, Y., Mme. Francoise Calmes-Perrault and Marie Therese Durand, presentee' par M. Jean Lacomte, "La constante du dimethylsulfoxyde pur et ses melanges aqueux", C.R. Acad. Sc. Paris, t 260, pp 1878-1881, (1965).

(18) England, T.S., "Dielectric Properties for the Human Body for Wavelengths in the 1-10 cm. range", Nature, 166, 480, (1950).

(19) Schwan, H.P., "Electrical Characteristics of Tissue - A Survey", Biophysik 1, pp 198-208, (1964).

(20) Tinga, W.R. and S.O. Nelson, "Dielectric Properties for Microwave Processing - Tabulated", J. Microwave Power 8(1), pp 23-65, (1973).

(21) Presman, A.S., Electromagnetic Fields and Life, Plenum Press, New York, (1970).

(22) Foster, K.R., Bell, R.T., Whittington, R. and Bohdan Denysk, "Effect of DMSO on the Dielectric Properties of Canine Kidney Tissue", Cryobiology 13, pp 581-585, (1976).

(23) Tressler, D.K. and C.F. Evers, The Freezing Preservation of Foods, Vol. 1, 3rd edition. Avi Publishing Co., Westport, Connecticut, (1957).

(24) Awberry, J.H. and E. Griffiths, "Thermal Properties of Meat", J. Soc. Chem. Ind., 52, 326-328, (1933).

(25) Dickerson, R.W., "Thermal Properties of Food", The

Freezing Preservation of Foods, 4th Edition, Avi Pub. Co., Westport, Conn., (1968).

(26) Ohlsson, and N.E. Bengtsson, "Microwave Heating Profiles in Foods", Microwave Energy Applications Newsletter, IV(6), 1-8, (1971).

(27) Hill, J.E., J.D. Leitman and J.E. Sunderland, "Thermal Conductivity of Various Meats", Food Tech., 21(8), 91-96, (1967).

(28) Nykvist, W.E. and R.V. Decareau, "Microwave Meat Roasting", J. Microwave Power, 11(1), pp 3-24, (1976).

(29) Alexander, D.A., "A Mathematical Model of Microwave Heating of Three-layer Composite Bodies", Private Communication, (1974).

(30) Guy, A.W., J.C. Lin, P.O. Kramar and A.F. Emery, "Effect of 2450 Mhz Radiation on the Rabbit Eye", IEEE Trans. Microwave Theory Tech., vol. MTT-23, pp 492-498, (1975).

(31) Taflove, A. and M.E. Brodwin, "Computation of the Electromagnetic Fields and Induced Temperatures within a Model of the Microwave Irradiated Human Eye", IEEE Trans. on Microwave Theory and Techniques, vol MTT-23, pp 888-896, (1975).

(32) Stratton, J.A., Electromagnetic Theory, New York, McGraw-Hill, (1941).

(33) Bussey, H.E., "Measurement of RF Properties of Materials. A Survey", Proc. IEEE, 55(6), pp 1046-1053, (1967).

(34) Altschuler, H.M., Handbook of Microwave Measurements, Chapter IX, Vol. II. Max Sucher and Jerome Fox, Eds., Polytechnic Press, New York, pp 495-547, (1963).

(35) Iskander, M.F. and S.S. Stuchly, "A Time Domain Technique for measurement of the Dielectric Properties of Biological Substances", IEEE Trans. I-M, 21(4), pp 425-429, (1972).

(36) Rueggenberg, W., "Determination of Complex Permittivity of Arbitrarily Dimensioned Dielectric Modules at Microwave Frequencies", IEEE Trans. on Microwave Theory and Techniques, MTT-19(6), pp 517-521, (1971).

(37) Rzepecka, M.A. "A Cavity Perturbation Method for Routine Permittivity Measurement", J. Microwave Power, 8(1), pp 3-12, (1973).

(38) Risman, P.O and N.E. Bengtsson, "Dielectric Properties of Food at 3 Ghz. as Determined by a Cavity Perturbation Technique", J. Microwave Power, 6(2), pp 101-106, (1971).

(39) Bengtsson, N.E. and P.O. Risman, "Dielectric Properties of Foods at 3Ghz as Determined by a Cavity Perturbation Technique", J. Microwave Power, 6(2), pp 107-123, (1971).

(40) von Hippel, A.R., Dielectric Materials and Applications, E.J. Wiley, p 301,360, (1954).

(41) Cocks, F.H. and W.E. Brower, "Phase Diagram Relationships in Cryobiology", Cryobiology 11, pp 340-

358, (1974).

(42) Hasted, J.B., Aqueous Dielectrics, Chapman and Hall, London, pp 65-99, (1973).

(43) Hasted, J.B., Aqueous Dielectrics, Chapman and Hall, London, pp 32-64, (1973).

(44) Tinga, W.R., " Multiphase Dielectric Theory Applied to Cellulose Mixtures", Phd. Thesis, University of Alberta, Edmonton, Alberta, Canada, (1969).

(45) Pegg, D.E., "An Apparatus for Simultaneous Programmed Control of DMSO Concentration and Temperature in an Organ Perfusion System", Abs. 9, 5th Annual Meeting of the Soc. for Cryobiology, Cryobiology 4, p 249, (1968).

(46) Ohlsson, T., N.E. Bengtsson and P.O. Risman, "The Frequency and Temperature Dependence of Dielectric Food Data as Determined by a Cavity Perturbation Technique", J. Microwave Power, 9(2), pp 129-145, (1974).

(47) Deficis, A. and A. Priou, "Non-perturbing Microprobes for Measurement in Electromagnetic Fields", IMPI Symposium, Leuven, Belgium, (1976).

(48) Panslow, G.E. and J.R. Pavlat, "Field values in Slotted Waveguides", J. Microwave Power, 11(1), pp 25-27, (1976).

(49) Brodwin, M.E., "Passive Telemetry for in-vivo Measurements of Fields in Biological Materials", IMPI Symposium, Leuven, Belgium, (1976).

(50) Guy, A.W., "Analyses of Electromagnetic Fields Induced in Biological Tissues by Thermographic Studies on Equivalent Phantom Models", IEEE Trans. Microwave Theory and Tech., vol. MTT-19, pp 205-215, (1971).

(51) Bielec, M. and S. Szmigielski, "Use of Thermography for Quantitation of Energy Absorbtion in Animals Irradiated with Microwaves", IMPI Symposium, Leuven, Belgium, (1976).

(52) Bates, R.H.T., "Analytic Constraints on Electromagnetic Field Computations", IEEE Trans. Microwave Theory and Tech., MTT-23, pp 605-622, (1975).

(53) Shapiro, A.R., R.P. Lutomirski and H.T. Yura, "Induced Fields and Heating within a Cranial Structure Irradiated by an Electromagnetic Plane Wave", IEEE Microwave Theory and Tech., Vol. MTT-19, pp187- 196, (1971).

(54) Durney, C.H. and Habib Massoudi, "Long Wavelength Analysis of Plane Wave Irradiation of a Prolate Spheroid Model of Man, IEEE Microwave Theory and Tech., MTT-23, pp529-532, (1975).

(55) Livesay, D.E. and Kun-Mu Chen, "Electromagnetic Fields Induced Inside Arbitrary Shaped Biological Bodies", IEEE Trans. Microwave Theory Tech., vol. MTT-22, pp 1273-1280, (1974).

(56) Yee, K.S., "Numerical Solution of Initial Boundary Value Problems Involving Maxwell's Equations in

Isotropic Media", IEEE Trans. Ant. Propag., vol. AP-14, pp 302-307, (1966).

(57) Taflove, A. and M.E. Brodwin, "Numerical Solution of Steady State Scattering Problems using the Time-Dependent Maxwell's Equations", IEEE Trans. Microwave Theory Tech., vol. MTT-23, pp 623-629, (1975).

(58) Evans, H.E. and A. de Lahunta, Miller's Guide to the Dissection of the Dog, W.B. Saunders Co., Philadelphia, pp 162-164, (1971).

(59) Pitts, R.F., Physiology of the Kidney and Body Fluids, Yearbook Medical Publishers Inc., Chicago, (1969).

(59) Taflove, A., Private Communication.

(60) Lin, J.C., "Microwave Auditory Effect - Acomparison of some Possible Transconduction Mechanisms", J. Microwave Power, 11(1), pp 77-81, 1976.

(61) Frey, A.H., "Auditory System Responses to Radio-Frequency Energy", Aerospace Med., 32, pp1140-1142, (1961).

Appendix A

As explained in Chapter 5, two computer programs were used to analyse the raw data obtained from the dielectric measurements. A brief description of the function of each program is given below, followed by FORTRAN listings of the programs.

Calibration Program (CALCOEFF)

This program takes the values of ϵ' and ϵ'' for the 5 standard solutions, and, using measured values of frequency shift and attenuation, performs a bicubic spline fit of the data. The spline coefficients are stored for use in the second program. Three separate spline fits are performed, representing the mean and the upper and lower bounds of the standard deviation.

Calculation program (CALCULATE)

Using the values of the coefficients obtained in the CALCOEFF program, this program calculates ϵ' and ϵ'' from the frequency shift and attenuation data obtained from measurements on the unknown solutions. Again, three values are calculated in each case, these being the mean and standard deviation bounds.

PROGRAM CALCOEFF

```
C       THIS PROGRAM CALCULATES THE VALUES OF E' AND E" FOR
C       UNKNOWN SUBSTANCES. FOR EACH TEMPERATURE, THE MEAN
C       AND STANDARD DEVIATION OF NDATA VALUES OF FREQUENCY
C       SHIFT AND ATTENUATION ARE FOUND, GIVING DATAL, DATAM
C       AND DATAU AS THE ERROR BOUNDS. IN EACH CASE THE
C       SUBSCRIPTS ARE USED AS FOLLOWS;
C                          .....(I,1)=TEMPERATURE
C                          .....(I,2)=FREQUENCY SHIFT
C                          .....(I,3)=ATTENUATION
C
        DIMENSION DATA(100,3),DATAL(3),DATAM(3),DATAU(3)
        DIMENSION COEFFL(4),COEFFM(4),COEFFU(4)
        DIMENSION COEPPL(4),COEPPM(4),COEPPU(4)
        DIMENSION EPL(100),EPM(100),EPU(100)
        DIMENSION EPPL(100),EPPM(100),EPPU(100)
        LOGICAL*1 ITYPE(4),STRING(16),TITLE(50),EQUC,
        BUFFER(60)
C
C       THE COEFFICIENT DATA, AS CALCULATED BY "CALCOEFF", IS
C       READ FROM "COEFFICIENTS".
        DO 4567 I=1,5
 4567   CALL MOVEC(12,'            ',BUFFER(((I-1)*12)+1))
        READ(5,3456) ITLEN,(TITLE(I),I=1,50)
 3456   FORMAT(I2,1X,50A1)
        ISTART=(60-ITLEN)/2
        CALL MOVEC(ITLEN,TITLE(1),BUFFER(ISTART))
        WRITE(6,5678) (BUFFER(I),I=1,60)
 5678   FORMAT('1',60A1)
        READ(5,2121) ITYPE
 2121   FORMAT(4A1)
        IF (EQUC(ITYPE,'TEMP')) GOTO 2323
        CALL MOVEC(16,' % CONCENTRATION',STRING)
        GOTO 2324
 2323   CALL MOVEC(16,'   TEMPERATURE  ',STRING)
 2324   WRITE(6,1000) (STRING(I),I=1,16)
        READ(8,1003) (COEFFL(I),I=1,4)
        READ(8,1003) (COEFFM(I),I=1,4)
        READ(8,1003) (COEFFU(I),I=1,4)
        READ(8,1003) (COEPPL(I),I=1,4)
        READ(8,1003) (COEPPM(I),I=1,4)
        READ(8,1003) (COEPPU(I),I=1,4)
C
C       THE DATA FOR NTEMP DIFFERENT TEMPERATURES (IN ORDER
C       OF INCREASING TEMPERATURE) IS NOW READ IN. THERE ARE
C       NDATA FREQUENCY SHIFTS AND ATTENUATIONS FOR EACH
C       TEMPERATURE.
C       MEANS AND STANDARD DEVIATIONS ARE THEN CALCULATED
C       FOR EACH TEMPERATURE
C
        READ(5,1002) NDATA,NTEMP
        DO 130 L=1,NTEMP
        SUMF=0
```

```
      SUMA=0
      SUM2F=0
      SUM2A=0
      DO 100 I=1,NDATA
      READ(5,1004)(DATA(L,J),J=1,3)
      SUMF=DATA(L,2)+SUMF
      SUMA=DATA(L,3)+SUMA
      SUM2F=DATA(L,2)**2.+SUM2F
      SUM2A=DATA(L,3)**2.+SUM2A
100   CONTINUE
      AK=SUMF*SUMF/NDATA
      BK=(ABS(SUM2F-AK))/(NDATA-1)
      SDF=SQRT(BK)
      AA=SUMA*SUMA/NDATA
      BB=(ABS(SUM2A-AA))/(NDATA-1)
      SDA=SQRT(BB)
      DATAL(2)=SUMF/NDATA-SDF
      DATAL(3)=SUMA/NDATA-SDA
      DATAM(2)=SUMF/NDATA
      DATAM(3)=SUMA/NDATA
      DATAU(2)=SUMF/NDATA+SDF
      DATAU(3)=SUMA/NDATA+SDA
C
C     VALUES OF E' AND E" AND THEIR LOWER AND UPPER
C     BOUNDS ARE NOW CALCULATED FOR EACH TEMPERATURE.
C
      K1=K-1
      EPL(L)=0
      EPM(L)=0
      EPU(L)=0
      EPPL(L)=0
      EPPM(L)=0
      EPPU(L)=0
      DO 110 I=1,4
      EPL(L)=EPL(L)+COEFFL(I)*DATAL(2)**(I-1)
      EPM(L)=EPM(L)+COEFFM(I)*DATAM(2)**(I-1)
110   EPU(L)=EPU(L)+COEFFU(I)*DATAU(2)**(I-1)
      DO 120 I=1,4
      EPPL(L)=EPPL(L)+COEPPL(I)*ALOG10(EPL(L-1)**(I-1)
      EPPM(L)=EPPM(L)+COEPPM(I)*ALOG10(EPM(L-1)**(I-1)
120   EPPU(L)=EPPU(L)+COEPPU(I)*ALOG10(EPU(L-1)**(I-1)
      EPPL(L)=10.**(DATAL(3)/20+EPPL(L-1.25)
      EPPM(L)=10.**(DATAM(3)/20+EPPM(L-1.25)
      EPPU(L)=10.**(DATAU(3)/20+EPPU(L-1.25)
      TANL=EPPL(L)/EPU(L)
      TANM=EPPM(L)/EPM(L)
      TANU=EPPU(L)/EPL(L)
      PRINT 1005,EPL(L),EPPL(L),TANL
      PRINT 1006,DATA(L,1),EPM(L),EPPM(L),TANM
      PRINT 1007,EPU(L),EPPU(L),TANU
C     WRITE DATA FOR PLOT ROUTINE
      WRITE(3,2000) DATA(L,1),EPL(L),EPM(L),EPU(L)
      WRITE(4,2000) DATA(L,1), EPPL(L), EPPM(L), EPPU(L)
130   CONTINUE
```

```
1000  FORMAT('0',T8,16A1,T27,'EP',T41,'EPP',T53,'LOSS TAN')
1001  FORMAT(' ',2F7.2)
1002  FORMAT(I1,I4)
1003  FORMAT(1X,6E15.4)
1004  FORMAT(3F8.1)
1005  FORMAT('0',T25,F5.2,T40,F5.2,T54,F6.3)
1006  FORMAT(' ',T12,F6.1,T25,F5.2,T40,F5.2,T54,F6.3)
1007  FORMAT(' ',T25,F5.2,T40,F5.2,T54,F6.3)
1010  FORMAT(' ',3F8.1)
2000  FORMAT(4F6.2)
      STOP
      END
```

PROGRAM CALCULATE

```
C     THIS PROGRAM CALCULATES THE COEFFICIENTS FOR A LEAST
C     SQUARES FIT OF FREQUENCY SHIFT DATA (FS) TO E' (EP).
C     3 DISTINCT CURVES (MEAN, MEAN+S.DEVIATION AND
C     MEAN-S.DEVIATION FOR N SEPARATE READINGS) ARE FOUND,
C     ENABLING THE STANDARD DEVIATION OF ANY
C     MEASUREMENT ON UNKNOWN SUBSTANCES TO BE ESTIMATED.
C
      DIMENSION EP(7),EPP(7),FS(7,10),AT(7,10)
      DIMENSION FU(7),FL(7),FM(7)
      DIMENSION AL(7),AM(7),AU(7)
      DIMENSION COEFFL(4),COEFFM(4),COEFFU(4)
      DIMENSION C(6),S(6),A(3),B(3),X(7)
      DIMENSION EP1(7),EPP25L(7),EPP25M(7),EPP25U(7)
      DOUBLE PRECISION P(14),T(16)
C
C     N (MAX. 20) IS THE NUMBER OF READINGS FOR EACH
C     CALIBRATION LIQUID AND NCL (MAX. 10) IS THE NUMBER
C     OF CALIBRATION LIQUIDS.
C
      N=6
      NCL=7
      READ 1001,(EP(I),I=1,NCL)
      READ 1001,(EPP(I),I=1,NCL)
      DO 100 I=1,NCL
      READ 1002, (FS(I,J),J=1,N)
      READ 1002, (AT(I,J),J=1,N)
100   CONTINUE
      DO 120 I=1,NCL
      FS1=0
      FS2=0
      AT1=0
      AT2=0
C
C     CALCULATE THE MEANS AND STANDARD DEVIATIONS OF THE
C     INPUT DATA AND PLACE THEM IN THE APPROPRIATE
C     COEFFICIENT MATRIX.
C
      DO 110 J=1,N
      FS1=FS1+FS(I,J)
      FS2=FS2+FS(I,J)**2.
      AT1=AT1+AT(I,J)
      AT2=AT2+AT(I,J)**2.
110   CONTINUE
      AK=FS1*FS1/N
      BK=(FS2-AK)/(N-1)
      SDF=SQRT(BK)
      AA=AT1*AT1/N
      BB=(AT2-AA)/(N-1)
      SDA=SQRT(BB)
      FU(I)=FS1/N+SDF
      FM(I)=FS1/N
      FL(I)=FS1/N-SDF
```

```
      AU(I)=AT1/N+SDA
      AM(I)=AT1/N
      AL(I)=AT1/N-SDA
120   CONTINUE
      DO 260 J=1,3
      IF(J-2)130,150,170
130   DO 140 I=1,NCL
140   X(I)=PU(I)
      GO TO 190
150   DO 160 I=1,NCL
160   X(I)=PM(I)
      GO TO 190
170   DO 180 I=1,NCL
180   X(I)=PL(I)
190   CONTINUE
      CALL RLFOTH (X,EP,NCL,100.,3,ID,P,C,S,A,B,IER)
      CALL RLDOPM (C,ID,A,B,T)
      KD=ID+1
      IF(J-2)200,220,240
200   WRITE(6,1004)(C(I),I=1,KD)
      GO TO 260
220   WRITE(6,1004)(C(I),I=1,KD)
      GO TO 260
240   WRITE(6,1004)(C(I),I=1,KD)
260   CONTINUE
C
C     ESTABLISH VECTORS OF LOG(E'-1) (EP1) AND LOG(E")
C     AT 25 DB (EPP25).
C
      DO 270 I=1,NCL
      EP1(I)=ALOG10(EP(I-1)
      EPP25L(I)=ALOG10(EPP(I)-AU(I)/20+1.25
      EPP25M(I)=ALOG10(EPP(I)-AM(I)/20+1.25
      EPP25U(I)=ALOG10(EPP(I)-AL(I)/20+1.25
270   CONTINUE
C
C     CALCULATE THE LEAST SQUARES COEFFICIENTS FOR THE ABOVE
C     VECTORS FOR THE THREE CASES, MEAN-SD, MEAN AND MEAN+SD
C     COEPPL,COEPPM AND COEPPU ARE THE COEFFICIENT VECTORS
C     FOR THE CURVES REPRESENTING THE MEAN-SD, MEAN AND
C     MEAN+SD OF EP-1 VS. EPP25
C
      DO 280 I=1,NCL
280   X(I)=EP1(I)
      CALL RLFOTH (X,EPP25L,NCL,100.,3,ID,P,C,S,A,B,IER)
      CALL RLDOPM (C,ID,A,B,T)
      KD=ID+1
      PRINT 1004,(C(I),I=1,KD)
      DO 290 I=1,NCL
290   X(I)=EP1(I)
      CALL RLFOTH (X,EPP25M,NCL,100.,3,ID,P,C,S,A,B,IER)
      CALL RLDOPM (C,ID,A,B,T)
      KD=ID+1
      PRINT 1004,(C(I),I=1,KD)
```

```
      DO 300 I=1,NCL
300   X(I)=EP1(I)
      CALL RLFOTH (X,EPP25U,NCL,100.,3,ID,P,C,S,A,B,IER)
      CALL RLDOPM (C,ID,A,B,T)
      KD=ID+1
      PRINT 1004,(C(I),I=1,KD)
1000  FORMAT(I1)
1001  FORMAT(F5.2,1X,F5.2,1X,F5.2,1X,F5.2,1X,F5.2,1X,
     CF5.2,1X,F5.2)
1002  FORMAT(F5.2,1X,F5.2,1X,F5.2,1X,F5.2,1X,F5.2,1X,F5.2)
1003  FORMAT('0','IER =',I3)
1004  FORMAT(' ',6E15.4)
1005  FORMAT('0','VALUES OF EP',7F6.2)
1006  FORMAT('0','VALUES OF EPP',7F6.2)
1007  FORMAT('0','VALUES OF FS')
1008  FORMAT('0',6F6.1)
1009  FORMAT('0','VALUES OF AT')
1010  FORMAT('0','FU(',I1,')=',F5.1,5X,'FM(',I1,')=',F5.1,
     C5X,'FL(', I1,')=',F5.1)
1011  FORMAT('0','AU(',I1,')=',F5.1,5X,'AM(',I1,')=',F5.1,
     C5X,'AL(', I1,')=',F5.1)
      STOP
      END
```

Appendix B

As explained in Chapter 8, a program to calculate the heating index of a plane incident microwave field on an arbitrary shaped body was written based on a similar program due to Taflove (T3). This program is called SCAT.KID.2 and a FORTRAN listing is given below.

Input to the program includes the frequency, the total number of steps for which the program is to be run, the number of steps for which the envelope is to be scanned and the step at which scanning is to begin. Also included are the number of media and their dielectric properties, and a media lattice describing the distribution of the various media. Output from the program is an index from 0-9 representing the amount of energy dissipated at each point within the lattice. The maximum dissipated power in W/m^3, corresponding to an index of 9, is also returned.

PROGRAM SCAT.KID.2

```
C       PROGRAM SCAT.KID.2
C
C       STEADY TEM IRRADIATION OF A CANINE KIDNEY
C       INCIDENT WAVE HAS THE COMPONENTS EZ,HX,KY
C       5 DIFFERENT DIELECTRICS ARE DEFINED
C       27 X 34 X 15 CELL YEE LATTICE IS USED
C       UNIT CELL DIAMETER = 0.05*LAMBDA(MIN)=DX
C       EVEN SYMMETRY ABOUT PLANES X=27.5*DX AND Z=15.0*DX
C       IS ASSUMED AND ADAPTIVE SOFT LATTICE TRUNCATIONS
C       ARE USED.
C
C       THE MEDIA LATTICE AND THE ENVELOPE PRINTOUT
C       ARE TIED TO UNIT 6.
C       CONTROL INPUT IS ON UNIT 5, DATA INPUT ON 8.
C
        REAL MUZ
        COMPLEX JKAY, CMPLX, CSQRT
        INTEGER IPR(27),N(27),IVF(9)
        REAL EX0(15,27), EZ0(15,27), EXT1F(15,27),
       1     EXT2F(15,27), EYT(34,14,27), ENY(34,15,27),
       2     EZT1F(15,27), EZT2F(15,27), EXT(34,14,27),
       3     HYT(34,14,15), HZT(34,14,15), ENX(34,15,27),
       4     ENZ(34,15,27), EX(34,16,28), EY(34,16,28),
       5     HX(34,16,28), HY(34,16,28), HZ(34,16,28),
       6     EZ(34,16,28), MEDIA(34,15,27), EPS(9),
       7     EXTR(14,15,27), EZTR(14,15,27)
       6     SIG(9),CA(9),CB(9)
C
C       .....I. PROBLEM PARAMETERS.....
        READ  (5,1100) FREQ
 1100 FORMAT(E6.1)
        PRINT 1102, FREQ
 1102 FORMAT('1','THE FREQUENCY IS = ',E9.2,' HZ')
        DX=1.5E-3
C
C       MAXDT IS THE TOTAL NO OF STEPS REQUIRED.
C       MINDT IS THE TIME AT WHICH ENVELOPE SCANNING BEGINS.
C       MIDDT IS THE NUMBER OF STEPS FOR WHICH THE ENVELOPE
C       IS SCANNED.
        READ(5,1110) MAXDT, MINDT, MIDDT
 1110   FORMAT(I3,1X,I3,1X,I3)
        PRINT 1103, MAXDT,MINDT,MIDDT
 1103   FORMAT(' ','MAXDT = ',I3,/,'MINDT = ',I3,
       1/'MIDDT = ',I2)
C
C       .....II. DIELECTRIC MEDIA.....
        MPR=5
        READ (5,1101)  (EPS(I),I=1,MPR)
        READ (5,1101)  (SIG(I),I=1,MPR)
 1101 FORMAT(9(F5.2,1X))
        DO 1104 I=1,MPR
 1104 PRINT 1105, I,EPS(I),I,SIG(I)
```

```
 1105 FORMAT(' ','EPS(',I1,') = ',F5.2,5X,
     1'SIG(',I1,') = ',F5.2)
C
C      EQUATE MTS AND FORTRAN LOGICAL UNITS
C      CALL FTNCMD('EQUATE 9=9',10)
C
C      .....III. BASIC AND DERIVED CONSTANTS.....
       PI=3.1415927
       MUZ=4.0*PI*1.0E-7
       EPSZ=8.854E-12
       OMEGA=2.0*PI*FREQ
       DT=DX/5.99585E+8
       MDT=MINDT+MIDDT
       R=DT/EPSZ
       RA=DT*DT/DX/DX/MUZ/EPSZ
       RB=DT/DX/MUZ
       RC=MUZ*EPSZ*OMEGA**2
       RD=MUZ*OMEGA
       RE=5.99585E+8/OMEGA
       RF=1000.0*RB
       RG=OMEGA*DT
       RH=2.0*RF**2
       FMPR=FLOAT(MPR)
       NTEST=0
       DO 1 IAA=1,27
     1 N(IAA)=IAA
C
C      .....IV. CALCULATE THE PROPAGATION CONSTANT AND.....
C           HENCE THE MAXIMUM DELAY FOR EACH TISSUE TYPE
       DO 2 IB=1,MPR
       JKAY=CMPLX(0.0,1.0)*CSQRT(CMPLX(EPS(IB)*RC,
      1SIG(IB)*RD))
       IVF(IB)=AMIN1(RE*AIMAG(JKAY-0.5,13.5)
       CA(IB)=1.0-R*SIG(IB)/EPS(IB)
     2 CB(IB)=RA/EPS(IB)
C
C      .....V. LOAD THE STORAGE VECTOR.....
C      .....A. ZERO INITIAL FIELDS (FRONT REAR).....
       DO 3 ICA=1,27
       DO 3 IC=1,15
       EX0(IC,ICA)=0.0
     3 EZ0(IC,ICA)=0.0
       DO 3010 ICA=1,27
       DO 3010 IC=1,15
       EXT1F(IC,ICA)=0.0
  3010 EZT1F(IC,ICA)=0.0
       DO 3011 ICA=1,27
       DO 3011 IC=1,15
       EXT2F(IC,ICA)=0.0
  3011 EZT2F(IC,ICA)=0.0
       DO 301 ICB=1,27
       DO 301 ICA=1,15
       DO 301 IC=1,14
       EXTR(IC,ICA,ICB)=0.0
```

```
  301 EZTR(IC,ICA,ICB)=0.0
C
C     .....B. TYPE OF DIELECTRIC MEDIUM.....
      DO 4 IK=1,15
      DO 4 ID=1,34
      IE=16-IK
      READ(8,1113)(MEDIA(ID,IE,IEA),IEA=1,27)
 1113 FORMAT(27F1.0)
    4 CONTINUE
C
C     .....C. ZERO INITIAL FIELDS (CENTRE).....
      DO 402 IC=1,27
      DO 402 IB=1,14
      DO 402 IA=1,34
      EXT(IA,IB,IC)=0.0
  402 EYT(IA,IB,IC)=0.0
      DO 4020 IC=1,15
      DO 4020 IB=1,14
      DO 4020 IA=1,34
      HYT(IA,IB,IC)=0.0
 4020 HZT(IA,IB,IC)=0.0
      DO 403 IC=1,27
      DO 403 IB=1,15
      DO 403 IA=1,34
      ENX(IA,IB,IC)=0.0
      ENY(IA,IB,IC)=0.0
  403 ENZ(IA,IB,IC)=0.0
      DO 4030 IC=1,28
      DO 4030 IB=1,16
      DO 4030 IA=1,34
      EX(IA,IB,IC)=0.0
      EY(IA,IB,IC)=0.0
 4030 EZ(IA,IB,IC)=0.0
      DO 4031 IC=1,28
      DO 4031 IB=1,16
      DO 4031 IA=1,34
      HX(IA,IB,IC)=0.0
      HY(IA,IB,IC)=0.0
 4031 HZ(IA,IB,IC)=0.0
C
C     .....VI. PRINT THE DIELECTRIC MEDIA LATTICE.....
      DO 8 IP=1,15
      PRINT 6,IP
    6 FORMAT(1H1,////////,55X,'DIELECTRIC MEDIA LATTICE',
     1          //,62X,'PLANE K = ',I2,//,38X,'J',//)
      DO 67 IG=1,34
      IH=35-IG
      DO 66 II=1,27
      IPR(II)= MEDIA(IH,IP,II)
      IF(IPR(II).LT.1.0.OR.IPR(II).GT.FMPR)GO TO 70
   66 CONTINUE
   67 PRINT 7,IH,(IPR(IJ),IJ=1,27)
    7 FORMAT (37X,I2,4X,27I2)
    8 PRINT 9,(N(IK),IK=1,9),(N(IL),IL=1,9),(N(IM),IM=1,7)
```

```
    9 FORMAT (///,40X,'I',2X,9I2,10(' 1'),8(' 2'),/,
     161X,' 0',9I2,' 0',7I2)
C
C       .....VII. TIME STEPPING LOOP.....
        DO 65 J=1,MAXDT
C
C       .....ESTABLISH LOOP AND FIELD PARAMETERS.....
  109   TERM=RF*SIN(FLOAT(J)*RG)
        MAXY=MIN0(6+IFIX(FLOAT(J)/2.0),34)
C
C       .....A. E FIELD LOOP.....
        DO 22 JA=1,MAXY
        IF(JA.EQ.34)GO TO 14
C
C          .....1. EX ITERATION.....
        IF(J.GE.MINDT)GO TO 111
        DO 110 JCA=2,27
        DO 110 JBA=2,15
        NF=MEDIA(JA,JBA,JCA)
  110   EX(JA,JBA,JCA)=CA(NF)*EX(JA,JBA,JCA)+CB(NF)*
       1                (HY(JA,JBA-1,JCA) - HY(JA,JBA,JCA)+
       2                 HZ(JA+1,JBA,JCA-HZ(JA,JBA,JCA))
        GO TO 112
  111   DO 10 JC=2,27
        DO 10 JB=2,15
        NF=MEDIA(JA,JB,JC)
        EX(JA,JB,JC)=CA(NF)*EX(JA,JB,JC)+CB(NF)*
       1                (HY(JA,JB-1,JC) - HY(JA,JB,JC)+
       2                 HZ(JA+1,JB,JC-HZ(JA,JB,JC))
   10   ENX(JA,JB,JC)=AMAX1(ABS(EX(JA,JB,JC)),ENX(JA,JB,JC))
  112   REX=EX(JA,2,10)/RB
        IF(ABS(REX).GT.1.0E+4)GO TO 42
C
C       .....2. EX SOFT LATTICE TRUNCATION.....
        EX(JA,1,2)=(EXT(JA,1,2)+EXT(JA,1,3))/2.0
        EX(JA,1,27)=(EXT(JA,1,26)+EXT(JA,1,27))/2.0
        DO 11 JD=3,26
   11   EX(JA,1,JD)=(EXT(JA,1,JD-1)+EXT(JA,1,JD)
       1            +EXT(JA,1,JD+1))/3.0
        DO 13 JE=2,27
        NF=MEDIA(JA,1,JE)
        JF=IVF(NF)
        DO 12 JG=1,JF
   12   EXT(JA,JG,JE)=EXT(JA,JG+1,JE)
   13   EXT(JA,JG+1,JE)=EX(JA,2,JE)
C
C          .....3. EY ITERATION.....
   14   IF(J.GE.MINDT)GO TO 116
        DO 115 JIA=1,27
        DO 115 JHA=2,15
        NF=MEDIA(JA,JHA,JIA)
        EY(JA,JHA,JIA)=CA(NF)*EY(JA,JHA,JIA)+CB(NF)*
       1                (HX(JA,JHA,JIA-HX(JA,JHA-1,JIA)
       2                +HZ(JA,JHA,JIA-HZ(JA,JHA,JIA+1))
```

```
  115 CONTINUE
      GO TO 117
  116 DO 15 JI=1,27
      DO 15 JH=2,15
      NP=MEDIA(JA,JH,JI)
      EY(JA,JH,JI)=CA(NP)*EY(JA,JH,JI)+CB(NP)*
     1                    (HX(JA,JH,JI-HX(JA,JH-1,JI)
     2                    +HZ(JA,JH,JI-HZ(JA,JH,JI+1))
   15 ENY(JA,JH,JI)=AMAX1(ABS(EY(JA,JH,JI)),ENY(JA,JH,JI))
  117 REY=EY(JA,2,10)/RB
      IF(ABS(REY).GT.1.0E+4)GO TO 42
C
C          .....4. EY SOFT LATTICE TRUNCATION.....
      EY(JA,1,1)=(EYT(JA,1,1)+EYT(JA,1,2))/2.0
      EY(JA,1,27)=(EYT(JA,1,26)+2.0*EYT(JA,1,27))/3.0
      DO 16 JJ=2,26
   16 EY(JA,1,JJ)=(EYT(JA,1,JJ-1)+EYT(JA,1,JJ)
     1             +EYT(JA,1,JJ+1))/3.0
      DO 18 JK=1,27
      NP=MEDIA(JA,1,JK)
      JF=IVF(NP)
      DO 17 JL=1,JF
   17 EYT(JA,JL,JK)=EYT(JA,JL+1,JK)
   18 EYT(JA,JL+1,JK)=EY(JA,2,JK)
      IF(JA.EQ.34)GO TO 23
C
C          .....5. EZ ITERATION.....
      IF(J.GE.MINDT)GO TO 120
      DO 119 JNA=1,27
      DO 119 JMA=1,15
      NP=MEDIA(JA,JMA,JNA)
      EZ(JA,JMA,JNA)=CA(NP)*EZ(JA,JMA,JNA)+CB(NP)
     1                *(HX(JA,JMA,JNA-HX(JA+1,JMA,JNA)
     2                +HY(JA,JMA,JNA+1-HY(JA,JMA,JNA))
  119 CONTINUE
      GO TO 121
  120 DO 19 JN=1,27
      DO 19 JM=1,15
      NP=MEDIA(JA,JM,JN)
      EZ(JA,JM,JN)=CA(NP)*EZ(JA,JM,JN)+CB(NP)*(HX(JA,JM,JN)
     1             -HX(JA+1,JM,JN)+HY(JA,JM,JN+1)
     2             -HY(JA,JM,JN))
   19 ENZ(JA,JM,JN)=AMAX1(ABS(EZ(JA,JM,JN)),ENZ(JA,JM,JN))
  121 REZ=EZ(JA,1,10)/RB
      IF(ABS(REZ).GT.1.0E+4)GO TO 42
      IF(JA.EQ.1)GO TO 122
      IF(JA-3)22,123,22
C
C     .....6. EX,EZ TRUNCATIONS AT FRONT LATTICE FACE.....
  122 DO 1221 JZB=1,27
      DO 1221 JZA=1,15
      EX0(JZA,JZB)=EXT1F(JZA,JZB)
      EXT1F(JZA,JZB)=EXT2F(JZA,JZB)
 1221 EXT2F(JZA,JZB)=EX(1,JZA,JZB)
```

```
      DO 1222 JZB=1,27
      DO 1222 JZA=1,15
      EZ0(JZA,JZB)=EZT1F(JZA,JZB)
      EZT1F(JZA,JZB)=EZT2F(JZA,JZB)
 1222 EZT2F(JZA,JZB)=EZ(1,JZA,JZB)
      GO TO 21
C
C          .....7. SOFT TEM WAVE SOURCE CONDITION.....
  123 DO 20 JP=1,27
      DO 20 JO=1,15
   20 EZ(JA,JO,JP)=TERM+EZ(JA,JO,JP)
   21 CONTINUE
   22 CONTINUE
      GO TO 27
   23 CONTINUE
C
C       .....8. EX,EZ TRUNCATIONS AT REAR LATTICE FACE.....
      DO 230 JSA=1,27
      DO 230 JRA=1,15
      EX(34,JRA,JSA)=EXTR(1,JRA,JSA)
  230 EZ(34,JRA,JSA)=EZTR(1,JRA,JSA)
      DO 25 JS=1,27
      DO 25 JR=1,15
      NF=MEDIA(34,JR,JS)
      JF=IVF(NF)
      DO 24 JT=1,JF
      EXTR(JT,JR,JS)=EXTR(JT+1,JR,JS)
   24 EZTR(JT,JR,JS)=EZTR(JT+1,JR,JS)
      EXTR(JF+1,JR,JS)=EX(33,JR,JS)
   25 EZTR(JF+1,JR,JS)=EZ(33,JR,JS)
C
C          .....B. H FIELD LOOP.....
   27 DO 40 K=1,MAXY
      IF(K.GE.2)GO TO 28
      GO TO 29
C
C          .....1. HX ITERATION.....
   28 DO 30 KB=1,27
      DO 30 KA=1,15
      HX(K,KA,KB)=HX(K,KA,KB)+EY(K,KA+1,KB-EY(K,KA,KB)
     1           +EZ(K-1,KA,KB-EZ(K,KA,KB)
   30 CONTINUE
      GOTO 306
   29 DO 305 KBZ=1,27
      DO 305 KAZ=1,15
      HX(K,KAZ,KBZ)=HX(K,KAZ,KBZ)+EY(K,KAZ+1,KBZ)
     1         -EY(K,KAZ,KBZ)+EZ0(KAZ,KBZ-EZ(K,KAZ,KBZ)
  305 CONTINUE
  306 CONTINUE
      IF(K.EQ.34)GO TO 35
C
C          .....2. HY ITERATION.....
      DO 31 KD=2,27
      DO 31 KC=1,15
```

```
      HY(K,KC,KD)=HY(K,KC,KD)+EX(K,KC,KD-EX(K,KC+1,KD)
     1            +EZ(K,KC,KD-EZ(K,KC,KD-1)
   31 CONTINUE
C
C          .....3. HY SOFT LATTICE TRUNCATION.....
      HY(K,1,1)=(HYT(K,1,1)+HYT(K,1,2))/2.0
      HY(K,15,1)=(HYT(K,1,14)+2.0*HYT(K,1,15))/3.0
      DO 32 KE=2,14
   32 HY(K,KE,1)=(HYT(K,1,KE-1)+HYT(K,1,KE)
     1            +HYT(K,1,KE+1))/3.0
      DO 34 KF=1,15
      NF=MEDIA(K,KF,1)
      KG=IVF(NF)
      DO 33 KH=1,KG
   33 HYT(K,KH,KF)=HYT(K,KH+1,KF)
   34 HYT(K,KH+1,KF)=HY(K,KF,2)
C
C          .....4. HZ ITERATION.....
      IF(K.GE.2)GO TO 35
      DO 341 KJ=2,27
      DO 341 KI=2,15
  341 HZ(K,KI,KJ)=HZ(K,KI,KJ)+EX(K,KI,KJ-EX0(KI,KJ)
     1            +EY(K,KI,KJ-1-EY(K,KI,KJ)
      GO TO 351
   35 DO 36 KJ=2,27
      DO 36 KI=2,15
   36 HZ(K,KI,KJ)=HZ(K,KI,KJ)+EX(K,KI,KJ-EX(K-1,KI,KJ)
     1            +EY(K,KI,KJ-1-EY(K,KI,KJ)
  351 CONTINUE
C
C          .....5. HZ SOFT LATTICE TRUNCATION.....
      HZ(K,2,1)=(HZT(K,1,2)+HZT(K,1,3))/2.0
      HZ(K,15,1)=(HZT(K,1,14)+HZT(K,1,15))/2.0
      DO 37 KK=3,14
   37 HZ(K,KK,1)=(HZT(K,1,KK-1)+HZT(K,1,KK)
     1            +HZT(K,1,KK+1))/3.0
      DO 39 KL=2,15
      NF=MEDIA(K,KL,1)
      KG=IVF(NF)
      DO 38 KH=1,KG
   38 HZT(K,KH,KL)=HZT(K,KH+1,KL)
   39 HZT(K,KH+1,KL)=HZ(K,KL,2)
   40 CONTINUE
C
C          .....C. PRINT-OUT ROUTINE.....
      DO 41 L=NDT,MAXDT,MIDDT
      IF(J.EQ.L)GO TO 43
   41 CONTINUE
      GO TO 64
   42 NTEST=1
C
C          .....1. FIND THE NORMALISING PARAMETER.....
   43 EMAX=0.0
      DO 45 LC=1,27
```

```
      DO 45 LB=1,15
      DO 45 LA=1,34
      LD=MEDIA(LA,LB,LC)
      ER=(ENX(LA,LB,LC)**2+ENY(LA,LB,LC)**2
     1+ENZ(LA,LB,LC)**2)*SIG(LD)/RH
      IF(ER-EMAX)45,45,44
   44 EMAX=ER
   45 CONTINUE
      PRINT 46, EMAX
   46 FORMAT('1','THE MAXIMUM DISSIPATED POWER IS ',E10.3,
     11X,'WATTS/M**3 FOR UNIT INCIDENT ELECTRIC FIELD')
      EMAX=EMAX/9
      PRINT 47, EMAX
   47 FORMAT(' ','THE NORMALISING FACTOR IS ',E10.3)
C
C     .....2. CALCULATE THE DISSIPATED POWER AT EACH .....
C             POINT, NORMALISE IT TO AN INDEX IN THE
C             RANGE 0-9, AND PRINT OUT THE INDEX IN
C             THE SAME FORM AS IN THE MEDIA LATTICE.
      DO 52 LF=1,15
      PRINT 48, J, LF
   48 FORMAT(1H1,////////,46X,'NORMALISED HEATING INDEX AT',
     1' TIME STEP ',I3,//,62X,'PLANE K = ',I2,//,38X,'J',//)
      DO 50 LH=1,34
      LE=35-LH
      DO 49 LG=1,27
      LI=MEDIA(LE,LF,LG)
   49 IPR(LG)=(ENX(LE,LF,LG)**2+ENY(LE,LF,LG)**2
     1+ENZ(LE,LF,LG)**2)*SIG(LI)/(RH*EMAX)
   50 PRINT 51,LE,(IPR(LJ),LJ=1,27)
   51 FORMAT(37X,I2,4X,27I2)
   52 PRINT 53,(N(LK),LK=1,9),(N(LL),LL=1,9),(N(LM),LM=1,7)
   53 FORMAT(///,40X,'I',2X,9I2,10(' 1'),8(' 2'),/,61X,' 0',
     19I2,' 0',7I2)
C
C         .....5. DEFAULT OPTION.....
      IF(NTEST.EQ.1)GO TO 70
C
C         .....6. ENVELOPE RESET TO ZERO.....
      DO 62 LV=1,27
      DO 62 LU=1,15
      DO 62 LT=1,34
      ENX(LT,LU,LV)=0.0
      ENY(LT,LU,LV)=0.0
   62 ENZ(LT,LU,LV)=0.0
   64 CONTINUE
   65 CONTINUE
   70 STOP
      END
|ENCHAP
```

Appendix C

Selected Physical Properties of DMSO

Property	Value
Boiling Point at 760mm Hg, °C	189.0
Vapour pressure at 20°C, mm Hg	0.37,0.417
Specific heat at 25°C, cal/gm	.4698
Specific heat of vaporization at b.p., cal/gm	175
Molar Heat of vaporization at b.p., kcal/mole	13.67
Entropy of vaporization at b.p., cal/deg.mole	29.6
Enthalpy of vaporization at 25°C, kcal/mole	12.64
Coefficient of expansion, ml/gm.deg	0.00088
Specific gravity at 25°C, g/ml	1.096
Melting point, °C	18.55
Specific heat of fusion, cal/gm	38.8
Molar heat of fusion, kcal/mole	3.43,3.03
Entropy of fusion, cal/deg.mole	10.4,11.7
Specific heat of solid at 18.45°C, cal/gm	0.5
Heat of formation, kcal/mole	-47.7
Heat of combustion, cal/gm	6050
Flash point, open vessel, °C	95
Molal f.p. depression, deg/mole/1000gm	4.4,4.36
Refractive index (nD^{20})	1.4783
Refractive index (nD^{25})	1.47674
Molar refractivity, Rm	20.12
Polarizability, cm^3	7.97×10^{-24}
Dielectric constant at 20°C (Estatic)	48.9
Dielectric constant at 25°C (Estatic)	46.4
Dipole moment, 25°C, D	4.11
Viscosity, 20°C, cP	2.473
Viscosity, 25°C, cP	1.99
Surface tension at 20°C, dyne/cm	46.2
Surface tension at 25°C, dyne/cm	42.86
Specific conductance at 20°C, $ohm^{-1}cm^{-1}$	3×10^{-8}

The above properties are obtained from (S4), page 5. This source lists the references in which the above data was published.

Appendix D

In order to make available the numerical data obtained from the dielectric measurements, the tables in this section are presented. Some comments regarding their presentation are in order.

Fourteen different sets of measurement parameters were used, as outlined below:

(1) Distilled water	
(2) 1% DMSO	
(3) 5% DMSO	measurements in the
(4) 10% DMSO	temperature range
(5) 20% DMSO	-60°C to +100°C
(6) 70% DMSO	
(7) 100% DMSO	
(8) 5% dextran	measurements in the
(9) 0.1% NaCl + 10% DMSO	temperature range
(10) 1.0% NaCl + 10% DMSO	-60°C to +40°C
(11) 5% dextran + 10% DMSO	
(12) DMSO at 5°C	concentrations in 10%
(13) DMSO at 23°C	steps from 0% to 100%
(14) DMSO at 50°C	at each temperature

The data obtained in the measurements has been reduced

to values of ϵ', ϵ'', loss tangent and conductivity (mho). The standard deviation as a percentage of the value is quoted in the case of ϵ' and ϵ'', except for cases where this exceeds 100% as in the vicinity of the freezing point of some mixtures. In these cases, the deviation is left blank. Standard deviations are not quoted for the derived quantities, loss tangent and conductivity, because they are not measured directly. The quoted value is calculated from the mean values of ϵ' and ϵ''. In the case of sets 1-11, the figures quoted for decreasing temperatures were those obtained during cooling, and the figures quoted for increasing temperatures were those obtained during heating. The differences are attributable to supercooling effects, and to the existence of mixtures of solid and liquid material just beyond the state transition point. For purposes of plotting the curves of chapter 6, some liberties were taken in these regions, as described in that chapter.

DIELECTRIC DATA FOR DISTILLED WATER

TEMP. DEG.C	EP	EPP	L.TAN (AVG)	COND. MHO
24.5	76.58+- 1.9%	11.48+- 8.9%	0.150	1.784
21.5	79.04+- 1.8%	11.83+- 7.5%	0.150	1.841
16.5	80.20+- 2.0%	13.06+- 7.3%	0.163	2.029
10.5	81.09+- 1.9%	14.68+- 7.8%	0.181	2.281
1.5	81.23+- 1.8%	18.26+- 8.8%	0.225	2.840
-2.0	77.90+- 4.0%	22.21+- 9.1%	0.285	3.456
-2.0	65.72+- 7.2%	21.91+-14.5%	0.333	3.405
-2.5	41.85+-13.3%	16.43+-17.9%	0.393	2.557
-3.5	18.56+-18.2%	6.52+-33.1%	0.351	1.012
-15.0	4.21+-29.7%	0.28+- 0.0%	0.067	0.044
-30.5	3.11+-10.9%	0.12+-16.7%	0.039	0.019
-43.5	3.04+-12.5%	0.12+- 8.3%	0.039	0.019
-50.5	3.06+-12.4%	0.12+- 8.3%	0.039	0.019
-54.0	2.92+-12.7%	0.12+-16.7%	0.041	0.019
-47.5	2.66+-14.3%	0.11+-18.2%	0.041	0.017
-42.5	2.80+-13.2%	0.12+-16.7%	0.043	0.019
-36.0	2.64+-13.6%	0.11+-18.2%	0.042	0.017
-28.5	2.80+-14.3%	0.12+-16.7%	0.043	0.019
-21.0	2.83+-14.5%	0.12+-16.7%	0.042	0.019
-13.0	2.80+-16.1%	0.12+-16.7%	0.043	0.019
-6.0	2.80+-16.1%	0.12+-16.7%	0.043	0.019
-2.0	2.87+-13.6%	0.12+-16.7%	0.042	0.019
-1.5	4.39+-31.4%	0.30+-83.3%	0.068	0.047
-1.5	8.99+-26.8%	1.36+-58.8%	0.151	0.212
-1.5	15.46+-18.5%	3.91+-29.4%	0.253	0.608
-1.0	22.76+-16.5%	6.81+-22.6%	0.299	1.062
-1.0	30.86+-16.9%	9.42+-22.1%	0.305	1.464
0.0	41.01+-14.3%	12.27+-20.0%	0.299	1.910
1.0	52.03+-11.4%	14.92+-18.1%	0.287	2.319
1.0	63.12+- 9.1%	16.77+-15.9%	0.266	2.608
6.0	72.25+- 5.3%	17.56+-13.8%	0.243	2.733
12.0	76.45+- 5.6%	17.21+-12.5%	0.225	2.677
17.0	78.44+- 4.7%	16.61+-14.6%	0.212	2.582
22.0	77.97+- 4.7%	14.08+-13.7%	0.181	2.193
27.0	75.22+- 2.5%	9.39+- 9.9%	0.125	1.458
33.0	73.69+- 2.8%	8.41+- 9.2%	0.114	1.307
38.0	72.31+- 4.5%	7.80+-10.8%	0.108	1.213
43.0	71.38+- 4.2%	7.23+-10.8%	0.101	1.125
49.0	70.65+- 4.2%	6.85+-11.8%	0.097	1.068
55.0	68.97+- 4.5%	6.45+-13.6%	0.094	1.005
61.0	65.50+- 2.5%	5.71+-12.6%	0.087	0.886
67.0	64.43+- 2.3%	5.24+-11.8%	0.081	0.817
74.0	63.39+- 2.6%	4.76+-11.8%	0.075	0.741
80.0	62.09+- 2.7%	4.35+-12.0%	0.070	0.679
87.0	61.40+- 2.5%	4.05+-10.9%	0.066	0.628
93.0	60.30+- 2.5%	3.79+-10.3%	0.063	0.589
98.0	59.21+- 3.0%	3.52+- 9.9%	0.059	0.547

DIELECTRIC DATA FOR 1% DMSO IN WATER

TEMP. DEG.C	EP	EPP	L.TAN (AVG)	COND. MHO
23.2	75.02+- 1.8%	11.24+- 7.7%	0.150	1.747
16.7	74.45+- 3.0%	12.81+-11.2%	0.172	1.992
9.7	75.35+- 3.3%	15.35+-13.3%	0.204	2.388
1.1	74.26+- 5.0%	18.22+-15.6%	0.245	2.834
-0.4	60.56+- 6.9%	16.84+-13.8%	0.278	2.620
-0.7	43.53+-22.0%	13.80+-29.4%	0.317	2.149
-1.1	23.41+-31.5%	7.05+-50.2%	0.301	1.100
-2.5	9.38+-29.6%	1.60+-60.6%	0.171	0.249
-14.8	3.44+-16.9%	0.33+-36.4%	0.096	0.051
-31.1	3.02+- 8.6%	0.19+-26.3%	0.063	0.030
-43.7	2.85+- 8.4%	0.14+-21.4%	0.049	0.022
-54.7	2.69+- 8.2%	0.12+-16.7%	0.045	0.019
-46.7	2.37+-11.0%	0.12+-25.0%	0.051	0.019
-40.7	2.54+-10.2%	0.14+-21.4%	0.055	0.022
-34.0	2.47+-12.6%	0.16+-18.8%	0.065	0.025
-26.6	2.76+-12.7%	0.22+-22.7%	0.080	0.034
-18.7	2.95+-13.9%	0.28+-21.4%	0.095	0.044
-11.6	3.76+-15.7%	0.38+-18.4%	0.101	0.059
-5.9	5.56+-21.4%	0.61+-27.9%	0.110	0.095
-2.8	8.99+-23.9%	1.20+-41.7%	0.133	0.187
-1.6	13.98+-24.7%	2.47+-45.7%	0.177	0.384
-1.1	20.79+-36.5%	4.63+-56.2%	0.223	0.723
-0.9	29.72+-35.3%	7.64+-51.6%	0.257	1.188
-0.7	41.15+-28.1%	10.80+-33.9%	0.262	1.678
-0.5	53.03+-19.6%	13.69+-30.3%	0.258	2.130
-0.4	64.88+-17.4%	16.13+-26.8%	0.249	2.507
0.8	71.57+-13.3%	15.06+-35.6%	0.210	2.344
5.2	76.65+- 1.5%	14.16+-16.0%	0.185	2.205
10.4	76.19+- 2.0%	13.08+-14.1%	0.172	2.036
14.4	75.73+- 2.3%	12.32+-11.7%	0.163	1.916
20.6	73.50+- 2.7%	10.02+-10.5%	0.136	1.558
25.0	74.13+- 2.3%	11.19+- 9.9%	0.151	1.740
30.0	73.50+- 2.0%	10.32+- 9.3%	0.140	1.602
38.0	72.43+- 2.5%	9.24+-10.0%	0.128	1.439
43.0	71.57+- 2.1%	8.50+- 8.0%	0.119	1.319
55.0	67.33+- 5.3%	7.39+-11.8%	0.110	1.150
61.0	65.39+- 3.4%	6.60+-12.7%	0.101	1.024
67.0	64.32+- 2.8%	6.08+-14.1%	0.095	0.949
74.0	63.50+- 2.8%	5.39+-11.5%	0.085	0.836
80.0	62.04+- 2.9%	5.07+-12.0%	0.082	0.792
87.0	61.29+- 3.1%	4.54+-12.1%	0.074	0.704
93.0	60.19+- 2.9%	4.21+-11.9%	0.070	0.653
98.0	59.11+- 3.0%	3.88+-11.9%	0.066	0.603

DIELECTRIC DATA FOR 5% DMSO IN WATER

TEMP. DEG.C	EP	EPP	L.TAN (AVG)	COND. MHO
23.5	74.90+- 2.0%	11.98+-13.0%	0.160	1.866
14.5	73.12+- 2.0%	12.48+-10.3%	0.171	1.942
7.0	74.38+- 2.9%	14.78+-10.1%	0.199	2.300
-2.5	75.48+- 3.2%	17.58+-13.4%	0.233	2.733
-8.0	72.06+- 5.9%	21.05+-18.0%	0.292	3.274
-6.0	54.27+-12.7%	19.80+-27.4%	0.365	3.079
-9.0	33.56+-22.1%	14.25+-34.0%	0.425	2.218
-17.0	17.20+-29.3%	8.13+-34.4%	0.473	1.263
-30.0	7.72+-24.4%	3.24+-44.8%	0.420	0.504
-42.5	4.97+-34.0%	1.31+-71.8%	0.264	0.204
-52.0	3.78+-15.1%	0.58+-60.3%	0.153	0.090
-60.0	3.67+-12.3%	0.32+-43.7%	0.087	0.050
-51.0	3.62+-13.5%	0.42+-33.3%	0.116	0.065
-45.5	3.69+-14.1%	0.55+-34.5%	0.149	0.085
-38.5	4.10+-14.1%	0.81+-33.3%	0.198	0.126
-31.5	4.50+-16.2%	1.27+-34.6%	0.282	0.197
-24.5	5.79+-16.4%	2.10+-34.3%	0.363	0.327
-18.5	7.97+-15.3%	3.47+-31.7%	0.435	0.540
-13.5	10.63+-13.0%	5.25+-29.1%	0.494	0.817
-9.5	15.53+-20.9%	7.63+-37.1%	0.491	1.188
-7.5	20.94+-20.1%	9.91+-31.6%	0.473	1.539
-6.0	27.72+-21.1%	12.09+-30.8%	0.436	1.879
-5.0	36.39+-24.4%	14.43+-34.9%	0.397	2.243
-4.0	46.65+-21.8%	16.50+-31.1%	0.354	2.564
-1.5	59.16+-14.0%	18.10+-23.6%	0.306	2.815
3.5	69.03+-12.7%	18.33+-24.6%	0.266	2.853
9.0	75.28+- 2.5%	17.44+-13.6%	0.232	2.714
13.5	75.48+- 2.0%	15.58+-11.9%	0.206	2.425
18.0	75.22+- 1.6%	14.00+-10.2%	0.186	2.180
21.5	74.77+- 1.9%	12.89+- 9.9%	0.172	2.004
26.0	74.38+- 2.3%	12.17+-11.7%	0.164	1.891
31.0	73.43+- 1.9%	10.77+- 9.3%	0.147	1.678
38.0	72.74+- 2.4%	9.98+-10.6%	0.137	1.552
43.0	71.94+- 2.3%	9.30+-10.1%	0.129	1.445
49.0	71.08+- 2.3%	8.84+- 9.7%	0.124	1.376
55.0	67.04+- 5.9%	7.87+-13.9%	0.117	1.225
61.0	64.71+- 2.8%	7.00+-10.4%	0.108	1.087
67.0	63.77+- 2.9%	6.45+-10.5%	0.101	1.005
74.0	62.68+- 2.8%	5.88+-10.5%	0.094	0.917
80.0	61.45+- 3.0%	5.37+-10.6%	0.087	0.836
87.0	60.66+- 2.9%	5.05+-10.5%	0.083	0.785
93.0	59.52+- 2.8%	4.72+-10.4%	0.079	0.735
98.0	58.25+- 2.7%	4.35+-10.3%	0.075	0.679

DIELECTRIC DATA FOR 10% DMSO IN WATER

TEMP. DEG.C	EP	EPP	L.TAN (AVG)	COND. MHO
23.0	73.56+- 2.9%	11.99+-14.0%	0.163	1.866
15.5	74.32+- 2.4%	13.73+-14.2%	0.185	2.136
8.0	75.15+- 2.4%	16.00+-13.4%	0.213	2.488
-1.5	75.67+- 2.0%	20.20+-14.8%	0.267	3.142
-11.5	74.58+- 3.1%	26.04+-15.9%	0.349	4.053
-6.5	49.71+-21.3%	23.30+-36.4%	0.469	3.625
-11.0	26.47+-27.9%	17.17+-39.4%	0.649	2.670
-18.0	12.66+-46.0%	8.38+-44.6%	0.662	1.301
-28.0	6.18+-20.7%	3.01+-29.9%	0.487	0.468
-39.5	5.04+-14.3%	1.35+-27.4%	0.268	0.210
-49.5	4.19+-12.6%	0.68+-26.5%	0.162	0.106
-57.5	3.89+-12.3%	0.42+-19.0%	0.108	0.065
-48.5	4.03+-13.2%	0.62+-19.4%	0.154	0.096
-43.0	4.08+-13.7%	0.83+-19.3%	0.203	0.129
-37.0	4.53+-10.6%	1.22+-18.9%	0.269	0.190
-30.5	5.12+- 9.6%	1.88+-17.6%	0.367	0.292
-23.0	6.37+-17.1%	3.12+-22.1%	0.490	0.485
-17.5	8.48+-18.8%	5.10+-21.0%	0.601	0.792
-12.5	12.58+-35.3%	8.30+-34.5%	0.660	1.288
-8.5	22.05+-21.8%	13.87+-36.7%	0.629	2.155
-6.5	33.20+-17.8%	17.85+-36.5%	0.538	2.777
-5.0	46.93+-14.0%	20.56+-30.8%	0.438	3.198
-2.5	59.73+- 9.6%	21.13+-24.3%	0.354	3.286
2.5	70.77+- 5.5%	21.20+-19.1%	0.300	3.299
7.5	73.62+- 2.3%	18.99+-15.1%	0.258	2.953
12.5	73.94+- 2.9%	17.03+-15.2%	0.230	2.652
18.0	73.94+- 3.1%	14.49+-14.7%	0.196	2.256
25.5	72.18+- 2.1%	11.84+-13.0%	0.164	1.841
32.0	70.83+- 2.4%	10.66+-13.2%	0.151	1.659
43.0	71.69+- 4.3%	9.07+-11.5%	0.127	1.414
55.0	67.21+- 2.2%	7.07+- 7.8%	0.105	1.100
67.0	65.10+- 2.3%	6.13+- 9.8%	0.094	0.955
80.0	61.93+- 2.9%	5.13+- 8.2%	0.083	0.798
93.0	59.26+- 3.1%	4.53+- 9.5%	0.076	0.704

DIELECTRIC DATA FOR 20% DMSO IN WATER

TEMP. DEG.C	EP	EPP	L.TAN (AVG)	COND. MHO
23.0	74.83+- 2.1%	15.96+-10.3%	0.213	2.482
15.0	73.43+- 2.7%	17.67+-11.5%	0.241	2.746
7.0	73.69+- 3.2%	20.32+-13.1%	0.276	3.160
-3.0	73.50+- 4.6%	26.06+-16.7%	0.355	4.053
-15.0	72.49+- 4.2%	33.70+-15.9%	0.465	5.240
-25.0	67.50+- 8.0%	40.07+-19.4%	0.594	6.233
-19.0	30.43+-64.0%	23.93+-66.0%	0.786	3.720
-28.0	8.97+-21.2%	8.07+-25.8%	0.900	1.257
-36.5	5.92+-14.9%	3.90+-23.8%	0.659	0.606
-45.0	5.49+- 9.8%	2.11+-20.9%	0.384	0.328
-53.5	5.01+- 9.8%	1.19+-17.6%	0.238	0.185
-60.5	4.55+- 7.0%	0.71+-18.3%	0.156	0.111
-53.5	4.73+- 8.5%	1.01+-27.7%	0.214	0.157
-48.0	4.88+- 6.8%	1.35+-30.4%	0.277	0.210
-41.5	5.21+- 8.3%	1.94+-33.5%	0.372	0.302
-33.5	5.60+-10.5%	2.88+-36.5%	0.514	0.448
-29.5	6.95+-18.1%	4.58+-38.6%	0.659	0.710
-23.5	8.54+-17.0%	6.87+-33.2%	0.804	1.068
-19.0	10.05+-10.6%	8.43+-43.3%	0.839	1.313
-15.0	10.57+- 7.3%	10.67+-19.3%	0.009	1.659
-11.5	53.90+-26.1%	30.58+-47.5%	0.567	4.756
-6.0	66.81+-15.3%	28.52+-29.3%	0.427	4.436
0.0	72.99+- 7.4%	26.19+-14.8%	0.359	4.072
5.5	75.48+- 3.2%	23.67+- 9.0%	0.314	3.682
9.0	75.09+- 2.9%	21.69+- 9.8%	0.289	3.374
12.0	74.51+- 2.3%	19.33+- 8.5%	0.259	3.003
19.0	74.51+- 2.1%	17.36+-11.0%	0.233	2.702
26.0	73.69+- 2.1%	15.01+-10.6%	0.204	2.337
33.0	73.50+- 2.4%	13.37+- 9.1%	0.182	2.080
43.0	72.31+- 2.2%	11.48+-10.5%	0.159	1.784
55.0	66.81+- 2.1%	8.86+-11.9%	0.133	1.376
67.0	64.32+- 2.5%	7.60+-13.2%	0.118	1.181
80.0	61.13+- 3.0%	6.24+-11.9%	0.102	0.968
93.0	58.65+- 3.4%	5.45+-11.7%	0.093	0.848

DIELECTRIC DATA FOR 70% DMSO IN WATER

TEMP. DEG.C	EP	EPP	L.TAN (AVG)	COND. MHO
22.5	51.45+- 5.4%	26.41+-12.9%	0.513	4.109
16.0	37.51+-20.2%	23.37+-34.1%	0.623	3.638
9.0	26.53+-27.9%	19.04+-37.4%	0.718	2.959
-1.0	13.19+- 7.5%	10.63+-16.9%	0.806	1.652
-12.0	12.75+-12.7%	9.05+-19.9%	0.710	1.407
-22.0	12.13+-49.7%	7.47+-44.2%	0.616	1.162
-31.5	7.99+-21.7%	4.37+-20.1%	0.547	0.679
-40.0	7.44+-10.1%	3.05+-13.4%	0.410	0.474
-48.0	7.28+- 5.4%	2.23+-11.7%	0.306	0.347
-54.0	7.20+- 5.6%	1.69+-12.4%	0.235	0.263
-62.0	6.78+- 3.1%	1.12+- 9.8%	0.165	0.174
-52.0	6.83+- 5.9%	2.10+-12.9%	0.307	0.327
-45.5	7.20+- 4.9%	2.90+- 9.7%	0.403	0.451
-39.0	7.24+-18.1%	3.90+-19.7%	0.539	0.606
-32.0	7.11+-22.2%	5.13+-20.9%	0.722	0.798
-22.5	9.63+-35.2%	7.68+-33.7%	0.798	1.194
-15.0	11.88+- 8.7%	10.11+-17.5%	0.851	1.571
-7.0	13.35+- 8.5%	12.03+-18.4%	0.901	1.872
0.0	21.47+-25.9%	16.38+-42.2%	0.763	2.545
5.5	24.83+-40.9%	17.74+-58.0%	0.714	2.758
9.5	29.20+-43.7%	19.47+-56.3%	0.667	3.029
13.0	33.03+-53.9%	20.72+-72.0%	0.627	3.223
17.5	33.31+-55.8%	20.31+-75.7%	0.610	3.160
20.0	46.77+-18.9%	24.79+-35.5%	0.530	3.858
25.5	49.41+- 8.1%	23.85+-24.2%	0.483	3.707
30.0	52.21+- 7.1%	23.18+-23.9%	0.444	3.607
34.0	53.26+- 7.0%	22.12+-23.3%	0.415	3.443
38.0	52.71+- 5.3%	22.99+-13.8%	0.436	3.575
43.0	53.21+- 4.3%	20.91+-12.5%	0.393	3.255
49.0	53.53+- 4.2%	19.32+-13.7%	0.361	3.003
55.0	53.16+- 4.0%	17.48+-13.4%	0.329	2.721
61.0	53.53+- 6.4%	15.86+-15.8%	0.296	2.469
67.0	53.35+- 4.6%	14.50+-13.0%	0.272	2.256
74.0	53.21+- 4.2%	13.14+-14.0%	0.247	2.042
80.0	51.72+- 4.5%	11.63+-13.7%	0.225	1.810
87.0	51.72+- 4.1%	10.69+-13.8%	0.207	1.665
93.0	50.57+- 5.2%	9.70+-15.4%	0.192	1.508
98.0	50.36+- 4.4%	8.95+-14.5%	0.178	1.395

DIELECTRIC DATA FOR 100% DMSO

TEMP. DEG.C	EP	EPP	L.TAN (AVG)	COND. MHO
23.0	46.49+- 5.3%	13.06+-11.6%	0.281	2.029
19.5	46.69+- 5.1%	13.73+-11.4%	0.294	2.136
12.5	47.01+- 4.8%	15.35+-10.9%	0.327	2.388
14.0	33.56+-10.8%	11.65+-22.6%	0.347	1.810
13.5	20.79+-14.1%	6.38+-69.4%	0.307	0.993
10.0	9.18+-16.8%	1.92+-38.5%	0.209	0.298
-4.0	4.66+-13.5%	0.60+-26.7%	0.129	0.094
-20.0	3.46+-13.0%	0.29+-27.6%	0.084	0.045
-33.0	3.32+-10.5%	0.20+-20.0%	0.060	0.031
-43.5	3.18+-11.0%	0.16+-18.8%	0.050	0.025
-52.5	3.04+-11.8%	0.14+-14.3%	0.046	0.022
-61.5	2.97+-10.4%	0.13+-15.4%	0.044	0.020
-52.0	3.04+-11.8%	0.15+-20.0%	0.049	0.023
-46.5	3.06+-11.1%	0.16+-18.8%	0.052	0.025
-39.5	2.95+-11.2%	0.26+- 0.0%	0.088	0.040
-33.0	3.25+-12.9%	0.21+-19.0%	0.065	0.033
-25.0	3.18+-14.2%	0.25+-24.0%	0.079	0.039
-17.0	3.64+-13.2%	0.34+-20.6%	0.093	0.053
-10.0	4.08+-12.5%	0.46+-19.6%	0.113	0.072
-4.0	4.84+-16.1%	0.65+-26.2%	0.134	0.101
0.5	5.96+-16.4%	0.93+-28.0%	0.156	0.145
5.0	7.24+-16.3%	1.29+-30.2%	0.178	0.200
8.0	8.46+-14.4%	1.75+-28.0%	0.207	0.272
9.5	10.12+-12.3%	2.49+-24.5%	0.246	0.387
11.5	12.24+-13.0%	3.53+-25.2%	0.288	0.549
12.5	14.75+-14.2%	4.83+-22.2%	0.327	0.754
13.0	18.20+-14.5%	6.41+-21.2%	0.352	0.999
13.5	21.69+-12.9%	7.76+-18.7%	0.358	1.206
14.0	25.65+-14.0%	9.42+-21.5%	0.367	1.464
14.5	30.79+-13.9%	11.15+-20.9%	0.362	1.734
18.0	35.93+-13.5%	12.53+-19.6%	0.349	1.948
20.5	41.50+-11.4%	13.62+-21.1%	0.328	2.117
23.0	45.82+- 5.8%	13.63+-16.2%	0.297	2.117
27.5	46.33+- 5.0%	12.32+-11.8%	0.266	1.916
33.0	44.85+- 4.9%	10.89+-13.9%	0.243	1.696
43.0	43.86+- 5.0%	9.48+-14.9%	0.216	1.477
55.0	42.94+- 6.7%	8.00+-17.3%	0.186	1.244
67.0	41.29+- 5.3%	6.79+-15.9%	0.164	1.056
80.0	39.44+- 5.5%	5.72+-12.1%	0.145	0.892
93.0	37.93+- 5.7%	5.03+-13.7%	0.133	0.785

DIELECTRIC DATA FOR 5% DEXTRAN IN WATER

TEMP. DEG.C	EP	EPP	L.TAN (AVG)	COND. MHO
23.2	74.32+- 2.9%	14.13+-14.9%	0.190	2.199
17.5	75.15+- 5.2%	15.22+-22.1%	0.203	2.369
11.3	75.41+- 5.7%	18.08+-17.9%	0.240	2.815
2.5	74.45+- 5.0%	21.21+-14.9%	0.285	3.299
-7.5	69.56+-14.2%	24.30+-30.1%	0.349	3.782
-0.2	43.57+-14.3%	16.82+-20.9%	0.386	2.614
-0.5	24.96+-17.4%	9.79+-28.8%	0.392	1.521
-1.8	11.24+-20.4%	2.21+-72.4%	0.197	0.344
-14.1	3.67+-10.6%	0.25+-36.0%	0.068	0.039
-27.8	3.06+- 8.8%	0.14+-14.3%	0.046	0.022
-39.0	3.02+- 8.6%	0.13+-15.4%	0.043	0.020
-45.6	2.97+- 6.7%	0.12+-16.7%	0.040	0.019
-50.3	2.76+- 7.2%	0.12+-16.7%	0.043	0.019
-45.2	2.71+-10.3%	0.12+-16.7%	0.044	0.019
-39.9	2.87+-10.8%	0.13+-15.4%	0.045	0.020
-34.2	2.78+-11.2%	0.14+-21.4%	0.050	0.022
-27.3	2.90+-10.3%	0.15+-20.0%	0.052	0.023
-20.0	3.04+-11.2%	0.16+-12.5%	0.053	0.025
-12.5	3.09+-12.3%	0.18+-16.7%	0.058	0.028
-6.4	3.62+-11.3%	0.33+-18.2%	0.091	0.051
-2.2	5.43+-15.7%	0.71+-15.5%	0.131	0.111
-0.6	8.91+-15.2%	1.42+-23.9%	0.159	0.221
-0.3	14.45+-17.2%	3.32+-34.6%	0.230	0.516
-0.2	21.30+-18.5%	6.18+-36.1%	0.290	0.961
-0.2	31.89+-21.1%	10.40+-40.2%	0.326	1.615
0.0	41.22+-13.1%	13.25+-24.9%	0.321	2.061
0.1	54.65+-11.9%	16.32+-17.6%	0.299	2.538
0.5	64.60+- 8.3%	18.73+-16.6%	0.290	2.915
2.4	75.67+- 9.1%	21.23+-15.1%	0.281	3.305
5.9	77.31+- 4.6%	19.86+-13.5%	0.257	3.091
10.5	76.19+- 4.2%	17.82+-11.7%	0.234	2.771
13.7	75.80+- 4.1%	16.67+-11.1%	0.220	2.595
17.9	75.48+- 4.0%	15.20+- 9.7%	0.201	2.362
20.5	75.41+- 4.1%	14.09+-12.6%	0.187	2.193

DIELECTRIC DATA FOR 0.1% NACL IN 10% DMSO

TEMP. DEG.C	EP	EPP	L.TAN (AVG)	COND. MHO
20.5	73.75+- 5.7%	14.32+-11.5%	0.194	2.224
16.0	76.19+- 4.1%	15.79+-10.3%	0.207	2.457
9.8	76.78+- 4.4%	18.41+-11.0%	0.240	2.865
1.5	76.98+- 3.5%	21.77+-13.6%	0.283	3.387
-8.3	68.14+-17.2%	23.91+-31.5%	0.351	3.720
-5.5	44.51+-23.0%	19.24+-39.2%	0.432	2.991
-7.3	22.82+-24.0%	10.97+-30.5%	0.481	1.709
-12.5	10.10+-22.4%	4.59+-26.1%	0.454	0.716
-22.0	6.49+-13.3%	1.97+-21.8%	0.304	0.307
-32.8	4.30+-17.2%	0.81+-24.7%	0.188	0.126
-44.3	3.64+- 9.9%	0.40+-20.0%	0.110	0.062
-53.0	3.46+-10.4%	0.29+-20.7%	0.084	0.045
-55.0	3.13+- 9.9%	0.23+-21.7%	0.073	0.036
-48.3	3.11+- 9.6%	0.32+-25.0%	0.103	0.050
-42.5	3.50+- 9.7%	0.44+-27.3%	0.126	0.068
-36.5	3.64+-10.2%	0.62+-27.4%	0.170	0.096
-29.5	4.41+- 9.1%	0.99+-29.3%	0.224	0.154
-22.5	5.43+-13.4%	1.63+-33.7%	0.300	0.253
-16.5	7.72+-18.8%	2.90+-37.9%	0.376	0.451
-11.8	11.72+-25.7%	5.01+-39.7%	0.427	0.779
-8.5	17.29+-35.5%	7.87+-45.7%	0.455	1.225
-6.8	28.64+-31.9%	12.91+-46.5%	0.451	2.011
-5.3	44.01+-21.4%	16.91+-38.7%	0.384	2.633
-4.0	59.06+-17.9%	19.40+-34.5%	0.328	3.016
-1.3	69.87+-10.8%	19.35+-29.6%	0.277	3.010
6.3	74.64+- 7.1%	18.63+-14.9%	0.250	2.897
11.8	74.90+- 3.5%	15.88+-18.0%	0.212	2.469
15.8	74.32+- 2.4%	14.54+-17.3%	0.196	2.262
19.5	74.58+- 3.1%	13.18+-18.7%	0.177	2.048
24.3	73.75+- 2.2%	12.02+-17.2%	0.163	1.872
29.8	72.99+- 1.8%	11.15+-15.7%	0.153	1.734

DIELECTRIC DATA FOR 1.0% NACL IN 10% DMSO

TEMP. DEG.C	EP	EPP	L.TAN (AVG)	COND. MHO
23.1	73.62+- 2.3%	21.39+- 9.8%	0.291	3.324
16.0	73.56+- 2.9%	21.00+- 7.3%	0.285	3.267
8.9	73.62+- 3.2%	22.57+- 7.4%	0.307	3.512
-0.2	72.06+- 4.7%	25.07+-10.5%	0.348	3.902
-6.3	62.41+- 9.4%	25.99+-14.6%	0.416	4.040
-6.0	40.83+-14.9%	20.24+-23.8%	0.496	3.148
-8.5	18.62+-20.2%	10.58+-23.8%	0.568	1.646
-14.0	10.57+-14.1%	5.39+-21.0%	0.510	0.836
-22.8	7.36+-10.6%	2.65+-23.4%	0.360	0.412
-33.1	4.66+- 5.2%	1.14+-15.8%	0.245	0.177
-42.4	3.85+- 8.6%	0.56+-14.3%	0.145	0.087
-48.7	3.76+- 6.1%	0.36+-11.1%	0.096	0.056
-52.0	3.44+- 6.1%	0.30+-10.0%	0.087	0.047
-46.5	3.44+- 8.1%	0.42+-14.3%	0.122	0.065
-41.3	3.87+- 7.5%	0.61+-14.8%	0.158	0.095
-35.6	4.21+- 5.0%	0.98+-15.3%	0.233	0.153
-29.3	5.17+- 8.1%	1.66+-20.5%	0.321	0.258
-22.6	7.16+-11.2%	3.27+-42.5%	0.457	0.508
-16.8	9.99+-14.7%	4.65+-18.5%	0.465	0.723
-12.5	12.28+-13.4%	6.48+-17.7%	0.528	1.005
-9.4	18.65+-19.0%	10.28+-20.9%	0.551	1.596
-7.3	28.86+-18.4%	14.92+-25.1%	0.517	2.319
-5.9	41.78+-15.8%	19.42+-23.6%	0.465	3.022
-4.9	60.71+- 9.3%	25.07+-20.9%	0.413	3.902
-1.3	69.81+- 6.8%	25.93+-15.1%	0.371	4.034
4.7	74.83+- 3.0%	24.72+-10.1%	0.330	3.845
10.4	74.51+- 2.7%	23.01+- 8.9%	0.309	3.581
17.1	73.56+- 3.1%	21.70+- 8.6%	0.295	3.374
21.5	73.12+- 2.1%	21.08+- 6.5%	0.288	3.280
26.6	72.81+- 2.3%	20.67+- 6.3%	0.284	3.217
30.6	72.68+- 2.3%	20.83+- 7.2%	0.287	3.242

DIELECTRIC DATA POR 5% DEXTRAN IN 10% DMSO

TEMP. DEG.C	EP	EPP	L.TAN (AVG)	COND. MHO
22.1	67.44+- 2.8%	13.06+-12.5%	0.194	2.029
20.6	71.87+- 3.0%	13.66+-12.7%	0.190	2.124
15.9	72.06+- 3.2%	14.73+-12.9%	0.204	2.293
8.3	73.37+- 4.3%	17.46+-15.6%	0.238	2.714
-0.2	73.37+- 4.5%	21.39+-19.6%	0.292	3.324
-11.7	68.26+-12.6%	22.61+-35.8%	0.331	3.519
-6.4	39.20+-36.4%	16.38+-75.3%	0.418	2.545
-9.6	23.32+-35.7%	11.74+-46.7%	0.503	1.828
-15.3	11.53+-44.3%	5.09+-77.6%	0.441	0.792
-24.3	7.07+-36.9%	2.07+-76.8%	0.293	0.322
-34.8	4.59+-30.3%	0.80+-57.5%	0.174	0.124
-44.1	4.03+-14.6%	0.41+-36.6%	0.102	0.063
-57.3	3.55+-10.1%	0.25+-24.0%	0.070	0.039
-51.1	3.46+- 9.0%	0.27+-22.2%	0.078	0.042
-42.3	3.78+- 7.4%	0.46+-13.0%	0.122	0.072
-37.8	4.01+- 7.7%	0.66+-15.2%	0.165	0.102
-30.1	4.77+- 7.1%	1.07+-15.9%	0.224	0.167
-23.8	5.90+-11.5%	1.83+-18.0%	0.310	0.285
-17.6	8.44+-26.3%	3.34+-30.8%	0.396	0.520
-12.9	11.81+-22.1%	5.51+-25.0%	0.467	0.855
-9.9	16.64+-24.9%	8.74+-25.5%	0.525	1.357
-7.7	25.91+-26.9%	12.93+-34.4%	0.499	2.011
-5.9	39.64+-38.8%	17.35+-52.1%	0.438	2.695
-3.8	50.10+-22.4%	19.55+-38.6%	0.390	3.041
-0.4	63.28+-14.4%	21.53+-29.7%	0.340	3.349
2.9	67.44+- 7.1%	19.84+-17.4%	0.294	3.085
7.4	68.38+- 5.7%	18.09+-14.3%	0.265	2.815
11.5	68.26+- 5.4%	16.60+-11.8%	0.243	2.582
15.5	68.20+- 4.5%	15.45+- 9.3%	0.227	2.400
20.9	68.32+- 5.0%	13.71+-10.2%	0.201	2.130
25.6	68.03+- 4.7%	12.24+-12.4%	0.180	1.904
29.1	67.79+- 4.4%	11.36+-14.9%	0.168	1.766

DIELECTRIC DATA FOR DMSO IN WATER AT 5 C

CONC. %	EP	EPP	L.TAN (AVG)	COND. MHO
0.0	80.00+- 2.8%	14.95+- 8.4%	0.187	2.325
10.0	75.00+- 3.6%	18.77+- 9.7%	0.250	2.922
20.0	73.44+- 3.3%	23.65+- 7.6%	0.328	3.676
30.0	71.38+- 3.3%	30.03+-10.1%	0.322	4.668
40.0	62.47+- 2.9%	34.09+- 8.4%	0.546	5.303
50.0	50.18+-10.6%	32.94+-17.2%	0.656	5.121
60.0	38.20+-13.5%	28.00+-19.1%	0.733	4.355
70.0	27.00+- 8.2%	20.84+-13.9%	0.772	3.239
80.0	32.50+- 9.3%	24.50+-16.7%	0.754	3.813
90.0	43.34+- 5.6%	25.94+-12.6%	0.598	4.034
91.0	8.42+- 1.8%	25.94+-12.6%	0.599	0.281
100.0	8.42+- 1.8%	1.81+- 2.2%	0.215	0.281

DIELECTRIC DATA FOR DMSO IN WATER AT 23 C

CONC. %	EP	EPP	L.TAN (AVG)	COND. MHO
0.0	76.58+- 1.9%	11.48+- 8.9%	0.150	1.782
10.0	73.24+- 2.0%	11.99+- 8.4%	0.164	1.862
20.0	72.06+- 3.5%	13.91+- 9.8%	0.193	2.161
30.0	70.53+- 2.6%	17.31+- 8.8%	0.245	2.689
40.0	67.21+- 3.1%	20.74+- 9.6%	0.309	3.223
50.0	65.22+- 2.8%	24.97+-11.8%	0.383	3.883
60.0	61.03+- 3.9%	27.63+-13.2%	0.453	4.298
70.0	57.95+- 5.8%	28.45+-14.5%	0.491	4.423
80.0	55.60+- 4.2%	25.93+-11.1%	0.466	4.034
90.0	52.80+- 4.2%	20.40+- 9.8%	0.386	3.173
100.0	47.50+- 5.7%	13.42+-10.1%	0.283	2.086

DIELECTRIC DATA FOR DMSO IN WATER AT 50 C

CONC. %	EP	EPP	L.TAN (AVG)	COND. MHO
0.0	66.64+- 3.6%	7.58+-12.1%	0.114	1.181
10.0	66.35+- 3.3%	8.79+-12.1%	0.132	1.370
20.0	65.89+- 3.4%	11.12+- 9.8%	0.169	1.728
30.0	65.55+- 3.3%	13.04+-11.5%	0.199	2.029
40.0	64.55+- 3.3%	16.12+-17.9%	0.250	2.507
50.0	61.40+- 5.3%	19.41+-13.3%	0.316	3.016
60.0	55.03+- 5.4%	18.97+-11.1%	0.345	2.953
70.0	54.23+- 7.0%	18.35+-20.3%	0.338	2.853
80.0	52.44+- 5.2%	17.59+-12.4%	0.335	2.733
90.0	50.14+- 4.8%	14.40+-12.2%	0.287	2.237
100.0	46.77+- 6.5%	10.70+-22.1%	0.229	1.665